CHEMICAL REVIEWS

pubs.acs.org/CR

Review

Smart Textiles for Electricity Generation

Guorui Chen, Yongzhong Li, Michael Bick, and Jun Chen*

Cite This: *Chem. Rev.* 2020, 120, 3668−3720

Read Online

ACCESS | Metrics & More | Article Recommendations

ABSTRACT: Textiles have been concomitant of human civilization for thousands of years. With the advances in chemistry and materials, integrating textiles with energy harvesters will provide a sustainable, environmentally friendly, pervasive, and wearable energy solution for distributed on-body electronics in the era of Internet of Things. This article comprehensively and thoughtfully reviews research activities regarding the utilization of smart textiles for harvesting energy from renewable energy sources on the human body and its surroundings. Specifically, we start with a brief introduction to contextualize the significance of smart textiles in light of the emerging energy crisis, environmental pollution, and public health. Next, we systematically review smart textiles according to their abilities to harvest biomechanical energy, body heat energy, biochemical energy, solar energy as well as hybrid forms of energy. Finally, we provide a critical analysis of smart textiles and insights into remaining challenges and future directions. With worldwide efforts, innovations in chemistry and materials elaborated in this review will push forward the frontiers of smart textiles, which will soon revolutionize our lives in the era of Internet of Things.

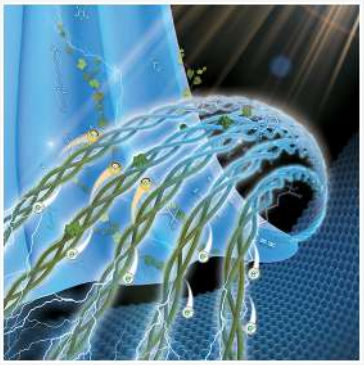

CONTENTS

Received: December 17, 2019
Published: March 23, 2020

https://dx.doi.org/10.1021/acs.chemrev.9b00821
Chem. Rev. 2020, 120, 3668−3720

1. INTRODUCTION

Fossil fuels contribute to up to 86% of global primary energy consumption, which would be exhausted in 150 years,[1−3] given the fact that the energy consumption growth rate has nearly doubled since 2010.[4−9] Moreover, burning fossil fuels exacerbates the greenhouse effect,[10−12] toxic air pollution,[13−15] and particulate matter emissions,[16−18] which all have lasting, detrimental impacts on global climate,[19−21] public health,[22−24] local communities,[25−27] and ecosystems.[28−30] Since the Second Industrial Revolution in 1870, CO_2 release from fossil fuel combustion has increased average earth surface temperature by 0.76 °C and is expected to lead to another warming of 1.1−6.4 °C by the end of the 21st century.[31−33] The resulting toxic air pollutants would also cause heart-related diseases,[34−36] lung cancer,[37−39] and respiratory illness.[40−42] Additionally, mining and drilling procedures of removing fossil fuels from the earth pose serious public health[43−45] and environmental threats.[46−48] With the threats of energy crises, environmental pollution , and public health in mind, searching for renewable and environmentally friendly energy solutions to complement and eventually replace fossil fuels is imperative for sustainable development of human civilization.

Meanwhile, as the world marches into the era of Internet of Things (IoT), wireless sensor networks, big data, robotics, and artificial intelligence are forcing the world to use a new form of pervasive energy to sustainably power billions of distributed devices.[49−51] It is estimated that the number of IoT devices will reach 26 billion by 2020,[52] which will greatly revolutionize our conventional means of communications and lifestyles. The need for a pervasive energy solution exceeds the capability of traditional central power supply systems,[53] providing a considerable challenge for people to overcome.

Portable energy storage units such as batteries seem like the intuitive choice to render a pervasive energy solution.[54−58] Wearable electronics, especially skin electronics, are key elements of the IoT for personalized healthcare,[59−64] as well as information and communications.[65−68] However, the wide-ranging adoption of battery systems for wearable electronics will be largely inhibited by the following factors. First, rigid and bulky battery systems render devices unfit for skin interfaces.[69−74] Second, a majority of battery systems are built on toxic chemicals, which hinder their potential toward biointegrated applications and introduce possible environmental risks.[75−79] Lastly, the limited lifetime of batteries also precludes their applications in widely distributed device systems.[80−84] Therefore, a pervasive, environmentally friendly, and sustainable energy solution is highly desired to power on-body electronics.

The human body and its surroundings, including biomechanical motions, body heat, body fluids, and sunshine, are rich sources of renewable energy.[85−87] For example, the available energy associated with body heat and biomechanical motions are respectively up to 4.8 W[88−91] and 67 W,[92−95] and body fluids even contain energy up to 100 W.[96−98] Besides the available energy from the body, its surroundings are also filled with renewable energy sources, such as solar irradiance, which has an energy density up to 100 mW/cm^2.[99−102] The energy requirements of modern on-body electronics are within the range of 200 μW−1 W,[103] which can be fully met by harnessing the energy associated with the human body.

In recent years, various working mechanisms and wearable device designs have sprung up to harvest these types of energy,[104−110] including triboelectric nanogenerators (TENGs),[111−144] piezoelectric nanogenerators (PENGs),[145−151] thermoelectric generators (TEGs),[152−160] biofuel cells (BFCs),[161−167] solar cells (SCs),[168−186] and hybrid generators (HGs).[187−198] However, these electricity generators exhibit certain deficiencies for driving on-body electronics. Thick and bulky structure designs make them uncomfortable to wear and would likely impair body movement.[199] Also, most of the reported wearable energy harvesters are built on polymer thin films, which have poor air permeability and ability to endure frequent mechanical deformation.[200−202] Maintaining electricity generation without compromising wearability remains a challenge for on-body energy harvesters.

Clothing is a feature of all human societies. The discovery of textile-like materials dates back to 34 000 BCE, even possibly to prehistoric times.[203] Since then, textiles have been made from a wide range of materials, from natural products (e.g., silk, wool, and cotton) to synthetic compounds (e.g., peptide, polyamide, and polyester), and many of them are biocompatible, biodegradable, and even bioabsorbable, which are desired properties for textiles working as the interface between skin and electronics. Merging electronics with textiles is becoming increasingly desirable, as this can lead to an excellent on-body platform for pervasive computing while retaining compelling features of textiles, including superior wearing comfort, excellent mechanical strength, softness to accommodate complex deformation, light weight, low cost, flexibility, and even foldability.[204−208] However, up to now, the functionalities of textiles have been limited to skin protection,[209−211] body temperature maintenance,[212−215] decoration, and aestheticism.[216] The rapid advancements of materials science and chemistry continue revolutionizing traditional textiles, making them smart, especially toward the capability of harvesting energy from the human body and its surroundings.[217,218]

https://dx.doi.org/10.1021/acs.chemrev.9b00821
Chem. Rev. 2020, 120, 3668−3720

Figure 1. Schematic illustration of smart textiles for energy harvesting. The human body and its surroundings, including biomechanical motions, body heat, biofluids, and sunshine, are rich sources of renewable energy. Fusion of textiles and generators to generate electricity from the human body and its ambient environment renders a pervasive, environmentally friendly, and sustainable energy solution for wearable electronics in the era of the Internet of Things.

In the following sections, we present a broad picture of the research on smart textiles for energy harvesting. We comprehensively and thoughtfully discuss all of the research activities on utilizing smart textiles to harvest biomechanical energy, body heat energy, biochemical energy, solar energy as well as hybrid energy forms simultaneously (Figure 1). To achieve a better understanding and all-inclusive scope of the whole field, this review exhaustively covers the working mechanisms, material innovations, advanced device designs, energy efficiency, and on-body applications of smart textiles. Finally, this review provides a critical analysis of smart textiles and insights into remaining challenges and future directions. With worldwide efforts, innovations in chemistry and materials elaborated in this review will push forward the frontiers of smart textiles, which will soon revolutionize our lives in the era of Internet of Things.

2. BIOMECHANICAL ENERGY HARVESTING

The human body is a rich source of biomechanical energy. Biomechanical motions, such as blood flow, breathing, upper limb movement, finger typing, and walking, can release approximately 0.93 W, 0.83 W, 3.0 W, 6.9 mW, and 67 W of energy, respectively.[219] Harvesting various forms of biomechanical energy from the human body via smart textiles could provide a renewable, convenient, and comfortable energy solution for on-body electronics. The reported working mechanisms for mechanical energy harvesting include the electromagnetic effect,[220−222] electrostatic effect,[223−225] triboelectrification,[226−234] and piezoelectric effect.[235−249] Combining biomechanical energy harvesters with textiles brings a number of compelling features. First, the pliancy of textiles ensures a sensitive response to mechanical deformation for high performance biomechanical energy harvesting. Second, the great breathability of textiles offers wearable comfort while harvesting energy. Lastly, taking advantage of the textile industry, textile generators can be massively produced. However, electromagnetic transduction relies on magnets and coils with a rigid structure,[250−252] while electrostatic transduction requires sophisticated structure and external high direct current (DC) voltage.[253−255] Both can hardly be merged with textiles to effectively harvest on-body biomechanical energy. In contrast, because of the wide range of low-cost, light weight, and flexible material choices with simple structural design, the triboelectric effect and piezoelectric effect based nanogenerators show potential for integration with the textile industry to provide a wearable and comfortable energy source for on-body electronics.[256−260] In this section, we comprehensively cover the research progress on textile-based biomechanical energy harvesting by using both a triboelectric nanogenerator (TENG) and a piezoelectric nanogenerator

https://dx.doi.org/10.1021/acs.chemrev.9b00821
Chem. Rev. 2020, 120, 3668−3720

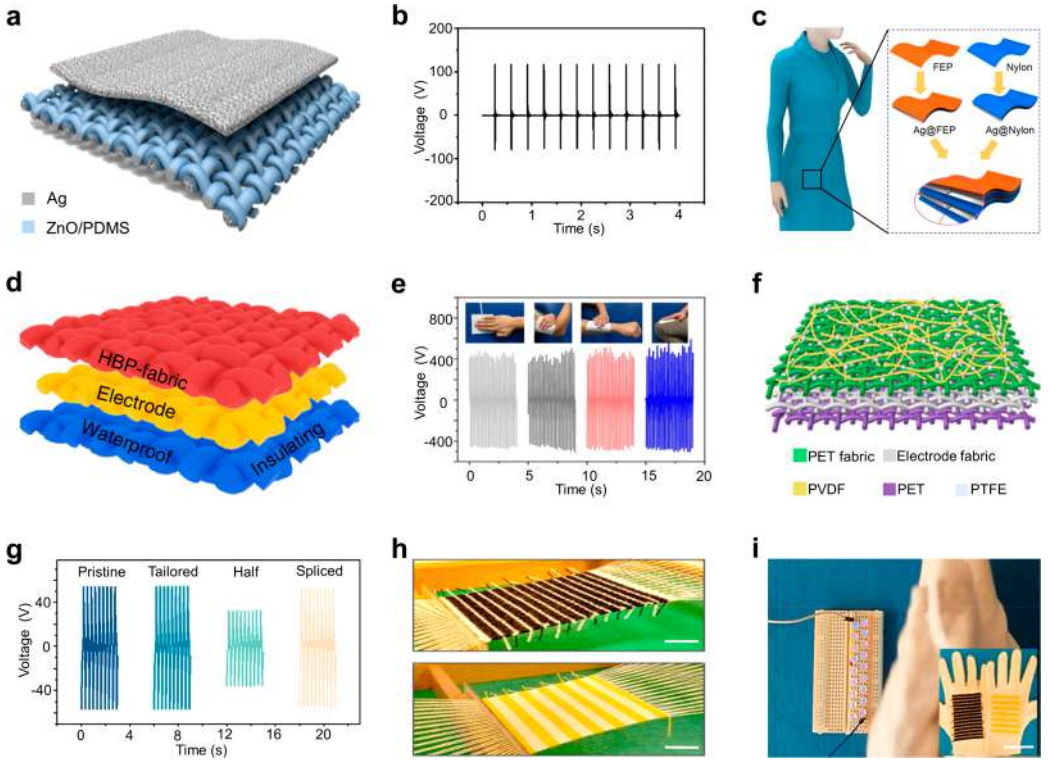

Figure 2. Textile TENGs based on layer stacking for biomechanical energy harvesting. (a) Schematic illustration of a nanopatterned textile TENG based on the contact-separation mode. (b) Output voltage of the nanopatterned textile TENG under compressive force. Reproduced with permission from ref 329. Copyright 2015 American Chemical Society. (c) Schematic illustration of a textile TENG based on the lateral sliding mode. Reproduced with permission from ref 333. Copyright 2015 American Chemical Society. (d) Schematic illustration of a textile TENG based on the single-electrode mode. (e) Output voltage of the textile TENG by harvesting biomechanical energy from the human body. Reproduced with permission from ref 334. Copyright 2018 Nature Publishing Group under Creative Commons Attribution 4.0 (http://creativecommons.org/licenses/by/4.0/). (f) Schematic illustration of a textile TENG modified with PVDF nanofibers and PTFE nanoparticles. (g) Output voltage of the textile TENG in different tailored shapes. Reproduced with permission from ref 335. Copyright 2019 Elsevier. (h) Photographs of the textile electrode (top) and the grating dielectric textile (bottom). Scale bar, 4.5 cm. (i) Photograph of the FT mode textile TENG that was knitted onto to a pair of gloves and lighted up LEDs under natural rubbing/patting of hands. Scale bar, 6 cm. Reproduced with permission from ref 336. Copyright 2018 Elsevier.

(PENG) and summarize challenges and opportunities in each field.

2.1. Textile TENGs

Physical contact between two dissimilar materials with different electron affinities can generate opposite electrostatic charges on the contacted surfaces.[261,262] A gap or perturbation created by an external mechanical force can establish an electric potential difference between the two charged surfaces, thus generating a voltage and polarization-induced current.[263] This is the mechanism behind the triboelectric nanogenerator, which originates from Maxwell's displacement current[264] and was first brought up in 2012.[265] Within the past eight years, TENGs have proved to be an efficient energy technology to convert ambient mechanical motions into electricity as either sustainable power sources[266−282] or self-powered active sensors.[283−298] Integrating TENGs with conventional textiles can achieve a human-friendly, convenient, and sustainable energy solution for on-body electronics.[299] To realize a textile-based TENG for biomechanical energy harvesting, three fabrication techniques have been systematically developed: layer stacking, yarn intersection, and 3D printing, as introduced one by one in the following sections.

2.1.1. Layer Stacking. On the basis of the surface charging effect, layer stacking of textile materials with different electron affinities could be a simple way to realize a textile TENG. The rough surfaces of textiles are naturally favorable to enhance triboelectrification for higher electric output. To construct a layer-stacked textile TENG, dielectric and electrode layers are laminated vertically. Four fundamental working modes of TENGs have been widely involved,[300] including the vertical contact-separation mode,[301−304] the lateral-sliding mode,[305−310] the single-electrode mode,[311−315] and the freestanding triboelectric-layer mode.[316−318] We introduce the layer-stacked textile TENGs one by one according to the four working modes.

2.1.1.1. Contact-Separation Mode. Vertical contact-separation friction is commonly observed with body motions, such as finger pressing, elbow bending, and foot tapping. In layer-stacked textile TENGs based on the contact-separation mode,[319−327] the two dielectric textile layers with different electron affinities will be oppositely charged during contact. When biomechanical movements associated with body motions bring them to a separation state, a flow of induced electrons goes through the external circuits to balance the electrostatic field.

For example, on the basis of the contact-separation mode, Andrew et al. reported an all-textile TENG, which consisted of four stacked layers.[328] In this configuration, cotton and nylon fabric served as dielectric layers with different electron affinities and were placed face-to-face between two electrode layers.

https://dx.doi.org/10.1021/acs.chemrev.9b00821
Chem. Rev. 2020, 120, 3668−3720

With a vertical force of 6 N applied onto the all-textile TENGs, an average areal power density of 7 μW/cm^2 was demonstrated during the contact and separation process of the cotton and nylon fabric layers.

Similarly, Kim et al. developed a layer-stacked textile TENG decorated with zinc oxide (ZnO) nanorods to promote energy efficiency under the vertical contact-separation mode.[329] In this work, ZnO nanorods were grown on the Ag-coated textile and further coated with polydimethylsiloxane (PDMS). After stacking another unprocessed Ag-coated textile on the nanopatterned dielectric layer, a textile TENG with full flexibility, foldability, and robustness was constructed (Figure 2a). Under a vertical compressive force of 10 kgf, as shown in Figure 2b, the nanopatterned textile TENG generated an output voltage and power of up to 120 V and 1.1 mW, respectively. The enhancement of the electric output was mainly attributed to the created surface nanopatterns, which effectively increased the contact area between the two textile layers.

2.1.1.2. Lateral Sliding Mode. Sliding biomechanical movements, such as arm and leg swings, are also quite common in humans. Layer-stacked textile TENGs based on the lateral sliding mode can take advantage of horizontal friction and harvest energy for on-body electronics.[330,331] In this configuration, body movements drive stacked dielectric textiles to slide against each other, which generates triboelectric charges and induces a lateral polarization. Periodic body movement drives electrons to flow back and forth to balance the lateral polarization, generating electricity in external circuits.

For example, Qin et al. developed a grating-structured textile TENG based on the lateral sliding working mode.[332] By using cotton fabrics as the substrates and supporting layers, nylon and Dacron with back-coated copper electrodes were laminated onto the cotton fabrics, acting as the two triboelectric layers. Attaching these two triboelectric layers onto the tester's inner forearm and waist with natural arm swinging, the constructed textile TENG was subjected to a relative lateral sliding, generating an output voltage and current of up to 0.7 kV and 50 μA, respectively.

However, these conventional textile TENGs based on the lateral siding mode usually consist of two separate triboelectric layers, which might be inconvenient to be integrated with practical clothes that usually have a one-body design. In that case, Zhou et al. developed a layer-stacked textile TENG that assembled two triboelectric layers into one piece. In this simplified configuration (Figure 2c),[333] Ag-covered fluorinated ethylene propylene (FEP) was first stacked onto Ag-covered nylon with an adhesive tape, which was then stacked onto a piece of nylon cloth for added protection. With a sliding range of 5 mm and a frequency of 5 Hz, the textile TENG generated an output power density of up to 4.65 μW/cm^2. Meanwhile, when this integrated textile TENG with a size of 10 cm by 10 cm was easily fastened to the armpit area in practical clothes and slid by the tester' sleeve, 11 blue light-emitting diodes (LEDs) connected in parallel were lit up simultaneously, which demonstrated outstanding applicability for on-body energy harvesting.

Additionally, it is worth mentioning that both the lateral sliding and vertical contact-separation working modes can coexist in textile TENGs during human body movement. With this in mind, Kim et al. developed a similarly structured textile TENG that could work in both the lateral sliding and contact-separation working modes.[337] Two dielectric textiles with different electron affinities were used: one of them was fabricated by coating polyurethane (PU) and polyimide (PI) onto a carbon fabric, and the other was based on coating PDMS and Al electrodes onto the carbon fabric. These two dielectric textiles were separately placed on the elbow and armpit regions to harvest energy from both vertical and horizontal friction caused by the tester running, producing an output power density of up to 0.18 μW/cm^2.

2.1.1.3. Single-Electrode Mode. Compared to the aforementioned working modes that require two textile electrodes, textile TENGs based on the single-electrode working mode have a relatively simple structure, and their integration with practical clothes proves to be straightforward.[338−343] In this configuration, the bottom textile electrode is grounded, and vertical or lateral movements of the dielectric textile manipulate the electron distribution on the textile electrode surface, thus inducing a flow of electrons oscillating between the textile electrode and ground.

For example, Lee et al. demonstrated a layer-stacked textile TENG based on the single-electrode working mode (Figure 2d).[334] First, the triboelectric fabric (HBP fabric) was fabricated by coating black phosphorus and hydrophobic cellulose oleoyl ester nanoparticles (HCOENPs) onto the polyethylene terephthalate (PET) fabric successively. Then the enhanced triboelectric fabric layer was stacked onto the textile electrode to form a single-electrode based textile TENG. By applying the hand touching of ∼5 N at a frequency of 4 Hz, the contact and separation between the textile TENG and the human skin generated an output voltage and current density of up to 880 V and 1.1 μA/ cm^2, respectively (Figure 2e). This textile TENG based on the single-electrode working mode takes advantage of the human skin as a dielectric layer, which effectively simplifies the device structure and shows promise for incorporation into practical clothes.

More recently, Ding et al. designed a single-electrode mode textile TENG with a similar structure.[335] In this work, the PET textile was first modified with polyvinylidene difluoride (PVDF) nanofibers and polytetrafluoroethylene (PTFE) nanoparticles to obtain a triboelectric layer with considerable electronegativity and enlarged contact area. Then a conductive textile was employed as the single electrode, and another PET textile substrate was placed at the bottom to form the textile TENG (Figure 2f). By undertaking the contact and separation process with another dielectric layer such as clothes or human skin, this textile TENG could effectively harvest biomechanical energy and deliver a maximum power density of 80 mW/m^2. Meanwhile, this tailored textile TENG maintained the same output current and voltage as the original one (Figure 2g), demonstrating its outstanding capability of merging with practical clothes in any shape.

2.1.1.4. Freestanding Triboelectric-Layer Mode. Last but not least, textile TENGs based on the freestanding triboelectric-layer mode (FT mode) involve the absence of physical contact between the moving and stationary components, which prove to be ideal in biomechanical energy harvesting with versatile applications and long-term durability.[344] In this working mode, symmetric electrodes are underneath the dielectric textile. With the approach and departure of the moving object on the surface, the charges redistribute on the paired electrodes to balance the potential changes, forming an alternating flow of electrons through the external circuits.

https://dx.doi.org/10.1021/acs.chemrev.9b00821
Chem. Rev. 2020, 120, 3668−3720

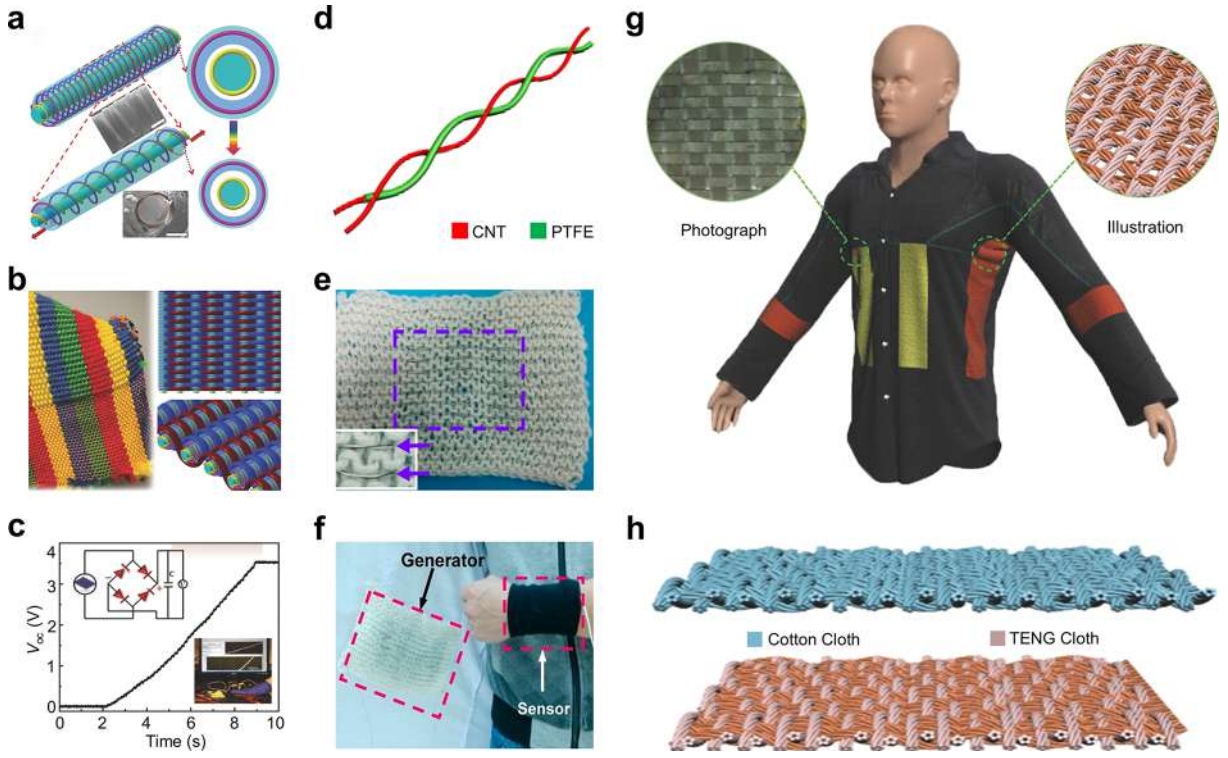

Figure 3. Textile TENGs based on yarn intersection for biomechanical energy harvesting. (a) Schematic illustration of a coaxial yarn-shaped TENG. (b) Photograph of an interlaced textile TENG. (c) The interlaced textile TENG charged a 1 μF capacitor to 3.5 V in 7 s under hand flapping. Reproduced with permission from ref 363. Copyright 2018 Wiley-VCH. (d) Schematic illustration of a pretwisted yarn-shaped TENG. (e) Photograph of pretwisted yarn-shaped TENG woven with a textile. (f) Photograph of the power shirt triggering a temperature sensor. Reproduced with permission from ref 364. Copyright 2014, American Chemical Society. (g) Schematic illustration of a whole-textile TENG cloth. (h) Schematic illustration of the whole-textile TENG operating in the vertical contact-separation mode with a cotton cloth. Reproduced with permission from ref 365. Copyright 2016, Wiley-VCH.

For example, Chen et al. developed a textile TENG based on the FT mode for harnessing lateral body motion energy.[336] The textile TENG consisted of an interdigital textile electrode and a grating dielectric textile comprised of PTFE and cotton threads (Figure 2h). At sliding speeds of 20 cm/s, the grating dielectric textile approached and departed from the electrodes periodically, generating an output voltage and current of up to 118 V and 1.5 μA, respectively. Meanwhile, 80% of the initial output could be maintained after cycling the sliding process 15 000 times at a speed of 10 cm/s. Furthermore, the two layers of this textile TENG were knitted separately onto a pair of gloves. The natural rubbing and patting of the human hands resulted in glove-generated electricity, lighting up 18 LEDs (Figure 2i). More recently, Beeby et al. developed a FT mode textile TENG with a novel grated strip textile design,[345] which consisted of alternating positive nylon strips and negative polyvinyl chloride (PVC) heat transfer vinyl strips. Then the textile TENG with five pairs of alternating strips was attached to practical clothes. With the arm swinging at a frequency of 2.5 Hz, the FT mode textile TENG generated an output voltage of up to 46.72 V, which was able to drive a digital watch.

In summary, by fully exploring and utilizing the advantages of the four working modes, the textile TENGs based on layer stacking configuration can harvest various types of biomechanical energy to generate electricity from the human body.

2.1.2. Yarn Intersection. Although a textile TENG based on layer stacking has a convenient and straightforward fabrication process, stacking functional layers with required spacers between them greatly increases device thickness and undermines its inherent wearing comfort, such as flexibility and breathability, as well as its sensitivity to biomechanical deformation induced by body movement. These concerns can be eliminated by developing woven or knitted textile TENGs based on yarn intersection. Specifically, woven textiles are mainly constructed by intersecting two sets of straight yarns at right angles. In contrast, knitted textiles consist of symmetric loops of yarn following a meandering path.

To realize a woven or knitted textile TENG, functional yarns are the building blocks. To construct a functional yarn, there are two types of configuration. The first configuration is a coaxial structure,[346−349] in which each yarn is a single TENG comprised of coaxial triboelectric materials and electrodes. The second configuration consists of various functional fibers, and they can be pretwisted into a single thicker yarn[350−352] or directly woven or knitted into the textile form for energy harvesting.[353−361] Yarn intersection-based textile TENGs could hold enhanced breathability and wearability due to the porous weaving/knitting structure. Moreover, textile TENGs constructed via yarn intersection create tiny nanogenerators at each interface, which respond more efficiently to tiny localized textile deformations than layer-stacked TENGs. These yarn intersection-based textile TENGs can be designed with two types of structure: two-dimensional (2D) interlacing and three-dimensional (3D) interlacing, introduced as follows.

2.1.2.1. 2D Interlacing. Interlacing functional yarns into a 2D form is a convenient method for achieving a textile TENG for biomechanical energy harvesting. For example, Baik et al.

https://dx.doi.org/10.1021/acs.chemrev.9b00821
Chem. Rev. 2020, 120, 3668−3720

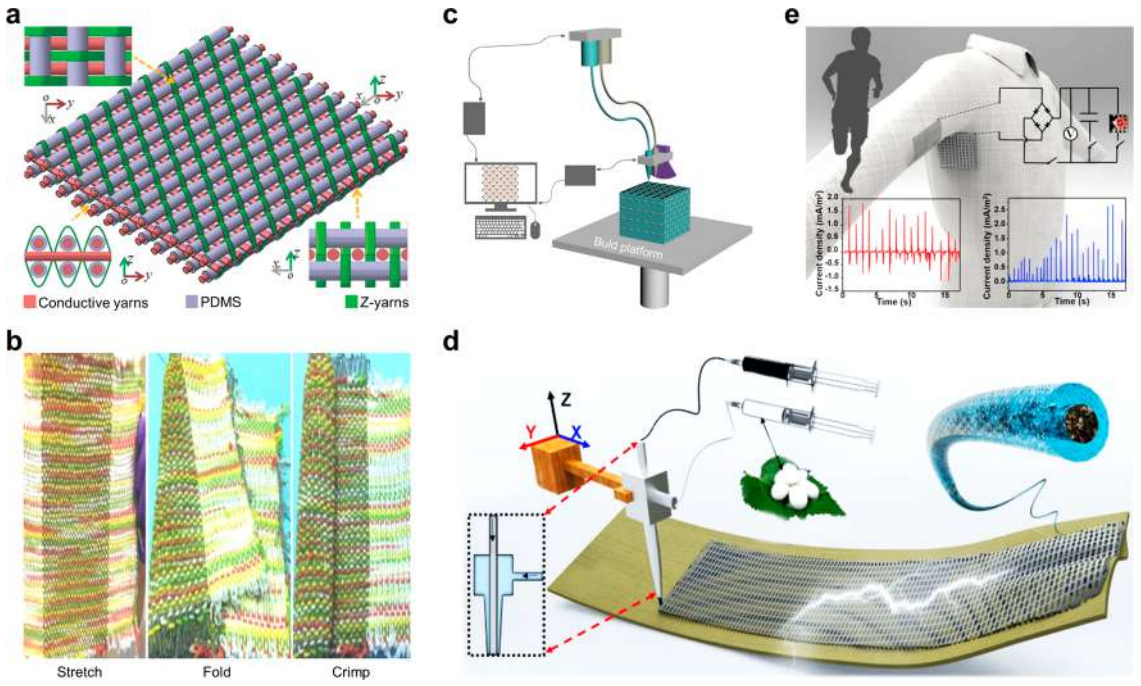

Figure 4. Textile TENGs based on 3D interlacing or 3D printing for biomechanical energy harvesting. (a) Schematic illustration of a 3D orthogonal woven textile TENG. (b) Photograph of the as-prepared 3D textile TENG. Reproduced with permission from ref 367. Copyright 2017 Wiley-VCH. (c) Schematic illustration of a hybrid 3D printing system and ultraflexible 3D TENG. Reproduced with permission from ref 368. Copyright 2018 Elsevier. (d) Schematic illustration of the 3D printing process and a coaxial fiber-shaped TENG. (e) Schematic illustration of the ultraflexible 3D TENG on commercial clothes for biomechanical energy harvesting. Reproduced with permission from ref 369. Copyright 2019 Elsevier.

developed a 2D stretchable textile TENG by weaving strands of coaxial yarns.[362] In these coaxial triboelectric yarns, PDMS tube was sandwiched between the external sheath of Al foil and internal core of Au-coated Al wire. The triboelectric effect was observed in the gap between the PDMS tube and Al wire in the vertical contact-separation working mode. This woven textile TENG demonstrated incredible sensitivity in harvesting energy from the stretched direction, exhibiting an output voltage of 40 V and current value of 210 μA when employing a cycled 50 N compressive force on a 14 cm by 14 cm effective area. Applying this textile TENG with 30 by 30 yarns onto the elbow of a tester, with a bending angle of up to 130°, an output current of 7 μA was generated, which is sufficient to light up a green LED.

Recently, a more intricate coaxial yarn-based 2D textile TENG was brought up by Dong et al.[363] In this coaxial structure, the inner core yarn was achieved by twisting a conductive yarn onto the silicone rubber fiber. Then the core yarn was coaxially inserted into an elastic silicone rubber tube, which was entangled with another conductive yarn as the external electrode. After being packed with a silicone rubber film, a coaxial yarn-shaped TENG was finally realized (Figure 3a). The gap between the core yarn and the silicone rubber provided enough spaces for contact and separation between triboelectric layers. Because of the high elasticity, flexibility, and performance endowed by this novel spring-like coaxial structure, these coaxial yarn-shaped TENGs can be readily woven with insulating acrylic yarns into a 2D interlacing textile (Figure 3b). By applying hand flapping on the 2D textile TENG, the generated electricity was able to charge a 1 μF capacitor to 3.5 V in 7 s (Figure 3c).

In addition to interlacing the coaxial yarn-shaped TENGs into a plane pattern, 2D textile TENGs can be constructed by weaving or knitting the dielectric yarns and electrode yarns. For example, Zhou et al. established the first proof-of-concept of weaving entangled dielectric yarns and electrode yarns with textiles.[364] In this work, separated carbon nanotube (CNT) yarns and PTFE-coated CNT yarns were pretwisted together to form a yarn-shaped fiber TENG (Figure 3d). With a length of 9 cm, this yarn-shaped TENG generated a peak output power of 11.08 nW under 2.15% strain at a frequency of 5 Hz. Then the flexible and lightweight yarn-shaped TENGs were woven into a textile to obtain a power shirt (Figure 3e). By harvesting biomechanical energy from the wearer, this power shirt was able to light up a red LED and trigger a wireless body temperature sensor (Figure 3f), which proved to be a promising start for on-body electricity generation.

Furthermore, Pu et al. proposed a whole-textile TENG cloth by weaving Ni-coated polyester strips and parylene-Ni-coated strips into a plane pattern (Figure 3g).[365] This whole-textile TENG could be integrated into many positions on the human body, such as the arm, leg, and foot, to harvest biomechanical energy. When the whole-textile TENG with a size of 10 cm by 10 cm was operated in the vertical contact-separation mode with a cotton cloth at a frequency of 5 Hz (Figure 3h), it delivered an open-circuit voltage (V_{oc}) and a short-circuit current (I_{sc}) of up to 40 V and 5 μA, respectively.

Similarly, Zhao et al. developed a 2D interlacing textile TENG by directly weaving Cu-PET warp and PI-Cu-PET weft on an industrial loom.[350] Specifically, each crisscross intersection area between the two types of yarn served as an individual TENG, thus boosting triboelectric charge generation, especially in response to subtle friction. This 2D interlacing textile TENG with a size of 6 cm by 4 cm delivered an output power density of up to 33.16 mW/m^2 when being tapped at a speed of 10 cm/s.

https://dx.doi.org/10.1021/acs.chemrev.9b00821
Chem. Rev. 2020, 120, 3668−3720

Table 1. Materials and Energy Performance of Representative Textile TENGs

triboelectric materials	electrodes	performance	modes	year	ref
Layer Stacking					
PI/PU and Al/PDMS	carbon fabric	0.18 μW/cm^2	CS[a]/LS	2014	337
ZnO NWs-PDMS/Ag	Ag coated textile	120 V, 1.1 mW	CS	2015	329
nylon and dacron	Cu strips	0.7 kV, 50 μA	LS[b]	2015	332
PDMS and Al NPs	Au coated textile	33.6 mW/cm^2	SE[c]	2015	342
FEP and nylon	Ag coated textile	4.65 μW/cm^2	LS	2015	333
graphene and polyester	Ag NWs	7 nW/cm^2	LS	2016	330
nylon and cotton	Ag coated nylon textile	7 μW/cm^2	CS	2016	328
water drop and PET	Au	15 V, 4 μA, 0.14 W/m^2	SE	2017	341
silk and skin	CNT ink	0.18 V (40 cm^2)	SE	2018	339
PET and conductive fabric	conductive fabric	3.4 V, 15 nA	SE	2018	340
PTFE and PA6	Ag plated filament	11.0 mW/m^2	CS	2018	323
PTFE and nylon	Cr/Cu coated fabrics	1.95 μW/m^2	LS	2018	331
PTFE and cotton	conductive carbon wires	118 V, 1.5 μA (30 cm^2)	CS/FT[d]	2018	336
skin and PET	Ag coated textile	880 V, 1.1 μA/cm^2	SE	2018	334
Ag and PTFE	Ag NFs	600 μW/cm^2	CS	2019	325
PTFE/PVDF and skin	conductive textile	112.7 V, 1.98 μA, 80 mW/m^2	SE	2019	335
PTFE and PEDOT:PSS-coated textile	Al	2 W/cm^2	CS	2019	319
rubber membrane and Mesh fabric	conductive textile	16 mW/m^2	CS	2019	321
PTFE and Ag coated textile	Ag coated textile	900 V, 19 μA	FT	2019	344
Yarn Intersection					
PTFE and CNT	CNT	11.08 nW (9 cm)	CS	2014	364
nylon and PET	Ag coated fabric	1 μA, 90 V	FT	2014	353
PDMS and Al wire	Al	40 V, 210 μA	CS	2015	362
Ni and parylene	Ni coated cloth	50 V, 4 μA (25 cm^2)	CS/LS	2015	357
PI and Cu	Cu coated fiber	4.98 V, 15.50 mA/m^2	CS	2016	350
parylene, Ni, and cotton	Ni coated fiber	40V, 5 μA (100 cm^2)	CS	2016	365
skin and silicone rubber	stainless steel wire	85 mW/m^2	SE	2017	338
polymer and natural fiber	stainless steel fiber	75 V, 1.2 μA, 60 mW/m^2	CS/SE	2017	360
silicone rubber and skin	stainless steel thread	200 V, 200 μA, 14 mW	SE	2017	355
silicone rubber and Ni	Ni coated fabric	0.892 mW/cm^2	FT	2017	359
Ag and PTFE	Ag	23.5 V, 1.05 μA, 60 μW	CS	2017	354
silicone rubber and nylon	carbon fiber	42.9 V, 0.51 μA, 1.12 μW	SE	2018	349
nylon and silicone rubber	Ag coated fibers	0.88 W/m^3	CS	2018	363
silicone rubber and skin	Ag-coated Cu thread	34.4 μW/cm^2	SE	2018	348
PVDF and nylon	Al	130 nA, 1.2 V	CS	2018	358
PTFE and skin	Cu coated fiber	0.56 W/m^2	SE	2018	347
silicone rubber and skin	stainless steel wire	12.5 μW/m	SE	2019	352
nylon and PET	steel and copper	6.35 V, 575 nA, 2.33 mW/m^2	LS	2019	356
3D Structure					
PDMS and stainless steel wire	stainless steel wire	263.36 mW/m^2	CS	2017	367
PAN and Ag	Ag plated nylon fibers	1768.2 mW/m^2	SE	2019	370
silk fibroin and PET	CNT	18 mW/m^2	CS	2019	369

[a]CS: the vertical contact-separation mode. [b]LS: the lateral sliding mode. [c]SE: the single-electrode mode. [d]FT: the freestanding triboelectric-layer mode.

2.1.2.2. 3D Interlacing. In general, 2D textile TENGs based on yarn interlacing exhibit a collection of compelling features, including simple structure, light weight, and scalable fabrication. However, wide-range adoption of 2D textile TENGs for biomechanical energy harvesting is largely limited by their insufficient energy delivery for on-body electronics. To boost output power to a practical level, more advanced 3D-structured TENGs have been introduced based on advancing 3D interlacing technology.[366] For example, Dong et al. reported a 3D orthogonal woven textile TENG for harnessing biomechanical energy.[367] In this work, nonconductive binding yarns were woven with weft PDMS-coated dielectric yarns (top and bottom) and warp 3-ply twisted stainless steel/polyester conductive yarns (middle) together in the normal direction (Figure 4a). This as-prepared textile TENG (Figure 4b) demonstrated an output power density of 263.36 mW/m^2 when undertaken with a tapping frequency of 3 Hz, which was far better than the energy performance of 2D interlacing textile TENG, which lacked sufficient contact-separation space in the thickness direction. In addition, this 3D textile TENG was found to be able to power a warning indicator, a capacitor, and a watch, demonstrating its capability to drive on-body electronics.

Recently, Gong et al. developed a 3D full fabric TENG by employing computerized 3D knitting technology.[370] Conductive fibers, polyacrylonitrile (PAN) fibers, and cotton fibers were used to knit the top electrode layer, bottom dielectric layer, and middle linking layer, respectively. This innovative

https://dx.doi.org/10.1021/acs.chemrev.9b00821
Chem. Rev. 2020, 120, 3668−3720

3D full fabric structure contributed to a doubled contact and separation process in the textile TENG for electricity generation. Therefore, with an applied force of 1200 N, this 3D full fabric TENG delivered an outstanding power density of up to 1768.2 mW/m^2, which could light up 320 LEDs.

To sum up, the three-dimensional weaving or knitting technology can interlace triboelectric yarns omnidirectionally, thus opening up an avenue for constructing textile TENGs with a novel 3D structure, which could effectively boost their output power for on-body biomechanical energy harvesting.

2.1.3. 3D Printing. As an emerging manufacturing technique, 3D printing has revolutionized how people design and fabricate objects.[371−375] Wide applications of 3D printing range across both academia and industry such as manufacturing smart robotics,[376] flexible electronics,[377] innovative composites,[378] and life-like organs.[379] Because of the ability to rapidly print complex objects with fully tailored designs, utilizing 3D printing to develop textile TENGs with advanced geometries and novel materials for optimized energy efficiency has attracted tremendous research interests.

For example, Wang et al.[368] first explored this potential by fabricating an ultraflexible 3D TENG consisting of composite resin materials as electrification layers and ionic hydrogel electrodes via hybrid 3D printing technology (Figure 4c). On the basis of a single-electrode working mode, the novel 3D structure endowed the TENG with ultraflexibility and enough space in the normal direction for accommodating the deformation. An enhanced output power density of up to 10.98 W/m^3 was delivered when the 3D TENG was applied to harvest biomechanical energy from human motions.

Furthermore, the method to directly print fiber-shaped TENGs onto textiles for harvesting biomechanical energy was proved by Zhang et al.[369] The 3D printer equipped with a multiaxial spinneret constructed coaxial fiber-shaped TENGs, which consisted of a CNTs core and silk fibroin sheath, onto a conventional textile (Figure 4d). With the vertical contact-separation working mode, the one-step fabricated textile TENG could reach an output power density of up to 18 mW/m^2 by harvesting biomechanical energy at a displacement speed of 10 cm/s (Figure 4e).

Overall, 3D printing technology paves an innovative way for rapidly producing fully tailored textile TENGs for biomechanical energy harvesting. However, many challenges still exist in this field. For example, the available materials for 3D printing are still limited, thus constraining its applications in smart textile fabrication.[380] Meanwhile, the mechanical properties of the complete 3D printing textiles, such as tensile strength,[381] are weaker than their conventionally manufactured counterparts like woven or knitted textiles. Hence, totally unlocking the potential of 3D printing in smart textile manufacturing requires intensive research in the future.

2.1.4. Outlook on Textile TENGs. Since the first demonstration of TENGs in 2012,[265] the interdisciplinary research areas of textile TENGs have witnessed rapid development, and a summary of research progress of recent textile TENGs is illustrated in Table 1. However, several challenges that hinder their future applications must be addressed.

2.1.4.1. Packaging. Moisture and liquid contaminants are common in daily scenarios, which largely impair the power output of textile TENGs. Traditional methods to resolve this problem involve encapsulation with waterproof property,[339] which in turn eliminates permeability and adds weight. To enhance encapsulation without losing wearability, hydrophobic or oleophobic coating materials such as HCOENPs[334] could be a superior solution to ensure liquid repellency. Furthermore, it is also applicable to directly use commercial waterproof fabric (i.e., Gore-Tex) as sacrificial substrate to accommodate triboelectric materials. A systematic study of related hydrophobic materials and existing waterproof yarns or fabrics, along with in-depth understanding of involved fabrication techniques, is highly desirable for achieving long-term reliability.

2.1.4.2. Mechanical Durability. Interfacial bonding between fiber/fabric electrodes and active triboelectric materials is another obstacle to achieving long-term mechanical durability. For textile TENGs, much attention has been focused on flexibility and stretchability, which in turn put forward stringent requirements for component assemblies. In this case, conductive components need to be extremely close to triboelectric materials in order to collect transported electrons. Interfacial bonding is likely to break down, resulting from either brittle fiber/fabric electrodes or peel-off of triboelectric materials when they experience intense deformation. Hence, rational selection of conductive materials and corresponding interfacial designs should be thoroughly investigated to ensure that devices can withstand accompanying deformations throughout daily use.

2.1.4.3. Scalable Fabrication. Efficient weaving/knitting techniques are fundamental for realizing commercial manufacturing of textile TENGs. Given that textile TENGs incorporate multiple components and require hierarchal assembly, the existing hand-based, lab-scale, centimeter-length weaving methods offer limited potential for scalable manufacture, which casts a shadow on practical applications. There are two ways to address this issue. First, redesign the functional fiber in regard to its diameter and mechanical strength so as to meet the standards of the well-developed modern textile industry. In this case, machine-based weaving/knitting methods such as modern looms could be used to facilitate the fabrication process. Second, specialized weaving/knitting equipment is efficient in dealing with peculiar TENGs system. For example, in terms of textile TENGs with coaxial-yarn intersection, a roller-guided assembly line demonstrated impressive efficiency in scalable manufacture.[352] However, to the best of our knowledge, few research efforts have been put forth for using specialized weaving/knitting methods to enhance the fabrication efficiency.

2.1.4.4. Structure Design. Textile TENG fabrication methods are categorized into layer stacking, yarn intersection, and 3D printing. Generally speaking, 3D textile TENGs exhibited the largest amount of areal power density. This is because 3D structure increased separation distance for electricity generation. Nonetheless, it does not mean future development should merely focus on increasing structural dimensions to achieve greater power output. On one hand, other determinants such as rational selections of triboelectric material usage, structure sensitivity to tiny deformations, etc., all contribute to the final outcome. On the other hand, the structural designs of textile TENGs are highly application-oriented. For example, light weight and air permeability are more desirable when textile TENGs are deployed around human joints such as the wrist or elbow.[359] In this case, a 2D-structured textile TENG with apparent simplicity is more suitable than a 3D one.

Accordingly, a layer stacking structure is not necessarily bulky compared to plain woven 2D textile TENGs. For

https://dx.doi.org/10.1021/acs.chemrev.9b00821
Chem. Rev. 2020, 120, 3668−3720

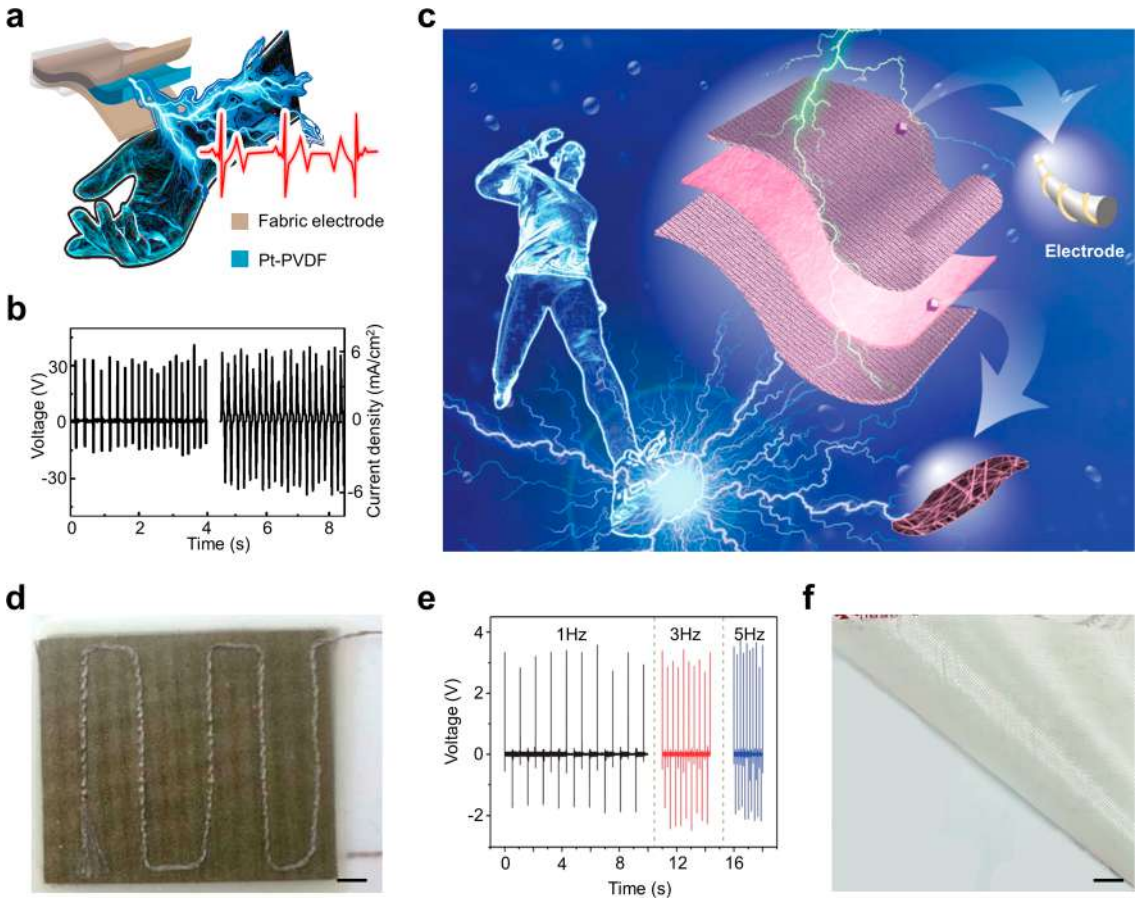

Figure 5. Textile PENGs based on layer stacking for biomechanical energy harvesting. (a) Schematic illustration of an all-fiber textile PENG. (b) Electrical output of the all-fiber textile PENG under iterative stress. Reproduced with permission from ref 434. Copyright 2018 Elsevier. (c) Schematic illustration of a layer-stacked textile PENG based on a nonwoven piezoelectric fabric. (d) Photograph of the as-prepared layer-stacked textile PENG. Scale bar, 1 cm. (e) The output voltage of the layer-stacked textile PENG under a periodic force. Reproduced with permission from ref 435. Copyright 2013 Royal Society of Chemistry. (f) Photograph of a PZT-Glass fiber fabric composite. Scale bar, 1 cm. Adapted with permission from ref 436. Copyright 2019 Elsevier.

instance, when two dielectric layers are separately placed around the human body in order to harvest energy from humans while walking, the reserved spacers between two dielectric layers are enlarged to the existing gap distance, such as the distance between the elbow and bilateral chest, resulting in no actual thickness accumulation in the stacked direction.[337] In this case, the original drawback of a layer stacking structure is effectively avoided in actual on-body applications. In conclusion, the diverse structures of textile TENGs are complementary. In-depth understanding of the associated structure designs of each category and keen insights into corresponding applicable scenarios are crucial in dealing with textile TENG systems.

2.2. Textile PENGs

To harvest biomechanical energy, the piezoelectric effect is another feasible working mechanism that could be integrated with textiles for on-body electricity generation. In certain types of materials, inner positive and negative charge centers are shifted in response to applied mechanical stress, inducing an internal electrical field.[382−384] In this process, mechanical motions are converted into electricity.[385−390] Since the first discovery of the direct piezoelectric effect in 1880,[391] there has been an abundance of piezoelectric materials reported, including organics, e.g., PVDF, vinylidene fluoride-*co*-trifluoroethylene (PVDF-TrFE), and inorganics, e.g., ZnO, lead zirconate titanate (PZT), and barium titanate ($BaTiO_3$). Human beings have utilized these piezoelectric materials to convert mechanical motions into electricity for a long time;[392−394] it was Wang in 2006 that first used ZnO nanowires to develop a piezoelectric nanogenerator (PENG) for electricity generation from tiny ambient mechanical motions.[395] Since then, PENGs have demonstrated tremendous potential for harvesting ambient mechanical energy[396−408] and working as self-powered active sensors.[409−420] With features of a unique working principle, ease of implementation, and simple structural design, merging PENGs with textiles has become a compelling approach to realizing a comfortable, flexible, convenient, and sustainable energy solution for on-body electronics. According to device configurations and fabrication processes, to realize a textile PENG, two approaches are usually adopted: layer stacking and yarn intersection, as introduced one by one in the following sections.

2.2.1. Layer Stacking. Layer stacking of functional textiles could be a simple approach to realizing a textile PENG because a typical PENG contains three layers: a piezoelectric material layer sandwiched by two layers of electrodes.[421−423] The thin electrode textiles can effectively transfer external mechanical forces to deform the piezoelectric layer and induce a flow of electrons in response to biomechanical motions.

https://dx.doi.org/10.1021/acs.chemrev.9b00821
Chem. Rev. 2020, 120, 3668−3720

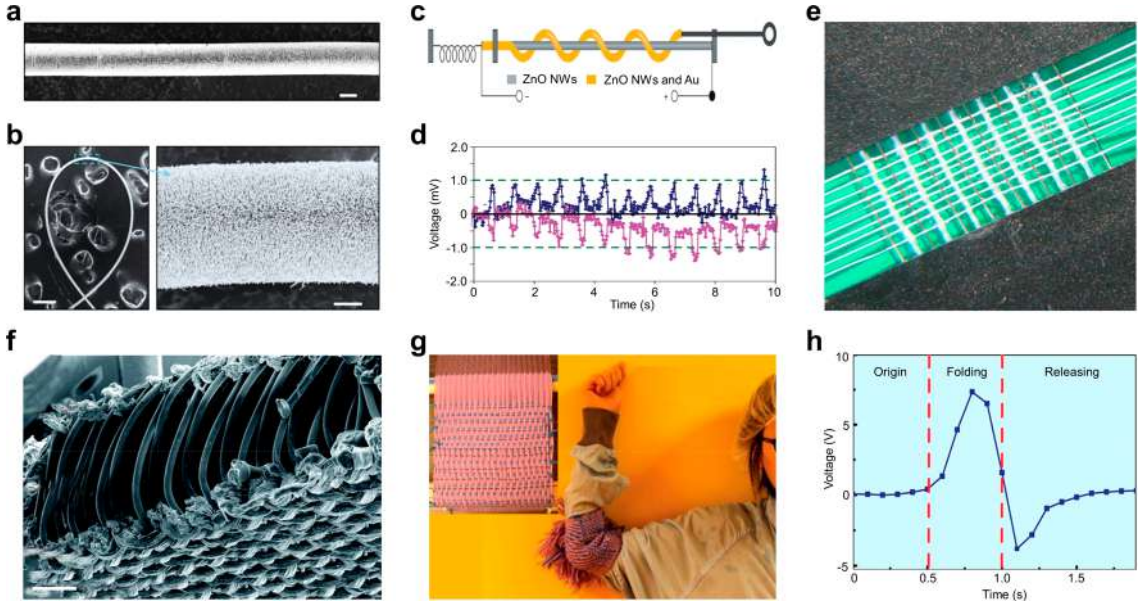

Figure 6. Textile PENGs based on yarn intersection for biomechanical energy harvesting. (a) A SEM image of radially growing ZnO nanowires on the fibers. Scale bar, 20 μm. (b) A SEM image of bending the composite piezoelectric fiber (left), scale bar, 200 μm, and an enlarged view showing the distribution of the ZnO nanowires (right), scale bar, 10 μm. (c) Schematic illustration of the fabrication process of a fiber-based PENG. (d) The open-circuit voltage of the fiber-based PENG under an external pulling force. Reproduced with permission from ref 439. Copyright 2008 Nature Publishing Group. (e) Photograph of a 2D textile PENG by intersecting three kinds of yarns. Reproduced with permission from ref 444. Copyright 2015 Elsevier. (f) A cross-sectional SEM image of a 3D spacer textile PENG. Scale bar, 1 mm. Reproduced with permission from ref 445. Copyright 2014 Royal Society of Chemistry. (g) Photograph of a textile PENG mixed weaving with cotton to form an energy elbow pad. (h) The open-circuit voltage of the textile PENG under 90° arm bend-release actions. Reproduced with permission from ref 446. Copyright 2017 American Chemical Society.

For example, Kim et al. developed a layer-stacked textile PENG comprised of vertically grown ZnO nanowires (NWs) between two Au-coated textile electrodes.[424] To enhance the piezoelectricity, an insulating film was also stacked into the multilayer structure to take advantage of electrostatic effects. Applying a 100 dB sound wave onto the textile PENG with a size of 10 cm^2 induced a flow of electrons in the ZnO NWs layer and generated an V_{oc} of up to 8 V and a I_{sc} of up to 2.5 mA, which was able to light up a green organic LED. Similarly, Willander et al. developed a textile PENG by vertically growing ZnO nanorods[425−428] and nanoflowers[429] onto an Ag-coated textile electrode. With a size of 2 μm by 2 μm, the textile PENG generated a voltage output of 9.5 mV during consecutive bending.[425]

The previously mentioned textile PENGs were constructed by vertically growing aligned piezoelectric materials onto textile electrodes.[430] This configuration might weaken the mechanical robustness of the textile PENGs, especially when subjected to the continuous stretching and twisting on the human body.[249] Developing textile PENGs in which the piezoelectric materials flatly lie on the textile electrode could address this challenge.[431−433]

For example, Mandal et al. designed a textile PENG with a piezoelectric layer consisting of horizontally aligned Pt-PVDF nanofibers sandwiched between top−bottom Cu-Ni-plated fabric electrodes (Figure 5a).[434] This multilayer textile PENG demonstrated long-term durability under a mechanical bending test of up to 90 000 cycles. Meanwhile, by impacting an iterative stress on this textile PENG, a piezoelectric potential was induced vertically to the Pt-PVDF nanofibers that delivered an output power density of up to 22 $\mu W/cm^2$ (Figure 5b), which was capable of driving a digital calculator. Decent mechanical robustness and electric output were mainly attributed to the composite structure with laterally aligned piezoelectric nanofiber arrays.

In addition to textile PENGs with well-aligned piezoelectric nanowires, the nonwoven active textile layer with randomly and chaotically oriented piezoelectric fibers could also convert biomechanical energy into electrical energy.[437] Tao et al. demonstrated a layer-stacked textile PENG based on a nonwoven piezoelectric fabric comprised of lateral PVDF-$NaNbO_3$ nanofibers that were randomly aligned with each other (Figure 5c).[435] After sandwiching the piezoelectric fabric between two knitted fabric electrodes, the as-prepared textile PENG was flexible and lightweight due to the all-fiber layer stacking structure, thus ensuring exceptional wearing comfort (Figure 5d). Under periodic impact force, the textile PENG with a size of 2.5 by 2.5 by 0.2 cm^3 generated an V_{oc} and a I_{sc} of up to 3.2 V and 4.2 μA, respectively (Figure 5e). Similarly, a piezoelectric membrane was fabricated by hydrothermally growing ZnO nanorods on randomly orientated PVDF nanofibers.[438] The composite piezoelectric layer was then sandwiched between two soft fabric electrodes to form a layer-stacked textile PENG. This soft textile PENG with an effective area of 15 cm^2 produced a high output voltage of up to 6.36 V in response to a 0.10 MPa pressure.

More recently, Guo et al. developed an innovative textile PENG based on a large-scale and superflexible PZT thin film.[436] Although PZT has demonstrated a considerable piezoelectric effect, its brittle and rigid structure has limited further application on the human body. This work utilized a simple dipping method to grow a PZT thin film on a commercial glass fiber fabric (PZT-GFF) (Figure 5f), which was quite flexible and soft for on-body generators. Stacking the

https://dx.doi.org/10.1021/acs.chemrev.9b00821
Chem. Rev. 2020, 120, 3668−3720

Table 2. Materials and Energy Performance of Representative Textile PENGs

piezoelectric materials	electrodes	performance	year	ref
Layer Stacking				
PZT	Ag	200 μw/cm^3, 6 V, 45 nA	2012	431
ZnO	Au coated textile	8 V, 25 μA (10 cm^2)	2012	424
ZnO	Ag coated textile	9.5 mV (2 × 2 μm^2)	2012	425
PVDF/$NaNbO_3$	Ag coated fabric	3.2 V, 4.2 μA (2.5 × 2.5 × 0.2 cm^3)	2013	435
PVDF	Cu foil	577.6 pW/cm^2	2013	432
PZT/Ag/polymer	Ag polymer ink	34 J/m^3	2017	422
ZnO/PVDF	Ag conductive fabric	6.36 V, 0.17 μA (15 cm^2)	2018	438
PVDF	PEDOT	48 V, 6 μA	2018	421
Pt/PVDF	Cu−Ni plated fabrics	30 V, 6 mA/cm^2, 22 μW/cm^2	2018	434
PZT	Carbon film	110 V, 1.05 μA (8 × 8 cm^2)	2019	436
ZnO	Ag coated fabric	4 V, 20 nA (2 × 1.5 cm^2)	2019	430
Yarn Intersection				
ZnO/Pd covered ZnO	Cu wires	3 mV, 17 pA	2013	442
PVDF	Ag-coated fiber	5.10 μW/cm^2, 14 V, 29.8 μA	2014	445
$BaTiO_3$	Cu wire	1.9 V, 24 nA	2015	444
PVDF-TrFE	Ag coated nylon, CNT sheet	50 μW/cm^3, 2.6 V, 15 nA	2015	460
PVDF	Ni/Cu alloy	51 V, 850 μW	2015	462
PVDF	Ni/Cu alloy	42.5 V, 125 μW/cm^2	2015	461
PVDF	PEDOT	1 V, 0.15 mA	2017	457
$BaTiO_3$/PZT/CNT/PVDF	carbon filled polyethylene	6V, 4 nA, 4 yarns (20 cm)	2017	446
PVDF-TrFE	conductive thread	16.2 mV	2017	443
PVDF	Cu wire	2.3 V, 10.5 μJ/m^2	2018	447
PVDF	Ag coated nylon yarn	0.38 V, 29.62 μW/cm^3	2019	463

PZT-GFF layer with top and bottom carbon-based electrodes, a textile PENG with a size of 8 cm by 8 cm was manufactured and produced a substantial current of 1.05 μA with a voltage of up to 110 V under human hand pressing and releasing cycles, which was able to light 20 LEDs. In a word, layer stacking is a straightforward method to manufacture textile PENGs for biomechanical energy harvesting.

2.2.2. Yarn Intersection. Although layer stacking provides an effective and straightforward approach to constructing textile PENGs, the multilayer structure might add thickness, thus curbing wearability and breathability. These drawbacks could be well addressed by developing a textile PENG via yarn intersection because the weaving or knitting of piezoelectric yarns can achieve a single-layer textile PENG, and the inner porous structure adds decent air permeability and wearable comfort.

As for textile PENGs based on yarn intersection, a single piezoelectric fiber is the building block, which is flexible and capable of being seamlessly integrated into a textile form. In Figure 6a, the first fiber-based PENG was presented by Wang et al. in 2008 via radially growing ZnO nanowires on fibers (Figure 6b).[439] Then the composite piezoelectric fiber was entangled by an Au-coated conductive fiber over the surface to form a fiber-based PENG (Figure 6c). By applying an external pulling force on the fiber-based PENG with an effective length of 4−5 mm, a V_{oc} of 1 mV and a I_{sc} of 5 nA were delivered (Figure 6d).

Since then, fiber-based PENGs have attracted substantial interest and demonstrated the possibility of harvesting biomechanical energy by stitching or sewing them into commercial textiles.[440,441] However, to promote the output power, weaving or knitting these single fibers together to form a textile PENG is highly desired. The same group further developed a 2D woven PENG by intersecting ZnO nanowires grown fibers and Pd-coated conductive wires as electrodes together.[442] The 2D woven PENG consisting of 20 intersection yarns was able to harvest tiny mechanical energy even from airflow and delivered an output voltage and current of up to 3 mV and 17 pA, respectively. However, in this work, each yarn had to be intersected at a certain distance to avoid short-circuit, which resulted in a large porous structure and impaired the wearability of the textile PENG.

To reduce the risk of a short circuit and enhance the wearing comfort of these 2D textile PENGs, introducing conventional fibers like cotton or silk during the weaving or knitting process could be a promising choice.[443] For example, Xue et al. designed a 2D textile PENG by intersecting three kinds of yarns.[444] In this work, first, the hybrid piezoelectric fiber was made of aligned $BaTiO_3$ nanowires to enhance energy efficiency and polyvinyl chloride to improve flexibility. Second, metal copper wires worked as electrodes. Finally, conventional insulating cotton yarns served as spacers to avoid a short circuit as well as provided wearers with comfortable tactile sensations (Figure 6e). Mounting this woven textile PENG onto an elbow pad, an output voltage, current, and power of up to 1.9 V, 24 nA, and 10.02 nW, respectively, were delivered while undertaking 90° folding−release cycles of the human arm.

To optimize the output power of the textile PENGs, weaving or knitting the piezoelectric yarns along a third direction, namely, the thickness direction, to fabricate a 3D textile PENG could be an effective approach because the thickness of the 3D textile PENG could increase maximum displacement and even stress distribution.[447] For example, in 2014, Soin et al. developed an all textile PENG using three-dimensional yarn knitting technology.[445] In this work, Ag-coated conductive yarns, polyester insulating yarns, and highly oriented β-phase (~80%) PVDF yarns were knitted together to fabricate a novel 3D spacer textile PENG (Figure 6f). Undertaking an impact pressure of 0.106 MPa, the as-fabricated 3D textile PENG demonstrated an enhanced output power density, V_{oc}, and I_{sc}

https://dx.doi.org/10.1021/acs.chemrev.9b00821
Chem. Rev. 2020, 120, 3668−3720

of up to 5.10 $\mu W/cm^2$, 14 V, and 29.8 μA, respectively. This output performance was higher than that of the previously reported 2D woven and nonwoven textile PENGs. This is attributed to the uniformly distributed stress among the PVDF yarns and the tight connection of electrodes in this novel 3D structure.

Nevertheless, interlacing piezoelectric yarns and electrode yarns might reduce their contact area, thus increasing junction resistances and impairing charge flowing in textile PENGs. In that case, using the all-in-one design of fiber-shaped PENGs as building blocks for constructing textile PENGs via weaving or knitting could be another suitable configuration.[448−460] For example, Song et al. coated Ni/Cu alloy electrodes onto both sides of a PVDF thin film to obtain a strap-shaped PENG.[461,462] Then these strap PENGs were woven with conventional yarns to form a large-scale and wearable textile PENG, which generated a maximum output power density of 125 $\mu W/cm^2$ with stretch motions.

In addition, Skorobogatiy et al. fabricated spiral yarn-shaped PENGs via fiber drawing technology to further enlarge the contact area between the electrodes and piezoelectric materials.[446] In this work, the spiral yarn-shaped PENG consisted of a soft hollow polycarbonate core wrapped by alternating PVDF-based piezoelectric active layers and electrode layers, which could easily achieve a length magnitude of kilometers and a diameter magnitude of submillimeter. Because of the compelling features of yarn PENGs such as flexibility, light weight, robustness, mass production, and a small diameter, these yarn PENGs were mixedly woven with cotton into a textile elbow pad by using a commercial Dobby loom (Figure 6g). Under a series of 90° arm bend−release actions, the textile PENG delivered a voltage of up to 10 V and current of up to 15 nA (Figure 6h). This high output performance came from the tight and enlarged contact area between the PVDF composites and electrodes in this novel spiral structure.

More recently, Spinks et al. developed a woven textile PENG based on triaxial braided yarns with extreme durability, which demonstrated appreciable potential for applications in practical clothes.[463] The novel triaxial braided yarn-shaped PENG was fabricated by braiding Ag coated nylon (inner and outer electrodes) and PVDF fibers (intermediate piezoelectric layer) in a commercial braiding machine. Then these as-prepared yarn-shaped PENGs were woven into a textile form, which could yield an output voltage and power of up to 380 mV and 0.8 μW, respectively, under an external pressure of 0.023 MPa.

Overall, yarn intersection has attracted substantial interest in building textile PENGs with improved flexibility, breathability, and wearability. However, insufficient power output and complex yarn fabrication are still the main barriers that require intensive research efforts in the future.

2.2.3. Outlook on Textile PENGs. We have witnessed rapid progress in textile PENGs for biomechanical energy harvesting, and a summary of the research progress of recent textile PENGs is illustrated in Table 2. However, there is still a considerable gap between present textile PENGs and expected real applications on the human body, which requires continuous research input.

2.2.3.1. Energy Efficiency. Although integrating PENGs with textiles has remarkably expanded on-body applications, it has a negative effect on energy efficiency, which is the most significant metric for evaluating textile PENGs. Promising solutions in material innovations, device configurations, and working modes are proposed to address the challenges in the community, as follows.

First, developing materials that exhibit the desired piezoelectric effect could completely revolutionize energy efficiency of textile PENGs.[399,464] Because the piezoelectric coefficients of piezoelectric materials are dictated by their intrinsic crystal structure, creatively designing the piezoelectric architecture might be attainable to enhance their piezoelectric performance, thus boosting energy efficiency of textile PENGs.[465] For example, introducing numerous air voids into the polypropylene could effectively optimize the piezoelectric architecture. These air voids could generate charges with opposite polarity on their two internal sides to form giant dipoles, which could yield a remarkably high piezoelectric performance.[466,467] Meanwhile, appropriate chemical doping such as embedding ceramic nanoparticles, nanofibers, and nano thin films into a polymer matrix like PVDF could enhance its piezoelectric performance, thus promoting higher energy efficiency of textile PENGs.[468]

Second, designing the shape of piezoelectric materials in textile PENGs could also contribute to high energy efficiency. For example, trapezoidal piezoelectric wires on textile or fiber substrates might distribute external stress more uniformly than the commonly used cylinder shape, thus accommodating larger deformation and resulting in enhanced energy efficiency.[469]

Furthermore, electrode designs could also optimize energy efficiency of textile PENGs. Scientists have claimed that utilizing electrodes partially covering piezoelectric layers might mitigate the redistribution of electrons induced by stress, thus boosting output voltages.[470−472] In that case, twisting external fiber electrodes onto piezoelectric fibers or utilizing segment electrodes in multilayer textile PENGs might be promising methods for promoting biomechanical energy efficiency.

In addition, it is worth mentioning that the mainstream operating modes of textile PENGs are the d_{31} mode and d_{33} mode, which refer to the direction of the induced electric field perpendicular or parallel with external stress.[222] Nevertheless, the d_{15} working mode, in which the induced electric field is simultaneously vertical to the polarization and external stress,[473] is exiguous in textile PENGs due to its complicated device structure. Because the d_{15} mode is more efficient than the two previous modes, especially in response to shear/torsion stress,[150,474,475] simplifying device structures and merging them with textiles is a potential approach to enhance energy efficiency of textile PENGs in response to shear and torsion motions on the human body.

2.2.3.2. Materials and Fabrication. Many popular piezoelectric materials such as PZT still depend on complicated manufacturing processes, including hours of lattice growth, a high temperature sintering process (~1200 °C), and high voltage polarization (~2 kV/mm).[476] Meanwhile, the thermal stability of textiles is an obstacle for efficient fabrication of piezoelectric materials in textile PENGs. In this light, applying emerging 3D printing technology to directly print one-step fabricated piezoelectric materials onto textile substrates or into the fiber shape may be a highly promising method,[477] especially for efficient fabrication of textile PENGs.

In addition, abundant natural materials, such as fish scales[478] and spider silk,[479] have been determined to have distinctive piezoelectric coefficients. Applying these easily obtainable natural biomaterials to construct textile PENGs could easily achieve a biocompatible, biodegradable, and cost-effective approach to harvesting on-body mechanical energy.

https://dx.doi.org/10.1021/acs.chemrev.9b00821
Chem. Rev. 2020, 120, 3668−3720

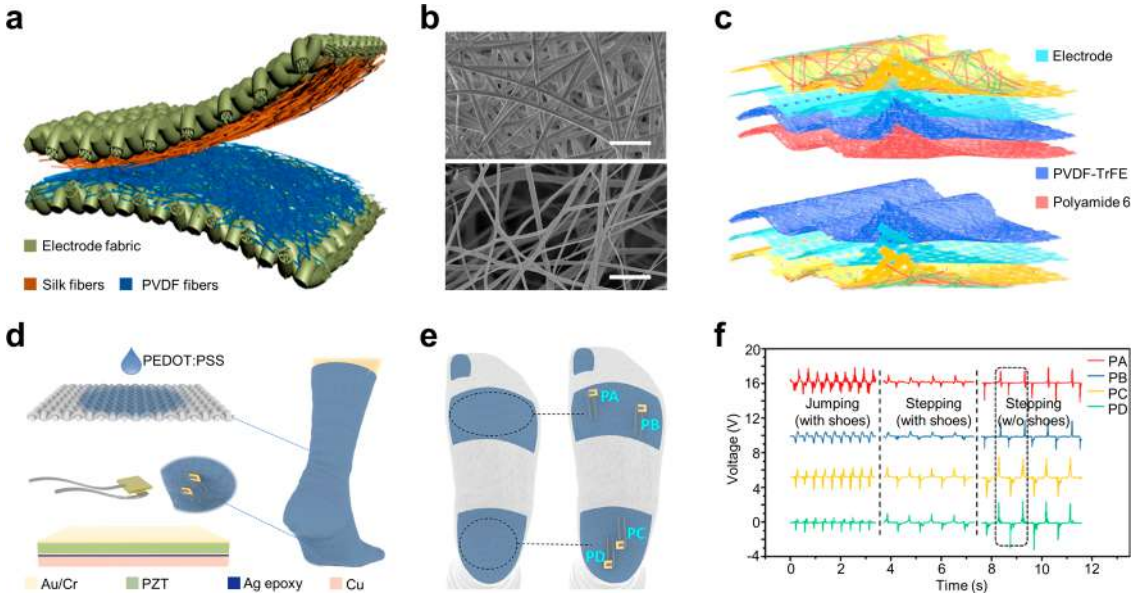

Figure 7. Textile TPENGs for biomechanical energy harvesting. (a) Schematic illustration of an all-fiber textile TPENG. (b) SEM images of silk nanofibers (top) and PVDF nanofibers (bottom). Scale bar, 3 μm. Reproduced with permission from ref 490. Copyright 2018 Elsevier. (c) Schematic illustration of the e-textile based on the triboelectric–ferroelectric synergistic effect. Reproduced with permission from ref 489. Copyright 2019 Nature Publishing Group under Creative Commons Attribution 4.0 (http://creativecommons.org/licenses/by/4.0/). (d) Schematic illustration of a cotton sock using the piezoelectric and triboelectric hybrid mechanism. (e) Embedded PZT force sensors labeled as "PA", "PB", "PC", and "PD". (f) Voltage signals of the textile TPENG under various conditions. Reproduced with permission from ref 493. Copyright 2019 Wiley and American Chemical Society.

2.2.3.3. Beyond Body Motions. There are abundant mechanical energy sources available for on-body electricity generation in the environment, ranging from human motions to the wind,[480] water flow,[481] and rain droplets.[482] Developing both textile TENGs and PENGs with reliable and resistant encapsulation to simultaneously harvest mechanical energy from the human body and its surroundings may be an attractive research direction.

2.3. Textile TPENGs

Both textile TENGs and textile PENGs are capable of converting biomechanical motions into electricity. Because body motions can concurrently cause mechanical friction and deformation in textile nanogenerators, combining textile TENGs and PENGs to form textile triboelectric–piezoelectric nanogenerators (TPENGs) could take full advantage of the features of body biomechanical motions for optimized energy efficiency.[483−487] For effective combination, a natural configuration would be sandwiching triboelectric and piezoelectric layers between two electrodes.[488,489] For example, Guo et al. developed a textile TPENG based on two conductive fabrics that were electrospun with silk and PVDF nanofibers (Figure 7a).[490] These two modified fabrics served as top and bottom electrodes as well as a triboelectric pair (Figure 7b). Meanwhile, the PVDF nonwoven fabric also worked as the piezoelectric-enhanced layer for boosting electric output. Then attaching these two functional fabric layers on different parts of clothes achieved a vertical contact-separation working mode of the TENG component. By applying a hand tapping of 27.5 N with a frequency of 2 Hz on the textile TPENG, the triboelectric potential between the silk and PVDF drove electrons to flow through the external load and a pressure-induced piezoelectric potential was simultaneously established in the PVDF nanofibers. With the piezoelectric-enhanced triboelectric effect, the textile TPENG achieved a maximum output power density of 0.31 mW/cm^2, which exhibited a better energy performance than the individual textile TENG and textile PENG components. Because of strengthened output power and capability of being easily merged with real clothes, this textile TPENG exhibits great potential for harvesting biomechanical energy on the human body. Similarly, Wang et al. presented an e-textile by stacking PVDF-TrFE nonwoven fabrics and a layer of polyamide 6 (Figure 7c).[489] With the triboelectric–ferroelectric synergistic effect, the e-textile generated an enhanced output power density of 5.2 W/m^2 by harvesting biomechanical energy from low frequency motions.

Another textile TPENG configuration was demonstrated by introducing a shared electrode or an insulation layer to separate the triboelectric and piezoelectric components, which facilitated their cooperation with the assistance of external power management circuits.[491] For example, Tao et al. developed a cascaded textile TPENG for effectively harvesting biomechanical energy by layer stacking triboelectric and piezoelectric textiles.[492] First, PVDF/CNT/$BaTiO_3$-based nonwoven fabric, which worked as a piezoelectric layer, was sandwiched between two conductive electrode textiles. Meanwhile, the top electrode also served as the contact surface and was stacked with a PDMS/MWCNT/graphite-based triboelectric layer. Finally, another conductive fabric was stacked onto the top of the triboelectric layer. Under a 3.3 Hz periodic force of 580 N, the vertically aligned textile TPENG achieved an output power density of up to 2.22 W/m^2, which was sufficient to light up 150 LEDs.

More recently, a smart cotton sock dependent on the triboelectric-piezoelectric effect was demonstrated by Lee et al.[493] In this configuration, an as-prepared PZT chip was inserted into the poly(3,4-ethylenedioxythiophene) polystyrene sulfonate (PEDOT:PSS)-coated triboelectric sock (Figure

https://dx.doi.org/10.1021/acs.chemrev.9b00821
Chem. Rev. 2020, 120, 3668−3720

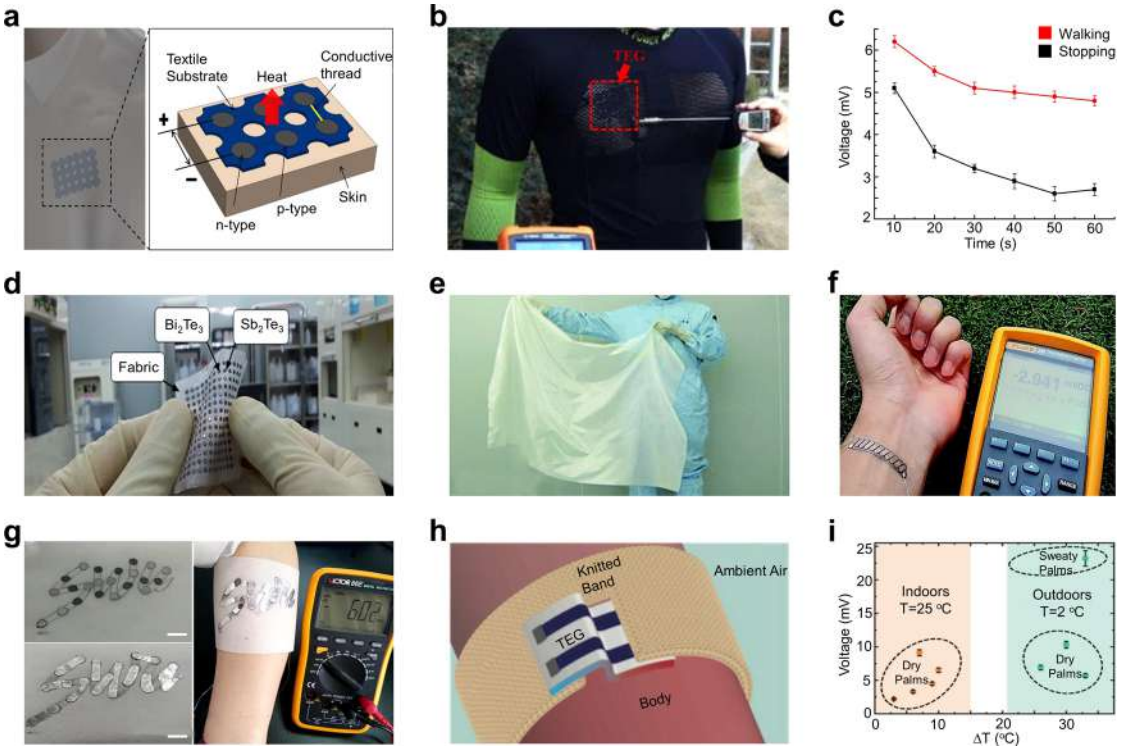

Figure 8. TEGs using textiles as substrates for body heat energy harvesting. (a) Schematic illustration of a textile TEG with large holes. (b) Photographs of the shirt embedded with the textile TEG for powering on-body electronics. (c) The output voltage of the textile TEG at an ambient temperature of 25 °C. Reproduced with permission from ref 528. Copyright 2014 IOP Publishing Ltd. (d) Photograph of a textile TEG consisting of Bi_2Te_3 and Sb_2Te_3 legs on a glass fabric. (e) Photograph of the large-scale glass fabric with decent flexibility and softness. (f) Photograph of the textile TEG generating electricity from body heat at an air temperature of 15 °C. Reproduced with permission from ref 531. Copyright 2014 Royal Society of Chemistry. (g) Photograph of a silk-based TEG and harvesting thermal energy from the human body. Scale bar, 1 cm. Reproduced with permission from ref 532. Copyright 2016 Elsevier. (h) Schematic illustration of a textile TEG in a Z type mounted on the human body. (i) Dependence of the output voltage of the textile TEG on different wearing sites, and it delivered an output voltage up to 10 mV at a room temperature of 25 °C. Reproduced with permission from ref 533. Copyright 2019 Wiley-VCH.

7d), and then a PTFE film and an aluminum electrode were attached onto the inner surface of the shoes to construct a textile TPENG in a vertical contact-separation mode. When a tester in this smart cotton sock was jumping or stepping at a frequency of 2 Hz (Figure 7e), this textile TPENG could deliver a triboelectric power density of up to 11 $\mu W/cm^2$ and a piezoelectric power density of up to 128 $\mu W/cm^2$ (Figure 7f).

Overall, textile TPENGs can take full advantage of biomechanical motions with enhanced energy efficiency. However, the sophisticated configurations of textile TPENGs require a complex fabrication process and external power management circuits to effectively produce an electric output. In addition, the stacked triboelectric and piezoelectric layers might further obstruct the wearability of textile nanogenerators. In that case, designing an all-in-one fiber-shape TPENG with the coupling of the triboelectric and piezoelectric effects and then weaving or knitting them into a textile could be an innovative approach to optimize wearability. Furthermore, a mixed weaving or knitting of individual triboelectric yarns and piezoelectric yarns could also resolve this dilemma.

3. BODY HEAT ENERGY HARVESTING

Compared to intermittent biomechanical energy that requires body motions, another energy source, body heat, constantly exists on the human body even in stationary scenarios, which originates from metabolic byproducts and has become an available energy source for continuous electricity generation over the past decades.[494,495] The released body heat of an adult can reach up to approximately 100−525 W.[496−498] Using smart textiles to harvest energy from body heat could be a promising approach to powering on-body electronics. Two working mechanisms can be employed to harvest body heat energy, including the pyroelectric effect by using temperature differences over time[499−503] and the thermoelectric effect by using temperature differences over space.[504−513] Because the human body surface temperature shows little variation over time and stays around 33.5 °C,[514] the pyroelectric effect is less efficient to harvest body heat energy. On the other hand, the spatial temperature difference between an adult and its surroundings can continuously produce heat flow of up to 10 mW/cm^2,[515] and thus the thermoelectric effect shows its talent here. When a thermoelectric generator (TEG) is attached to human skin, induced by the spatial temperature gradient, charge carriers in thermoelectric materials diffuse from the hot side (skin) to the cold side (ambient environment) to generate electricity.[516] As for the thermoelectric materials, the thermoelectric figure of merit, the ZT value, is a standard to evaluate their quality.[517−519] The ZT value is derived from three fundamental physical properties, including electrical conductivity σ, thermal conductivity κ, and Seebeck coefficient S, with a governing equation $ZT = (\sigma S^2)T/\kappa$.

Recently, because of advanced device designs and high-quality thermoelectric materials, merging TEGs with textiles for body heat energy harvesting has become a tantalizing

https://dx.doi.org/10.1021/acs.chemrev.9b00821
Chem. Rev. 2020, 120, 3668−3720

option for wearable electricity generation. Textile TEGs have been endowed with high electric output,[520,521] stability,[522] flexibility,[523,524] and light weight.[525] Fabricating textile TEGs generally relies on two configurations, namely textiles as substrates and yarns as building blocks, as introduced respectively in the following sections. At the end, the critical challenges in textile TEGs are discussed, and future research efforts to address these concerns are suggested.

3.1. Textiles as Substrates

Building TEGs on textile substrates is an effective approach to harvesting body heat energy. The textile materials can not only show good conformability to enable effective contact with curved skin for heat absorption but also hold low thermal conductivity,[526] e.g., cotton fabric ~0.0633 W/(m·K), to reduce heat loss.[527] By using textiles as a substrate, a series of thermoelectric (TE) materials, known as TE legs, can be either vertically or parallelly coated/printed/sewed onto the textile substrates.

3.1.1. Vertical Alignment. A spatial temperature gradient can be created and well-maintained from the bottom of TE legs at the skin side to the top of TE legs facing the ambient environment. Thus, via vertical alignment, TE legs can effectively convert body heat energy into electricity. For example, utilizing textile substrates with large holes for perpendicular penetration of TE legs is a feasible method for constructing textile TEGs.[528,529] As in Figure 8a, TE legs consisting of $Bi_{0.5}Sb_{1.5}Te_3$ (p-type) and $Bi_2Se_{0.3}Te_{2.7}$ (n-type) were filled in the holes of a textile substrate by using dispenser printing.[528] Then conductive threads were sewn onto the textile substrate to connect 12 pairs of p-type and n-type TE legs together (Figure 8b). To test it, the textile TEG was worn by a tester with a body temperature of 32 °C. In a cold ambient environment of 5 °C, this textile TEG could deliver an output power density of up to 292.4 nW/cm^2 (Figure 8c).

However, dispenser printing is not favorable when it comes to mass production. On the other hand, screen printing, which is capable of fabricating TE legs onto the textile substrate vertically, is an effective method for realizing large-scale fabrication of textile TEGs.[530] For example, Kim et al. developed a textile TEG by screen printing Bi_2Te_3 (n-type) and Sb_2Te_3 (p-type) pastes onto a glass fabric (Figure 8d),[531] which not only endowed the TE layer with decent flexibility and softness for wearing (Figure 8e) but also served as a thermal blocker to reduce body heat loss. Then the TE active layer was combined with two Cu-based plates by using conductive Ag paste. This as-prepared textile TEG consisting of 11 TE leg couples was attached to the human wrist. Each TE leg had a diameter of 12.7 mm and a thickness of 0.5 mm. This textile TEG generated an output power and voltage of up to 3 μW and 2.9 mV, respectively, at an ambient temperature of 15 °C (Figure 8f).

Similarly, Lu et al. demonstrated a textile TEG by depositing Bi_2Te_3 and Sb_2Te_3 columns onto both sides of a silk substrate.[532] Then 12 couples of these p-type and n-type TE legs with a diameter of 4 mm and a thickness of 0.30 mm were connected by conductive silver foils (Figure 8g). The formed textile TEG could harvest thermal energy at a temperature difference ranging from 5 to 35 °C with a maximum voltage and power of up to 10 mV and 15 nW, respectively. A voltage of up to 3 mV was realized when a tester wore the textile TEG on the arm while walking. In addition, this textile TEG was still stable after enduring 100 cycles of bending and twisting.

3.1.2. Parallel Alignment. TE legs can also be oriented along the in-plane direction of a textile substrate. Compared to the previous design, parallelly aligned TE legs endow the textile TEG with a thinner and more flexible design.[534−539] For example, Lin et al. demonstrated a textile TEG by mounting PEDOT:PSS-coated fabric strips along a cotton substrate.[540,541] Then opposite ends of these TE legs were consecutively connected by using Ag paint and constantan wire. The as-prepared textile TEG consisted of five TE legs, each having a size of 35 mm by 5 mm. With a temperature difference of 74.3 °C in the textile in-plane direction, an output voltage of 18.7 mV and a power of up to 212.6 nW were consistently obtained even after continuous operating for 10 days.[541]

However, parallel alignment usually shows lower power output than that of textile TEGs with vertically aligned TE legs. This is because the temperature difference between the human body and its surrounding is normally distributed along the thickness direction of the textiles, rather than the in-plane direction.[542,543] To create a decent temperature difference in the parallel configuration, Andrew et al. reported a rationally designed textile TEG in a Z formation to ensure that half of the textile TEG was in contact with hot skin and the other half was exposed to the cold ambient environment (Figure 8h).[533] This structural design and heat-insulated textile substrate contributed together to effectively increase the temperature gradient along the textile in-plane direction. The as-fabricated textile TEG with two TE legs of 5 mm by 7 mm mounted on human skin generated an output voltage of up to 10 mV at a room temperature of 25 °C (Figure 8i).

In a word, TEGs built on textile substrates create a convenient, low cost, and effective option for harvesting body energy to power wearable electronics. However, a tradeoff has been widely recognized between device flexibility and spatial temperature gradient utilization. Further efforts in realizing larger temperature differences in thinner textile TEGs are highly desired.

3.2. Yarns as Building Blocks

TEGs based on textile substrates show a number of compelling features due to thermal insulation and relative conformity to human skin. However, this configuration requires coating/printing/sewing the TE legs onto textile substrates, which largely impairs the breathability of the smart textiles. Constructing TEG textiles by weaving or knitting with TE yarns as building blocks could be a superior strategy to address the above concern. In this configuration, the design of the yarn-shaped TE leg is an important determinant of the structure of a textile TEG.[544,545]

3.2.1. 1D Thermoelectric Yarns. To design a one-dimensional (1D) TE yarn, inorganic/organic TE materials could be coated onto various flexible fibers, including carbon fibers, glass fibers, cotton fibers, or directly spun into a yarn shape via spinning technology.[546−548] For example, in 2012, Wu et al. developed inorganic composite-based flexible yarns that were fabricated by uniformly coating PbTe nanocrystals onto glass fibers with a diameter of 10 μm. The coating thickness was precisely controlled at 300 nm.[549] These thermoelectric yarns demonstrated a relatively high Seebeck coefficient of 1201.7 μV/K at 27 °C, which resulted in a power factor of 0.41 W/(m·K^2). Organic thermoelectric materials, like polyurethane, multiwalled carbon nanotube (MWCNT), and PEDOT:PSS composite, were also coated onto a polyester

https://dx.doi.org/10.1021/acs.chemrev.9b00821
Chem. Rev. 2020, 120, 3668−3720

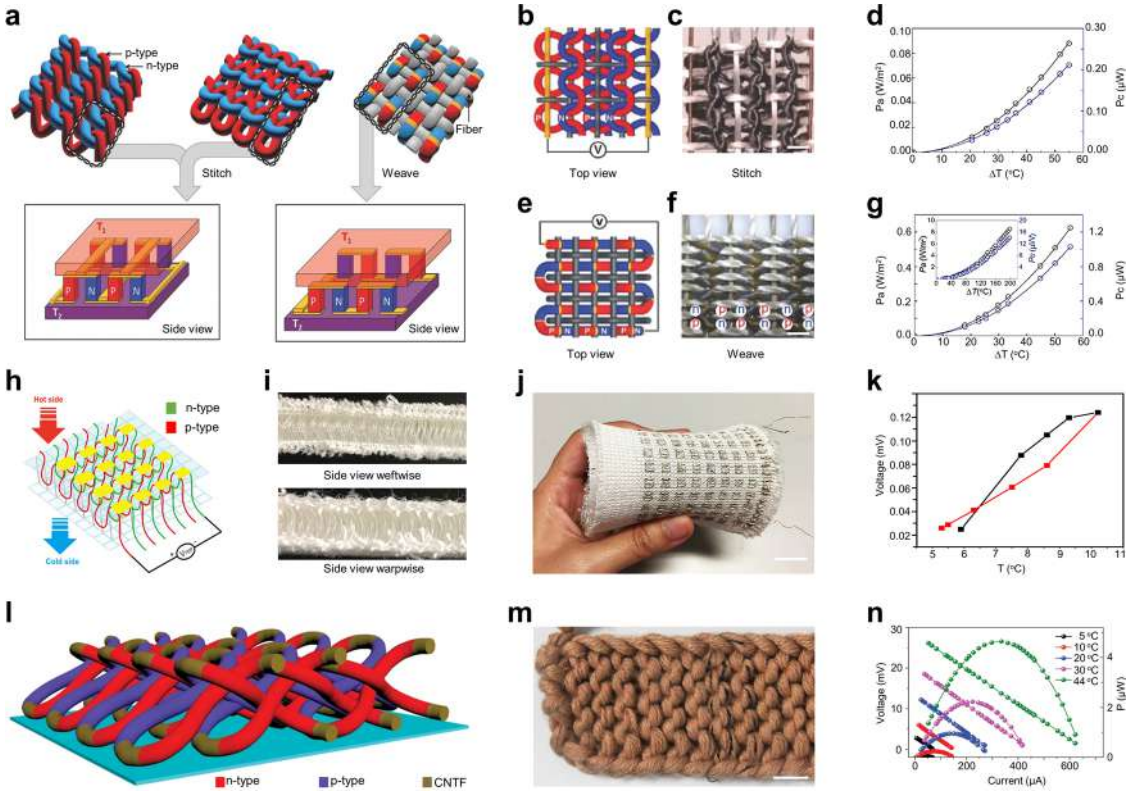

Figure 9. Yarn-constructed TEGs for body heat energy harvesting. (a) Schematic illustration of textile TEGs based on zigzag stitch, garter stitch, and plain weave. Schematic illustration (b), photograph (c), and output power (d) of the garter-stitch textile TEG. Schematic illustration (e), photograph (f), and output power (g) of the plain-woven textile TEG. All scale bars, 2 mm. Reproduced with permission from ref 551. Copyright 2016 Wiley-VCH. (h) Schematic illustration of a 3D textile TEG. (i) A side view of substrate and superstrate fabrics. (j) Photograph of the 3D textile TEG. Scale bar, 1 cm. (k) The on-body power generation of the 3D textile TEG with increased temperature difference (black line) and decreased temperature difference (red line). Reproduced with permission from ref 552. Copyright 2017 IOP Publishing Ltd. (l) Schematic illustration of the 3D textile TEG without substrate. (m) Photograph of the 3D textile TEG without substrate. Scale bar, 1 cm. (n) The electricity generation performance of the 3D textile TEG without substrate in different temperature difference. Reproduced with permission from ref 560. Copyright 2020 Nature Publishing Group under Creative Commons Attribution 4.0 (http://creativecommons.org/licenses/by/4.0/).

fiber to form a 1D TE yarn.[550] The Seebeck coefficient and the resulting power factor of these yarns achieved 10 μV/K and 1.41 μW/(m·K^2) at room temperature, respectively.

3.2.2. 2D Interlacing. 1D TE yarns are the basic functional units for body heat energy harvesting. To boost output power, building 2D textile TEGs on thermoelectric yarns is an effective approach. The first concept demonstration was performed by Takai et al. in 2002. They reported yarn intersection-based TEGs by interlacing alumel and chromel wires as a thermocouple.[553] Since then, more research efforts led to the development of two-dimensional textile TEGs. By using TE yarns to construct woven/knitted TEGs, the yarns can be interfaced either along the in-plane direction or the thickness direction.[551,554,555] Wei et al. reported a textile TEG by weaving TE yarns along the in-plane direction of a 2D fabric with p-type and n-type crystalline TE nanowires.[556] Cu electrode-interlaced p-type $Bi_{0.5}Sb_{1.5}Te_3$ and n-type Bi_2Se_3 fibers with a diameter of 80 μm and a length of 5 cm were employed in this configuration. An output power of 0.36 μW was obtained by using two pairs of p−n TE legs at a temperature difference of 50 °C.

Nevertheless, temperature differences between the human body and ambient environment were often observed in the textile thickness direction rather than in-plane direction. Thermocouples should be placed vertically to optimize body heat energy harvesting. Baughman et al. reported 2D TE textiles by weaving or knitting n-type Bi_2Te_3 yarns and p-type Sb_2Te_3 yarns.[551] As shown in Figure 9a, three textile designs, including zigzag stitch, garter stitch, and plain weave, were systematically demonstrated to harvest body heat energy in the thickness direction. For the garter stitch textile TEG (Figure 9b), insulating fibers were introduced to maintain the intersection structure of n- and p-type TE yarns (Figure 9c). With a temperature difference of 55 °C, a power density of 0.09 W/m^2 was delivered (Figure 9d). For the plain-weave textile TEG (Figure 9e), n-type and p-type TE leg segments were alternatingly integrated into a one-body yarn, which was interlaced with insulating fibers (Figure 9f). At the same temperature difference, a higher output power density of 0.62 W/m^2 was delivered (Figure 9g).

To construct a 2D textile TEG, beyond the weaving and knitting structures, a third configuration can be employed by assembling multiple 1D TE yarns onto a 2D fabric.[557] For example, p-type PEDOT:PSS dyed silk yarns were evenly sewed onto a wool fabric.[558] Silver wires were used as conductive yarns to connect adjacent TE yarns. An output voltage of 26 μV/K at a temperature gradient of 50 °C was delivered in this 2D textile TEG.

3.2.3. 3D Interlacing. Constructing a 3D textile TEG along the temperature gradient between the human body and ambient environment could further the harvesting of body heat energy. In this design, the thickness of the textile and the

https://dx.doi.org/10.1021/acs.chemrev.9b00821
Chem. Rev. 2020, 120, 3668−3720

Table 3. Materials and Energy Performance of Representative Textile TEGs

thermoelectric materials					
P-type	N-type	performance	temperature difference (°C)	year	ref
Textiles as Substrates					
Sb_2Te_3	Bi_2Te_3	3 μW, 2.9 mV (D^a =12.7 mm, T^b = 0.5 mm, 11 pairs)	8.5[c]	2014	531
$Bi_{0.5}Sb_{1.5}Te_3$	$Bi_2Se_{0.3}Te_{2.7}$	292.4 nW/cm^2, 11.5 mV	27[c]	2014	528
Ag_2Se	PEDOT:PSS	5 nW (3 × 13 mm^2, 4 legs)	20	2015	536
Sb_2Te_3	Bi_2Te_3	15 nW, 10 mV (D = 4 mm, T = 0.3 mm, 12 pairs)	5−35	2016	532
Sb_2Te_3	$Bi_{1.8}Te_{3.2}$	2.3 μW (20 × 2 × 0.07 mm^3, 8 pairs)	20	2016	530
PEDOT:PSS	Ni foil	2.6 μW/cm^2	48.5	2017	542
PEDOT:PSS	constantan wire	212.6 nW, 18.7 mV (35 × 5 mm^2, 5 legs)	74.3	2017	541
PEDOT-Cl	carbon fiber	10 mV (45 × 5 mm^2, 2 legs)	8.5[c]	2019	540
Yarns as Building Blocks					
Sb_2Te_3	Bi_2Te_3	0.62 W/m^2 (plain weave) 0.11 W/m^2 (zigzag stitch) 0.09 W/m^2 (garter stitch)	55	2016	551
PEDOT:PSS	Ag wire	12 nW (5 cm, 26 legs)	66	2017	558
p-doped CNTs	n-doped CNTs	54 mV (240 pairs)	6	2017	555
$Bi_{0.5}Sb_{1.5}Te_3$	Bi_2Se_3	24.2 mV, 59.1 μA, 0.36 μW (2 pairs)	50	2017	556
NWPU/PEDOT:PSS/MWCNT	NWPU/n-doped MWCNT	0.025 mV (6 cm × 6 cm × 7 mm)	6.4	2017	552
PEDOT:PSS	MWCNT/PVP coated yarn	7.1 nW (4 cm, 38 pairs)	80	2018	557
p-doped CNTs	n-doped CNTs	70 mW/m^2	44	2020	560

[a]D: diameter. [b]T: thickness. [c]Estimated value.

captured air in porous structure can block body heat loss and will maintain temperature differences, thus obtaining a higher energy performance.[559] For example, Hu et al. developed a 3D textile TEG, which incorporated piles of embroidered p-type (nonionic waterborne polyurethane (NWPU)/PEDOT:PSS/MWCNT coated) and n-type (NWPU/n-doped MWCNT coated) yarns along the thickness direction (Figure 9h).[552] As shown in Figure 9i, two tightly knitted fabrics separately served as substrate and superstrate, which demonstrated thermoregulation capability for keeping the temperature difference. Connecting these two fabrics with interlaced p-type and n-type TE legs, a flexible 3D textile TEG was achieved (Figure 9j). With a size of 6 cm by 6 cm by 7 mm, the 3D textile TEG was adhered to a human wrist and generated a voltage of 0.025 mV at a 6.4 °C temperature difference between the human skin and the room air. The voltage could be further enlarged to 0.1242 mV under a temperature difference of 10.7 °C by cooling the outside layer of the textile TEG with iced water (Figure 9k).

However, the substrate and superstrate fabrics of the 3D textile TEGs would limit the energy performance. Recently, Snyder et al. presented a 3D textile TEG without substrates by weaving thermoelectric yarns consisting of alternately doped carbon nanotube fibers (CNTF) (Figure 9l).[560] The 3D architecture of the textile TEG was formed owing to the elastic force rather than the traditional substrate fabric (Figure 9m), thus exhibiting better mechanical properties and yielding higher temperature differences. This 3D textile TEG composed of 15 units with a fixed length of 16 mm generated an output power of 4.64 μW at a 44.4 °C temperature difference (Figure 9n), which is higher than that of previous organic TEGs. Furthermore, when the 3D textile TEG covered 40% of the total body surface area of an adult at an ambient temperature of 26 °C, it produced as much as 200 μW of output power.

Although yarn-based textile TEGs, including 1D, 2D and 3D structures, exhibit improved breathability, uniformly and tightly coating the thermoelectric materials onto the round fibers could be a challenging process. The low adhesion usually makes the coating layers easily damaged under mechanical deformation. Therefore, constructing robust thermoelectric yarns with a reproducible manufacturing process is in need of solutions.

3.3. Outlook on Textile TEGs

Rapid advancements in textile TEGs for body heat energy harvesting are well underway, and a summary of recent research progress is illustrated in Table 3. However, there are still many challenges that need to be addressed.

3.3.1. Thermoelectric Materials. Applied TE materials could greatly determine the output performance of the textile TEGs.[561,562] Given that the ZT values of inorganic TE materials are much higher than organic ones at room temperature, it seems more promising to adopt inorganic ones for better output performance, but further analysis reveals that inorganic materials are relatively brittle and thus are not capable of withstanding intensive abrasion due to human body motions. Besides, inorganic TE materials like Bi-Te alloys have poor biocompatibility for on-body applications as a result of their toxicity. To overcome these obstacles, fabricating low-dimensional TE materials, such as copper iodide thin films,[563] and then depositing them on textile substrates could be an effective way.[564] Meanwhile, advanced encapsulation is highly desired to reduce abrasion, along with ensuring isolation of materials from human skin to improve biocompatibility. Also, owing to high flexibility and light weight, organic TE materials can overcome the drawback of relatively low TE performance by implementing a densely knitting or weaving method so as to increase the number of p-n pairs in the assigned textile area.[552] Meanwhile, mixing TE polymers with inorganic TE materials[565,566] and chemical doping could also improve TE properties without sacrificing flexibility.[567] Recently, thermo-

https://dx.doi.org/10.1021/acs.chemrev.9b00821
Chem. Rev. 2020, 120, 3668−3720

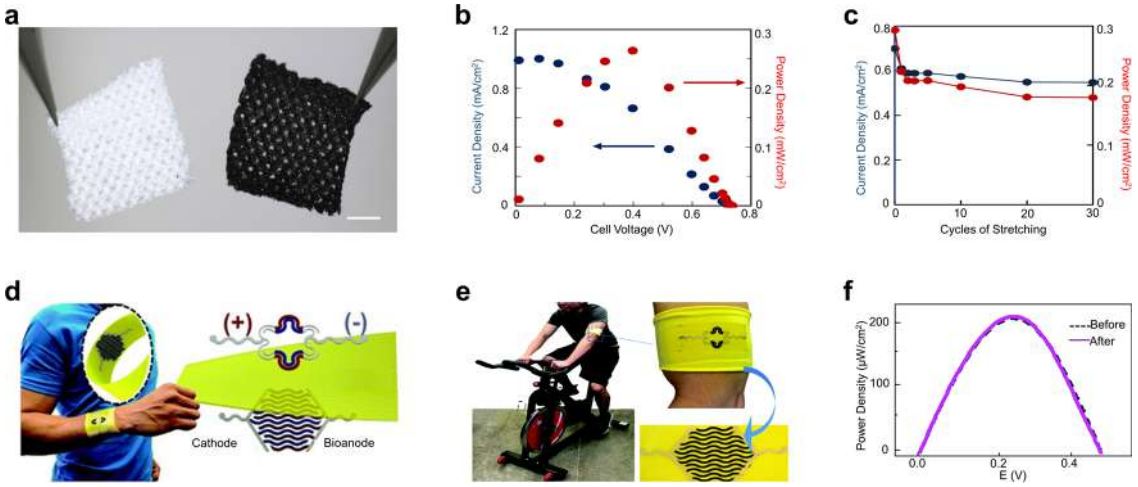

Figure 10. EBFCs using textiles as substrates for biochemical energy harvesting. (a) Photograph comparing a virgin and a CNT-modified textile substrate. Scale bar, 4 mm. (b) Dependence of the current density and the power density of the textile EBFCs on cell voltage. (c) Dependence of the current density and the power density of the textile EBFCs on cycles of stretching. Reproduced with permission from ref 614. Copyright 2015 Elsevier. (d) Schematic illustration of a stretchable EBFC by using the textile as a substrate. (e) Photograph of the stretchable textile EBFC harvesting biochemical energy during sports. (f) The output power of the stretchable textile EBFC before and after 100 folding cycles. Reproduced with permission from ref 617. Copyright 2018 Royal Society of Chemistry.

galvanic gel electrolytes have aroused research interests because of their decent Seebeck coefficient, high flexibility, and easy fabrication processes.[568−570] The thermogalvanic gel electrolytes can be easily molded into thin film or fiber shape for integrating with textiles, which demonstrate a promising solution for harvesting energy from low grade body heat. In conclusion, a deep understanding of the constraints and corresponding solutions of applying organic and inorganic TE materials is essential in dealing with textile TEG systems.

3.3.2. Temperature Gradient. Because the output power of textile TEGs is proportional to the spatial temperature difference, the present textile TEGs are usually incapable of continuously driving on-body electronics due to the limited temperature gradient. In that case, increasing thermal insulation of textile TEGs and decreasing contact thermal resistance could be promising pathways to increase the temperature difference between the bottom and top of textile TEGs and, thus, the output power.

3.3.3. Thermal Radiation. With a normal temperature of 33.5 °C and emissivity of 0.98, the human skin strongly emits thermal radiation in the mid-infrared range for human body heat dissipation.[571−574] This component of body heat is usually ignored in the field of heat energy harvesting. Recently, metafabrics, which concentrate thermal radiation into high energy spots, could shed some light on this issue. The infrared detector material layer based on the thermophotovoltaic effect can convert the thermal radiation into electricity.[575] However, the wearability and biocompatibility of metafabrics require further enhancement for on-body applications.

3.3.4. Intimate Contact. Intimate contact between textile TEGs with curved/hairy skin surfaces is critical to perform body heat energy harvesting. Compared to thin film base TEGs,[154,576−579] the weaving/ knitting structures in textile TEGs, although they increase wearability, largely reduce contact area due to their rough topography.[580] Undermined heat conduction with the skin greatly lowers output performance. Hence, optimizing architectures of textile TEGs to achieve intimate and continuous contact with the skin is highly desired for efficiently harvesting body heat energy.

4. BIOCHEMICAL ENERGY HARVESTING

Beyond the aforementioned electricity generation from biomechanical motions and body heat, biochemical energy is a type of on-body energy source that is generally available but usually ignored, which is presented in forms like body fluids, including sweat, tears, blood, and saliva.[581−583] They are also renewable and eco-friendly for electricity generation.[584−586] On-body biochemical energy is stored in biofuels such as glucose, lactate, and fructose, which can reach up to 100 W in total for a healthy adult.[98] These rich biofuels can be oxidized using biocatalysts in a biofuel cell (BFC) for electricity generation.[587−589] In principle, biocatalysts in the anode first facilitate the oxidation of biofuels like glucose, which release electrons that flow into the cathode via external circuits, as expressed in eq 1.[590−594] Then the cathode collects these electrons for oxygen reduction and converts the biochemical energy into electricity, as expressed in eq 2.

$$\text{2glucose} \rightarrow \text{2gluconolactone} + 4H^+ + 4e^- \quad (1)$$

$$O_2 + 4H^+ + 4e^- \rightarrow 2H_2O \quad (2)$$

Two types of biocatalysts are widely recognized in the community: microbials and enzymes corresponding to the microbial biofuel cell (MBFC)[595−597] and enzyme biofuel cell (EBFC), respectively.[598−601] The latter, EBFC, has been endowed with brighter prospects for on-body scenarios due to its high biofuel conversion efficiency,[602−605] biocompatibility,[606−608] and miniaturization.[609−612] More specifically, on-body EBFCs have been merged into a textile form and attracted remarkable research attention. According to the device configuration, there are two feasible solutions for realizing textile EBFCs, including utilizing textiles as substrates to support the enzymes, as well as starting from a yarn design to construct fiber electrodes as building blocks, as introduced in the following sections. Finally, the key challenges of textile EBFCs are discussed, along with potential solutions and future prospects.

https://dx.doi.org/10.1021/acs.chemrev.9b00821
Chem. Rev. 2020, 120, 3668−3720

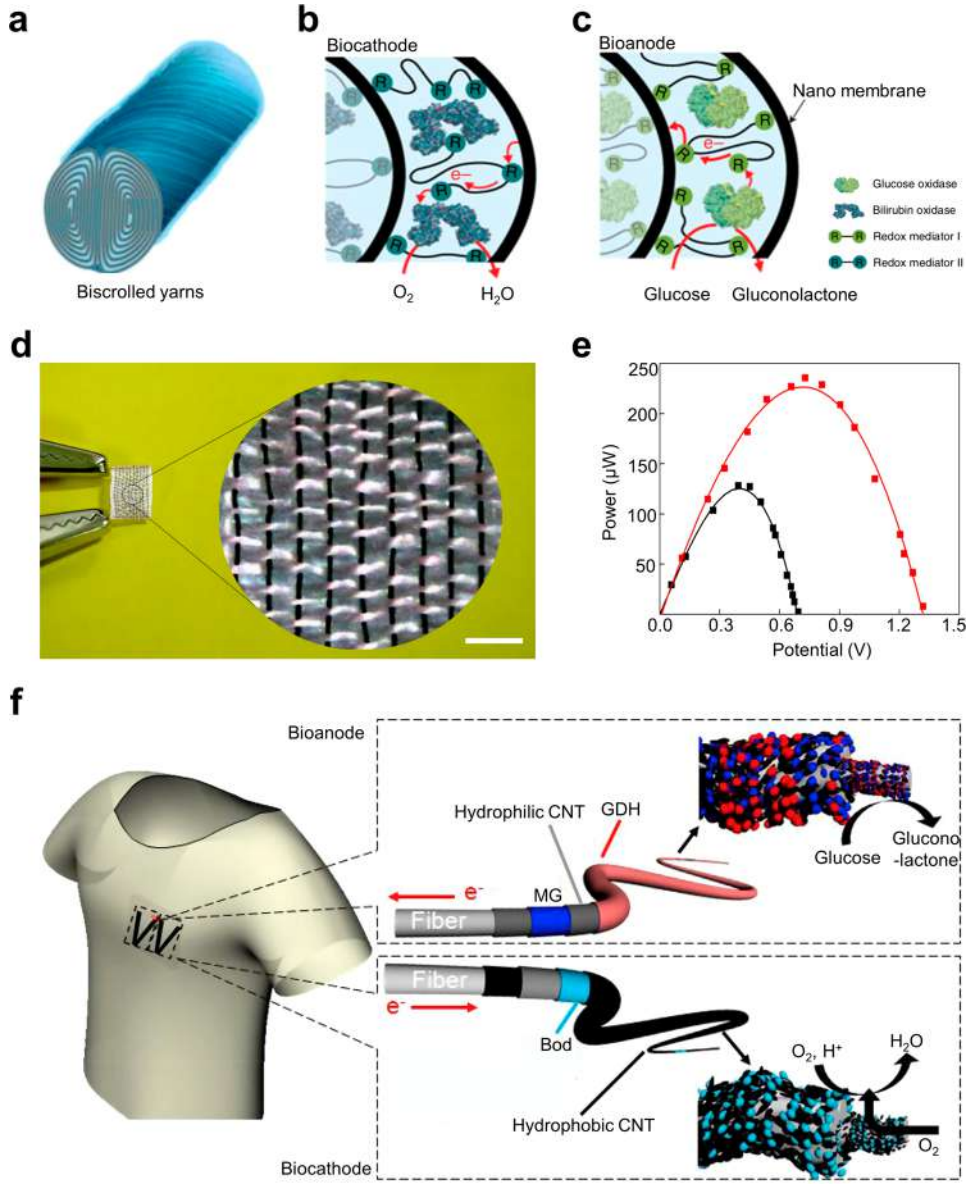

Figure 11. Yarn-constructed EBFCs for biochemical energy harvesting. (a) Schematic illustration of the biscrolled yarn electrodes. (b) Schematic illustration of the biscrolled yarn cathode and its working mechanism. (c) Schematic illustration of the biscrolled yarn anode and its working mechanism. (d) Photograph of the woven EBFC textile that consists of biscrolled yarn anodes and cathodes. Scale bar, 500 μm. (e) The power density of textile EBFC when harvesting the biomechanical energy in glucose. Reproduced with permission from ref 619. Copyright 2014 Nature Publishing Group. (f) Schematic illustration of weaving the yarn electrodes into conventional clothes to realize a textile EBFC. Reproduced with permission from ref 622. Copyright 2019 Elsevier.

4.1. Textiles as Substrates

With natural micro/nanoscale roughness, textiles are an ideal substrate for constructing a biofuel cell due to the ease of enzyme loading. Specifically, textile substrates are flexible, permeable, and conform to skin curvature to enable tight contact on a large scale for body fluids absorption, thus promoting high electricity output.

For example, the Nishizawa group developed a multilayer EBFC based on textile substrates.[613,614] First, commercial pantyhose textiles were coated with CNTs to achieve high conductivity and specific surface area for enzyme loading (Figure 10a).[614] After that, the anode and cathode were formed via modifying these functional textiles with D-fructose dehydrogenase and bilirubin oxidase, respectively. Finally, a hydrogel film containing 200 mM fructose fuel was sandwiched between these two modified textile electrodes. While the redox reaction occurred in the anode and cathode, this EBFC based on textile substrates yielded an output power density of up to 0.25 mW/cm^2 (Figure 10b), which was able to drive a red LED. Although the meshwork structure of electrodes endowed the textile EBFC with stretchability, a 25% decrease of the output power was demonstrated after the initial stretching cycles (Figure 10c). Further efforts to increase the stretchability of textile EBFCs are highly desired because human body movement will cause long-term, random deformations on these wearable devices in practical applications.

To this end, the Wang group developed stretchable textile EBFCs for extracting biochemical energy from body fluids by directly printing electrodes on textile substrates.[615−617] For example, serpentine-shaped and interdigitated CNT electrodes

https://dx.doi.org/10.1021/acs.chemrev.9b00821
Chem. Rev. 2020, 120, 3668−3720

Table 4. Materials and Energy Performance of Representative Textile EBFCs

bioanode	biocathode	biofuels	performance	year	ref
Textiles as Substrates					
conductive carbon ink	conductive carbon ink	lactate, 15 mM	0.1 mW/cm^2	2014	616
lactate oxidase	platinum black				
CNTs coated textile	CNTs coated textile	fructose, 200 mM	0.25 mW/cm^2	2015	614
D-fructose dehydrogenase	bilirubin oxidase				
printed CNT	printed Ag_2O/Ag	glucose, 50 mM	0.16 mW/cm^2	2016	615
glucose oxidase		lactate, 20 mM	0.25 mW/cm^2		
lactate oxidase					
printed CNT	printed Ag_2O/Ag	lactate, 15 mM	0.252 mW/cm^2	2018	617
lactate oxidase					
Yarns as Building Blocks					
PEDOT coated MWCNT	PEDOT coated MWCNT Bilirubin oxidase	glucose, 60 mM	0.375 mW/cm^2[a]	2014	619
glucose oxidase					
MWCNTs/rubber fiber	MWCNTs/rubber fiber	glucose, 7 mM	0.042 mW/cm^2	2018	624
glucose oxidase	bilirubin oxidase				
CNT coated carbon fibers	CNT coated carbon fibers	glucose, 200 mM	0.216 mW/cm^2	2019	622
glucose dehydrogenase	bilirubin oxidase				

[a]Estimated value.

were screen printed on the inner side of the textile substrate by using stretchable CNT ink.[617] Then the Ag wires for connecting the anode and cathode were similarly printed on the textile substrate by using stretchable Ag ink. Finally, the bioanode was modified with the lactate oxidase enzyme and naphthoquinone redox mediator by drop casting. Analogously, the biocathode was fabricated by drop casting Ag_2O/CNTs solutions. The lactate was enzymatically oxidized on the bioanode, and liberated electrons flowed toward the silver-oxide cathode, generating electrical power (Figure 10d). With a lactate concentration of 15 mM, which is comparable to body fluids, these textile EBFCs exhibited an output voltage and power density of up to 0.49 V and 252 μW/cm^2 respectively, which was able to light three LEDs. Meanwhile, a tester was wearing a sweatband with printed textile EBFC and exercising continuously. By harvesting biochemical energy from the tester's perspiration, this textile EBFC could charge a capacitor to 0.40 V in 37 min (Figure 10e). In addition, 98.7%, 95.4%, and 86.4% of the initial output power was maintained after imposing 100 repeated folding, twisting, and stretching processes on the stretchable textile EBFCs, respectively (Figure 10f). Because of the high stretchability and great output power density, this EBFC based on textile substrates is very valuable for harvesting biochemical energy from body fluids to power on-body electronics.

Although coating or printing electrodes on a textile substrate is a convenient approach to producing textile EBFCs,[618] only limited surface area on the electrode can be used for loading enzymes, which inhibits the redox reaction rate and results in a decrease in energy conversion efficiency. As a consequence, the energy efficiency and longevity of current textile EBFCs are not high enough to serve as a practical power source. More research efforts are needed to push forward the frontiers of the field. Investigating different textile substrates, such as silk, wool, cotton, and polyester, which possess various surface roughnesses and microstructure modifications, could be an effective approach to maximizing enzyme loading and immobilization.

4.2. Yarns as Building Blocks

Beyond the previous configuration of using common textiles as substrates, constructing textile EBFC starting with yarn-shaped electrodes as building blocks by relying on current textile technologies, such as weaving, knitting, or sewing, could easily achieve higher guest molecule loading and immobilization by using the total volume of yarn-shaped electrodes.

For example, a high-powered glucose-based textile EBFC was demonstrated by weaving biscrolled yarn electrodes in 2014.[619] The yarn electrodes were fabricated by twisting PEDOT-coated MWCNT nanomembranes (Figure 11a), which loaded a large amount of guest molecules like glucose oxidase/bilirubin oxidase and redox mediator from aqueous solution, counting to over 95 wt % of the biocathode (Figure 11b) and bioanode (Figure 11c). Because of the full exploitation of the yarn volume, the EBFC based on a yarn-shaped anode/cathode pair achieved an V_{oc} and a power density of up to 0.70 V and 2.18 mW/cm^2, respectively, in a 60 mM glucose solution. Furthermore, because of the robustness, flexibility, and stretchability of the yarn electrodes, a 5 mm by 7 mm textile EBFC was realized by weaving 14 mm anode yarns and 56 mm cathode yarns together (Figure 11d). This single layer interlaced textile EBFC exhibited an output power of up to 128 mW and an V_{oc} of 0.70 V by harnessing biochemical energy in glucose (Figure 11e).

The following research on textile EBFCs built on yarn electrodes has concentrated on enhancing both output power and wearability,[620] such as utilizing highly conductive Au nanoparticles to achieve efficient electrical communication between oxidase enzyme and a yarn anode,[621] as well as fabricating highly biocompatible yarn electrodes without toxic mediators or chemical cross-linkers.[623] However, the stretchability and robustness of these innovative yarn electrodes require further improvement, as the textile EBFCs built on these yarns should be capable of accommodating various deformations caused by body movements. To this end, Kim et al. fabricated highly stretchable and soft yarn electrodes by wrapping MWCNTs on to a stretched rubber fiber.[624] Then the MWCNTs/rubber fiber was coated with different active enzyme layers and rewrapped with another layer of MWCNT sheet to realize yarn-shaped anodes and cathodes separately.

https://dx.doi.org/10.1021/acs.chemrev.9b00821
Chem. Rev. 2020, 120, 3668−3720

The as-prepared yarn electrodes were connected with external circuits and yielded an output voltage of up to 0.55 V and a power density of up to 42 $\mu W/cm^2$ in a 7 mM glucose solution. Meanwhile, this energy performance of the yarn electrodes only decreased by 5% after undertaking 1000 stretch−release cycles.

More recently, Miyake et al. developed a textile EBFC by using a similar electrode structure.[622] After decorating the MWCNT modified carbon fibers with glucose dehydrogenase and bilirubin oxidase, the yarn-shaped bioanode for glucose oxidation and yarn-shaped biocathode for oxygen reduction were woven onto conventional clothes to realize a textile EBFC (Figure 11f). With a 200 mM glucose solution, this textile EBFC built on yarn electrodes produced an output power density of up to 216 $\mu W/cm^2$, which was able to light a red LED device.

Textile EBFCs built on yarn electrodes highlight promising potential for harvesting biochemical energy in body fluids that is an indispensable component for powering on-body electronics in the near future. However, engineering long and robust yarn electrodes that are capable of taking advantage of the current textile industry for large-scale textile EBFCs fabrication remains a great challenge.

4.3. Outlook on Textile EBFCs

Converting biochemical energy from body fluids into electricity via textile EBFCs has been substantially developed and has attracted increasing research efforts in recent years. However, many challenges remain due to their unique working principle compared to other on-body energy harvesting technologies. A summary of recent textile EBFCs is illustrated in Table 4.

4.3.1. Stability. The predominant challenge in the textile EBFCs community is output stability, which is largely determined by external chemical or mechanical factors. On one hand, fluctuating body conditions like varying temperature, biomolecule concentrations, and pH of body fluids could chemically impair the rate of redox reactions, resulting in poor output power. Meanwhile, surface fouling and ambient humidity could degrade the activation of loaded enzymes that constrains the energy efficiency of textile EBFCs. On the other hand, rigorous mechanical deformation could pose a significant risk of enzyme desorption and whittle down the effective contact area between the textile EBFCs and skin surface. Hence, further enhancing the mechanical robustness and chemical durability of electrodes is still highly desired for maintaining output stability of textile EBFCs.

4.3.2. Energy Efficiency. The low utilization efficiency of biofuels in body fluids is another challenge. To solve this problem, it is imperative to enlarge the effective area of textile substrates so as to achieve larger enzyme loading for fully oxidizing these rich biofuels. Meanwhile, most textile EBFCs only consist of one kind of enzyme and cannot oxidize coexisting biofuels like glucose, lactate, and fructose in body fluids simultaneously. Introducing an enzymatic cascade to textile EBFCs could address this concern and lead to enhanced energy efficiency and output power.

4.3.3. Biocompatibility. Enhancing biocompatibility without compromising electron transfer between enzymes and bioanodes is also critical for the epidermal application of textile EBFCs. Possible leakage of toxic chemicals in textile EBFCs, such as commonly used osmium in mediators, renders it highly risky for on-body applications. To solve this problem, mediator-free EBFCs could be a solution.[625−627] In addition, developing textile microbial BFCs that are innocuous to the human body is another promising approach with greatly improved biocompatibility for on-body biochemical energy harvesting.[628,629]

4.3.4. Evaluation Standard. The energy performance evaluation standard for textile EBFCs is valuable but lacking in the community. Abundant external factors, such as body temperature, pH of body fluids, biofuel concentration, and environmental humidity, influence output power of textile EBFCs. Therefore, researchers are encouraged to test textile EBFCs in standard conditions such as using biofuels with the same concentration as body fluids. To sum up, establishing widely accepted protocols of evaluating and comparing the energy performance of textile EBFCs is challenging but will be beneficial for tracking and promoting research development.

5. SOLAR ENERGY HARVESTING

In the previous sections, we introduced smart textiles for harvesting energy from the human body such as biomechanical motions, body heat, and body fluids. Moving toward environmental sources, ambient solar energy produced from direct sunlight is about 100 mW/cm^2,[630] which shows great potential of powering on-body electronics. Moreover, the annual potential of solar energy is 1575−49 837 exajoules (EJ) in the world, which is three times larger than the total world energy consumption of 578 EJ in 2018 and even exceeds the estimated global energy consumption of 1000 EJ in 2050.[631−633] Thus, solar irradiance, which is available in huge quantities, is another clean and renewable energy source around the human body. Known as the photovoltaic effect, this is when sunlight hits a solar cell (SC) and the absorbed photons excite and separate electrons and holes in the active layers to generate a photocurrent. In regard to photoactive materials, solar cells are typically categorized into three main generations.[634−637] The first generation is wafer-based, e.g., crystalline silicon (c-Si). The second generation of solar cells depends on thin film materials, e.g., cadmium telluride (CdTe), amorphous silicon (a-Si), and copper indium gallium selenide (CIGS). The third-generation solar cells include organic solar cells (OSCs), dye-sensitized solar cells (DSSCs), perovskite solar cells (PSCs), and so on. Among these solar cells, the emerging third-generation solar cells like OSCs,[638−640] DSSCs,[641−643] and PSCs[644−646] have been endowed with compelling features including flexibility, light weight, abundant raw materials, easy fabrication, and low cost. Merging them with the textile industry has attracted tremendous attention for powering on-body electronics. To construct a textile solar cell, two configurations are widely adopted, including layer stacking and yarn intersection, as elaborated in the following sections.

5.1. Layer Stacking

A typical solar cell has a multilayered structure consisting of electrode layers and photoactive material layers. Thus, to construct a textile solar cell, layer stacking is a simple and effective approach. Technically, it could be fabricated by transferring an as-prepared solar cell vertically onto the textile substrate or building the solar cell on textile substrates via a layer-by-layer coating/printing technology.

5.1.1. Direct Transfer. Direct transfer of as-prepared solar cells onto textile substrates is a straightforward and effective method for constructing textile solar cells,[647,648] as this allows

https://dx.doi.org/10.1021/acs.chemrev.9b00821
Chem. Rev. 2020, 120, 3668−3720

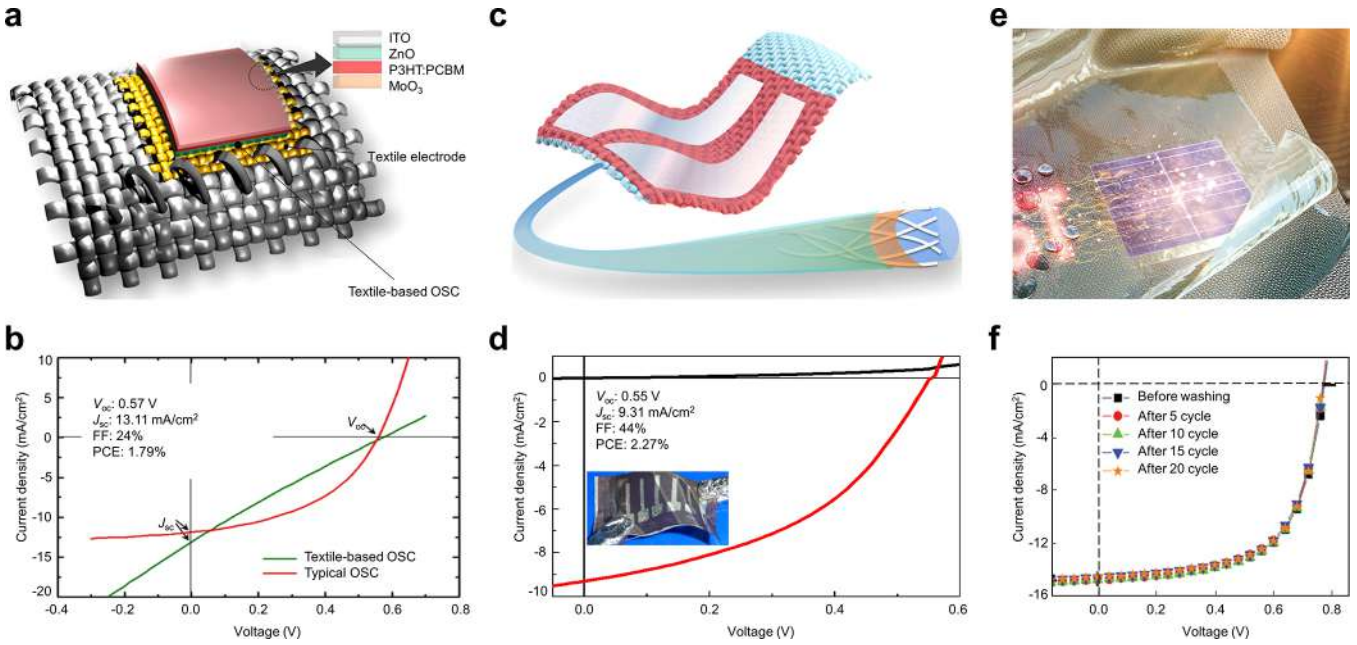

Figure 12. Textile SCs based on layer stacking. (a) Schematic illustration of a stitchable textile OSC. (b) Current density−voltage characteristic (J−V curves) of the textile-based stitchable OSC (green line) and the typical OSC (red line). Reproduced with permission from ref 651. Copyright 2014 Elsevier. (c) Schematic illustration of a textile OSC built on a polyester fiber-based substrate. (d) J−V curves of the textile OSC under light (red line) and in the dark (black line), and a photograph of the textile OSC. Reproduced with permission from ref 663. Copyright 2017 Elsevier. (e) Schematic illustration of a washable textile OSC working in water. (f) J−V curves of the washable textile OSC before and after various washing cycles. Reproduced with permission from ref 664. Copyright 2019 Royal Society of Chemistry.

for textile solar cell fabrication without exposing the textile substrates to higher temperatures, which could lead to instability of certain textiles. Common direct transfer methods include wet transferring,[649] hot-melt adhering,[650] stitching, and so on. For example, Lee et al. developed a textile solar cell by vertically transferring an OSC onto a commercial textile via a stitching process (Figure 12a).[651] In this work, a photoactive layer contained poly(3-hexylthiophene) (P3HT) as the electron donor and [6,6]-phenyl-C61-butyric acid methyl ester (PCBM) as the acceptor. A ZnO-based electron transport layer with indium tin oxide (ITO) coating worked as the top electrode, and a MoO_3 (hole transport layer) deposited gold textile worked as the bottom electrode. The stitched textile solar cell generated an V_{oc}, a short-circuit current density (J_{sc}), a fill-factor (FF), and a power conversion efficiency (PCE) of up to 0.57 V, 13.11 mA/cm^2, 24% and 1.79%, respectively, under AM 1.5G illumination at 100 mW/cm^2 (Figure 12b).

5.1.2. Building on Textiles. Building solar cells on textile substrates via layer-by-layer coating[652−655] or printing[656−659] technology is also a promising method of fabricating textile solar cells. Compared with the direct transfer technique,[660,661] layer-by-layer construction ensures a stable interface and, thus, long-term stability and mechanical durability against biomechanical motions. For example, Peng et al. developed a flexible and lightweight textile OSC via a layer-by-layer dip-coating of photoactive materials onto a textile substrate.[662] First, a highly flexible Ti textile worked as the electrode, which was then coated with TiO_2 nanoparticle, P3HT:PCBM, and PEDOT:PSS on the surfaces in succession. Finally, two CNT sheets were stacked on both sides as the external electrodes. The textile OSC demonstrated a PCE of 1.08%, and the performance was still stable after being bent for 200 cycles, exhibiting long-term durability under mechanical motions.

However, the Ti wires and CNT sheets might decrease the wearing comfort of the textile solar cell. In consideration of improving wearability, Kim et al. demonstrated a flexible, stretchable, and even foldable textile solar cell by coating the P3HT:PCBM and the electrode layer by layer on a polyester fiber-based conductive textile (Figure 12c).[663] This as-fabricated textile solar cell exhibited an V_{oc} of up to 0.55V, a J_{sc} of 9.31 mA/cm^2, and a PCE of 2.27%, as well as good stability after 400 cycles of curling and folding (Figure 12d). The relatively low PCE might be due to the limited contact area between the P3HT:PCBM and the rough surface of the textile anode, which could interfere with charge transfer.

To further improve output power, Cho et al. laminated a PU layer on the textile substrate before layer-by-layer spin-coating of the photoactive materials and electrodes.[665] The PU layer provided a planarization platform for uniform coating and enlarged the contact area between the functional layers by relieving the surface roughness. As a consequence, the multilayer textile OSC was uniform, flexible, and compatible with a practical cloth. It produced a constant V_{oc} of up to 0.77 V, a J_{sc} of 15.91 mA/cm^2, and a PCE of 8.71% under a bending cycle of 100 times.

More recently, a similarly structured textile OSC was reported by Jeong et al. in 2019. The textile OSC was fabricated via layer-by-layer coated electrodes, carrier transporting layers, and PTB7-Th:PC71BM on a barrier-covered textile substrate.[664] Noticeably, SiO_2−polymer composite encapsulation was finally attached to the as-prepared textile OSC as a superstrate to enhance its stability by protecting it from ambient chemicals and moisture (Figure 12e). This highly durable textile OSC generated a stable V_{oc}, J_{sc}, and PCE of up to 0.77 V, 14.85 mA/cm^2, and 7.24%, respectively, even under 20 washing cycles in 10 min (Figure 12f), which exhibited a promising potential for practical wearing. To sum

https://dx.doi.org/10.1021/acs.chemrev.9b00821
Chem. Rev. 2020, 120, 3668−3720

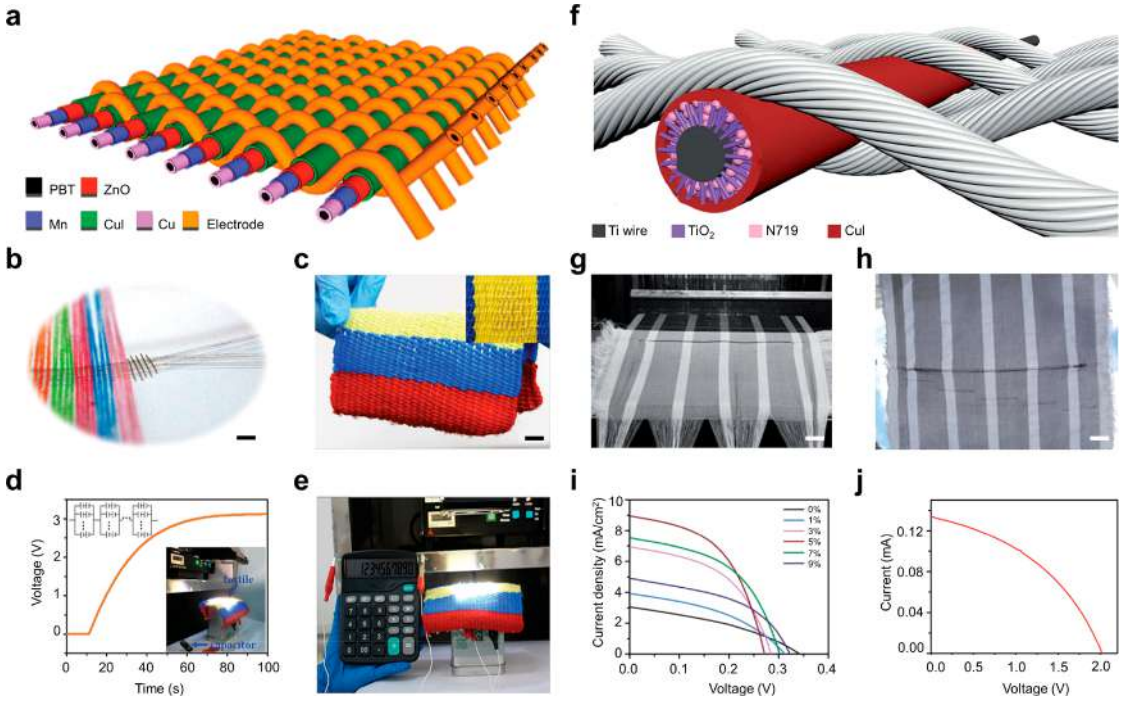

Figure 13. Textile SCs based on yarn intersection. (a) Schematic illustration of a solid-state textile DSSC. (b) Photograph of the weaving process. Scale bar, 1 cm. (c) Photograph of the as-fabricated light, flexible, and colorful solid-state textile DSSC. Scale bar, 1 cm. (d) The textile DSSC charged a 2 mF capacitor under natural solar irradiation. (e) Photograph of the all solid-state textile DSSC powering a digital calculator under natural solar irradiation. Reproduced with permission from ref 676. Copyright 2016 Wiley. (f) Schematic illustration of the TiO_2-based large-scale textile DSSC. (g) Photograph showing large-scale weaving of the textile DSSC on a loom. Scale bar, 5 cm. (h) Photograph of the lightweight TiO_2-based textile DSSC with flexibility and breathability. Scale bar, 5 cm. Current density−voltage characteristic of the textile DSSC (i) under different EMISCN concentrations, and (j) with five modified photoanodes connected in series. Reproduced with permission from ref 677. Copyright 2019 the Royal Society of Chemistry.

up, layer stacking is a convenient and feasible approach to fabricate a textile solar cell with a collection of compelling features, including flexibility, high performance, and long-term durability.

5.2. Yarn Intersection

Despite layer stacking bringing us a simple and effective approach for constructing a textile solar cell, both the conventional solar cell direct transfer and building on textiles largely impede the breathability of textile solar cells with possible wearing discomfort. In addition, the limited transparency of the upper electrode in the textile stacking configuration might impair light absorption and, thus, energy efficiency. These concerns could be well addressed if we were to construct a textile solar cell by weaving or knitting functional yarns such as photoactive fibers or electrode fibers. The yarn intersection-based textile solar cell could hold greatly improved breathability and absorbed solar radiation with different light incident angles due to its surface morphology and the bare area of photoactive fibers.

As for yarn intersection-based textile solar cells, a fiber-shaped solar cell is the basic component, which starts with an elastic core with photoactive materials coating and follows with a conductive yarn twisting[666−669] or external electrode coating.[670−674] For example, Yang et al. developed a fiber-shaped stretchable DSSC by twisting a N719-dyed, spring-like Ti wire on conductive rubber elastic fibers.[675] A single fiber-shaped DSSC exhibited a PCE of up to 7.13%, which was still stable after weaving 5 fibers by 5 fibers into a textile form.

The solar cell unified as a single fiber usually shows excessive diameter due to the one-body design, which leads to a huge pore size and reduced wearability when intersected into a textile form. In that case, Zhang et al. demonstrated a solid-state textile DSSC by seamlessly weaving strings of photoanode (PE) yarns and counter electrode (CE) yarns with a diameter of about 1 mm (Figure 13a).[676] In this textile DSSC, ZnO nanoarrays sensitized by N719 dye was deposited on Mn-plated polybutylene terephthalate (PBT) polymer wires. Then the functional wires were coated with the hole transport active material CuI to form PE yarns. These PE yarns and Cu-based CE yarns were interlaced on a loom to achieve the solid-state textile DSSC (Figure 13b). This low-cost, flexible, and lightweight textile DSSC based on yarn interaction (Figure 13c) reached a PCE of up to 1.3%, an V_{oc} of 0.46 V, and a J_{sc} of 7.8 mA/cm^2, which was capable of charging a 2 mF capacitor (Figure 13d) and powering a digital calculator (Figure 13e) via harvesting energy from natural solar irradiation. In this work, by taking advantage of the technology in the textile industry, convenient large-scale production of textile DSSCs was achieved for the first time. Furthermore, the usage of all solid-state, flexible, and lightweight material endowed the woven textile DSSC with outstanding wearability, representing a significant step toward on-body applications of textile solar cells.

After that, a similar all-solid textile DSSC by weaving N719 dye sensitized PEs and Cu-coated polymer CEs was also developed by Chai et al.[678] This well-designed textile DSSC based on yarn intersection exhibited a PCE of up to 0.9%, as well as superior tailorability and excellent stability for operation after 60 days. Similarly, Peng et al. reported a textile OSC by weaving P3HT:PCBM-based cathode yarns and Ag-plated

https://dx.doi.org/10.1021/acs.chemrev.9b00821
Chem. Rev. 2020, 120, 3668−3720

Table 5. Materials and Energy Performance of Representative Textile SCs

types	photoactive materials	performance				fabrication	year	ref
		V_{oc} V	J_{sc} mA/cm^2	FF %	PCE %			
Layer Stacking								
DSSC	N719, TiO_2	0.69	19.70	43	5.83	sewing	2014	647
DSSC	N719, Ti	0.625	7.28	60	3.67	stacking	2014	660
DSSC	N719, TiO_2	0.31	5.2	25	0.4	printing	2019	658
DSSC	N719, TiO_2	0.73	10.24	54	4.04	printing	2019	659
OSC	P3HT:PCBM	0.57	13.11	24	1.79	stitching	2014	651
OSC	P3HT:PCBM	0.53	5.2		1.08	coating	2014	662
OSC	P3HT:PC61BM	0.58	12.10	41	2.90	wet transfer	2017	649
OSC	P3HT:PCBM	0.55	9.31	44	2.27	coating	2017	663
OSC	PBDTTT:PC71BM	0.8	10			hot-melt	2018	650
OSC	P3HT:ICBA	0.54	6.05	37	1.23	coating	2018	654
OSC	PFN/PTB7-Th:PC71BM	0.77	15.91	71	8.71	coating	2019	665
OSC	PTB7-Th:PC71BM	0.77	14.85	63	7.24	coating	2019	664
PSC	$CH_3NH_3PbI_3$	1.06	20.53	66	14.3	stacking	2017	661
PSC	$CH_3NH_3PbI_3$	0.82	12.69	50	5.72	coating	2018	655
Yarn Intersection								
DSSC	N719, Ti	0.71	16.17	62	7.13	weaving	2014	675
DSSC	N719, ZnO	0.4	4		0.9	weaving	2016	678
DSSC	N719, ZnO	0.46	7.80	36.23	1.30	weaving	2016	676
DSSC	N719, TiO_2	0.725	19.34	71	10.0	weaving	2018	673
DSSC	N719, TiO_2	0.4	9.42	51	1.92	weaving	2019	677
OSC	P3HT:PCBM	0.52	9.06	38	1.78	weaving	2014	668
OSC	P3HT:PCBM	0.48	7.39	45.88	1.62	weaving	2018	679
PSC	$CH_3NH_3PbI_3$	0.96	16.44	66	10.41	weaving	2016	672

nylon-based anode yarns in a loom.[679] This thin, lightweight, flexible, and large-scale textile OSC based on yarn intersection reached a PCE of up to 1.62%, an V_{oc} of 0.48 V, and a J_{sc} of 7.39 mA/cm^2, which was able to power an electronic watch under natural solar irradiation.

More recently, the same research group developed a large-scale textile DSSC with a size magnitude of meters (Figure 13f).[677] By utilizing similar weaving technology, TiO_2-based PE yarns and Ag-plated nylon yarns were intersected together (Figure 13g). The as-prepared all solid-state textile DSSC was compatible with conventional clothes due to its flexibility, light weight, and breathability (Figure 13h). Noticeably, by optimizing the diameter of CuI particles in PE yarns via changing the concentration of 1-methyl-3-ethylimidazolium thiocyanate (EMISCN) during the synthesis process (Figure 13i), this textile DSSC exhibited an V_{oc} of 0.4 V, an J_{sc} of 9.42 mA/cm^2, and an enhanced PCE of up to 1.92% (Figure 13j), which was higher than all previous solid-state woven textile DSSCs.

In a word, yarn intersection has become a monumental method for achieving large-scale, comfortable, and flexible textile solar cells for harvesting ambient solar energy. However, the cylindrical surface of the fiber-shaped core in functional yarns may easily cause coating defects, such as fractures, perforation, and wrinkling on photoactive layers, which will debilitate carrier transfer and mechanical robustness in yarn-shaped electrodes. Hence, further research in controllably and precisely coating photoactive materials onto the curved yarn surface is highly desired to advance the frontier of textile solar cells with both durability and high energy conversion efficiency.

5.3. Outlook on Textile SCs

Everybody wears clothes, and sunshine is generally available with a high energy density of about 100 mW/cm^2. Tremendous research efforts and great achievements have been made in the field of textile solar cells for on-body electricity generation, and a summary of recent research progress in textile solar cells is illustrated in Table 5. However, opportunities and challenges coexist, requiring further research to boost the field to the next level.

5.3.1. Energy Efficiency. Improving wearability at the expense of energy conversion efficiency renders a low output performance for textile solar cells. To enhance their energy efficiency, three research directions are pointed out as follows.

First, constructing 3D tandem structure textile solar cells by weaving or knitting spectrally matched photoactive yarns in the thickness direction could be a promising method to enhance energy conversion efficiency.[680] Because the majority of current textile solar cells only absorb light in a specific range of the spectrum, this approach could effectively broaden the working wavelength range with a result of improved energy efficiency.

Moreover, designing an optical fiber-shaped photoanode may effectively enhance the amount of light captured by textile solar cells.[681−683] For example, coating photoactive materials and electrode layers onto the inner wall of a tubular yarn, the incident light from one end of the yarn could be essentially trapped due to the multiple reflections in the tubular geometry. Hence, weaving or knitting the optical fiber-based solar cell into a textile may be a tempting idea to achieve stronger light absorption and higher energy conversion efficiency.

Finally, heat always accompanies any form of energy conversion. To fully utilize solar energy, introducing thermoelectric or pyroelectric materials into textile solar cells could

https://dx.doi.org/10.1021/acs.chemrev.9b00821
Chem. Rev. 2020, 120, 3668−3720

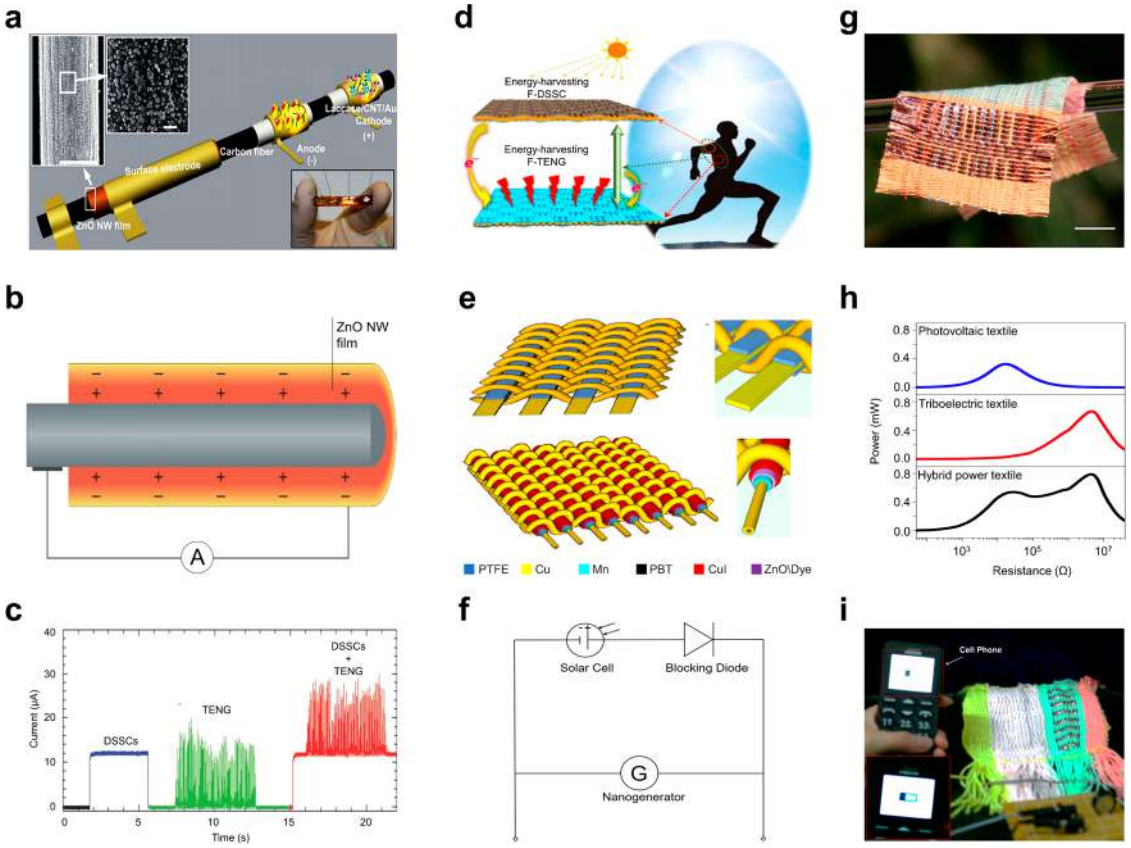

Figure 14. Smart textiles for hybrid energy harvesting. (a) Schematic illustration of a coaxial fiber-shaped HG consisting of a ZnO-based PENG and a biofuel cell. Scale bars, 5 μm and 300 nm. (b) Working principle of the piezoelectric component in the coaxial fiber-shaped HG. Reproduced with permission from ref 713. Copyright 2011 Wiley VCH. (c) The short-circuit current of the fiber DSSC, the textile TENG, and the hybrid power textile. Reproduced with permission from ref 714. Copyright 2016 Wiley VCH. (d) Schematic illustration of the textile HG consisting of a fabric TENG and a fabric DSSC. Reproduced with permission from ref 715. Copyright 2016 American Association for the Advancement of Science. (e) Schematic illustration of a hybrid power textile, including a textile TENG and a textile DSSC. (f) Power management circuit diagram. (g) Photograph of the hybrid power textile mixed with colorful yarns. Scale bar, 1 cm. (h) Dependence of the output power of the textile DSSC, textile TENG, as well as the hybrid power textile on the load resistances. (i) Photograph of the hybrid power textile charging a cell phone. Reproduced with permission from ref 716. Copyright 2016 Nature Publishing Group.

explore photothermally generated heat, potentially resulting in enhanced electric output and improved energy efficiency.[684]

5.3.2. Stability. For on-body applications, long-term stability is a critical concern. To protect textile solar cells from abrasion during wearing and corrosion caused by water and oxygen, adding an encapsulation that has mechanical flexibility and good optical transmittance is of great necessity.[685] Specifically, polymer materials have fair flexibility and are easy to process, which make them suitable for encapsulation.[686] However, it remains difficult to obtain robust packaging performance due to their high water vapor transmission rate. On the other hand, widely adopted ceramic packaging materials such as aluminum nitride are too brittle to endure frequent deformations caused by biomechanical motions.[687] Integrating organic and inorganic materials to form a composite network with sacrificial hydrogen bonds could dissipate applied stress, largely optimizing their mechanical properties.[688] Also, organic components could release interfacial tension of fragile inorganic components.[689,690] Consequently, encapsulating textile solar cells with an organic/inorganic composite could improve the stability without compromising performance and wearability.[691]

5.3.3. Biocompatibility. Biocompatibility is another critical concern for on-body applications. In the current textile solar cell system, possible leakage of toxic materials found in DSSC and PSC fibers, such as the N719 dye and heavy metal ions, e.g., lead, renders textile solar cells a high risk for wearing purposes.[692] Silicon-based solar cells could be a superior solution due to their low cost, abundance, and high biocompatibility.[693−695] Silicon could even be implanted in feline cortical tissue.[696] However, the rigid structure of current silicon solar cells makes them unsuitable for textile integration. Recent technological advancements have produced an ultrathin silicon film with superior flexibility,[697−699] which sheds some light of hope on the possibility of constructing a silicon-based textile solar cell with greatly improved biocompatibility and energy efficiency.

5.3.4. Beyond DSSCs. Among all of the solar cells, the third-generation ones have been widely made into textile forms, especially DSSCs. Merging other types of solar cells with the textile industry, such as silicon and thin film-based solar cells, has been an untapped research area that requires more research efforts. For example, integrating flexible CIGS solar cells with textiles could provide a stable energy solution even in low lighting conditions like indoor scenarios and

https://dx.doi.org/10.1021/acs.chemrev.9b00821
Chem. Rev. 2020, 120, 3668−3720

cloudy days due to the outstanding weak light performance of CIGS.[700−702]

6. HYBRID ENERGY HARVESTING

In the preceding sections, we have comprehensively reviewed the research progress in smart textiles for energy harvesting from biomechanical motions, body heat, body fluids, and solar irradiance. However, with the increasing number and power requirements of on-body electronics,[703] electricity generation from a single energy source might become insufficient.[704] Moreover, some energy sources are not always available.[705] For example, textile solar cells cannot generate electricity constantly in cloudy or dark situations with limited solar radiation.[706] Noticeably, multiple energy sources commonly coexist.[195] For example, when people walk during sunshine, all the solar energy, biomechanical energy, body heat energy, and even biochemical energy from perspiration are generally available for electricity generation.

Therefore, harvesting multiple types of energy simultaneously presents an effective method for optimizing the power output of smart textiles. In the following sections, we comprehensively review current progress of textile hybrid generators (HGs) for energy harvesting. To promote field development, problems pressing for solutions and onward research directions are also presented.

6.1. Body Heat and Biomechanical Energy

Body heat and biomechanical energy (BHBE) always coexist in a living human. Body motions such as walking, running, and jumping can also lead to enhanced heat flow from the skin to the surroundings due to an increased metabolic rate, which results in a larger spatial temperature difference for electricity generation.[707−710]

For example, Lee et al. developed a flexible hybrid generator by vertically stacking a thermoelectric generator, which consisted of six pairs of TE legs with a size of 2 mm by 2 mm by 1 mm, on a ZnO-based PENG.[711] Attached to a human forearm, this flexible hybrid generator produced an enhanced output voltage of up to 0.12 V and a current of 90 nA. Similarly, Kim et al. demonstrated a hybrid generator by mounting a PTFE-based triboelectric generator on a thermoelectric generator consisting of Bi-Te pellet arrays.[712] Under a sliding rate of 12 cm/s and ambient temperature of 24 °C, this HG delivered an output power density of 14.98 mW/cm^2, which could light up 100 commercial LED bulbs. It is worth mentioning that all reported wearable BHBE hybrid generators are built on a thin film platform and seldomly merged with textile technologies, which is an uncharted area requiring future research efforts.

6.2. Biochemical and Biomechanical Energy

On the human body, biomechanical motions can boost body fluid secretion, which results in a strong correlation between biochemical and biomechanical energy (BCBE). This combination for energy harvesting is highly desired, especially when there is a lack of significant spatial temperature differences for harvesting BHBE.[717]

For example, Pan et al. constructed a coaxial fiber-shaped hybrid nanogenerator by integrating a ZnO-based PENG and a biofuel cell with the two ends of a carbon fiber (Figure 14a).[713] Working with coexisting body fluid and biomechanical motions, the yarn nanogenerator was capable of simultaneously converting biochemical energy from glucose and yarn deformation into electricity (Figure 14b), which yielded an output voltage of up to 3 V and a current of 200 nA. Although the output power could be effectively boosted by weaving or knitting the yarn-shaped nanogenerators, further advancement in the field of hybrid BCBE harvesting by smart textiles is much slower than expected due to technological challenges.

6.3. Solar and Biomechanical Energy

The hybrid energy generator based on glass/silicon/GaN substrates for simultaneously harvesting solar and biomechanical energy (SBE) was first proposed by Wang et. al in 2009.[718] Since then, tremendous research efforts have been made by the community to improve output performance and wearability.[719−728]

For example, Pu et al. explored this kind of hybrid power textile by simply sewing a pair of contact-separation mode triboelectric layers and seven fiber-based DSSCs on clothes, connecting them via an external circuit.[714] By harvesting energy from a human jogging under an AM 1.5G solar radiation, this hybrid power textile could deliver a current of up to 30 μA (Figure 14c). Another hybrid textile generator was also reported to harvest SBE by integrating fiber-shaped TENGs and DSSCs (Figure 14d).[715] In this work, the textile DSSC layer was fabricated by intersecting three fiber-shaped DSSCs and then pairing them with PDMS-covered and Cu-coated ethylene vinyl acetate (EVA) tubes to construct the textile TENG.

Furthermore, a high performance, foldable, and lightweight hybrid power textile designed by weaving fiber-based TENG and DSSC was developed by Chen et al.[716] The Cu-coated PTFE stripes, photoanode yarns, and Cu electrode yarns were woven into a hybrid power textile via a shuttle-flying process in an industrial loom (Figure 14e). To optimize the energy output of the power textile, a blocking diode was introduced to the power textile to serve as the electrical interconnection between the textile TENG and textile DSSC to realize impedance matching (Figure 14f). The as-prepared hybrid power textile was flexible, aesthetically pleasing, and exhibited outstanding wearability and breathability (Figure 14g). The DSSC component of the hybrid power textile was capable of converting solar irradiance into usable electricity, and the contact-separation process between the PTFE strips and Cu electrode yarns was able to harvest biomechanical energy. When a tester walked under a solar intensity of 80 mW/cm^2, the hybrid power textile with a size of 4 cm by 5 cm stably generated a power output of 0.5 mW under a wide range of load resistances (Figure 14h), which was able to directly charge a cell phone (Figure 14i).

It is worth noting that the majority of solar energy harvesting with textiles uses DCCSs due to their low cost and scalability. However, the wide adoption of this technology is largely hindered by its relatively low efficiency and the toxicity of the dye used. Organic or perovskite solar cells show a possibility of being integrated with textiles for on-body solar energy harvesting and a further hybridization with other energy harvesting technologies.[729−733]

6.4. Multiple Energy Harvesting

Hybrid generators for concurrently harnessing three or more energy forms were also developed to further enhance output power with advanced and fine designs.[196,734] For example, Zhang et al. developed a hybrid nanogenerator based on multifunctional PZT for simultaneously harvesting biomechanical, thermal, and solar energy.[735] By harnessing three kinds of energy at the same time, this hybrid generator with an active

https://dx.doi.org/10.1021/acs.chemrev.9b00821
Chem. Rev. 2020, 120, 3668−3720

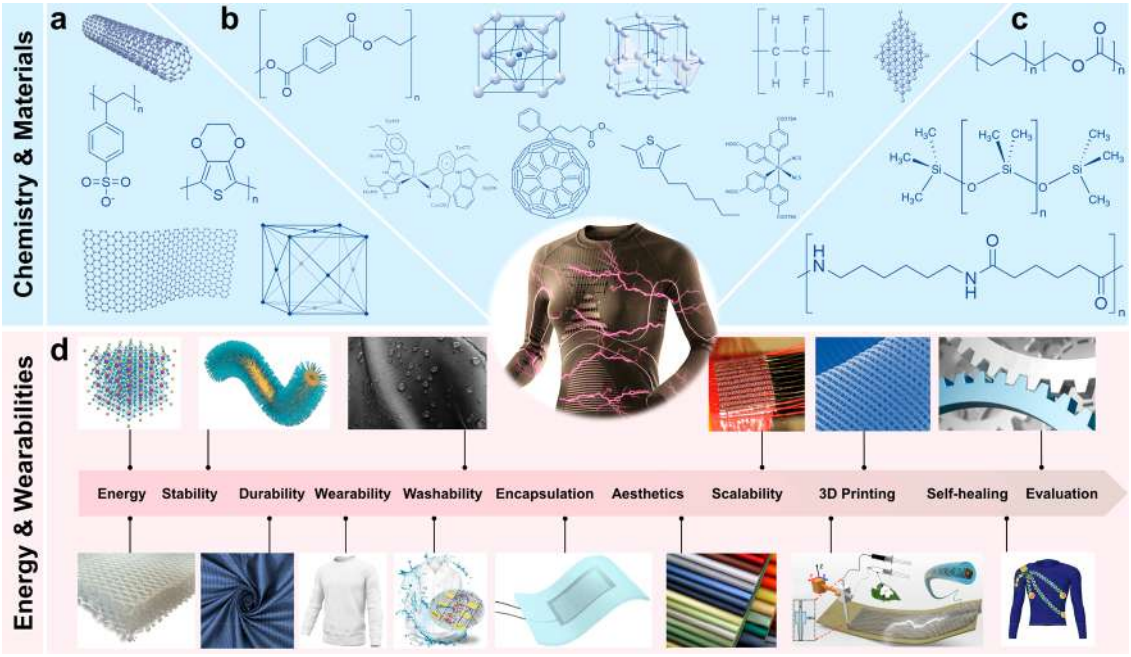

Figure 15. Conclusions and perspectives regarding smart textiles for electricity generation. Chemistry and materials: major materials for smart textiles, including the conductive materials as electrodes or functional coating on textiles (a), e.g., CNTs, PEDOT:PSS, graphene, Ag, and Cu (left to right); the representative materials for each textile generator (b), e.g., PET (TENGs), PZT (PENGs), ZnO (PENGs, TENGs), PVDF (PENGs), Sb-Te alloy (TEGs), glucose oxidase (EBFCs), P3HT:PCBM (SCs), and N719 (SCs) (left to right); the encapsulating materials for smart textiles (c), e.g., EVA, PDMS, and nylon (top to bottom). (d) Energy and wearabilities: prospective research directions of energy harvesting textiles with improved energy conversion efficiency and wearability, which repose mainly on the innovation of chemistry and materials.

area of 70 mm by 70 mm could easily reach a voltage of up to 80 V, which could charge a 10 μF capacitor to 5.1 V in 90 s.

However, because of complicated structural requirements, developing smart textiles capable of simultaneously harvesting three or more energy forms has yet to be explored. Integrating these hybrid generators with textiles will be a promising research direction to provide a sustainable power source for on-body electronics in the near future.

6.5. Outlook on Textile HGs

As an emerging research field, textile HGs have demonstrated rapid advancement in the past decades. However, it is also confronted with serious challenges.

6.5.1. Output Power. Delivering an optimized output power from all components is the main challenge for textile HGs because each of the components has different electrical properties, such as inner impedances, working frequencies, and alternate-current/direct-current characteristics. To effectively sum all electrical output, power management circuits, such as a microscale rectifier[711] or buffer,[736] that could be seamlessly integrated with textile HGs is required.

6.5.2. Hybridization Methods. Current progress in textile HGs is mainly based on device-level hybridization. In this configuration, different textile-based generators are connected by using the external power management circuits to effectively integrate the electric output from each individual component. For example, fiber-based TENGs and DSSCs were woven together with blocking diodes to form a hybrid power textile.[716] However, the increased configuration complexity and HG device size associated with the growing number of electronic components have been major challenges in device-level hybridization for wearable applications. Meanwhile, optimized power outputs may not be realized simultaneously because of the mismatched electrical output properties of each component.

A promising approach to solving these problems in textile HGs is developing active materials with hybrid energy conversion mechanisms. In that case, various electricity generation technologies could be unified in a single textile-based generator, which could effectively miniaturize the device size and simplify the configuration.[737,738] For example, Zhang et al. reported a $(1-x)Pb(Mg,Nb)O_3$-$xPbTiO_3$ based ribbon,[739] which holds the hybridized piezoelectric and pyroelectric effect. This ribbon exhibited promising potential for harvesting biomechanical and thermal energy simultaneously. However, research on textile HGs based on mechanism-level hybridization remains at the prototype stage. Active materials with intrinsically hybrid energy conversion mechanisms are still limited, and various possible materials remain to be investigated and then integrated to textile form for wearable electricity generation.

6.5.3. More Combinations. Finally, several specific types of energy combinations have scarcely been studied. For example, little research has investigated concurrently harvesting body heat and biochemical energy, while these two energy sources are tightly correlated when people are exercising or enduring environmental temperature change. In addition, many aforementioned HGs with mature technology in harvesting various energy sources concurrently have not been merged with the textile platform, which may inhibit further on-body applications. Therefore, developing textile HGs for simultaneously harvesting as many types of energy sources as possible from the surroundings is an urgent issue for studying and exploring due to their bright prospects in energy harvesting and supporting next-generation on-body electronics.

https://dx.doi.org/10.1021/acs.chemrev.9b00821
Chem. Rev. 2020, 120, 3668−3720

7. CONCLUSIONS AND PERSPECTIVES

The projection of 26 billion IoT devices by 2020 has been pushing research to explore sustainable, eco-friendly, and pervasive energy solutions for distributed electronics.[52] Harvesting energy from on-body and ambient renewable energy sources, such as biomechanical motions, body heat, body fluids, and solar radiation using emerging energy technologies, is a promising method to fit the bill. Textiles, with which humans have been familiar for thousands of years, are ideal platforms to merge these energy harvesters for on-body applications due to their light weight, cost-effectiveness, ease of transport, and superior wearing comfort. In this review, we have comprehensively highlighted advances in textile-based sustainable energy technologies. These smart textiles with the capability of energy conversion have exciting prospects in revolutionizing the energy field and next-generation on-body electronics in the era of IoT. As highlighted in the preceding sections, smart textiles for energy harvesting have experienced a rapid advancement in functional material innovations, device configurations, and practical applications (Figure 15). To grow this nascent concept of smart textiles for energy harvesting to maturity, many challenges are waiting to be overcome, as follows.

7.1. Efficiency Enhancement

Considering the rising energy demands of on-body electronics,[740] e.g. the average power consumption of emerging smartwatches is about 30 mW, how to effectively boost energy conversion efficiency of smart textiles to match power needs is the essential challenge in this field. Functional material innovation and advancing device structure design represent the two most effective strategies for improving energy conversion efficiency of textile generators.

7.1.1. Applied Materials. Fundamental materials innovation will be the direct method to push forward the boundaries of energy conversion efficiency. For example, the *ZT* values of most reported thermoelectric materials in textile TEGs are below 0.85,[522] while state-of-the-art research has shown that $Mg_{3+\delta}Sb_xBi_{2-x}$ has a *ZT* of 1.05 near room temperature,[741] which could be a promising candidate material for high-performance textile TEGs. Although traditional $BaTiO_3$ has a high piezoelectric coefficient, its stiffness and brittleness impair its response to biomechanical stimuli and thus its efficiency.[245] Recently, scientists have developed ultraflexible $BaTiO_3$ membranes that can undergo 180° folding,[742] demonstrating great potential for being integrated with textiles for high-performance biomechanical energy harvesting.

7.1.2. Device Structures. Via advancing structural design, textile generators could be more responsive to environmental energy input to bring in a larger temperature gradient and effective contact area, better light absorption, and higher enzyme mass loading for high-performance energy harvesting. For example, using 3D printing or omnidirectional weaving technology, constructing 3D textile solar cells with spectrally matched photoelectric yarns in the thickness direction can fully absorb solar radiation to enhance energy conversion efficiency.[680] In addition, increasing the porous structure and surface roughness in textile electrodes of EBFCs can enlarge the area of active sites[165] and realize enzyme mass loading for an improved energy conversion efficiency.

7.2. Output Stability

Energy harvesting from the human body and its surroundings usually exhibits uncontrollable output fluctuations in electric outputs due to the variation of environmental energy input over time. It produces a practical problem in driving on-body electronics, which normally require a constant and stable power supply.

The first viable method to solve this problem is utilizing power management circuits, such as a rectifier or a buffer,[736,743] and then integrating them with textile generators to suppress electric output fluctuations. Developing sewable or weaveable power management circuits that can be merged with smart textiles will be a promising research direction in the future. Another possible approach is to integrate textile generators with textile-based energy storage devices, like a supercapacitor[744−746] or battery,[747,748] to form a textile-based self-charging power unit. Textile generators will first charge the energy storage devices, which can produce a steady and continuous electric output at its discharging plateau.

7.3. Mechanical Durability

To equip textiles with the capability of electricity generation, functional modifications, including physical, chemical, and even biological coatings,[749−751] need to be added onto traditional yarns and textiles, which are usually made from electronically insulating, chemically inert organic materials.[752] In practical wearing scenarios, various and ceaseless mechanical stresses routinely subject smart textiles to damage, such as the adhesive conductive layer cracking or even peeling off from the textile substrates.[753] Therefore, it is still a challenge to achieve good adhesion between functional coatings and soft textile materials for a decent mechanical strength and durability. Enhancing the surface roughness of yarn/textile substrates could yield large loading areas, which is especially favorable for coating functional material via solution process.[754] Meanwhile, the recently developed polymer-assisted metal deposition could also shed some light on this factor,[755] and more research on enhancing interface adhesion and stability is desired for improving the mechanical robustness of smart textiles.

7.4. Wearing Comfort

For electricity generation, having conductive pathways for electron transportation is the basic requirement for realizing its functionality. However, the majority of textile materials are insulating. To add this value, metal coating or metal wires are heavily involved in current smart textile fabrications,[750] which to some extent has a negative impact on textile softness, light weight, breathability, fit, and tactile comfort.

7.4.1. Light Weight. Despite decent electrical conductivity, metal-based electrodes in smart textiles might be too heavy for on-body applications. Replacing metal coatings or metal wires with conductive carbon-based materials like CNTs and graphene is a viable method for obtaining lightweight smart textiles.[756−760] Further research in optimizing the conductivity of carbon-based electrodes without sacrificing their light weight is highly desired. What is more, ultralight materials, including aerogels,[761] aerographite,[762] metallic foams,[763] polymeric foams,[764] and metallic microlattices,[765] could also make a significant contribution to reduce the weight of smart textiles.

7.4.2. Breathability. Beyond textile softness and light weight, breathability, which refers to the ability to allow transmission of moisture and air, is another critical parameter to measure textile wearability because it is indispensable for regulating body temperature and humidity. However, embedding functional materials, such as dispenser-printing thermo-

https://dx.doi.org/10.1021/acs.chemrev.9b00821
Chem. Rev. 2020, 120, 3668−3720

electric material legs onto textile substrates, would block air and moisture transport paths, causing damp and clammy sensations for wearers.[766] Manipulating the volume between the interlaced yarns to obtain appropriate pore structures and controlling the size of embedding functional materials could be possible solutions. Moreover, natural products with hygroscopicity, such as wool and cotton,[767] are capable of absorbing perspiration and releasing heat simultaneously. Hence, merging these hygroscopic materials with smart textiles might enhance ventilation of skin and the ambient environment.

7.4.3. Tactile Sensations. Tactile sensations are the direct feelings of the skin when in contact with smart textiles, especially in the scenarios of operating textile TEGs and EBFCs for on-body energy harvesting, which need a tight fit with the human body. For example, uncomfortable skin abrasion can be caused by a sewn-in functional stitchable textile solar cell due to its surface texture and swollen seams.[651]

In addition, prickle sensations and initial cold touch feelings might be caused by stiff metal wires that protrude from the surface of textile TEGs.[768] Improving the softness of the textile could be a possible solution, which can be achieved via both material innovation and structural design. On one hand, we can introduce more soft products such as silk, wool, and cotton to the smart textiles. On the other hand, woven/knitted smart textiles with porous structure are far preferable to increase soft tactile sensations. In addition, replacing metal conductors with carbon-based materials[769] or conductive polymers[770] could improve tactile sensations of smart textiles.

7.4.4. Biocompatibility. For on-body electricity generation and long-term epidermal applications, biocompatibility of smart textiles is another serious concern that needs to be considered. Hidden risks lurking in the leakage of toxic chemicals are prevalent in current textile generators, such as hazardous metal elements in PZT and Bi-Te alloys,[237,238,532] the most common N719 dye used in DSSCs,[676] and mediators in the electrodes of EBFCs.[619] Consequently, discovering suitable and toxic-free materials for textile generators is a pressing matter for on-body applications. For example, natural products have captured tremendous research interests in the field of energy harvesting, and blackberries could be used as a natural dye for DSSCs without toxic effects.

7.5. Washability

With functional coatings, washability is a widely recognizable challenge for smart textiles.[340] Constructing smart textiles that can withstand household laundering is still at the fundamental stage in view of their vulnerability to intensive mechanical deformation in water. Developing self-cleaning functional coatings with textiles is a promising solution. Mounting superhydrophobic surfaces on the textiles could resist surface contamination in practical situations,[771] and this concept is still at a budding stage.

7.6. Encapsulation

The compelling functionalities of smart textiles are built on the functional coating materials, which are usually not stable or safe when exposed to the ambient environment with oxygen,[772−774] water,[664,775] fluctuating temperature,[776−778] as well as mechanical stress.[779−781] For example, the textile EBFC is unstable under body fluid ion fouling.[782] Ceaseless body movements would lead to serious abrasion of the all-solid textile solar cell.[676] In addition, direct physical contact with PEDOT-Cl in an all-fabric TEG may cause allergic reactions like a mild tickle[533] and so on. Textile encapsulation is a good option to address these challenges. Admittedly, traditional encapsulating layers in smart textiles, e.g., hermetic plastic packages, might not only impair breathability but also undermine their energy performance by impeding, for instance, stress transport within TENGs and PENGs,[439] heat flow in TEGs,[228] body fluids absorption in EBFCs,[607] and translucency of solar cells.[180] Therefore, to achieve robustness without sacrificing wearability and output power of smart textiles, developing innovative encapsulant materials and technologies,[783] such as fully biobased films,[784] ultrathin White-EVA film,[785] and 3D printing packages,[786] are highly desired to stamp out this predicament.

7.7. Aesthetics Properties

Aesthetic properties such as color selection and style design of garments are pivotal factors that can make or break the wearable technology market.[753] However, current research on smart textiles shows few considerations for aesthetic needs. In that case, developing smart textiles in optional designs without compromising performance like light absorbtion and heat flow is a governing factor for commercialization.

7.8. Large-Scale Fabrication

To reduce cost and bring real impact to society, large-scale production of energy harvesting smart textiles is a must. Most of currently reported works are at the stage of lab-scale manual fabrication.[716] Although the sophisticated industry loom demonstrates the potential of commodity-scale manufacturability of smart textiles,[677] there are many challenges remaining.

First, as the building blocks of smart textiles, functional yarns remain challenging for scaling up because their electricity properties such as conductivity might decline progressively with increasing length.[787−789] Second, many functional inorganic material coatings usually enlarge the diameter of the yarns,[790,791] which may exceed the yarn count range (0.5−50 denier) of commercial looms. In addition, many of these yarns with brittle and stiff coatings are not stretchable enough to withstand the average tensile strength of 50 MPa during the shedding and insertion motions of machine weaving procedures,[792−794] which might easily cause crack propagation, delamination of these coatings, and performance degradation. Hence, mass production of robust functional yarns with proper diameter and mechanical strength is the premise of large-scale fabricated smart textiles and is highly desired to advance the field.

7.9. 3D Printing

3D printing has attracted tremendous attention in both academia and industry for its capability of easily producing freeform objects without design limitations. Recently, various 3D printing methods have been devised for advanced manufacturing[795] that could be employed to produce energy harvesting textiles, such as PZT for PENGs,[477] BiSbTe alloys for TEGs,[796] electrodes for EBFCs,[797,798] and organic−inorganic metal halide perovskites for PSCs,[799] paving the way for developing smart textiles with highly controllable material compositions and device structures. Nonetheless, the widespread adoption of 3D printing for smart textile manufacturing still requires more research due to limitations in printable filament materials, scalable fabrication, and the mechanical robustness of 3D-printed textiles. Therefore, further research to explore the applications of 3D printing in the smart textile community would be a bright direction

https://dx.doi.org/10.1021/acs.chemrev.9b00821
Chem. Rev. 2020, 120, 3668−3720

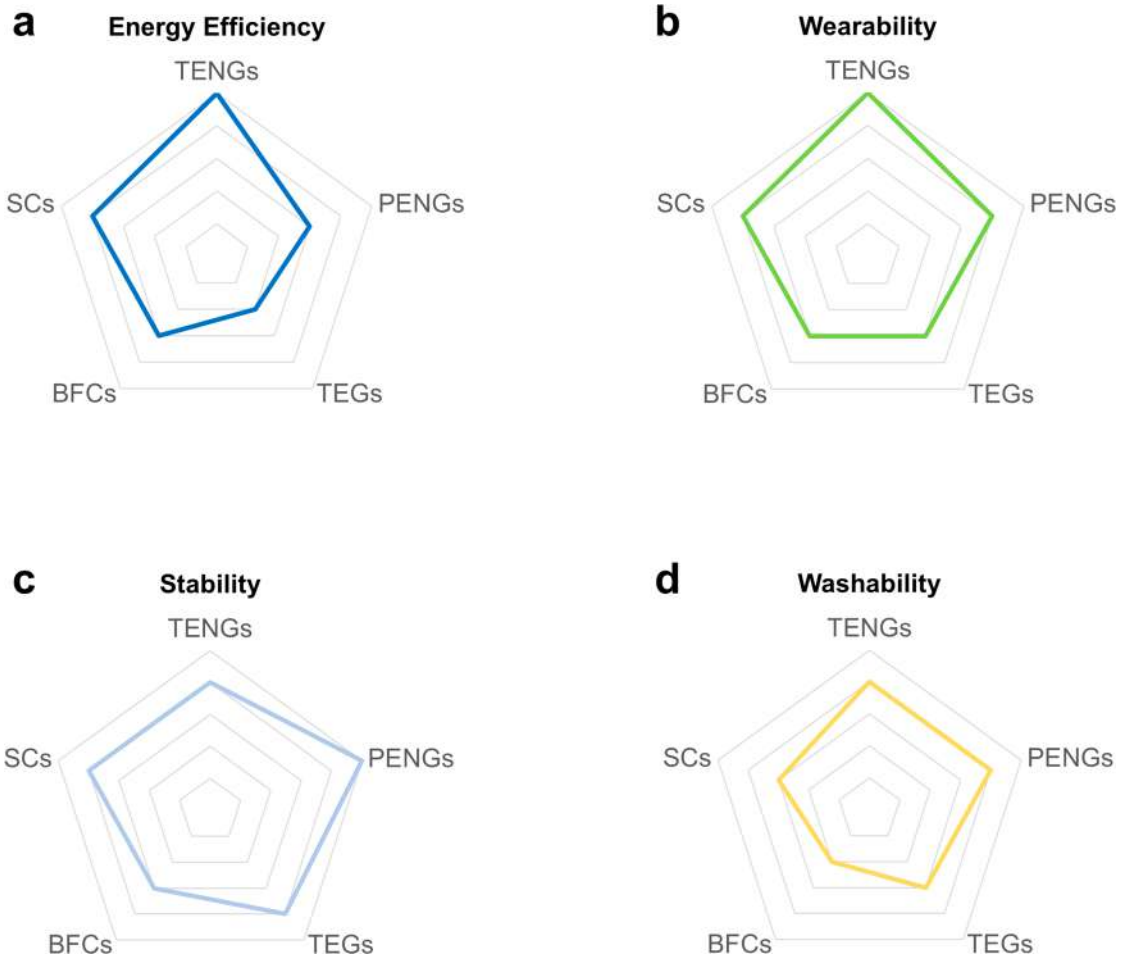

Figure 16. Schematic illustration of the proposed evaluation standard of smart textiles for energy harvesting. Each kind of textile generator was evaluated in terms of (a) energy efficiency, (b) wearability, (c) stability, and (d) washability. Perfect, good, fair, and poor performances are scored 5, 4, 3, and 2, respectively. Scale: each ring is 1 score, and the full score is 5.

considering its fabrication efficiency, as well as the customized and personalized requirements of individuals.

7.10. Self-Healing

While wearing smart textiles, they are constantly subjected to mechanical deformation, including bending, twisting, pressing, sliding, and so on, which may cause damage and malfunction.[240] Smart textiles with a self-healing ability, for example, a TENG consisting of self-healable PDMS elastomers,[800] could open a new door to address this issue. In that case, textile damage could be repaired by itself. Therefore, applying self-healing materials to smart textiles is highly desirable for long-term on-body applications.

7.11. Evaluation Standard

Although there have been hundreds of relevant research studies on smart textiles, it is still challenging to compare their performance, such as wearability and energy conversion efficiency, due to varied working principles, testing conditions, and application scenarios. Thus, the evaluation standard during commercialization of energy harvesting textiles is a matter of great urgency for consumers as well as businesses. To this end, we propose various merits with which to assess smart textiles simultaneously, including energy efficiency (Figure 16a), wearability (Figure 16b), stability (Figure 16c), washability (Figure 16d), and so on. This proposed evaluation standard may benefit the future perfection of an assessment for the field of smart textiles.

Overall, the rise of energy harvesting textiles opens an emerging route toward a prospective energy solution for next-generation on-body electronics. Challenges coexist with opportunities, and many more research efforts are highly desired to improve energy conversion efficiency, output stability, robustness, wearability, washability, packaging, aesthetics, scalable and advanced fabrication, self-healing, and an assessment system of smart textiles for energy harvesting. We anticipate the widespread applications and commercialization of smart textiles will be adopted in a variety of scenarios and improve our way of living in the near future.

AUTHOR INFORMATION

Corresponding Author

Jun Chen − *Department of Bioengineering, University of California, Los Angeles, Los Angeles, California 90095, United States*; orcid.org/0000-0002-3439-0495; Email: jun.chen@ucla.edu

Authors

Guorui Chen − *Department of Bioengineering, University of California, Los Angeles, Los Angeles, California 90095, United States*

https://dx.doi.org/10.1021/acs.chemrev.9b00821
Chem. Rev. 2020, 120, 3668−3720

Yongzhong Li − *Department of Bioengineering, University of California, Los Angeles, Los Angeles, California 90095, United States*

Michael Bick − *Department of Bioengineering, University of California, Los Angeles, Los Angeles, California 90095, United States*

Complete contact information is available at: https://pubs.acs.org/10.1021/acs.chemrev.9b00821

Notes

The authors declare no competing financial interest.

Biographies

Guorui Chen is currently a Ph.D. student in the Department of Bioengineering, University of California, Los Angeles, under the supervision of Prof. Jun Chen.

Yongzhong Li was a summer intern in the Department of Bioengineering, University of California, Los Angeles, under the supervision of Prof. Jun Chen.

Michael Bick is currently a junior undergraduate in the Department of Bioengineering at the University of California, Los Angeles, under the supervision of Prof. Jun Chen.

Jun Chen is currently an assistant professor in the Department of Bioengineering, University of California, Los Angeles. His current research focuses on nanotechnology and bioelectronics for energy, sensing, environment, and therapy applications in the form of smart textiles, wearables, and body area networks. He has already published two books and 100 journal articles, and 58 of them are as first/corresponding authors in *Nature Energy*, *Nature Electronics*, *Nature Sustainability*, *Nature Communications*, *Joule*, *Matter*, and many others. He also filed 14 U.S. patents and licensed one. He is currently an Associate Editor of *Biosensors and Bioelectronics*, and an Editorial Board Member of *Nano-Micro Letters*, *Frontiers in Pharmacology*, *Frontiers in Chemistry*, and *Smart Materials in Medicine*. With a current h-index of 58, he was identified to be one of the world's most influential researchers in the field of Materials Science by the Web of Science Group and on the global list of The Highly Cited Researchers 2019.

ACKNOWLEDGMENTS

We acknowledge the Henry Samueli School of Engineering & Applied Science and the Department of Bioengineering at the University of California, Los Angeles, for the startup support.

ABBREVIATIONS USED

PCBM = [6,6]-phenyl-C61-butyric acid methyl ester
PC71BM = [6,6]-phenyl-C71-butyric acid methyl ester
BFCs = biofuel cells
CdTe = cadmium telluride
CNT = carbon nanotube
CNTF = carbon nanotube fiber
CIGS = copper indium gallium selenide
CE = counter electrode
DSSCs = dye-sensitized solar cells
EJ = exajoules
FF = fill-factor
FEP = fluorinated ethylene propylene
HGs = hybrid generators
ITO = indium tin oxide
IoT = Internet of Things
PZT = lead zirconate titanate
LED = light emitting diode
MWCNT = multiwalled CNT
NWs = nanowires
NWPU = nonionic waterborne polyurethane
1D = one-dimensional
V_{oc} = open-circuit voltage
OSCs = organic solar cells
PSCs = perovskite solar cells
PE = photoanode
PENGs = piezoelectric nanogenerators
PEDOT:PSS = poly(3,4-ethylenedioxythiophene):polystyrene sulfonate
P3HT = poly(3-hexylthiophene)
PVP = poly(*N*-vinylpyrrolidone)
PTB7-Th = poly[4,8bis[5-(2-ethylhexyl)thiophen-2-yl]-benzo[1,2-*b*:4,5-*b*0]dithiophene2,6-diyl-*alt*-3-fluoro-2-[(2-ethylhexyl)carbonyl]thieno[3,4-*b*]thiophene-4,6-diyl]
PAN = polyacrylonitrile
PBT = polybutylene terephthalate
PDMS = polydimethylsiloxane
PET = polyethylene terephthalate
PI = polyimide
PTFE = polytetrafluoroethylene
PU = polyurethane
PVC = polyvinyl chloride
PVDF = polyvinylidene difluoride
PCE = power conversion efficiency
I_{sc} = short-circuit current
J_{sc} = short-circuit current density
SCs = solar cells
TEGs = thermoelectric generators
3D = three-dimensional
TENGs = triboelectric nanogenerators
TPENGs = triboelectric piezoelectric nanogenerators
2D = two-dimensional
ZnO = zinc oxide

REFERENCES

(1) Dudley, B. *BP Statistical Review of World Energy: An Unsustainable Path*. BP: London, 11 June 2019; https://www.bp.com/en/global/corporate/news-and-insights/press-releases/bp-statistical-review-of-world-energy-2019.html (accessed 2019-12-07).
(2) Shafiee, S.; Topal, E. When Will Fossil Fuel Reserves Be Diminished? *Energy Policy* **2009**, *37*, 181−189.
(3) Abas, N.; Kalair, A.; Khan, N. Review of Fossil Fuels and Future Energy Technologies. *Futures* **2015**, *69*, 31−49.
(4) Chu, S.; Cui, Y.; Liu, N. The Path Towards Sustainable Energy. *Nat. Mater.* **2017**, *16*, 16−22.
(5) Chu, S.; Majumdar, A. Opportunities and Challenges for a Sustainable Energy Future. *Nature* **2012**, *488*, 294−303.
(6) Guo, X.; Zhou, X.; Hale, L.; Yuan, M.; Ning, D.; Feng, J.; Shi, Z.; Li, Z.; Feng, B.; Gao, Q.; et al. Climate Warming Accelerates Temporal Scaling of Grassland Soil Microbial Biodiversity. *Nat. Ecol. Evol.* **2019**, *3*, 612−619.
(7) King, D. A. Climate Change Science: Adapt, Mitigate, or Ignore? *Science* **2004**, *303*, 176−177.
(8) Roemmich, D.; Church, J.; Gilson, J.; Monselesan, D.; Sutton, P.; Wijffels, S. Unabated Planetary Warming and Its Ocean Structure since 2006. *Nat. Clim. Chang.* **2015**, *5*, 240−245.
(9) Xue, G.; Xu, Y.; Ding, T.; Li, J.; Yin, J.; Fei, W.; Cao, Y.; Yu, J.; Yuan, L.; Gong, L.; et al. Water-Evaporation-Induced Electricity with Nanostructured Carbon Materials. *Nat. Nanotechnol.* **2017**, *12*, 317−321.
(10) Mercer, J. H. West Antarctic Ice Sheet and CO_2 Greenhouse Effect: A Threat of Disaster. *Nature* **1978**, *271*, 321−325.

(11) Von Blottnitz, H.; Curran, M. A. A Review of Assessments Conducted on Bio-Ethanol as a Transportation Fuel from a Net Energy, Greenhouse Gas, and Environmental Life Cycle Perspective. *J. Cleaner Prod.* **2007**, *15*, 607−619.
(12) Parker, R. W. R.; Blanchard, J. L.; Gardner, C.; Green, B. S.; Hartmann, K.; Tyedmers, P. H.; Watson, R. A. Fuel Use and Greenhouse Gas Emissions of World Fisheries. *Nat. Clim. Chang.* **2018**, *8*, 333−337.
(13) Burns, D. A.; Aherne, J.; Gay, D. A.; Lehmann, C. M. B. Acid Rain and Its Environmental Effects: Recent Scientific Advances Preface. *Atmos. Environ.* **2016**, *146*, 1−4.
(14) Likens, G. E.; Bormann, F. H. Acid Rain: A Serious Regional Environmental Problem. *Science* **1974**, *184*, 1176−1179.
(15) Livingston, R. A. Acid Rain Attack on Outdoor Sculpture in Perspective. *Atmos. Environ.* **2016**, *146*, 332−345.
(16) Cavicchioli, R.; Ripple, W. J.; Timmis, K. N.; Azam, F.; Bakken, L. R.; Baylis, M.; Behrenfeld, M. J.; Boetius, A.; Boyd, P. W.; Classen, A. T.; et al. Scientists' Warning to Humanity: Microorganisms and Climate Change. *Nat. Rev. Microbiol.* **2019**, *17*, 569−586.
(17) Teräväinen, T. Visions of Energy Futures. *Nat. Energy* **2018**, *3*, 923−924.
(18) Zhou, Y. J.; Kerkhoven, E. J.; Nielsen, J. Barriers and Opportunities in Bio-Based Production of Hydrocarbons. *Nat. Energy* **2018**, *3*, 925−935.
(19) Liu, Z.; Guan, D.; Wei, W.; Davis, S. J.; Ciais, P.; Bai, J.; Peng, S.; Zhang, Q.; Hubacek, K.; Marland, G.; et al. Reduced Carbon Emission Estimates from Fossil Fuel Combustion and Cement Production in China. *Nature* **2015**, *524*, 335−338.
(20) McGlade, C.; Ekins, P. The Geographical Distribution of Fossil Fuels Unused When Limiting Global Warming to 2 °C. *Nature* **2015**, *517*, 187−190.
(21) Jakob, M.; Hilaire, J. Climate Science: Unburnable Fossil-Fuel Reserves. *Nature* **2015**, *517*, 150−152.
(22) Shindell, D.; Smith, C. J. Climate and Air-Quality Benefits of a Realistic Phase-out of Fossil Fuels. *Nature* **2019**, *573*, 408−411.
(23) Sofiev, M.; Winebrake, J. J.; Johansson, L.; Carr, E. W.; Prank, M.; Soares, J.; Vira, J.; Kouznetsov, R.; Jalkanen, J. P.; Corbett, J. J. Cleaner Fuels for Ships Provide Public Health Benefits with Climate Tradeoffs. *Nat. Commun.* **2018**, *9*, 406.
(24) Landrigan, P. J.; Fuller, R.; Acosta, N. J. R.; Adeyi, O.; Arnold, R.; Basu, N. N.; Balde, A. B.; Bertollini, R.; Bose-O'Reilly, S.; Boufford, J. I.; et al. The Lancet Commission on Pollution and Health. *Lancet* **2018**, *391*, 462−512.
(25) Sutton, M. A.; Oenema, O.; Erisman, J. W.; Leip, A.; van Grinsven, H.; Winiwarter, W. Too Much of a Good Thing. *Nature* **2011**, *472*, 159−161.
(26) Hsu, A.; Cheng, Y.; Weinfurter, A.; Xu, K.; Yick, C. Track Climate Pledges of Cities and Companies. *Nature* **2016**, *532*, 303−306.
(27) Platt, S. M.; Haddad, I. E.; Pieber, S. M.; Huang, R. J.; Zardini, A. A.; Clairotte, M.; Suarez-Bertoa, R.; Barmet, P.; Pfaffenberger, L.; Wolf, R.; et al. Two-Stroke Scooters Are a Dominant Source of Air Pollution in Many Cities. *Nat. Commun.* **2014**, *5*, 3749.
(28) Yang, Y.; Tilman, D.; Lehman, C.; Trost, J. J. Sustainable Intensification of High-Diversity Biomass Production for Optimal Biofuel Benefits. *Nat. Sustain.* **2018**, *1*, 686−692.
(29) Gruber, N.; Galloway, J. N. An Earth-System Perspective of the Global Nitrogen Cycle. *Nature* **2008**, *451*, 293−296.
(30) Gustavsson, L.; Haus, S.; Lundblad, M.; Lundstrom, A.; Ortiz, C. A.; Sathre, R.; Truong, N. L.; Wikberg, P. E. Climate Change Effects of Forestry and Substitution of Carbon-Intensive Materials and Fossil Fuels. *Renew. Sustain. Energy Rev.* **2017**, *67*, 612−624.
(31) Cox, P. M.; Huntingford, C.; Williamson, M. S. Emergent Constraint on Equilibrium Climate Sensitivity from Global Temperature Variability. *Nature* **2018**, *553*, 319−322.
(32) Fernández-Martínez, M.; Sardans, J.; Chevallier, F.; Ciais, P.; Obersteiner, M.; Vicca, S.; Canadell, J.; Bastos, A.; Friedlingstein, P.; Sitch, S.; et al. Global Trends in Carbon Sinks and Their Relationships with CO_2 and Temperature. *Nat. Clim. Chang.* **2019**, *9*, 73−79.
(33) Rogelj, J.; Popp, A.; Calvin, K. V.; Luderer, G.; Emmerling, J.; Gernaat, D.; Fujimori, S.; Strefler, J.; Hasegawa, T.; Marangoni, G.; et al. Scenarios Towards Limiting Global Mean Temperature Increase Below 1.5 °C. *Nat. Clim. Chang.* **2018**, *8*, 325−332.
(34) Delfino, R. J.; Tjoa, T.; Gillen, D. L.; Staimer, N.; Polidori, A.; Arhami, M.; Jamner, L.; Sioutas, C.; Longhurst, J. Traffic-Related Air Pollution and Blood Pressure in Elderly Subjects with Coronary Artery Disease. *Epidemiology* **2010**, *21*, 396−404.
(35) Jerrett, M. Atmospheric Science: The Death Toll from Air-Pollution Sources. *Nature* **2015**, *525*, 330−331.
(36) Thurston, G. D.; Burnett, R. T.; Turner, M. C.; Shi, Y.; Krewski, D.; Lall, R.; Ito, K.; Jerrett, M.; Gapstur, S. M.; Diver, W. R.; Pope, C. A. Ischemic Heart Disease Mortality and Long-Term Exposure to Source-Related Components of U.S. Fine Particle Air Pollution. *Environ. Health Perspect.* **2016**, *124*, 785−794.
(37) Figueres, C.; Le Quere, C.; Mahindra, A.; Bate, O.; Whiteman, G.; Peters, G.; Guan, D. Emissions Are Still Rising: Ramp up the Cuts. *Nature* **2018**, *564*, 27−30.
(38) Lelieveld, J.; Evans, J. S.; Fnais, M.; Giannadaki, D.; Pozzer, A. The Contribution of Outdoor Air Pollution Sources to Premature Mortality on a Global Scale. *Nature* **2015**, *525*, 367−371.
(39) Raaschou-Nielsen, O.; Andersen, Z. J.; Beelen, R.; Samoli, E.; Stafoggia, M.; Weinmayr, G.; Hoffmann, B.; Fischer, P.; Nieuwenhuijsen, M. J.; Brunekreef, B.; et al. Air Pollution and Lung Cancer Incidence in 17 European Cohorts: Prospective Analyses from the European Study of Cohorts for Air Pollution Effects (ESCAPE). *Lancet Oncol.* **2013**, *14*, 813−822.
(40) Perera, F. Pollution from Fossil-Fuel Combustion Is the Leading Environmental Threat to Global Pediatric Health and Equity: Solutions Exist. *Int. J. Environ. Res. Public Health* **2018**, *15*, 16.
(41) Perera, F. P. Multiple Threats to Child Health from Fossil Fuel Combustion: Impacts of Air Pollution and Climate Change. *Environ. Health Perspect.* **2017**, *125*, 141−148.
(42) Watts, N.; Adger, W. N.; Agnolucci, P.; Blackstock, J.; Byass, P.; Cai, W.; Chaytor, S.; Colbourn, T.; Collins, M.; Cooper, A.; et al. Health and Climate Change: Policy Responses to Protect Public Health. *Lancet* **2015**, *386*, 1861−1914.
(43) Epstein, P. R.; Buonocore, J. J.; Eckerle, K.; Hendryx, M.; Stout, B. M., Iii; Heinberg, R.; Clapp, R. W.; May, B.; Reinhart, N. L.; Ahern, M. M.; et al. Full Cost Accounting for the Life Cycle of Coal. *Ann. N. Y. Acad. Sci.* **2011**, *1219*, 73−98.
(44) Howarth, R. W.; Ingraffea, A.; Engelder, T. Should Fracking Stop? Extracting Gas from Shale Increases the Availability of This Resource, but the Health and Environmental Risks May Be Too High. *Nature* **2011**, *477*, 271−276.
(45) Pandey, B.; Agrawal, M.; Singh, S. Assessment of Air Pollution around Coal Mining Area: Emphasizing on Spatial Distributions, Seasonal Variations and Heavy Metals, Using Cluster and Principal Component Analysis. *Atmos. Pollut. Res.* **2014**, *5*, 79−86.
(46) Allred, B. W.; Smith, W. K.; Twidwell, D.; Haggerty, J. H.; Running, S. W.; Naugle, D. E.; Fuhlendorf, S. D. Ecosystem Services Lost to Oil and Gas in North America. *Science* **2015**, *348*, 401−402.
(47) Spiegel, S.; Brown, B. Fossil Fuels: Heed Local Impact of Coal Mining. *Nature* **2017**, *550*, 43.
(48) Rozell, D. J.; Reaven, S. J. Water Pollution Risk Associated with Natural Gas Extraction from the Marcellus Shale. *Risk Anal* **2012**, *32*, 1382−1393.
(49) Ashton, K. That 'Internet of Things' Thing. *RFID J.* **2009**, *22*, 97−114.
(50) Gubbi, J.; Buyya, R.; Marusic, S.; Palaniswami, M. Internet of Things (Iot): A Vision, Architectural Elements, and Future Directions. *Future Gener. Comp. Sy* **2013**, *29*, 1645−1660.
(51) Lee, I.; Lee, K. The Internet of Things (IoT): Applications, Investments, and Challenges for Enterprises. *Bus. Horiz.* **2015**, *58*, 431−440.
(52) Atzori, L.; Iera, A.; Morabito, G. The Internet of Things: A Survey. *Comput. Netw* **2010**, *54*, 2787−2805.

https://dx.doi.org/10.1021/acs.chemrev.9b00821
Chem. Rev. 2020, 120, 3668−3720

(53) Wang, Z. L. Entropy Theory of Distributed Energy for Internet of Things. *Nano Energy* **2019**, *58*, 669−672.
(54) Grey, C. P.; Tarascon, J. M. Sustainability and in Situ Monitoring in Battery Development. *Nat. Mater.* **2017**, *16*, 45−56.
(55) Gu, P.; Zheng, M. B.; Zhao, Q. X.; Xiao, X.; Xue, H. G.; Pang, H. Rechargeable Zinc-Air Batteries: A Promising Way to Green Energy. *J. Mater. Chem. A* **2017**, *5*, 7651−7666.
(56) He, Y. H.; Matthews, B.; Wang, J. Y.; Song, L.; Wang, X. X.; Wu, G. Innovation and Challenges in Materials Design for Flexible Rechargeable Batteries: From 1D to 3D. *J. Mater. Chem. A* **2018**, *6*, 735−753.
(57) Wang, Y. X.; Liu, B.; Li, Q. Y.; Cartmell, S.; Ferrara, S.; Deng, Z. Q. D.; Xiao, J. Lithium and Lithium Ion Batteries for Applications in Microelectronic Devices: A Review. *J. Power Sources* **2015**, *286*, 330−345.
(58) Quartarone, E.; Mustarelli, P. Electrolytes for Solid-State Lithium Rechargeable Batteries: Recent Advances and Perspectives. *Chem. Soc. Rev.* **2011**, *40*, 2525−2540.
(59) Gao, W.; Emaminejad, S.; Nyein, H. Y. Y.; Challa, S.; Chen, K.; Peck, A.; Fahad, H. M.; Ota, H.; Shiraki, H.; Kiriya, D.; et al. Fully Integrated Wearable Sensor Arrays for Multiplexed in Situ Perspiration Analysis. *Nature* **2016**, *529*, 509−514.
(60) Kim, J.; Campbell, A. S.; de Avila, B. E.; Wang, J. Wearable Biosensors for Healthcare Monitoring. *Nat. Biotechnol.* **2019**, *37*, 389−406.
(61) Liu, Y.; Pharr, M.; Salvatore, G. A. Lab-on-Skin: A Review of Flexible and Stretchable Electronics for Wearable Health Monitoring. *ACS Nano* **2017**, *11*, 9614−9635.
(62) Trung, T. Q.; Lee, N. E. Flexible and Stretchable Physical Sensor Integrated Platforms for Wearable Human-Activity Monitoringand Personal Healthcare. *Adv. Mater.* **2016**, *28*, 4338−4372.
(63) Kenry; Yeo, J. C.; Lim, C. T. Emerging Flexible and Wearable Physical Sensing Platforms for Healthcare and Biomedical Applications. *Microsyst. Nanoeng.* **2016**, *2*, 16043.
(64) Zang, Y. P.; Zhang, F. J.; Di, C. A.; Zhu, D. B. Advances of Flexible Pressure Sensors toward Artificial Intelligence and Health Care Applications. *Mater. Horiz.* **2015**, *2*, 140−156.
(65) Hussain, A. M.; Ghaffar, F. A.; Park, S. I.; Rogers, J. A.; Shamim, A.; Hussain, M. M. Metal/Polymer Based Stretchable Antenna for Constant Frequency far-Field Communication in Wearable Electronics. *Adv. Funct. Mater.* **2015**, *25*, 6565−6575.
(66) Kim, J.; Banks, A.; Cheng, H.; Xie, Z.; Xu, S.; Jang, K. I.; Lee, J. W.; Liu, Z.; Gutruf, P.; Huang, X.; et al. Epidermal Electronics with Advanced Capabilities in near-Field Communication. *Small* **2015**, *11*, 906−912.
(67) Kim, J.; Banks, A.; Xie, Z.; Heo, S. Y.; Gutruf, P.; Lee, J. W.; Xu, S.; Jang, K. I.; Liu, F.; Brown, G.; et al. Miniaturized Flexible Electronic Systems with Wireless Power and near-Field Communication Capabilities. *Adv. Funct. Mater.* **2015**, *25*, 4761−4767.
(68) Son, D.; Kang, J.; Vardoulis, O.; Kim, Y.; Matsuhisa, N.; Oh, J. Y.; To, J. W.; Mun, J.; Katsumata, T.; Liu, Y.; et al. An Integrated Self-Healable Electronic Skin System Fabricated via Dynamic Reconstruction of a Nanostructured Conducting Network. *Nat. Nanotechnol.* **2018**, *13*, 1057−1065.
(69) Chen, R. J.; Zhang, Y. B.; Liu, T.; Xu, B. Q.; Lin, Y. H.; Nan, C. W.; Shen, Y. Addressing the Interface Issues in All-Solid-State Bulk-Type Lithium Ion Battery via an All-Composite Approach. *ACS Appl. Mater. Interfaces* **2017**, *9*, 9654−9661.
(70) Kim, J. G.; Son, B.; Mukherjee, S.; Schuppert, N.; Bates, A.; Kwon, O.; Choi, M. J.; Chung, H. Y.; Park, S. A Review of Lithium and Non-Lithium Based Solid State Batteries. *J. Power Sources* **2015**, *282*, 299−322.
(71) Liu, T.; Ren, Y. Y.; Shen, Y.; Zhao, S. X.; Lin, Y. H.; Nan, C. W. Achieving High Capacity in Bulk-Type Solid-State Lithium Ion Battery Based on $Li_{6.75}La_3Zr_{1.75}Ta_{0.25}O_{12}$ Electrolyte: Interfacial Resistance. *J. Power Sources* **2016**, *324*, 349−357.
(72) Ruiz, O.; Cochrane, M.; Li, M. N.; Yan, Y.; Ma, K.; Fu, J. T.; Wang, Z. Y.; Tolbert, S. H.; Shenoy, V. B.; Detsi, E. Enhanced Cycling Stability of Macroporous Bulk Antimony-Based Sodium-Ion Battery Anodes Enabled through Active/Inactive Composites. *Adv. Energy Mater.* **2018**, *8*, 1801781.
(73) Sun, C. W.; Liu, J.; Gong, Y. D.; Wilkinson, D. P.; Zhang, J. J. Recent Advances in All-Solid-State Rechargeable Lithium Batteries. *Nano Energy* **2017**, *33*, 363−386.
(74) Zhang, Y.; Lai, J.; Gong, Y.; Hu, Y.; Liu, J.; Sun, C.; Wang, Z. L. A Safe High-Performance All-Solid-State Lithium-Vanadium Battery with a Freestanding V_2O_5 Nanowire Composite Paper Cathode. *ACS Appl. Mater. Interfaces* **2016**, *8*, 34309−34316.
(75) Fu, J.; Cano, Z. P.; Park, M. G.; Yu, A.; Fowler, M.; Chen, Z. Electrically Rechargeable Zinc-Air Batteries: Progress, Challenges, and Perspectives. *Adv. Mater.* **2017**, *29*, 1604685.
(76) Kang, D. H.; Chen, M.; Ogunseitan, O. A. Potential Environmental and Human Health Impacts of Rechargeable Lithium Batteries in Electronic Waste. *Environ. Sci. Technol.* **2013**, *47*, 5495−5503.
(77) Li, Y.; Dai, H. Recent Advances in Zinc-Air Batteries. *Chem. Soc. Rev.* **2014**, *43*, 5257−5275.
(78) Slater, M. D.; Kim, D.; Lee, E.; Johnson, C. S. Sodium-Ion Batteries. *Adv. Funct. Mater.* **2013**, *23*, 947−958.
(79) Yabuuchi, N.; Kubota, K.; Dahbi, M.; Komaba, S. Research Development on Sodium-Ion Batteries. *Chem. Rev.* **2014**, *114*, 11636−11682.
(80) Goodenough, J. B.; Park, K. S. The Li-Ion Rechargeable Battery: A Perspective. *J. Am. Chem. Soc.* **2013**, *135*, 1167−1176.
(81) Lin, M. C.; Gong, M.; Lu, B.; Wu, Y.; Wang, D. Y.; Guan, M.; Angell, M.; Chen, C.; Yang, J.; Hwang, B. J.; Dai, H. An Ultrafast Rechargeable Aluminium-Ion Battery. *Nature* **2015**, *520*, 324−328.
(82) Placke, T.; Kloepsch, R.; Duhnen, S.; Winter, M. Lithium Ion, Lithium Metal, and Alternative Rechargeable Battery Technologies: The Odyssey for High Energy Density. *J. Solid State Electrochem.* **2017**, *21*, 1939−1964.
(83) Ponrouch, A.; Frontera, C.; Barde, F.; Palacin, M. R. Towards a Calcium-Based Rechargeable Battery. *Nat. Mater.* **2016**, *15*, 169−172.
(84) Whittingham, M. S. Lithium Batteries and Cathode Materials. *Chem. Rev.* **2004**, *104*, 4271−4301.
(85) Dagdeviren, C.; Li, Z.; Wang, Z. L. Energy Harvesting from the Animal/Human Body for Self-Powered Electronics. *Annu. Rev. Biomed. Eng.* **2017**, *19*, 85−108.
(86) Stephen, N. G. On Energy Harvesting from Ambient Vibration. *J. Sound Vib.* **2006**, *293*, 409−425.
(87) Yildiz, F. Potential Ambient Energy-Harvesting Sources and Techniques. *J. Technol. Studies.* **2009**, *35*, 40−48.
(88) Akhtar, F.; Rehmani, M. H. Energy Harvesting for Self-Sustainable Wireless Body Area Networks. *IT Professional* **2017**, *19*, 32−40.
(89) Im, H.; Moon, H. G.; Lee, J. S.; Chung, I. Y.; Kang, T. J.; Kim, Y. H. Flexible Thermocells for Utilization of Body Heat. *Nano Res.* **2014**, *7*, 443−452.
(90) Leonov, V. Thermoelectric Energy Harvesting of Human Body Heat for Wearable Sensors. *IEEE Sens. J.* **2013**, *13*, 2284−2291.
(91) Starner, T. Human-Powered Wearable Computing. *IBM Syst. J.* **1996**, *35*, 618−629.
(92) Huang, L. B.; Bai, G. X.; Wong, M. C.; Yang, Z. B.; Xu, W.; Hao, J. H. Magnetic-Assisted Noncontact Triboelectric Nanogenerator Converting Mechanical Energy into Electricity and Light Emissions. *Adv. Mater.* **2016**, *28*, 2744−2751.
(93) Wang, X.; Niu, S.; Yi, F.; Yin, Y.; Hao, C.; Dai, K.; Zhang, Y.; You, Z.; Wang, Z. L. Harvesting Ambient Vibration Energy over a Wide Frequency Range for Self-Powered Electronics. *ACS Nano* **2017**, *11*, 1728−1735.
(94) Zi, Y.; Guo, H.; Wen, Z.; Yeh, M. H.; Hu, C.; Wang, Z. L. Harvesting Low-Frequency (<5 Hz) Irregular Mechanical Energy: A Possible Killer Application of Triboelectric Nanogenerator. *ACS Nano* **2016**, *10*, 4797−4805.
(95) Zi, Y.; Wang, J.; Wang, S.; Li, S.; Wen, Z.; Guo, H.; Wang, Z. L. Effective Energy Storage from a Triboelectric Nanogenerator. *Nat. Commun.* **2016**, *7*, 10987.

https://dx.doi.org/10.1021/acs.chemrev.9b00821
Chem. Rev. 2020, 120, 3668−3720

(96) Bandodkar, A. J.; You, J. M.; Kim, N. H.; Gu, Y.; Kumar, R.; Mohan, A. M. V.; Kurniawan, J.; Imani, S.; Nakagawa, T.; Parish, B.; et al. Soft, Stretchable, High Power Density Electronic Skin-Based Biofuel Cells for Scavenging Energy from Human Sweat. *Energy Environ. Sci.* **2017**, *10*, 1581−1589.
(97) Szczupak, A.; Halamek, J.; Halamkova, L.; Bocharova, V.; Alfonta, L.; Katz, E. Living Battery - Biofuel Cells Operating in Vivo in Clams. *Energy Environ. Sci.* **2012**, *5*, 8891−8895.
(98) Zebda, A.; Alcaraz, J. P.; Vadgama, P.; Shleev, S.; Minteer, S. D.; Boucher, F.; Cinquin, P.; Martin, D. K. Challenges for Successful Implantation of Biofuel Cells. *Bioelectrochemistry* **2018**, *124*, 57−72.
(99) Freitag, M.; Teuscher, J.; Saygili, Y.; Zhang, X.; Giordano, F.; Liska, P.; Hua, J.; Zakeeruddin, S. M.; Moser, J.-E.; Grätzel, M.; Hagfeldt, A. Dye-Sensitized Solar Cells for Efficient Power Generation under Ambient Lighting. *Nat. Photonics* **2017**, *11*, 372−378.
(100) Kim, S.; Vyas, R.; Bito, J.; Niotaki, K.; Collado, A.; Georgiadis, A.; Tentzeris, M. M. Ambient RF Energy-Harvesting Technologies for Self-Sustainable Standalone Wireless Sensor Platforms. *Proc. IEEE* **2014**, *102*, 1649−1666.
(101) Li, Y.; Grabham, N. J.; Beeby, S. P.; Tudor, M. J. The Effect of the Type of Illumination on the Energy Harvesting Performance of Solar Cells. *Sol. Energy* **2015**, *111*, 21−29.
(102) Tan, Y. K.; Panda, S. K. Energy Harvesting from Hybrid Indoor Ambient Light and Thermal Energy Sources for Enhanced Performance of Wireless Sensor Nodes. *IEEE Trans. Ind. Electron.* **2011**, *58*, 4424−4435.
(103) Tao, X. Study of Fiber-Based Wearable Energy Systems. *Acc. Chem. Res.* **2019**, *52*, 307−315.
(104) Misra, V.; Bozkurt, A.; Calhoun, B.; Jackson, T. N.; Jur, J. S.; Lach, J.; Lee, B.; Muth, J.; Oralkan, O.; Ozturk, M.; et al. Flexible Technologies for Self-Powered Wearable Health and Environmental Sensing. *Proc. IEEE* **2015**, *103*, 665−681.
(105) Proto, A.; Penhaker, M.; Conforto, S.; Schmid, M. Nanogenerators for Human Body Energy Harvesting. *Trends Biotechnol.* **2017**, *35*, 610−624.
(106) Radousky, H. B.; Liang, H. Energy Harvesting: An Integrated View of Materials, Devices and Applications. *Nanotechnology* **2012**, *23*, 502001.
(107) Ray, T. R.; Choi, J.; Bandodkar, A. J.; Krishnan, S.; Gutruf, P.; Tian, L.; Ghaffari, R.; Rogers, J. A. Bio-Integrated Wearable Systems: A Comprehensive Review. *Chem. Rev.* **2019**, *119*, 5461−5533.
(108) Sue, C. Y.; Tsai, N. C. Human Powered Mems-Based Energy Harvest Devices. *Appl. Energy* **2012**, *93*, 390−403.
(109) Wang, Z. L.; Wu, W. Nanotechnology-Enabled Energy Harvesting for Self-Powered Micro-/Nanosystems. *Angew. Chem., Int. Ed.* **2012**, *51*, 11700−11721.
(110) Yi, F.; Ren, H.; Shan, J.; Sun, X.; Wei, D.; Liu, Z. Wearable Energy Sources Based on 2D Materials. *Chem. Soc. Rev.* **2018**, *47*, 3152−3188.
(111) Bai, P.; Zhu, G.; Lin, Z. H.; Jing, Q.; Chen, J.; Zhang, G.; Ma, J.; Wang, Z. L. Integrated Multilayered Triboelectric Nanogenerator for Harvesting Biomechanical Energy from Human Motions. *ACS Nano* **2013**, *7*, 3713−3719.
(112) Cheng, X. L.; Meng, B.; Zhang, X. S.; Han, M. D.; Su, Z. M.; Zhang, H. X. Wearable Electrode-Free Triboelectric Generator for Harvesting Biomechanical Energy. *Nano Energy* **2015**, *12*, 19−25.
(113) Hou, T. C.; Yang, Y.; Zhang, H. L.; Chen, J.; Chen, L. J.; Wang, Z. L. Triboelectric Nanogenerator Built inside Shoe Insole for Harvesting Walking Energy. *Nano Energy* **2013**, *2*, 856−862.
(114) Jeong, C. K.; Lee, J.; Han, S.; Ryu, J.; Hwang, G. T.; Park, D. Y.; Park, J. H.; Lee, S. S.; Byun, M.; Ko, S. H.; et al. A Hyper-Stretchable Elastic-Composite Energy Harvester. *Adv. Mater.* **2015**, *27*, 2866−2875.
(115) Kim, S.; Gupta, M. K.; Lee, K. Y.; Sohn, A.; Kim, T. Y.; Shin, K. S.; Kim, D.; Kim, S. K.; Lee, K. H.; Shin, H. J.; et al. Transparent Flexible Graphene Triboelectric Nanogenerators. *Adv. Mater.* **2014**, *26*, 3918−3925.
(116) Li, Z.; Chen, J.; Yang, J.; Su, Y.; Fan, X.; Wu, Y.; Yu, C.; Wang, Z. L. B-Cyclodextrin Enhanced Triboelectrification for Self-Powered Phenol Detection and Electrochemical Degradation. *Energy Environ. Sci.* **2015**, *8*, 887−896.
(117) Lin, Z. H.; Zhu, G.; Zhou, Y. S.; Yang, Y.; Bai, P.; Chen, J.; Wang, Z. L. A Self-Powered Triboelectric Nanosensor for Mercury Ion Detection. *Angew. Chem., Int. Ed.* **2013**, *52*, 5065−5069.
(118) Niu, S. M.; Wang, Z. L. Theoretical Systems of Triboelectric Nanogenerators. *Nano Energy* **2015**, *14*, 161−192.
(119) Pu, X.; Liu, M. M.; Chen, X. Y.; Sun, J. M.; Du, C. H.; Zhang, Y.; Zhai, J. Y.; Hu, W. G.; Wang, Z. L. Ultrastretchable, Transparent Triboelectric Nanogenerator as Electronic Skin for Biomechanical Energy Harvesting and Tactile Sensing. *Sci. Adv.* **2017**, *3*, No. e1700015.
(120) Su, Y. J.; Chen, J.; Wu, Z. M.; Jiang, Y. D. Low Temperature Dependence of Triboelectric Effect for Energy Harvesting and Self-Powered Active Sensing. *Appl. Phys. Lett.* **2015**, *106*, 013114.
(121) Su, Y.; Zhu, G.; Yang, W.; Yang, J.; Chen, J.; Jing, Q.; Wu, Z.; Jiang, Y.; Wang, Z. L. Triboelectric Sensor for Self-Powered Tracking of Object Motion inside Tubing. *ACS Nano* **2014**, *8*, 3843−3850.
(122) Tang, W.; Han, C. B.; Zhang, C.; Wang, Z. L. Cover-Sheet-Based Nanogenerator for Charging Mobile Electronics Using Low-Frequency Body Motion/Vibration. *Nano Energy* **2014**, *9*, 121−127.
(123) Tang, W.; Jiang, T.; Fan, F. R.; Yu, A. F.; Zhang, C.; Cao, X.; Wang, Z. L. Liquid-Metal Electrode for High-Performance Triboelectric Nanogenerator at an Instantaneous Energy Conversion Efficiency of 70.6%. *Adv. Funct. Mater.* **2015**, *25*, 3718−3725.
(124) Wang, J.; Zhang, H. L.; Xie, Y. H.; Yan, Z. C.; Yuan, Y.; Huang, L.; Cui, X. J.; Gao, M.; Su, Y. J.; Yang, W. Q.; et al. Smart Network Node Based on Hybrid Nanogenerator for Self-Powered Multifunctional Sensing. *Nano Energy* **2017**, *33*, 418−426.
(125) Wang, S. H.; Lin, L.; Wang, Z. L. Triboelectric Nanogenerators as Self-Powered Active Sensors. *Nano Energy* **2015**, *11*, 436−462.
(126) Wang, Z. L. Triboelectric Nanogenerators as New Energy Technology for Self-Powered Systems and as Active Mechanical and Chemical Sensors. *ACS Nano* **2013**, *7*, 9533−9557.
(127) Wang, Z. L. Triboelectric Nanogenerators as New Energy Technology and Self-Powered Sensors−Principles, Problems and Perspectives. *Faraday Discuss.* **2014**, *176*, 447−458.
(128) Wen, Z.; Chen, J.; Yeh, M. H.; Guo, H. Y.; Li, Z. L.; Fan, X.; Zhang, T. J.; Zhu, L. P.; Wang, Z. L. Blow-Driven Triboelectric Nanogenerator as an Active Alcohol Breath Analyzer. *Nano Energy* **2015**, *16*, 38−46.
(129) Wu, Y.; Jing, Q. S.; Chen, J.; Bai, P.; Bai, J. J.; Zhu, G.; Su, Y. J.; Wang, Z. L. A Self-Powered Angle Measurement Sensor Based on Triboelectric Nanogenerator. *Adv. Funct. Mater.* **2015**, *25*, 2166−2174.
(130) Xie, Y. N.; Wang, S. H.; Niu, S. M.; Lin, L.; Jing, Q. S.; Yang, J.; Wu, Z. Y.; Wang, Z. L. Grating-Structured Freestanding Triboelectric-Layer Nanogenerator for Harvesting Mechanical Energy at 85% Total Conversion Efficiency. *Adv. Mater.* **2014**, *26*, 6599−6607.
(131) Yang, J.; Chen, J.; Liu, Y.; Yang, W.; Su, Y.; Wang, Z. L. Triboelectrification-Based Organic Film Nanogenerator for Acoustic Energy Harvesting and Self-Powered Active Acoustic Sensing. *ACS Nano* **2014**, *8*, 2649−2657.
(132) Yang, J.; Chen, J.; Su, Y.; Jing, Q.; Li, Z.; Yi, F.; Wen, X.; Wang, Z.; Wang, Z. L. Eardrum-Inspired Active Sensors for Self-Powered Cardiovascular System Characterization and Throat-Attached Anti-Interference Voice Recognition. *Adv. Mater.* **2015**, *27*, 1316−1326.
(133) Yang, J.; Chen, J.; Yang, Y.; Zhang, H. L.; Yang, W. Q.; Bai, P.; Su, Y. J.; Wang, Z. L. Broadband Vibrational Energy Harvesting Based on a Triboelectric Nanogenerator. *Adv. Energy Mater.* **2014**, *4*, 1301322.
(134) Yang, W. Q.; Chen, J.; Zhu, G.; Wen, X. N.; Bai, P.; Su, Y. J.; Lin, Y.; Wang, Z. L. Harvesting Vibration Energy by a Triple-Cantilever Based Triboelectric Nanogenerator. *Nano Res.* **2013**, *6*, 880−886.

https://dx.doi.org/10.1021/acs.chemrev.9b00821
Chem. Rev. 2020, 120, 3668−3720

(135) Yang, W.; Chen, J.; Zhu, G.; Yang, J.; Bai, P.; Su, Y.; Jing, Q.; Cao, X.; Wang, Z. L. Harvesting Energy from the Natural Vibration of Human Walking. *ACS Nano* **2013**, *7*, 11317−11324.
(136) Yang, Y.; Zhang, H. L.; Lin, Z. H.; Zhou, Y. S.; Jing, Q. S.; Su, Y. J.; Yang, J.; Chen, J.; Hu, C. G.; Wang, Z. L. Human Skin Based Triboelectric Nanogenerators for Harvesting Biomechanical Energy and as Self-Powered Active Tactile Sensor System. *ACS Nano* **2013**, *7*, 9213−9222.
(137) Yi, F.; Lin, L.; Niu, S. M.; Yang, P. K.; Wang, Z. N.; Chen, J.; Zhou, Y. S.; Zi, Y. L.; Wang, J.; Liao, Q. L.; et al. Stretchable-Rubber-Based Triboelectric Nanogenerator and Its Application as Self-Powered Body Motion Sensors. *Adv. Funct. Mater.* **2015**, *25*, 3688−3696.
(138) Zhang, B.; Chen, J.; Jin, L.; Deng, W.; Zhang, L.; Zhang, H.; Zhu, M.; Yang, W.; Wang, Z. L. Rotating-Disk-Based Hybridized Electromagnetic-Triboelectric Nanogenerator for Sustainably Powering Wireless Traffic Volume Sensors. *ACS Nano* **2016**, *10*, 6241−6247.
(139) Zhang, H. L.; Yang, Y.; Su, Y. J.; Chen, J.; Adams, K.; Lee, S.; Hu, C. G.; Wang, Z. L. Triboelectric Nanogenerator for Harvesting Vibration Energy in Full Space and as Self-Powered Acceleration Sensor. *Adv. Funct. Mater.* **2014**, *24*, 1401−1407.
(140) Zhang, H. L.; Yang, Y.; Su, Y. J.; Chen, J.; Hu, C. G.; Wu, Z. K.; Liu, Y.; Wong, C. P.; Bando, Y.; Wang, Z. L. Triboelectric Nanogenerator as Self-Powered Active Sensors for Detecting Liquid/Gaseous Water/Ethanol. *Nano Energy* **2013**, *2*, 693−701.
(141) Zhang, K.; Wang, X.; Yang, Y.; Wang, Z. L. Hybridized Electromagnetic-Triboelectric Nanogenerator for Scavenging Biomechanical Energy for Sustainably Powering Wearable Electronics. *ACS Nano* **2015**, *9*, 3521−3529.
(142) Zhu, G.; Bai, P.; Chen, J.; Wang, Z. L. Power-Generating Shoe Insole Based on Triboelectric Nanogenerators for Self-Powered Consumer Electronics. *Nano Energy* **2013**, *2*, 688−692.
(143) Zhu, G.; Yang, W. Q.; Zhang, T.; Jing, Q.; Chen, J.; Zhou, Y. S.; Bai, P.; Wang, Z. L. Self-Powered, Ultrasensitive, Flexible Tactile Sensors Based on Contact Electrification. *Nano Lett.* **2014**, *14*, 3208−3213.
(144) Zi, Y.; Lin, L.; Wang, J.; Wang, S.; Chen, J.; Fan, X.; Yang, P. K.; Yi, F.; Wang, Z. L. Triboelectric-Pyroelectric-Piezoelectric Hybrid Cell for High-Efficiency Energy-Harvesting and Self-Powered Sensing. *Adv. Mater.* **2015**, *27*, 2340−2347.
(145) Park, K. I.; Son, J. H.; Hwang, G. T.; Jeong, C. K.; Ryu, J.; Koo, M.; Choi, I.; Lee, S. H.; Byun, M.; Wang, Z. L.; et al. Highly-Efficient, Flexible Piezoelectric PZT Thin Film Nanogenerator on Plastic Substrates. *Adv. Mater.* **2014**, *26*, 2514−2520.
(146) Ramadan, K. S.; Sameoto, D.; Evoy, S. A Review of Piezoelectric Polymers as Functional Materials for Electromechanical Transducers. *Smart Mater. Struct.* **2014**, *23*, 033001.
(147) Won, S. S.; Sheldon, M.; Mostovych, N.; Kwak, J.; Chang, B. S.; Ahn, C. W.; Kingon, A. I.; Kim, I. W.; Kim, S. H. Piezoelectric Poly(Vinylidene Fluoride Trifluoroethylene) Thin Film-Based Power Generators Using Paper Substrates for Wearable Device Applications. *Appl. Phys. Lett.* **2015**, *107*, 202901.
(148) Wu, H.; Huang, Y.; Xu, F.; Duan, Y.; Yin, Z. Energy Harvesters for Wearable and Stretchable Electronics: From Flexibility to Stretchability. *Adv. Mater.* **2016**, *28*, 9881−9919.
(149) Yang, B.; Yun, K. S. Piezoelectric Shell Structures as Wearable Energy Harvesters for Effective Power Generation at Low-Frequency Movement. *Sens. Actuators A: Phys.* **2012**, *188*, 427−433.
(150) Yang, Z. B.; Zhou, S. X.; Zu, J.; Inman, D. High-Performance Piezoelectric Energy Harvesters and Their Applications. *Joule* **2018**, *2*, 642−697.
(151) Zhao, J.; You, Z. A Shoe-Embedded Piezoelectric Energy Harvester for Wearable Sensors. *Sensors* **2014**, *14*, 12497−12510.
(152) Bahk, J.-H.; Fang, H.; Yazawa, K.; Shakouri, A. Flexible Thermoelectric Materials and Device Optimization for Wearable Energy Harvesting. *J. Mater. Chem. C* **2015**, *3*, 10362−10374.
(153) Jo, S. E.; Kim, M. K.; Kim, M. S.; Kim, Y. J. Flexible Thermoelectric Generator for Human Body Heat Energy Harvesting. *Electron. Lett.* **2012**, *48*, 1015−1016.
(154) Oh, J. Y.; Lee, J. H.; Han, S. W.; Chae, S. S.; Bae, E. J.; Kang, Y. H.; Choi, W. J.; Cho, S. Y.; Lee, J. O.; Baik, H. K.; et al. Chemically Exfoliated Transition Metal Dichalcogenide Nanosheet-Based Wearable Thermoelectric Generators. *Energy Environ. Sci.* **2016**, *9*, 1696−1705.
(155) Pietrzyk, K.; Soares, J.; Ohara, B.; Lee, H. Power Generation Modeling for a Wearable Thermoelectric Energy Harvester with Practical Limitations. *Appl. Energy* **2016**, *183*, 218−228.
(156) Takashiri, M.; Shirakawa, T.; Miyazaki, K.; Tsukamoto, H. Fabrication and Characterization of Bismuth-Telluride-Based Alloy Thin Film Thermoelectric Generators by Flash Evaporation Method. *Sens. Actuators A: Phys.* **2007**, *138*, 329−334.
(157) Tian, R.; Wan, C.; Wang, Y.; Wei, Q.; Ishida, T.; Yamamoto, A.; Tsuruta, A.; Shin, W.; Li, S.; Koumoto, K. A Solution-Processed TiS_2/Organic Hybrid Superlattice Film Towards Flexible Thermoelectric Devices. *J. Mater. Chem. A* **2017**, *5*, 564−570.
(158) Wan, C. L.; Tian, R. M.; Azizi, A. B.; Huang, Y. J.; Wei, Q. S.; Sasai, R.; Wasusate, S.; Ishida, T.; Koumoto, K. Flexible Thermoelectric Foil for Wearable Energy Harvesting. *Nano Energy* **2016**, *30*, 840−845.
(159) Wei, Q. S.; Mukaida, M.; Kirihara, K.; Naitoh, Y.; Ishida, T. Polymer Thermoelectric Modules Screen-Printed on Paper. *RSC Adv.* **2014**, *4*, 28802−28806.
(160) Rojas, J. P.; Conchouso, D.; Arevalo, A.; Singh, D.; Foulds, I. G.; Hussain, M. M. Paper-Based Origami Flexible and Foldable Thermoelectric Nanogenerator. *Nano Energy* **2017**, *31*, 296−301.
(161) Bandodkar, A. J.; Jeerapan, I.; You, J. M.; Nunez-Flores, R.; Wang, J. Highly Stretchable Fully-Printed CNT-Based Electrochemical Sensors and Biofuel Cells: Combining Intrinsic and Design-Induced Stretchability. *Nano Lett.* **2016**, *16*, 721−727.
(162) Halamkova, L.; Halamek, J.; Bocharova, V.; Szczupak, A.; Alfonta, L.; Katz, E. Implanted Biofuel Cell Operating in a Living Snail. *J. Am. Chem. Soc.* **2012**, *134*, 5040−5043.
(163) Kim, J.; Salvatore, G. A.; Araki, H.; Chiarelli, A. M.; Xie, Z.; Banks, A.; Sheng, X.; Liu, Y.; Lee, J. W.; Jang, K. I.; et al. Battery-Free, Stretchable Optoelectronic Systems for Wireless Optical Characterization of the Skin. *Sci. Adv.* **2016**, *2*, No. e1600418.
(164) MacVittie, K.; Halamek, J.; Halamkova, L.; Southcott, M.; Jemison, W. D.; Lobel, R.; Katz, E. From "Cyborg" Lobsters to a Pacemaker Powered by Implantable Biofuel Cells. *Energy Environ. Sci.* **2013**, *6*, 81−86.
(165) Reid, R. C.; Minteer, S. D.; Gale, B. K. Contact Lens Biofuel Cell Tested in a Synthetic Tear Solution. *Biosens. Bioelectron.* **2015**, *68*, 142−148.
(166) Chen, X. H.; Yin, L.; Lv, J.; Gross, A. J.; Le, M.; Gutierrez, N. G.; Li, Y.; Jeerapan, I.; Giroud, F.; Berezovska, A.; et al. Stretchable and Flexible Buckypaper-Based Lactate Biofuel Cell for Wearable Electronics. *Adv. Funct. Mater.* **2019**, *29*, 1905785.
(167) Ogawa, Y.; Kato, K.; Miyake, T.; Nagamine, K.; Ofuji, T.; Yoshino, S.; Nishizawa, M. Organic Transdermal Iontophoresis Patch with Built-in Biofuel Cell. *Adv. Healthcare Mater.* **2015**, *4*, 506−510.
(168) Bernechea, M.; Miller, N. C.; Xercavins, G.; So, D.; Stavrinadis, A.; Konstantatos, G. Solution-Processed Solar Cells Based on Environmentally Friendly $AgBiS_2$ Nanocrystals. *Nat. Photonics* **2016**, *10*, 521−525.
(169) Duan, C.; Zhang, K.; Zhong, C.; Huang, F.; Cao, Y. Recent Advances in Water/Alcohol-Soluble Pi-Conjugated Materials: New Materials and Growing Applications in Solar Cells. *Chem. Soc. Rev.* **2013**, *42*, 9071−9104.
(170) Gunes, S.; Neugebauer, H.; Sariciftci, N. S. Conjugated Polymer-Based Organic Solar Cells. *Chem. Rev.* **2007**, *107*, 1324−1338.
(171) He, Z. C.; Xiao, B.; Liu, F.; Wu, H. B.; Yang, Y. L.; Xiao, S.; Wang, C.; Russell, T. P.; Cao, Y. Single-Junction Polymer Solar Cells with High Efficiency and Photovoltage. *Nat. Photonics* **2015**, *9*, 174−179.

https://dx.doi.org/10.1021/acs.chemrev.9b00821
Chem. Rev. 2020, 120, 3668−3720

(172) Hu, X.; Huang, Z.; Zhou, X.; Li, P.; Wang, Y.; Huang, Z.; Su, M.; Ren, W.; Li, F.; Li, M.; et al. Wearable Large-Scale Perovskite Solar-Power Source via Nanocellular Scaffold. *Adv. Mater.* **2017**, *29*, 1703236.
(173) Jinno, H.; Fukuda, K.; Xu, X. M.; Park, S.; Suzuki, Y.; Koizumi, M.; Yokota, T.; Osaka, I.; Takimiya, K.; Someya, T. Stretchable and Waterproof Elastomer-Coated Organic Photovoltaics for Washable Electronic Textile Applications. *Nat. Energy* **2017**, *2*, 780−785.
(174) Kaltenbrunner, M.; Adam, G.; Glowacki, E. D.; Drack, M.; Schwodiauer, R.; Leonat, L.; Apaydin, D. H.; Groiss, H.; Scharber, M. C.; White, M. S.; et al. Flexible High Power-Per-Weight Perovskite Solar Cells with Chromium Oxide-Metal Contacts for Improved Stability in Air. *Nat. Mater.* **2015**, *14*, 1032−1039.
(175) Kim, B. J.; Kim, D. H.; Lee, Y. Y.; Shin, H. W.; Han, G. S.; Hong, J. S.; Mahmood, K.; Ahn, T. K.; Joo, Y. C.; Hong, K. S.; et al. Highly Efficient and Bending Durable Perovskite Solar Cells: Toward a Wearable Power Source. *Energy Environ. Sci.* **2015**, *8*, 916−921.
(176) Lee, J.; Wu, J.; Ryu, J. H.; Liu, Z.; Meitl, M.; Zhang, Y. W.; Huang, Y.; Rogers, J. A. Stretchable Semiconductor Technologies with High Areal Coverages and Strain-Limiting Behavior: Demonstration in High-Efficiency Dual-Junction Gainp/Gaas Photovoltaics. *Small* **2012**, *8*, 1851−1856.
(177) Li, R.; Xiang, X.; Tong, X.; Zou, J.; Li, Q. Wearable Double-Twisted Fibrous Perovskite Solar Cell. *Adv. Mater.* **2015**, *27*, 3831−3835.
(178) Liu, Y.; Zhao, J.; Li, Z.; Mu, C.; Ma, W.; Hu, H.; Jiang, K.; Lin, H.; Ade, H.; Yan, H. Aggregation and Morphology Control Enables Multiple Cases of High-Efficiency Polymer Solar Cells. *Nat. Commun.* **2014**, *5*, 5293.
(179) Mathew, S.; Yella, A.; Gao, P.; Humphry-Baker, R.; Curchod, B. F. E.; Ashari-Astani, N.; Tavernelli, I.; Rothlisberger, U.; Nazeeruddin, M. K.; Gratzel, M. Dye-Sensitized Solar Cells with 13% Efficiency Achieved through the Molecular Engineering of Porphyrin Sensitizers. *Nat. Chem.* **2014**, *6*, 242−247.
(180) Nam, J.; Lee, Y.; Choi, W.; Kim, C. S.; Kim, H.; Kim, J.; Kim, D. H.; Jo, S. Transfer Printed Flexible and Stretchable Thin Film Solar Cells Using a Water-Soluble Sacrificial Layer. *Adv. Energy Mater.* **2016**, *6*, 1601269.
(181) Peet, J.; Heeger, A. J.; Bazan, G. C. "Plastic" Solar Cells: Self-Assembly of Bulk Heterojunction Nanomaterials by Spontaneous Phase Separation. *Acc. Chem. Res.* **2009**, *42*, 1700−1708.
(182) Sun, Y. M.; Welch, G. C.; Leong, W. L.; Takacs, C. J.; Bazan, G. C.; Heeger, A. J. Solution-Processed Small-Molecule Solar Cells with 6.7% Efficiency. *Nat. Mater.* **2012**, *11*, 44−48.
(183) Tsai, H.; Nie, W.; Blancon, J. C.; Stoumpos, C. C.; Asadpour, R.; Harutyunyan, B.; Neukirch, A. J.; Verduzco, R.; Crochet, J. J.; Tretiak, S.; et al. High-Efficiency Two-Dimensional Ruddlesden-Popper Perovskite Solar Cells. *Nature* **2016**, *536*, 312−316.
(184) Wu, Z. W.; Li, P.; Zhang, Y. K.; Zheng, Z. J. Flexible and Stretchable Perovskite Solar Cells: Device Design and Development Methods. *Small Methods* **2018**, *2*, 1800031.
(185) Zhang, Q.; Kan, B.; Liu, F.; Long, G. K.; Wan, X. J.; Chen, X. Q.; Zuo, Y.; Ni, W.; Zhang, H. J.; Li, M. M.; et al. Small-Molecule Solar Cells with Efficiency over 9%. *Nat. Photonics* **2015**, *9*, 35−41.
(186) Zhao, J. B.; Li, Y. K.; Yang, G. F.; Jiang, K.; Lin, H. R.; Ade, H.; Ma, W.; Yan, H. Efficient Organic Solar Cells Processed from Hydrocarbon Solvents. *Nat. Energy* **2016**, *1*, 15027.
(187) Ahmed, I.; Ikhlef, A.; Ng, D. W. K.; Schober, R. Power Allocation for an Energy Harvesting Transmitter with Hybrid Energy Sources. *IEEE Trans. Wireless Commun.* **2013**, *12*, 6255−6267.
(188) Deng, F.; Yue, X.; Fan, X.; Guan, S.; Xu, Y.; Chen, J. Multisource Energy Harvesting System for a Wireless Sensor Network Node in the Field Environment. *IEEE Internet Things J.* **2019**, *6*, 918−927.
(189) Habibzadeh, M.; Hassanalieragh, M.; Ishikawa, A.; Soyata, T.; Sharma, G. Hybrid Solar-Wind Energy Harvesting for Embedded Applications: Supercapacitor-Based System Architectures and Design Tradeoffs. *IEEE Circuits Syst. Mag.* **2017**, *17*, 29−63.
(190) Lopez-Martin, A.; Algueta, J.; Matías, I. Energy Harvesting Approaches in IoT Scenarios with Very Low Ambient Energy. *Renew. Energy Power Qual. J.* **2019**, *10*, 183−187.
(191) Mohamad, T. N. T.; Sampe, J.; Berhanuddin, D. D. Architecture of Micro Energy Harvesting Using Hybrid Input of RF, Thermal and Vibration for Semi-Active RFID Tag. *Eng. J.* **2017**, *21*, 183−197.
(192) Ren, Z.; Zheng, Q.; Wang, H.; Guo, H.; Miao, L.; Wan, J.; Xu, C.; Cheng, S.; Zhang, H. Wearable and Self-Cleaning Hybrid Energy Harvesting System Based on Micro/Nanostructured Haze Film. *Nano Energy* **2020**, *67*, 104243.
(193) Wu, Y. C.; Zhong, X. D.; Wang, X.; Yang, Y.; Wang, Z. L. Hybrid Energy Cell for Simultaneously Harvesting Wind, Solar, and Chemical Energies. *Nano Res.* **2014**, *7*, 1631−1639.
(194) Xu, C.; Wang, Z. L. Compact Hybrid Cell Based on a Convoluted Nanowire Structure for Harvesting Solar and Mechanical Energy. *Adv. Mater.* **2011**, *23*, 873−877.
(195) Yang, Y.; Wang, Z. L. Hybrid Energy Cells for Simultaneously Harvesting Multi-Types of Energies. *Nano Energy* **2015**, *14*, 245−256.
(196) Yang, Y.; Zhang, H.; Zhu, G.; Lee, S.; Lin, Z. H.; Wang, Z. L. Flexible Hybrid Energy Cell for Simultaneously Harvesting Thermal, Mechanical, and Solar Energies. *ACS Nano* **2013**, *7*, 785−790.
(197) Yoo, D.; Park, S. C.; Lee, S.; Sim, J. Y.; Song, I.; Choi, D.; Lim, H.; Kim, D. S. Biomimetic Anti-Reflective Triboelectric Nanogenerator for Concurrent Harvesting of Solar and Raindrop Energies. *Nano Energy* **2019**, *57*, 424−431.
(198) Zheng, L.; Lin, Z. H.; Cheng, G.; Wu, W. Z.; Wen, X. N.; Lee, S. M.; Wang, Z. L. Silicon-Based Hybrid Cell for Harvesting Solar Energy and Raindrop Electrostatic Energy. *Nano Energy* **2014**, *9*, 291−300.
(199) Yang, W. Q.; Chen, J.; Jing, Q. S.; Yang, J.; Wen, X. N.; Su, Y. J.; Zhu, G.; Bai, P.; Wang, Z. L. 3D Stack Integrated Triboelectric Nanogenerator for Harvesting Vibration Energy. *Adv. Funct. Mater.* **2014**, *24*, 4090−4096.
(200) Bai, P.; Zhu, G.; Jing, Q.; Yang, J.; Chen, J.; Su, Y.; Ma, J.; Zhang, G.; Wang, Z. L. Membrane-Based Self-Powered Triboelectric Sensors for Pressure Change Detection and Its Uses in Security Surveillance and Healthcare Monitoring. *Adv. Funct. Mater.* **2014**, *24*, 5807−5813.
(201) Fan, X.; Chen, J.; Yang, J.; Bai, P.; Li, Z.; Wang, Z. L. Ultrathin, Rollable, Paper-Based Triboelectric Nanogenerator for Acoustic Energy Harvesting and Self-Powered Sound Recording. *ACS Nano* **2015**, *9*, 4236−4243.
(202) Xu, L.; Pang, Y. K.; Zhang, C.; Jiang, T.; Chen, X. Y.; Luo, J. J.; Tang, W.; Cao, X.; Wang, Z. L. Integrated Triboelectric Nanogenerator Array Based on Air-Driven Membrane Structures for Water Wave Energy Harvesting. *Nano Energy* **2017**, *31*, 351−358.
(203) Kvavadze, E.; Bar-Yosef, O.; Belfer-Cohen, A.; Boaretto, E.; Jakeli, N.; Matskevich, Z.; Meshveliani, T. 30,000-Year-Old Wild Flax Fibers. *Science* **2009**, *325*, 1359.
(204) Castano, L. M.; Flatau, A. B. Smart Fabric Sensors and E-Textile Technologies: A Review. *Smart Mater. Struct.* **2014**, *23*, 053001.
(205) Dong, K.; Peng, X.; Wang, Z. L. Fiber/Fabric-Based Piezoelectric and Triboelectric Nanogenerators for Flexible/Stretchable and Wearable Electronics and Artificial Intelligence. *Adv. Mater.* **2020**, *32*, 1902549.
(206) Weng, W.; Chen, P.; He, S.; Sun, X.; Peng, H. Smart Electronic Textiles. *Angew. Chem., Int. Ed.* **2016**, *55*, 6140−6169.
(207) Zeng, W.; Shu, L.; Li, Q.; Chen, S.; Wang, F.; Tao, X. M. Fiber-Based Wearable Electronics: A Review of Materials, Fabrication, Devices, and Applications. *Adv. Mater.* **2014**, *26*, 5310−5336.
(208) Weng, W.; Yang, J.; Zhang, Y.; Li, Y.; Yang, S.; Zhu, L.; Zhu, M. A Route toward Smart System Integration: From Fiber Design to Device Construction. *Adv. Mater.* **2020**, *32*, 1902301.
(209) Pan, N.; Sun, G. *Functional Textiles for Improved Performance, Protection and Health*; Woodhead Publishing: Cambridge, UK, 2011.

https://dx.doi.org/10.1021/acs.chemrev.9b00821
Chem. Rev. 2020, 120, 3668−3720

(210) Reinert, G.; Fuso, F.; Hilfiker, R.; Schmidt, E. UV-Protecting Properties of Textile Fabrics and Their Improvement. *Text. Chem. Color* **1997**, *29*, 36−43.
(211) Saravanan, D. UV Protection Textile Materials. *Autex Res. J.* **2007**, *7*, 53−62.
(212) Morris, G. Thermal Properties of Textile Materials. *J. Text. Inst.* **1953**, *44*, T449−T476.
(213) Clarke, M. O. S. E. B.; O'Mahony, M. *Sportstech: Revolutionary Fabrics, Fashion and Design*; Thames & Hudson: London, 2002.
(214) Cui, Y.; Gong, H.; Wang, Y.; Li, D.; Bai, H. A Thermally Insulating Textile Inspired by Polar Bear Hair. *Adv. Mater.* **2018**, *30*, 1706807.
(215) Lyu, S. Z.; He, Y. L.; Yao, Y. G.; Zhang, M.; Wang, Y. P. Photothermal Clothing for Thermally Preserving Pipeline Transportation of Crude Oil. *Adv. Funct. Mater.* **2019**, *29*, 1900703.
(216) Brand, R. Measurement of Fabric Aesthetics: Analysis of Aesthetic Components. *Text. Res. J.* **1964**, *34*, 791−804.
(217) Huang, L.; Lin, S.; Xu, Z.; Zhou, H.; Duan, J.; Hu, B.; Zhou, J. Fiber-Based Energy Conversion Devices for Human-Body Energy Harvesting. *Adv. Mater.* **2020**, *32*, 1902034.
(218) Wang, B.; Facchetti, A. Mechanically Flexible Conductors for Stretchable and Wearable E-Skin and E-Textile Devices. *Adv. Mater.* **2019**, *31*, 1901408.
(219) Wang, Z. L. *Nanogenerators for Self-Powered Devices and Systems*; Georgia Institute of Technology: Atlanta, GA, 2011; p 4.
(220) Choi, Y.-M.; Lee, M. G.; Jeon, Y. Wearable Biomechanical Energy Harvesting Technologies. *Energies* **2017**, *10*, 1483.
(221) Donelan, J. M.; Li, Q.; Naing, V.; Hoffer, J. A.; Weber, D. J.; Kuo, A. D. Biomechanical Energy Harvesting: Generating Electricity During Walking with Minimal User Effort. *Science* **2008**, *319*, 807−810.
(222) Rome, L. C.; Flynn, L.; Goldman, E. M.; Yoo, T. D. Generating Electricity While Walking with Loads. *Science* **2005**, *309*, 1725−1728.
(223) Baginsky, I.; Kostsov, E.; Sokolov, A. Electrostatic Microgenerators of Energy with a High Specific Power. *Optoelectron.Instrument.Proc.* **2010**, *46*, 580−592.
(224) Mitcheson, P. D.; Reilly, E. K.; Toh, T.; Wright, P. K.; Yeatman, E. M. Performance Limits of the Three Mems Inertial Energy Generator Transduction Types. *J. Micromech. Microeng.* **2007**, *17*, S211−S216.
(225) Xie, Y. B.; Bos, D.; de Vreede, L. J.; de Boer, H. L.; van der Meulen, M. J.; Versluis, M.; Sprenkels, A. J.; van den Berg, A.; Eijkel, J. C. T. High-Efficiency Ballistic Electrostatic Generator Using Microdroplets. *Nat. Commun.* **2014**, *5*, 3575.
(226) Chandrashekar, B. N.; Deng, B.; Smitha, A. S.; Chen, Y.; Tan, C.; Zhang, H.; Peng, H.; Liu, Z. Roll-to-Roll Green Transfer of CVD Graphene onto Plastic for a Transparent and Flexible Triboelectric Nanogenerator. *Adv. Mater.* **2015**, *27*, 5210−5216.
(227) Fan, F. R.; Lin, L.; Zhu, G.; Wu, W.; Zhang, R.; Wang, Z. L. Transparent Triboelectric Nanogenerators and Self-Powered Pressure Sensors Based on Micropatterned Plastic Films. *Nano Lett.* **2012**, *12*, 3109−3114.
(228) Jin, S.; Wang, Y.; Motlag, M.; Gao, S.; Xu, J.; Nian, Q.; Wu, W.; Cheng, G. J. Large-Area Direct Laser-Shock Imprinting of a 3D Biomimic Hierarchical Metal Surface for Triboelectric Nanogenerators. *Adv. Mater.* **2018**, *30*, 1705840.
(229) Wang, R.; Gao, S.; Yang, Z.; Li, Y.; Chen, W.; Wu, B.; Wu, W. Engineered and Laser-Processed Chitosan Biopolymers for Sustainable and Biodegradable Triboelectric Power Generation. *Adv. Mater.* **2018**, *30*, 1706267.
(230) Wang, Z. L. From Nanogenerators to Piezotronics-a Decade-Long Study of ZnO Nanostructures. *MRS Bull.* **2012**, *37*, 814−827.
(231) Wang, Z. L.; Chen, J.; Lin, L. Progress in Triboelectric Nanogenerators as a New Energy Technology and Self-Powered Sensors. *Energy Environ. Sci.* **2015**, *8*, 2250−2282.
(232) Meng, K.; Zhao, S.; Zhou, Y.; Wu, Y.; Zhang, S.; He, Q.; Wang, X.; Zhou, Z.; Fan, W.; Tan, X. et al. A Wireless Textile Based Sensor System for Self-Powered Personalized Health Care. *Matter* **2020**, DOI: 10.1016/j.matt.2019.12.025.
(233) Zhang, X. S.; Han, M. D.; Wang, R. X.; Zhu, F. Y.; Li, Z. H.; Wang, W.; Zhang, H. X. Frequency-Multiplication High-Output Triboelectric Nanogenerator for Sustainably Powering Biomedical Microsystems. *Nano Lett.* **2013**, *13*, 1168−1172.
(234) Zhu, G.; Chen, J.; Zhang, T.; Jing, Q.; Wang, Z. L. Radial-Arrayed Rotary Electrification for High Performance Triboelectric Generator. *Nat. Commun.* **2014**, *5*, 3426.
(235) Saadon, S.; Sidek, O. A Review of Vibration-Based Mems Piezoelectric Energy Harvesters. *Energy Convers. Manage.* **2011**, *52*, 500−504.
(236) Cha, S. N.; Seo, J. S.; Kim, S. M.; Kim, H. J.; Park, Y. J.; Kim, S. W.; Kim, J. M. Sound-Driven Piezoelectric Nanowire-Based Nanogenerators. *Adv. Mater.* **2010**, *22*, 4726−4730.
(237) Fan, F. R.; Tang, W.; Wang, Z. L. Flexible Nanogenerators for Energy Harvesting and Self-Powered Electronics. *Adv. Mater.* **2016**, *28*, 4283−4305.
(238) Gupta, M. K.; Lee, J. H.; Lee, K. Y.; Kim, S. W. Two-Dimensional Vanadium-Doped ZnO Nanosheet-Based Flexible Direct Current Nanogenerator. *ACS Nano* **2013**, *7*, 8932−8939.
(239) Kumar, B.; Kim, S. W. Energy Harvesting Based on Semiconducting Piezoelectric ZnO Nanostructures. *Nano Energy* **2012**, *1*, 342−355.
(240) Kumar, B.; Lee, K. Y.; Park, H. K.; Chae, S. J.; Lee, Y. H.; Kim, S. W. Controlled Growth of Semiconducting Nanowire, Nanowall, and Hybrid Nanostructures on Graphene for Piezoelectric Nanogenerators. *ACS Nano* **2011**, *5*, 4197−4204.
(241) Lee, J. H.; Lee, K. Y.; Kumar, B.; Tien, N. T.; Lee, N. E.; Kim, S. W. Highly Sensitive Stretchable Transparent Piezoelectric Nanogenerators. *Energy Environ. Sci.* **2013**, *6*, 169−175.
(242) Lee, K. Y.; Kim, D.; Lee, J. H.; Kim, T. Y.; Gupta, M. K.; Kim, S. W. Unidirectional High-Power Generation via Stress-Induced Dipole Alignment from $ZnSnO_3$ Nanocubes/Polymer Hybrid Piezoelectric Nanogenerator. *Adv. Funct. Mater.* **2014**, *24*, 37−43.
(243) Mao, Y. C.; Zhao, P.; McConohy, G.; Yang, H.; Tong, Y. X.; Wang, X. D. Sponge-Like Piezoelectric Polymer Films for Scalable and Integratable Nanogenerators and Self-Powered Electronic Systems. *Adv. Energy Mater.* **2014**, *4*, 1301624.
(244) Sun, C. L.; Shi, J.; Bayerl, D. J.; Wang, X. D. Pvdf Microbelts for Harvesting Energy from Respiration. *Energy Environ. Sci.* **2011**, *4*, 4508−4512.
(245) Wang, X. D. Piezoelectric Nanogenerators-Harvesting Ambient Mechanical Energy at the Nanometer Scale. *Nano Energy* **2012**, *1*, 13−24.
(246) Wang, X.; Song, J.; Liu, J.; Wang, Z. L. Direct-Current Nanogenerator Driven by Ultrasonic Waves. *Science* **2007**, *316*, 102−105.
(247) Wu, W.; Wang, L.; Li, Y.; Zhang, F.; Lin, L.; Niu, S.; Chenet, D.; Zhang, X.; Hao, Y.; Heinz, T. F.; Hone, J.; Wang, Z. L. Piezoelectricity of Single-Atomic-Layer MoS_2 for Energy Conversion and Piezotronics. *Nature* **2014**, *514*, 470−474.
(248) Xu, S.; Qin, Y.; Xu, C.; Wei, Y.; Yang, R.; Wang, Z. L. Self-Powered Nanowire Devices. *Nat. Nanotechnol.* **2010**, *5*, 366−373.
(249) Yang, R.; Qin, Y.; Dai, L.; Wang, Z. L. Power Generation with Laterally Packaged Piezoelectric Fine Wires. *Nat. Nanotechnol.* **2009**, *4*, 34−39.
(250) Li, Z.; Zuo, L.; Luhrs, G.; Lin, L.; Qin, Y.-X. Electromagnetic Energy-Harvesting Shock Absorbers: Design, Modeling, and Road Tests. *IEEE Trans. Veh. Technol.* **2013**, *62*, 1065−1074.
(251) Saha, C. R.; O'Donnell, T.; Loder, H.; Beeby, S.; Tudor, J. Optimization of an Electromagnetic Energy Harvesting Device. *IEEE Trans. Magn.* **2006**, *42*, 3509−3511.
(252) Yang, B.; Lee, C.; Xiang, W. F.; Xie, J.; He, J. H.; Kotlanka, R. K.; Low, S. P.; Feng, H. H. Electromagnetic Energy Harvesting from Vibrations of Multiple Frequencies. *J. Micromech. Microeng.* **2009**, *19*, 035001.

https://dx.doi.org/10.1021/acs.chemrev.9b00821
Chem. Rev. 2020, 120, 3668−3720

(253) Miljkovic, N.; Preston, D. J.; Enright, R.; Wang, E. N. Jumping-Droplet Electrostatic Energy Harvesting. *Appl. Phys. Lett.* **2014**, *105*, 013111.
(254) Torres, E. O.; Rincón-Mora, G. A. Electrostatic Energy-Harvesting and Battery-Charging Cmos System Prototype. *IEEE Trans. Circuits Syst. I, Reg. Papers* **2009**, *56*, 1938−1948.
(255) Wang, F.; Hansen, O. Electrostatic Energy Harvesting Device with out-of-the-Plane Gap Closing Scheme. *Sens. Actuators A: Phys.* **2014**, *211*, 131−137.
(256) Hu, Y. F.; Zheng, Z. J. Progress in Textile-Based Triboelectric Nanogenerators for Smart Fabrics. *Nano Energy* **2019**, *56*, 16−24.
(257) Paosangthong, W.; Torah, R.; Beeby, S. Recent Progress on Textile-Based Triboelectric Nanogenerators. *Nano Energy* **2019**, *55*, 401−423.
(258) Safaei, M.; Sodano, H. A.; Anton, S. R. A Review of Energy Harvesting Using Piezoelectric Materials: State-of-the-Art a Decade Later (2008−2018). *Smart Mater. Struct.* **2019**, *28*, 113001.
(259) Parvez Mahmud, M. A.; Huda, N.; Farjana, S. H.; Asadnia, M.; Lang, C. Recent Advances in Nanogenerator-Driven Self-Powered Implantable Biomedical Devices. *Adv. Energy Mater.* **2018**, *8*, 1701210.
(260) Zheng, Q.; Shi, B.; Li, Z.; Wang, Z. L. Recent Progress on Piezoelectric and Triboelectric Energy Harvesters in Biomedical Systems. *Adv. Sci.* **2017**, *4*, 1700029.
(261) Wang, Z. L.; Wang, A. C. On the Origin of Contact-Electrification. *Mater. Today* **2019**, *30*, 34−51.
(262) Wang, Z. L. On the First Principle Theory of Nanogenerators from Maxwell's Equations. *Nano Energy* **2020**, *68*, 104272.
(263) Chen, J.; Wang, Z. L. Reviving Vibration Energy Harvesting and Self-Powered Sensing by a Triboelectric Nanogenerator. *Joule* **2017**, *1*, 480−521.
(264) Wang, Z. L. On Maxwell's Displacement Current for Energy and Sensors: The Origin of Nanogenerators. *Mater. Today* **2017**, *20*, 74−82.
(265) Fan, F. R.; Tian, Z. Q.; Wang, Z. L. Flexible Triboelectric Generator. *Nano Energy* **2012**, *1*, 328−334.
(266) Chen, S. W.; Cao, X.; Wang, N.; Ma, L.; Zhu, H. R.; Willander, M.; Jie, Y.; Wang, Z. L. An Ultrathin Flexible Single-Electrode Triboelectric-Nanogenerator for Mechanical Energy Harvesting and Instantaneous Force Sensing. *Adv. Energy Mater.* **2017**, *7*, 1601255.
(267) Lee, S.; Lee, Y.; Kim, D.; Yang, Y.; Lin, L.; Lin, Z. H.; Hwang, W.; Wang, Z. L. Triboelectric Nanogenerator for Harvesting Pendulum Oscillation Energy. *Nano Energy* **2013**, *2*, 1113−1120.
(268) Wen, X.; Yang, W.; Jing, Q.; Wang, Z. L. Harvesting Broadband Kinetic Impact Energy from Mechanical Triggering/Vibration and Water Waves. *ACS Nano* **2014**, *8*, 7405−7412.
(269) Hu, Y. F.; Yang, J.; Jing, Q. S.; Niu, S. M.; Wu, W. Z.; Wang, Z. L. Triboelectric Nanogenerator Built on Suspended 3D Spiral Structure as Vibration and Positioning Sensor and Wave Energy Harvester. *ACS Nano* **2013**, *7*, 10424−10432.
(270) Wu, C. S.; Liu, R. Y.; Wang, J.; Zi, Y. L.; Lin, L.; Wang, Z. L. A Spring-Based Resonance Coupling for Hugely Enhancing the Performance of Triboelectric Nanogenerators for Harvesting Low-Frequency Vibration Energy. *Nano Energy* **2017**, *32*, 287−293.
(271) Xu, M. Y.; Wang, P. H.; Wang, Y. C.; Zhang, S. L.; Wang, A. C.; Zhang, C. L.; Wang, Z. J.; Pan, X. X.; Wang, Z. L. A Soft and Robust Spring Based Triboelectric Nanogenerator for Harvesting Arbitrary Directional Vibration Energy and Self-Powered Vibration Sensing. *Adv. Energy Mater.* **2018**, *8*, 1702432.
(272) Su, Y. J.; Wen, X. N.; Zhu, G.; Yang, J.; Chen, J.; Bai, P.; Wu, Z. M.; Jiang, Y. D.; Wang, Z. L. Hybrid Triboelectric Nanogenerator for Harvesting Water Wave Energy and as a Self-Powered Distress Signal Emitter. *Nano Energy* **2014**, *9*, 186−195.
(273) Chen, J.; Yang, J.; Li, Z.; Fan, X.; Zi, Y.; Jing, Q.; Guo, H.; Wen, Z.; Pradel, K. C.; Niu, S.; et al. Networks of Triboelectric Nanogenerators for Harvesting Water Wave Energy: A Potential Approach toward Blue Energy. *ACS Nano* **2015**, *9*, 3324−3331.
(274) Wang, X. F.; Niu, S. M.; Yin, Y. J.; Yi, F.; You, Z.; Wang, Z. L. Triboelectric Nanogenerator Based on Fully Enclosed Rolling Spherical Structure for Harvesting Low-Frequency Water Wave Energy. *Adv. Energy Mater.* **2015**, *5*, 1501467.
(275) Wang, Z. L.; Jiang, T.; Xu, L. Toward the Blue Energy Dream by Triboelectric Nanogenerator Networks. *Nano Energy* **2017**, *39*, 9−23.
(276) Xie, Y.; Wang, S.; Lin, L.; Jing, Q.; Lin, Z. H.; Niu, S.; Wu, Z.; Wang, Z. L. Rotary Triboelectric Nanogenerator Based on a Hybridized Mechanism for Harvesting Wind Energy. *ACS Nano* **2013**, *7*, 7119−7125.
(277) Bae, J.; Lee, J.; Kim, S.; Ha, J.; Lee, B. S.; Park, Y.; Choong, C.; Kim, J. B.; Wang, Z. L.; Kim, H. Y.; et al. Flutter-Driven Triboelectrification for Harvesting Wind Energy. *Nat. Commun.* **2014**, *5*, 4929.
(278) Seol, M. L.; Woo, J. H.; Jeon, S. B.; Kim, D.; Park, S. J.; Hur, J.; Choi, Y. K. Vertically Stacked Thin Triboelectric Nanogenerator for Wind Energy Harvesting. *Nano Energy* **2015**, *14*, 201−208.
(279) Zhang, L.; Zhang, B.; Chen, J.; Jin, L.; Deng, W.; Tang, J.; Zhang, H.; Pan, H.; Zhu, M.; Yang, W.; et al. Lawn Structured Triboelectric Nanogenerators for Scavenging Sweeping Wind Energy on Rooftops. *Adv. Mater.* **2016**, *28*, 1650−1656.
(280) Zhao, Z.; Pu, X.; Du, C.; Li, L.; Jiang, C.; Hu, W.; Wang, Z. L. Freestanding Flag-Type Triboelectric Nanogenerator for Harvesting High-Altitude Wind Energy from Arbitrary Directions. *ACS Nano* **2016**, *10*, 1780−1787.
(281) Yan, C.; Gao, Y.; Zhao, S.; Zhang, S.; Zhou, Y.; Deng, W.; Li, Z.; Jiang, G.; Jin, L.; Tian, G.; et al. A Linear-to-Rotary Hybrid Nanogenerator for High-Performance Wearable Biomechanical Energy Harvesting. *Nano Energy* **2020**, *67*, 104235.
(282) Xu, Z.; Duan, J.; Li, W.; Wu, N.; Pan, Y.; Lin, S.; Li, J.; Yuan, F.; Chen, S.; Huang, L.; et al. Boosting the Efficient Energy Output of Electret Nanogenerators by Suppressing Air Breakdown under Ambient Conditions. *ACS Appl. Mater. Interfaces* **2019**, *11*, 3984−3989.
(283) Yang, Y.; Lin, L.; Zhang, Y.; Jing, Q.; Hou, T. C.; Wang, Z. L. Self-Powered Magnetic Sensor Based on a Triboelectric Nanogenerator. *ACS Nano* **2012**, *6*, 10378−10383.
(284) Yang, Y.; Zhu, G.; Zhang, H. L.; Chen, J.; Zhong, X. D.; Lin, Z. H.; Su, Y. J.; Bai, P.; Wen, X. N.; Wang, Z. L. Triboelectric Nanogenerator for Harvesting Wind Energy and as Self-Powered Wind Vector Sensor System. *ACS Nano* **2013**, *7*, 9461−9468.
(285) Guo, H. Y.; Chen, J.; Tian, L.; Leng, Q.; Xi, Y.; Hu, C. G. Airflow-Induced Triboelectric Nanogenerator as a Self-Powered Sensor for Detecting Humidity and Airflow Rate. *ACS Appl. Mater. Interfaces* **2014**, *6*, 17184−17189.
(286) Lin, Z. H.; Cheng, G.; Wu, W. Z.; Pradel, K. C.; Wang, Z. L. Dual-Mode Triboelectric Nanogenerator for Harvesting Water Energy and as a Self-Powered Ethanol Nanosensor. *ACS Nano* **2014**, *8*, 6440−6448.
(287) Zhou, Y. S.; Zhu, G.; Niu, S.; Liu, Y.; Bai, P.; Jing, Q.; Wang, Z. L. Nanometer Resolution Self-Powered Static and Dynamic Motion Sensor Based on Micro-Grated Triboelectrification. *Adv. Mater.* **2014**, *26*, 1719−1724.
(288) Zheng, Q.; Shi, B.; Fan, F.; Wang, X.; Yan, L.; Yuan, W.; Wang, S.; Liu, H.; Li, Z.; Wang, Z. L. In Vivo Powering of Pacemaker by Breathing-Driven Implanted Triboelectric Nanogenerator. *Adv. Mater.* **2014**, *26*, 5851−5856.
(289) Shi, Q. F.; Wang, H.; Wang, T.; Lee, C. Self-Powered Liquid Triboelectric Microfluidic Sensor for Pressure Sensing and Finger Motion Monitoring Applications. *Nano Energy* **2016**, *30*, 450−459.
(290) Zheng, Q.; Zhang, H.; Shi, B.; Xue, X.; Liu, Z.; Jin, Y.; Ma, Y.; Zou, Y.; Wang, X.; An, Z.; et al. In Vivo Self-Powered Wireless Cardiac Monitoring via Implantable Triboelectric Nanogenerator. *ACS Nano* **2016**, *10*, 6510−6518.
(291) Zheng, Q.; Zou, Y.; Zhang, Y. L.; Liu, Z.; Shi, B. J.; Wang, X. X.; Jin, Y. M.; Ouyang, H.; Li, Z.; Wang, Z. L. Biodegradable Triboelectric Nanogenerator as a Life-Time Designed Implantable Power Source. *Sci. Adv.* **2016**, *2*, No. e1501478.

https://dx.doi.org/10.1021/acs.chemrev.9b00821
Chem. Rev. 2020, 120, 3668−3720

(292) Ouyang, H.; Tian, J.; Sun, G.; Zou, Y.; Liu, Z.; Li, H.; Zhao, L.; Shi, B.; Fan, Y.; Fan, Y.; et al. Self-Powered Pulse Sensor for Antidiastole of Cardiovascular Disease. *Adv. Mater.* **2017**, *29*, 1703456.
(293) Yang, W.; Chen, J.; Wen, X.; Jing, Q.; Yang, J.; Su, Y.; Zhu, G.; Wu, W.; Wang, Z. L. Triboelectrification Based Motion Sensor for Human-Machine Interfacing. *ACS Appl. Mater. Interfaces* **2014**, *6*, 7479−7484.
(294) Chen, J.; Zhu, G.; Yang, J.; Jing, Q.; Bai, P.; Yang, W.; Qi, X.; Su, Y.; Wang, Z. L. Personalized Keystroke Dynamics for Self-Powered Human-Machine Interfacing. *ACS Nano* **2015**, *9*, 105−116.
(295) Lim, S.; Son, D.; Kim, J.; Lee, Y. B.; Song, J. K.; Choi, S.; Lee, D. J.; Kim, J. H.; Lee, M.; Hyeon, T.; et al. Transparent and Stretchable Interactive Human Machine Interface Based on Patterned Graphene Heterostructures. *Adv. Funct. Mater.* **2015**, *25*, 375−383.
(296) Chandrasekhar, A.; Alluri, N. R.; Saravanakumar, B.; Selvarajan, S.; Kim, S. J. Human Interactive Triboelectric Nanogenerator as a Self-Powered Smart Seat. *ACS Appl. Mater. Interfaces* **2016**, *8*, 9692−9699.
(297) He, X.; Zi, Y. L.; Yu, H.; Zhang, S. L.; Wang, J.; Ding, W. B.; Zou, H. Y.; Zhang, W.; Lu, C. H.; Wang, Z. L. An Ultrathin Paper-Based Self-Powered System for Portable Electronics and Wireless Human-Machine Interaction. *Nano Energy* **2017**, *39*, 328−336.
(298) Luo, J.; Wang, Z.; Xu, L.; Wang, A. C.; Han, K.; Jiang, T.; Lai, Q.; Bai, Y.; Tang, W.; Fan, F. R.; Wang, Z. L. Flexible and Durable Wood-Based Triboelectric Nanogenerators for Self-Powered Sensing in Athletic Big Data Analytics. *Nat. Commun.* **2019**, *10*, 5147.
(299) Liu, J.; Gu, L.; Cui, N.; Xu, Q.; Qin, Y.; Yang, R. Fabric-Based Triboelectric Nanogenerators. *Research* **2019**, *2019*, 1091632.
(300) Zhu, G.; Peng, B.; Chen, J.; Jing, Q. S.; Wang, Z. L. Triboelectric Nanogenerators as a New Energy Technology: From Fundamentals, Devices, to Applications. *Nano Energy* **2015**, *14*, 126−138.
(301) Chen, J.; Zhu, G.; Yang, W. Q.; Jing, Q. S.; Bai, P.; Yang, Y.; Hou, T. C.; Wang, Z. L. Harmonic-Resonator-Based Triboelectric Nanogenerator as a Sustainable Power Source and a Self-Powered Active Vibration Sensor. *Adv. Mater.* **2013**, *25*, 6094−6099.
(302) Wang, S.; Lin, L.; Wang, Z. L. Nanoscale Triboelectric-Effect-Enabled Energy Conversion for Sustainably Powering Portable Electronics. *Nano Lett.* **2012**, *12*, 6339−6346.
(303) Zhu, G.; Lin, Z. H.; Jing, Q.; Bai, P.; Pan, C.; Yang, Y.; Zhou, Y.; Wang, Z. L. Toward Large-Scale Energy Harvesting by a Nanoparticle-Enhanced Triboelectric Nanogenerator. *Nano Lett.* **2013**, *13*, 847−853.
(304) Zhu, G.; Pan, C.; Guo, W.; Chen, C. Y.; Zhou, Y.; Yu, R.; Wang, Z. L. Triboelectric-Generator-Driven Pulse Electrodeposition for Micropatterning. *Nano Lett.* **2012**, *12*, 4960−4965.
(305) Lin, L.; Wang, S.; Xie, Y.; Jing, Q.; Niu, S.; Hu, Y.; Wang, Z. L. Segmentally Structured Disk Triboelectric Nanogenerator for Harvesting Rotational Mechanical Energy. *Nano Lett.* **2013**, *13*, 2916−2923.
(306) Wang, S.; Lin, L.; Xie, Y.; Jing, Q.; Niu, S.; Wang, Z. L. Sliding-Triboelectric Nanogenerators Based on in-Plane Charge-Separation Mechanism. *Nano Lett.* **2013**, *13*, 2226−2233.
(307) Zhu, G.; Chen, J.; Liu, Y.; Bai, P.; Zhou, Y. S.; Jing, Q.; Pan, C.; Wang, Z. L. Linear-Grating Triboelectric Generator Based on Sliding Electrification. *Nano Lett.* **2013**, *13*, 2282−2289.
(308) Bai, P.; Zhu, G.; Liu, Y.; Chen, J.; Jing, Q.; Yang, W.; Ma, J.; Zhang, G.; Wang, Z. L. Cylindrical Rotating Triboelectric Nanogenerator. *ACS Nano* **2013**, *7*, 6361−6366.
(309) Niu, S.; Liu, Y.; Wang, S.; Lin, L.; Zhou, Y. S.; Hu, Y.; Wang, Z. L. Theory of Sliding-Mode Triboelectric Nanogenerators. *Adv. Mater.* **2013**, *25*, 6184−6193.
(310) Xie, Y. N.; Wang, S. H.; Niu, S. M.; Lin, L.; Jing, Q. S.; Su, Y. J.; Wu, Z. Y.; Wang, Z. L. Multi-Layered Disk Triboelectric Nanogenerator for Harvesting Hydropower. *Nano Energy* **2014**, *6*, 129−136.
(311) Mao, Y. C.; Geng, D. L.; Liang, E. J.; Wang, X. D. Single-Electrode Triboelectric Nanogenerator for Scavenging Friction Energy from Rolling Tires. *Nano Energy* **2015**, *15*, 227−234.
(312) Niu, S. M.; Liu, Y.; Wang, S. H.; Lin, L.; Zhou, Y. S.; Hu, Y. F.; Wang, Z. L. Theoretical Investigation and Structural Optimization of Single-Electrode Triboelectric Nanogenerators. *Adv. Funct. Mater.* **2014**, *24*, 3332−3340.
(313) Yang, Y.; Zhou, Y. S.; Zhang, H. L.; Liu, Y.; Lee, S. M.; Wang, Z. L. A Single-Electrode Based Triboelectric Nanogenerator as Self-Powered Tracking System. *Adv. Mater.* **2013**, *25*, 6594−6601.
(314) Meng, B.; Tang, W.; Too, Z. H.; Zhang, X. S.; Han, M. D.; Liu, W.; Zhang, H. X. A Transparent Single-Friction-Surface Triboelectric Generator and Self-Powered Touch Sensor. *Energy Environ. Sci.* **2013**, *6*, 3235−3240.
(315) Yang, Y.; Zhang, H.; Chen, J.; Jing, Q.; Zhou, Y. S.; Wen, X.; Wang, Z. L. Single-Electrode-Based Sliding Triboelectric Nanogenerator for Self-Powered Displacement Vector Sensor System. *ACS Nano* **2013**, *7*, 7342−7351.
(316) Lin, L.; Wang, S. H.; Niu, S. M.; Liu, C.; Xie, Y. N.; Wang, Z. L. Noncontact Free-Rotating Disk Triboelectric Nanogenerator as a Sustainable Energy Harvester and Self-Powered Mechanical Sensor. *ACS Appl. Mater. Interfaces* **2014**, *6*, 3031−3038.
(317) Wang, S.; Xie, Y.; Niu, S.; Lin, L.; Wang, Z. L. Freestanding Triboelectric-Layer-Based Nanogenerators for Harvesting Energy from a Moving Object or Human Motion in Contact and Non-Contact Modes. *Adv. Mater.* **2014**, *26*, 2818−2824.
(318) Niu, S. M.; Liu, Y.; Chen, X. Y.; Wang, S. H.; Zhou, Y. S.; Lin, L.; Xie, Y. N.; Wang, Z. L. Theory of Freestanding Triboelectric-Layer-Based Nanogenerators. *Nano Energy* **2015**, *12*, 760−774.
(319) He, T. Y. Y.; Shi, Q. F.; Wang, H.; Wen, F.; Chen, T.; Ouyang, J. Y.; Lee, C. Beyond Energy Harvesting - Multi-Functional Triboelectric Nanosensors on a Textile. *Nano Energy* **2019**, *57*, 338−352.
(320) Ko, W. B.; Choi, D. S.; Lee, C. H.; Yang, J. Y.; Yoon, G. S.; Hong, J. P. Hierarchically Nanostructured 1D Conductive Bundle Yarn-Based Triboelectric Nanogenerators. *Adv. Mater.* **2017**, *29*, 1704434.
(321) Lai, Y. C.; Hsiao, Y. C.; Wu, H. M.; Wang, Z. L. Waterproof Fabric-Based Multifunctional Triboelectric Nanogenerator for Universally Harvesting Energy from Raindrops, Wind, and Human Motions and as Self-Powered Sensors. *Adv. Sci.* **2019**, *6*, 1801883.
(322) Lee, C.; Yang, S.; Choi, D.; Kim, W.; Kim, J.; Hong, J. Chemically Surface-Engineered Polydimethylsiloxane Layer Via Plasma Treatment for Advancing Textile-Based Triboelectric Nanogenerators. *Nano Energy* **2019**, *57*, 353−362.
(323) Li, H.; Zhao, S. Y.; Du, X. Y.; Wang, J. N.; Cao, R.; Xing, Y.; Li, C. J. A Compound Yarn Based Wearable Triboelectric Nanogenerator for Self-Powered Wearable Electronics. *Adv. Mater. Technol.* **2018**, *3*, 1800065.
(324) Liu, M.; Pu, X.; Jiang, C.; Liu, T.; Huang, X.; Chen, L.; Du, C.; Sun, J.; Hu, W.; Wang, Z. L. Large-Area All-Textile Pressure Sensors for Monitoring Human Motion and Physiological Signals. *Adv. Mater.* **2017**, *29*, 1703700.
(325) Sala de Medeiros, M.; Chanci, D.; Moreno, C.; Goswami, D.; Martinez, R. V. Waterproof, Breathable, and Antibacterial Self-Powered E-Textiles Based on Omniphobic Triboelectric Nanogenerators. *Adv. Funct. Mater.* **2019**, *29*, 1904350.
(326) Song, J.; Gao, L.; Tao, X.; Li, L. Ultra-Flexible and Large-Area Textile-Based Triboelectric Nanogenerators with a Sandpaper-Induced Surface Microstructure. *Materials* **2018**, *11*, 2120.
(327) Liu, L. M.; Pan, J.; Chen, P. N.; Zhang, J.; Yu, X. H.; Ding, X.; Wang, B. J.; Sun, X. M.; Peng, H. S. A Triboelectric Textile Templated by a Three-Dimensionally Penetrated Fabric. *J. Mater. Chem. A* **2016**, *4*, 6077−6083.
(328) Zhang, L.; Yu, Y.; Eyer, G. P.; Suo, G.; Kozik, L. A.; Fairbanks, M.; Wang, X.; Andrew, T. L. All-Textile Triboelectric Generator Compatible with Traditional Textile Process. *Adv. Mater. Technol.* **2016**, *1*, 1600147.

https://dx.doi.org/10.1021/acs.chemrev.9b00821
Chem. Rev. 2020, 120, 3668−3720

(329) Seung, W.; Gupta, M. K.; Lee, K. Y.; Shin, K. S.; Lee, J. H.; Kim, T. Y.; Kim, S.; Lin, J.; Kim, J. H.; Kim, S. W. Nanopatterned Textile-Based Wearable Triboelectric Nanogenerator. *ACS Nano* **2015**, *9*, 3501−3509.
(330) Wu, C.; Kim, T. W.; Li, F.; Guo, T. Wearable Electricity Generators Fabricated Utilizing Transparent Electronic Textiles Based on Polyester/Ag Nanowires/Graphene Core-Shell Nanocomposites. *ACS Nano* **2016**, *10*, 6449−6457.
(331) Kim, T.; Jeon, S.; Lone, S.; Doh, S. J.; Shin, D. M.; Kim, H. K.; Hwang, Y. H.; Hong, S. W. Versatile Nanodot-Patterned Gore-Tex Fabric for Multiple Energy Harvesting in Wearable and Aerodynamic Nanogenerators. *Nano Energy* **2018**, *54*, 209−217.
(332) Cui, N.; Liu, J.; Gu, L.; Bai, S.; Chen, X.; Qin, Y. Wearable Triboelectric Generator for Powering the Portable Electronic Devices. *ACS Appl. Mater. Interfaces* **2015**, *7*, 18225−18230.
(333) Li, S.; Zhong, Q.; Zhong, J.; Cheng, X.; Wang, B.; Hu, B.; Zhou, J. Cloth-Based Power Shirt for Wearable Energy Harvesting and Clothes Ornamentation. *ACS Appl. Mater. Interfaces* **2015**, *7*, 14912−14916.
(334) Xiong, J.; Cui, P.; Chen, X.; Wang, J.; Parida, K.; Lin, M.-F.; Lee, P. S. Skin-Touch-Actuated Textile-Based Triboelectric Nanogenerator with Black Phosphorus for Durable Biomechanical Energy Harvesting. *Nat. Commun.* **2018**, *9*, 4280.
(335) Qiu, Q.; Zhu, M.; Li, Z.; Qiu, K.; Liu, X.; Yu, J.; Ding, B. Highly Flexible, Breathable, Tailorable and Washable Power Generation Fabrics for Wearable Electronics. *Nano Energy* **2019**, *58*, 750−758.
(336) Chen, J.; Guo, H. Y.; Pu, X. J.; Wang, X.; Xi, Y.; Hu, C. G. Traditional Weaving Craft for One-Piece Self-Charging Power Textile for Wearable Electronics. *Nano Energy* **2018**, *50*, 536−543.
(337) Jung, S.; Lee, J.; Hyeon, T.; Lee, M.; Kim, D. H. Fabric-Based Integrated Energy Devices for Wearable Activity Monitors. *Adv. Mater.* **2014**, *26*, 6329−6334.
(338) Dong, K.; Wang, Y. C.; Deng, J.; Dai, Y.; Zhang, S. L.; Zou, H.; Gu, B.; Sun, B.; Wang, Z. L. A Highly Stretchable and Washable All-Yarn-Based Self-Charging Knitting Power Textile Composed of Fiber Triboelectric Nanogenerators and Supercapacitors. *ACS Nano* **2017**, *11*, 9490−9499.
(339) Cao, R.; Pu, X. J.; Du, X. Y.; Yang, W.; Wang, J. N.; Guo, H. Y.; Zhao, S. Y.; Yuan, Z. Q.; Zhang, C.; Li, C. J.; et al. Screen-Printed Washable Electronic Textiles as Self-Powered Touch/Gesture Tribo-Sensors for Intelligent Human-Machine Interaction. *ACS Nano* **2018**, *12*, 5190−5196.
(340) Lin, Z. M.; Yang, J.; Li, X. S.; Wu, Y. F.; Wei, W.; Liu, J.; Chen, J.; Yang, J. Large-Scale and Washable Smart Textiles Based on Triboelectric Nanogenerator Arrays for Self-Powered Sleeping Monitoring. *Adv. Funct. Mater.* **2018**, *28*, 1704112.
(341) Xiong, J. Q.; Lin, M. F.; Wang, J. X.; Gaw, S. L.; Parida, K.; Lee, P. S. Wearable All-Fabric-Based Triboelectric Generator for Water Energy Harvesting. *Adv. Energy Mater.* **2017**, *7*, 1701243.
(342) Lee, S.; Ko, W.; Oh, Y.; Lee, J.; Baek, G.; Lee, Y.; Sohn, J.; Cha, S.; Kim, J.; Park, J.; et al. Triboelectric Energy Harvester Based on Wearable Textile Platforms Employing Various Surface Morphologies. *Nano Energy* **2015**, *12*, 410−418.
(343) Mule, A. R.; Dudem, B.; Patnam, H.; Graham, S. A.; Yu, J. S. Wearable Single-Electrode-Mode Triboelectric Nanogenerator via Conductive Polymer-Coated Textiles for Self-Power Electronics. *ACS Sustainable Chem. Eng.* **2019**, *7*, 16450−16458.
(344) Huang, T.; Zhang, J.; Yu, B.; Yu, H.; Long, H. R.; Wang, H. Z.; Zhang, Q. H.; Zhu, M. F. Fabric Texture Design for Boosting the Performance of a Knitted Washable Textile Triboelectric Nanogenerator as Wearable Power. *Nano Energy* **2019**, *58*, 375−383.
(345) Paosangthong, W.; Wagih, M.; Torah, R.; Beeby, S. Textile-Based Triboelectric Nanogenerator with Alternating Positive and Negative Freestanding Grating Structure. *Nano Energy* **2019**, *66*, 104148.
(346) Sim, H. J.; Choi, C.; Kim, S. H.; Kim, K. M.; Lee, C. J.; Kim, Y. T.; Lepro, X.; Baughman, R. H.; Kim, S. J. Stretchable Triboelectric Fiber for Self-Powered Kinematic Sensing Textile. *Sci. Rep.* **2016**, *6*, 35153.
(347) Ning, C.; Tian, L.; Zhao, X. Y.; Xiang, S. X.; Tang, Y. J.; Liang, E. J.; Mao, Y. C. Washable Textile-Structured Single-Electrode Triboelectric Nanogenerator for Self-Powered Wearable Electronics. *J. Mater. Chem. A* **2018**, *6*, 19143−19150.
(348) Park, J.; Kim, D.; Choi, A. Y.; Kim, Y. T. Flexible Single-Strand Fiber-Based Woven-Structured Triboelectric Nanogenerator for Self-Powered Electronics. *APL Mater.* **2018**, *6*, 101106.
(349) Yang, Y.; Xie, L.; Wen, Z.; Chen, C.; Chen, X.; Wei, A.; Cheng, P.; Xie, X.; Sun, X. Coaxial Triboelectric Nanogenerator and Supercapacitor Fiber-Based Self-Charging Power Fabric. *ACS Appl. Mater. Interfaces* **2018**, *10*, 42356−42362.
(350) Zhao, Z. Z.; Yan, C.; Liu, Z. X.; Fu, X. L.; Peng, L. M.; Hu, Y. F.; Zheng, Z. J. Machine-Washable Textile Triboelectric Nanogenerators for Effective Human Respiratory Monitoring through Loom Weaving of Metallic Yarns. *Adv. Mater.* **2016**, *28*, 10267−10274.
(351) Park, J.; Choi, A. Y.; Lee, C. J.; Kim, Y.-H. *Flexible Fiber-Based Triboelectric Generator for Self-Powered Sensors*, 2016 IEEE SENSORS, Orlando, FL, **2016**; pp 1−3.
(352) Gong, W.; Hou, C.; Zhou, J.; Guo, Y.; Zhang, W.; Li, Y.; Zhang, Q.; Wang, H. Continuous and Scalable Manufacture of Amphibious Energy Yarns and Textiles. *Nat. Commun.* **2019**, *10*, 868.
(353) Zhou, T.; Zhang, C.; Han, C. B.; Fan, F. R.; Tang, W.; Wang, Z. L. Woven Structured Triboelectric Nanogenerator for Wearable Devices. *ACS Appl. Mater. Interfaces* **2014**, *6*, 14695−14701.
(354) Kwak, S. S.; Kim, H.; Seung, W.; Kim, J.; Hinchet, R.; Kim, S. W. Fully Stretchable Textile Triboelectric Nanogenerator with Knitted Fabric Structures. *ACS Nano* **2017**, *11*, 10733−10741.
(355) Lai, Y. C.; Deng, J.; Zhang, S. L.; Niu, S.; Guo, H.; Wang, Z. L. Single-Thread-Based Wearable and Highly Stretchable Triboelectric Nanogenerators and Their Applications in Cloth-Based Self-Powered Human-Interactive and Biomedical Sensing. *Adv. Funct. Mater.* **2017**, *27*, 1604462.
(356) Liu, J.; Gu, L.; Cui, N.; Bai, S.; Liu, S.; Xu, Q.; Qin, Y.; Yang, R.; Zhou, F. Core-Shell Fiber-Based 2D Woven Triboelectric Nanogenerator for Effective Motion Energy Harvesting. *Nanoscale Res. Lett.* **2019**, *14*, 311.
(357) Pu, X.; Li, L.; Song, H.; Du, C.; Zhao, Z.; Jiang, C.; Cao, G.; Hu, W.; Wang, Z. L. A Self-Charging Power Unit by Integration of a Textile Triboelectric Nanogenerator and a Flexible Lithium-Ion Battery for Wearable Electronics. *Adv. Mater.* **2015**, *27*, 2472−2478.
(358) Shin, Y. E.; Lee, J. E.; Park, Y.; Hwang, S. H.; Chae, H. G.; Ko, H. Sewing Machine Stitching of Polyvinylidene Fluoride Fibers: Programmable Textile Patterns for Wearable Triboelectric Sensors. *J. Mater. Chem. A* **2018**, *6*, 22879−22888.
(359) Tian, Z. M.; He, J.; Chen, X.; Zhang, Z. X.; Wen, T.; Zhai, C.; Han, J. Q.; Mu, J. L.; Hou, X. J.; Chou, X. J.; et al. Performance-Boosted Triboelectric Textile for Harvesting Human Motion Energy. *Nano Energy* **2017**, *39*, 562−570.
(360) Yu, A. F.; Pu, X.; Wen, R. M.; Liu, M. M.; Zhou, T.; Zhang, K.; Zhang, Y.; Zhai, J. Y.; Hu, W. G.; Wang, Z. L. Core-Shell-Yarn-Based Triboelectric Nanogenerator Textiles as Power Cloths. *ACS Nano* **2017**, *11*, 12764−12771.
(361) Zhang, L.; Zhang, N.; Yang, Y.; Xiang, S.; Tao, C.; Yang, S.; Fan, X. Self-Powered All-in-One Fluid Sensor Textile with Enhanced Triboelectric Effect on All-Immersed Dendritic Liquid-Solid Interface. *ACS Appl. Mater. Interfaces* **2018**, *10*, 30819−30826.
(362) Kim, K. N.; Chun, J.; Kim, J. W.; Lee, K. Y.; Park, J. U.; Kim, S. W.; Wang, Z. L.; Baik, J. M. Highly Stretchable 2d Fabrics for Wearable Triboelectric Nanogenerator under Harsh Environments. *ACS Nano* **2015**, *9*, 6394−6400.
(363) Dong, K.; Deng, J. A.; Ding, W. B.; Wang, A. C.; Wang, P. H.; Cheng, C. Y.; Wang, Y. C.; Jin, L. M.; Gu, B. H.; Sun, B. Z.; et al. Versatile Core-Sheath Yarn for Sustainable Biomechanical Energy Harvesting and Real-Time Human-Interactive Sensing. *Adv. Energy Mater.* **2018**, *8*, 1801114.

https://dx.doi.org/10.1021/acs.chemrev.9b00821
Chem. Rev. 2020, 120, 3668−3720

(364) Zhong, J.; Zhang, Y.; Zhong, Q.; Hu, Q.; Hu, B.; Wang, Z. L.; Zhou, J. Fiber-Based Generator for Wearable Electronics and Mobile Medication. *ACS Nano* **2014**, *8*, 6273−6280.
(365) Pu, X.; Li, L.; Liu, M.; Jiang, C.; Du, C.; Zhao, Z.; Hu, W.; Wang, Z. L. Wearable Self-Charging Power Textile Based on Flexible Yarn Supercapacitors and Fabric Nanogenerators. *Adv. Mater.* **2016**, *28*, 98−105.
(366) Zhu, M. S.; Huang, Y.; Ng, W. S.; Liu, J. Y.; Wang, Z. F.; Wang, Z. Y.; Hu, H.; Zhi, C. Y. 3D Spacer Fabric Based Multifunctional Triboelectric Nanogenerator with Great Feasibility for Mechanized Large-Scale Production. *Nano Energy* **2016**, *27*, 439−446.
(367) Dong, K.; Deng, J. N.; Zi, Y. L.; Wang, Y. C.; Xu, C.; Zou, H. Y.; Ding, W. B.; Dai, Y. J.; Gu, B. H.; Sun, B. Z.; et al. 3D Orthogonal Woven Triboelectric Nanogenerator for Effective Biomechanical Energy Harvesting and as Self-Powered Active Motion Sensors. *Adv. Mater.* **2017**, *29*, 1702648.
(368) Chen, B. D.; Tang, W.; Jiang, T.; Zhu, L. P.; Chen, X. Y.; He, C.; Xu, L.; Guo, H. Y.; Lin, P.; Li, D.; et al. Three-Dimensional Ultraflexible Triboelectric Nanogenerator Made by 3D Printing. *Nano Energy* **2018**, *45*, 380−389.
(369) Zhang, M.; Zhao, M.; Jian, M.; Wang, C.; Yu, A.; Yin, Z.; Liang, X.; Wang, H.; Xia, K.; Liang, X.; Zhai, J.; Zhang, Y. Printable Smart Pattern for Multifunctional Energy-Management E-Textile. *Matter* **2019**, *1*, 168−179.
(370) Gong, J. L.; Xu, B. G.; Guan, X. Y.; Chen, Y. J.; Li, S. Y.; Feng, J. Towards Truly Wearable Energy Harvesters with Full Structural Integrity of Fiber Materials. *Nano Energy* **2019**, *58*, 365−374.
(371) Lewis, J. A.; Ahn, B. Y. Device Fabrication: Three-Dimensional Printed Electronics. *Nature* **2015**, *518*, 42−43.
(372) Lipson, H.; Kurman, M. *Fabricated: The New World of 3D Printing*; John Wiley & Sons: New York, 2013.
(373) MacDonald, E.; Wicker, R. Multiprocess 3D Printing for Increasing Component Functionality. *Science* **2016**, *353*, aaf2093.
(374) Truby, R. L.; Lewis, J. A. Printing Soft Matter in Three Dimensions. *Nature* **2016**, *540*, 371−378.
(375) Capel, A. J.; Rimington, R. P.; Lewis, M. P.; Christie, S. D. R. 3D Printing for Chemical, Pharmaceutical and Biological Applications. *Nat. Rev. Chem.* **2018**, *2*, 422−436.
(376) Wallin, T. J.; Pikul, J.; Shepherd, R. F. 3D Printing of Soft Robotic Systems. *Nat. Rev. Mater.* **2018**, *3*, 84−100.
(377) Zarek, M.; Layani, M.; Cooperstein, I.; Sachyani, E.; Cohn, D.; Magdassi, S. 3D Printing of Shape Memory Polymers for Flexible Electronic Devices. *Adv. Mater.* **2016**, *28*, 4449−4454.
(378) Wang, X.; Jiang, M.; Zhou, Z. W.; Gou, J. H.; Hui, D. 3D Printing of Polymer Matrix Composites: A Review and Prospective. *Compos. B. Eng.* **2017**, *110*, 442−458.
(379) Ventola, C. L. Medical Applications for 3D Printing: Current and Projected Uses. *Pharm. Ther.* **2014**, *39*, 704−711.
(380) Valtas, A.; Sun, D. 3D Printing for Garments Production: An Exploratory Study. *J. Fash. Technol. Text. Eng.* **2016**, *4*, 3.
(381) Sabantina, L.; Kinzel, F.; Ehrmann, A.; Finsterbusch, K. Combining 3D Printed Forms with Textile Structures - Mechanical and Geometrical Properties of Multi-Material Systems. *IOP Conf. Ser.: Mater. Sci. Eng.* **2015**, *87*, 012005.
(382) Erturk, A.; Inman, D. J. *Piezoelectric Energy Harvesting*; John Wiley & Sons: Chichester, UK, 2011.
(383) Jaffe, B.; Cook, W. R.; Jaffe, H. *Piezoelectric Ceramics*; Academic Press: London, 1971.
(384) Kim, H. S.; Kim, J. H.; Kim, J. A Review of Piezoelectric Energy Harvesting Based on Vibration. *Int. J. Precis. Eng. Manuf.* **2011**, *12*, 1129−1141.
(385) Fang, H. B.; Liu, J. Q.; Xu, Z. Y.; Dong, L.; Wang, L.; Chen, D.; Cai, B. C.; Liu, Y. Fabrication and Performance of Mems-Based Piezoelectric Power Generator for Vibration Energy Harvesting. *Microelectron. J.* **2006**, *37*, 1280−1284.
(386) González, J. L.; Rubio, A.; Moll, F. Human Powered Piezoelectric Batteries to Supply Power to Wearable Electronic Devices. *Int. J. Soc. Mater. Eng. Resour.* **2002**, *10*, 34−40.
(387) Howells, C. A. Piezoelectric Energy Harvesting. *Energy Convers. Manage.* **2009**, *50*, 1847−1850.
(388) Shu, Y. C.; Lien, I. C. Efficiency of Energy Conversion for a Piezoelectric Power Harvesting System. *J. Micromech. Microeng.* **2006**, *16*, 2429−2438.
(389) Sodano, H. A.; Inman, D. J.; Park, G. A Review of Power Harvesting from Vibration Using Piezoelectric Materials. *Shock Vib. Digest* **2004**, *36*, 197−206.
(390) Taylor, G. W.; Burns, J. R.; Kammann, S. M.; Powers, W. B.; Welsh, T. R. The Energy Harvesting Eel: A Small Subsurface Ocean/River Power Generator. *IEEE J. Oceanic Eng.* **2001**, *26*, 539−547.
(391) Curie, J.; Curie, P. Développement Par Compression De L'électricité Polaire Dans Les Cristaux Hémièdres À Faces Inclinées. *Bulletin de Minéralogie* **1880**, *3*, 90−93.
(392) Ottman, G. K.; Hofmann, H. F.; Bhatt, A. C.; Lesieutre, L. G. A. Adaptive Piezoelectric Energy Harvesting Circuit for Wireless Remote Power Supply. *IEEE Trans. Power Electron.* **2002**, *17*, 669−676.
(393) Ottman, G. K.; Hofmann, H. F.; Lesieutre, G. A. Optimized Piezoelectric Energy Harvesting Circuit Using Step-Down Converter in Discontinuous Conduction Mode. *IEEE Trans. Power Electron.* **2003**, *18*, 696−703.
(394) Sodano, H. A.; Inman, D. J.; Park, G. Comparison of Piezoelectric Energy Harvesting Devices for Recharging Batteries. *J. Intell. Mater. Syst. Struct.* **2005**, *16*, 799−807.
(395) Wang, Z. L.; Song, J. Piezoelectric Nanogenerators Based on Zinc Oxide Nanowire Arrays. *Science* **2006**, *312*, 242−246.
(396) Calio, R.; Rongala, U. B.; Camboni, D.; Milazzo, M.; Stefanini, C.; de Petris, G.; Oddo, C. M. Piezoelectric Energy Harvesting Solutions. *Sensors* **2014**, *14*, 4755−4790.
(397) Hwang, G. T.; Park, H.; Lee, J. H.; Oh, S.; Park, K. I.; Byun, M.; Park, H.; Ahn, G.; Jeong, C. K.; No, K.; et al. Self-Powered Cardiac Pacemaker Enabled by Flexible Single Crystalline PMN-Pt Piezoelectric Energy Harvester. *Adv. Mater.* **2014**, *26*, 4880−4887.
(398) Chun, J.; Kang, N. R.; Kim, J. Y.; Noh, M. S.; Kang, C. Y.; Choi, D.; Kim, S. W.; Wang, Z. L.; Baik, J. M. Highly Anisotropic Power Generation in Piezoelectric Hemispheres Composed Stretchable Composite Film for Self-Powered Motion Sensor. *Nano Energy* **2015**, *11*, 1−10.
(399) Hwang, G. T.; Byun, M.; Jeong, C. K.; Lee, K. J. Flexible Piezoelectric Thin-Film Energy Harvesters and Nanosensors for Biomedical Applications. *Adv. Healthcare Mater.* **2015**, *4*, 646−658.
(400) Jung, W. S.; Lee, M. J.; Kang, M. G.; Moon, H. G.; Yoon, S. J.; Baek, S. H.; Kang, C. Y. Powerful Curved Piezoelectric Generator for Wearable Applications. *Nano Energy* **2015**, *13*, 174−181.
(401) Huang, Y. A.; Ding, Y. J.; Bian, J.; Su, Y. W.; Zhou, J.; Duan, Y. Q.; Yin, Z. P. Hyper-Stretchable Self-Powered Sensors Based on Electrohydrodynamically Printed, Self-Similar Piezoelectric Nano/Microfibers. *Nano Energy* **2017**, *40*, 432−439.
(402) Jeong, C. K.; Baek, C.; Kingon, A. I.; Park, K. I.; Kim, S. H. Lead-Free Perovskite Nanowire-Employed Piezopolymer for Highly Efficient Flexible Nanocomposite Energy Harvester. *Small* **2018**, *14*, No. 1704022.
(403) Lee, J. H.; Heo, K.; Schulz-Schonhagen, K.; Lee, J. H.; Desai, M. S.; Jin, H. E.; Lee, S. W. Diphenylalanine Peptide Nanotube Energy Harvesters. *ACS Nano* **2018**, *12*, 8138−8144.
(404) Ali, F.; Raza, W.; Li, X.; Gul, H.; Kim, K.-H. Piezoelectric Energy Harvesters for Biomedical Applications. *Nano Energy* **2019**, *57*, 879−902.
(405) Zhang, Y. Z.; Wu, M. J.; Zhu, Q. Y.; Wang, F. Y.; Su, H. X.; Li, H.; Diao, C. L.; Zheng, H. W.; Wu, Y. H.; Wang, Z. L. Performance Enhancement of Flexible Piezoelectric Nanogenerator via Doping and Rational 3D Structure Design for Self-Powered Mechanosensational System. *Adv. Funct. Mater.* **2019**, *29*, 1904259.
(406) Mo, X. W.; Zhou, H.; Li, W. B.; Xu, Z. S.; Duan, J. J.; Huang, L.; Hu, B.; Zhou, J. Piezoelectrets for Wearable Energy Harvesters and Sensors. *Nano Energy* **2019**, *65*, 104033.
(407) Chen, J.; Oh, S. K.; Nabulsi, N.; Johnson, H.; Wang, W. J.; Ryou, J. H. Biocompatible and Sustainable Power Supply for Self-

https://dx.doi.org/10.1021/acs.chemrev.9b00821
Chem. Rev. 2020, 120, 3668−3720

Powered Wearable and Implantable Electronics Using III-Nitride Thin-Film-Based Flexible Piezoelectric Generator. *Nano Energy* **2019**, *57*, 670−679.
(408) Shepelin, N. A.; Glushenkov, A. M.; Lussini, V. C.; Fox, P. J.; Dicinoski, G. W.; Shapter, J. G.; Ellis, A. V. New Developments in Composites, Copolymer Technologies and Processing Techniques for Flexible Fluoropolymer Piezoelectric Generators for Efficient Energy Harvesting. *Energy Environ. Sci.* **2019**, *12*, 1143−1176.
(409) Alluri, N. R.; Saravanakumar, B.; Kim, S.-J. Flexible, Hybrid Piezoelectric Film ($BaTi_{(1-x)}Zr_xO_3$)/PVDF Nanogenerator as a Self-Powered Fluid Velocity Sensor. *ACS Appl. Mater. Interfaces* **2015**, *7*, 9831−9840.
(410) Chen, X. L.; Li, X. M.; Shao, J. Y.; An, N. L.; Tian, H. M.; Wang, C.; Han, T. Y.; Wang, L.; Lu, B. H. High-Performance Piezoelectric Nanogenerators with Imprinted P(VDF-TrFE)/$BaTiO_3$ Nanocomposite Micropillars for Self-Powered Flexible Sensors. *Small* **2017**, *13*, 1604245.
(411) Chun, J.; Lee, K. Y.; Kang, C. Y.; Kim, M. W.; Kim, S. W.; Baik, J. M. Embossed Hollow Hemisphere-Based Piezoelectric Nanogenerator and Highly Responsive Pressure Sensor. *Adv. Funct. Mater.* **2014**, *24*, 2038−2043.
(412) Hu, Y. F.; Wang, Z. L. Recent Progress in Piezoelectric Nanogenerators as a Sustainable Power Source in Self-Powered Systems and Active Sensors. *Nano Energy* **2015**, *14*, 3−14.
(413) Lee, J. H.; Yoon, H. J.; Kim, T. Y.; Gupta, M. K.; Lee, J. H.; Seung, W.; Ryu, H.; Kim, S. W. Micropatterned P(VDF-TrFE) Film-Based Piezoelectric Nanogenerators for Highly Sensitive Self-Powered Pressure Sensors. *Adv. Funct. Mater.* **2015**, *25*, 3203−3209.
(414) Lee, M.; Bae, J.; Lee, J.; Lee, C. S.; Hong, S.; Wang, Z. L. Self-Powered Environmental Sensor System Driven by Nanogenerators. *Energy Environ. Sci.* **2011**, *4*, 3359−3363.
(415) Lee, S.; Bae, S. H.; Lin, L.; Yang, Y.; Park, C.; Kim, S. W.; Cha, S. N.; Kim, H.; Park, Y. J.; Wang, Z. L. Super-Flexible Nanogenerator for Energy Harvesting from Gentle Wind and as an Active Deformation Sensor. *Adv. Funct. Mater.* **2013**, *23*, 2445−2449.
(416) Mandal, D.; Yoon, S.; Kim, K. J. Origin of Piezoelectricity in an Electrospun Poly(Vinylidene Fluoride-Trifluoroethylene) Nanofiber Web-Based Nanogenerator and Nano-Pressure Sensor. *Macromol. Rapid Commun.* **2011**, *32*, 831−837.
(417) Shin, S. H.; Kim, Y. H.; Lee, M. H.; Jung, J. Y.; Nah, J. Hemispherically Aggregated $BaTiO_3$ Nanoparticle Composite Thin Film for High-Performance Flexible Piezoelectric Nanogenerator. *ACS Nano* **2014**, *8*, 2766−2773.
(418) Wang, X.; Shi, J. In *Piezoelectric Nanomaterials for Biomedical Applications*; Ciofani, G., Menciassi, A., Eds.; Springer: Berlin, 2012; pp 135−172.
(419) Zhou, J.; Gu, Y.; Fei, P.; Mai, W.; Gao, Y.; Yang, R.; Bao, G.; Wang, Z. L. Flexible Piezotronic Strain Sensor. *Nano Lett.* **2008**, *8*, 3035−3040.
(420) Zhong, J. W.; Zhong, Q. Z.; Hu, Q. Y.; Wu, N.; Li, W. B.; Wang, B.; Hu, B.; Zhou, J. Stretchable Self-Powered Fiber-Based Strain Sensor. *Adv. Funct. Mater.* **2015**, *25*, 1798−1803.
(421) Maity, K.; Mandal, D. All-Organic High-Performance Piezoelectric Nanogenerator with Multilayer Assembled Electrospun Nanofiber Mats for Self-Powered Multifunctional Sensors. *ACS Appl. Mater. Interfaces* **2018**, *10*, 18257−18269.
(422) Almusallam, A.; Luo, Z.; Komolafe, A.; Yang, K.; Robinson, A.; Torah, R.; Beeby, S. Flexible Piezoelectric Nano-Composite Films for Kinetic Energy Harvesting from Textiles. *Nano Energy* **2017**, *33*, 146−156.
(423) Kim, K. N.; Chun, J.; Chae, S. A.; Ahn, C. W.; Kim, I. W.; Kim, S. W.; Wang, Z. L.; Baik, J. M. Silk Fibroin-Based Biodegradable Piezoelectric Composite Nanogenerators Using Lead-Free Ferroelectric Nanoparticles. *Nano Energy* **2015**, *14*, 87−94.
(424) Kim, H.; Kim, S. M.; Son, H.; Kim, H.; Park, B.; Ku, J.; Sohn, J. I.; Im, K.; Jang, J. E.; Park, J. J.; et al. Enhancement of Piezoelectricity via Electrostatic Effects on a Textile Platform. *Energy Environ. Sci.* **2012**, *5*, 8932−8936.
(425) Khan, A.; Ali Abbasi, M.; Hussain, M.; Hussain Ibupoto, Z.; Wissting, J.; Nur, O.; Willander, M. Piezoelectric Nanogenerator Based on Zinc Oxide Nanorods Grown on Textile Cotton Fabric. *Appl. Phys. Lett.* **2012**, *101*, 193506.
(426) Khan, A.; Hussain, M.; Nur, O.; Willander, M. Mechanical and Piezoelectric Properties of Zinc Oxide Nanorods Grown on Conductive Textile Fabric as an Alternative Substrate. *J. Phys. D: Appl. Phys.* **2014**, *47*, 345102.
(427) Khan, A.; Hussain, M.; Abbasi, M. A.; Ibupoto, Z. H.; Nur, O.; Willander, M. Analysis of Junction Properties of Gold-Zinc Oxide Nanorods-Based Schottky Diode by Means of Frequency Dependent Electrical Characterization on Textile. *J. Mater. Sci.* **2014**, *49*, 3434−3441.
(428) Khan, A.; Edberg, J.; Nur, O.; Willander, M. A Novel Investigation on Carbon Nanotube/ZnO, Ag/ZnO and Ag/Carbon Nanotube/ZnO Nanowires Junctions for Harvesting Piezoelectric Potential on Textile. *J. Appl. Phys.* **2014**, *116*, 034505.
(429) Khan, A.; Abbasi, M. A.; Wissting, J.; Nur, O.; Willander, M. Harvesting Piezoelectric Potential from Zinc Oxide Nanoflowers Grown on Textile Fabric Substrate. *Phys. Status Solidi RRL* **2013**, *7*, 980−984.
(430) Zhang, Z.; Chen, Y.; Guo, J. S. Zno Nanorods Patterned-Textile Using a Novel Hydrothermal Method for Sandwich Structured-Piezoelectric Nanogenerator for Human Energy Harvesting. *Physica E* **2019**, *105*, 212−218.
(431) Wu, W.; Bai, S.; Yuan, M.; Qin, Y.; Wang, Z. L.; Jing, T. Lead Zirconate Titanate Nanowire Textile Nanogenerator for Wearable Energy-Harvesting and Self-Powered Devices. *ACS Nano* **2012**, *6*, 6231−6235.
(432) Liu, Z.; Pan, C.; Lin, L.; Huang, J.; Ou, Z. Direct-Write PVDF Nonwoven Fiber Fabric Energy Harvesters via the Hollow Cylindrical near-Field Electrospinning Process. *Smart Mater. Struct.* **2014**, *23*, 025003.
(433) Zhang, L. L.; Gui, J. Z.; Wu, Z. Z.; Li, R.; Wang, Y.; Gong, Z. Y.; Zhao, X. Z.; Sun, C. L.; Guo, S. S. Enhanced Performance of Piezoelectric Nanogenerator Based on Aligned Nanofibers and Three-Dimensional Interdigital Electrodes. *Nano Energy* **2019**, *65*, 103924.
(434) Ghosh, S. K.; Mandal, D. Synergistically Enhanced Piezoelectric Output in Highly Aligned 1D Polymer Nanofibers Integrated All-Fiber Nanogenerator for Wearable Nano-Tactile Sensor. *Nano Energy* **2018**, *53*, 245−257.
(435) Zeng, W.; Tao, X. M.; Chen, S.; Shang, S. M.; Chan, H. L. W.; Choy, S. H. Highly Durable All-Fiber Nanogenerator for Mechanical Energy Harvesting. *Energy Environ. Sci.* **2013**, *6*, 2631−2638.
(436) He, S. B.; Dong, W.; Guo, Y. P.; Guan, L.; Xiao, H. Y.; Liu, H. Z. Piezoelectric Thin Film on Glass Fiber Fabric with Structural Hierarchy: An Approach to High-Performance, Superflexible, Cost-Effective, and Large-Scale Nanogenerators. *Nano Energy* **2019**, *59*, 745−753.
(437) Chang, J. Y.; Dommer, M.; Chang, C.; Lin, L. W. Piezoelectric Nanofibers for Energy Scavenging Applications. *Nano Energy* **2012**, *1*, 356−371.
(438) Kim, M.; Wu, Y. S.; Kan, E. C.; Fan, J. Breathable and Flexible Piezoelectric ZnO@PVDF Fibrous Nanogenerator for Wearable Applications. *Polymers* **2018**, *10*, 745.
(439) Qin, Y.; Wang, X.; Wang, Z. L. Microfibre-Nanowire Hybrid Structure for Energy Scavenging. *Nature* **2008**, *451*, 809−813.
(440) Lee, M.; Chen, C. Y.; Wang, S.; Cha, S. N.; Park, Y. J.; Kim, J. M.; Chou, L. J.; Wang, Z. L. A Hybrid Piezoelectric Structure for Wearable Nanogenerators. *Adv. Mater.* **2012**, *24*, 1759−1764.
(441) Kim, M.; Yun, K. S. Helical Piezoelectric Energy Harvester and Its Application to Energy Harvesting Garments. *Micromachines* **2017**, *8*, 115.
(442) Bai, S.; Zhang, L.; Xu, Q.; Zheng, Y.; Qin, Y.; Wang, Z. L. Two Dimensional Woven Nanogenerator. *Nano Energy* **2013**, *2*, 749−753.
(443) Yang, E.; Xu, Z.; Chur, L. K.; Behroozfar, A.; Baniasadi, M.; Moreno, S.; Huang, J.; Gilligan, J.; Minary-Jolandan, M. Nanofibrous Smart Fabrics from Twisted Yarns of Electrospun Piezopolymer. *ACS Appl. Mater. Interfaces* **2017**, *9*, 24220−24229.

https://dx.doi.org/10.1021/acs.chemrev.9b00821
Chem. Rev. 2020, 120, 3668−3720

(444) Zhang, M.; Gao, T.; Wang, J. S.; Liao, J. J.; Qiu, Y. Q.; Yang, Q.; Xue, H.; Shi, Z.; Zhao, Y.; Xiong, Z. X.; et al. A Hybrid Fibers Based Wearable Fabric Piezoelectric Nanogenerator for Energy Harvesting Application. *Nano Energy* **2015**, *13*, 298−305.
(445) Soin, N.; Shah, T. H.; Anand, S. C.; Geng, J. F.; Pornwannachai, W.; Mandal, P.; Reid, D.; Sharma, S.; Hadimani, R. L.; Bayramol, D. V.; et al. Novel "3-D Spacer" All Fibre Piezoelectric Textiles for Energy Harvesting Applications. *Energy Environ. Sci.* **2014**, *7*, 1670−1679.
(446) Lu, X.; Qu, H.; Skorobogatiy, M. Piezoelectric Micro- and Nanostructured Fibers Fabricated from Thermoplastic Nanocomposites Using a Fiber Drawing Technique: Comparative Study and Potential Applications. *ACS Nano* **2017**, *11*, 2103−2114.
(447) Talbourdet, A.; Rault, F.; Lemort, G.; Cochrane, C.; Devaux, E.; Campagne, C. 3D Interlock Design 100% PVDF Piezoelectric to Improve Energy Harvesting. *Smart Mater. Struct.* **2018**, *27*, 075010.
(448) Egusa, S.; Wang, Z.; Chocat, N.; Ruff, Z. M.; Stolyarov, A. M.; Shemuly, D.; Sorin, F.; Rakich, P. T.; Joannopoulos, J. D.; Fink, Y. Multimaterial Piezoelectric Fibres. *Nat. Mater.* **2010**, *9*, 643−648.
(449) Li, Z.; Wang, Z. L. Air/Liquid-Pressure and Heartbeat-Driven Flexible Fiber Nanogenerators as a Micro/Nano-Power Source or Diagnostic Sensor. *Adv. Mater.* **2011**, *23*, 84−89.
(450) Hadimani, R. L.; Bayramol, D. V.; Sion, N.; Shah, T.; Qian, L. M.; Shi, S. X.; Siores, E. Continuous Production of Piezoelectric PVDF Fibre for E-Textile Applications. *Smart Mater. Struct.* **2013**, *22*, 075017.
(451) Liao, Q. L.; Zhang, Z.; Zhang, X. H.; Mohr, M.; Zhang, Y.; Fecht, H. J. Flexible Piezoelectric Nanogenerators Based on a Fiber/ZnO Nanowires/Paper Hybrid Structure for Energy Harvesting. *Nano Res.* **2014**, *7*, 917−928.
(452) Baniasadi, M.; Huang, J.; Xu, Z.; Moreno, S.; Yang, X.; Chang, J.; Quevedo-Lopez, M. A.; Naraghi, M.; Minary-Jolandan, M. High-Performance Coils and Yarns of Polymeric Piezoelectric Nanofibers. *ACS Appl. Mater. Interfaces* **2015**, *7*, 5358−5366.
(453) Zhang, L.; Bai, S.; Su, C.; Zheng, Y. B.; Qin, Y.; Xu, C.; Wang, Z. L. A High-Reliability Kevlar Fiber-ZnO Nanowires Hybrid Nanogenerator and Its Application on Self-Powered UV Detection. *Adv. Funct. Mater.* **2015**, *25*, 5794−5798.
(454) Choi, M.; Murillo, G.; Hwang, S.; Kim, J. W.; Jung, J. H.; Chen, C. Y.; Lee, M. Mechanical and Electrical Characterization of PVDF-ZnO Hybrid Structure for Application to Nanogenerator. *Nano Energy* **2017**, *33*, 462−468.
(455) Du, Y. Z.; Fu, C. K.; Gao, Y. Z.; Liu, L.; Liu, Y. W.; Xing, L. X.; Zhao, F. Carbon Fibers/ZnO Nanowires Hybrid Nanogenerator Based on an Insulating Interface Barrier. *RSC Adv.* **2017**, *7*, 21452−21458.
(456) Gao, H.; Minh, P. T.; Wang, H.; Minko, S.; Locklin, J.; Nguyen, T.; Sharma, S. High-Performance Flexible Yarn for Wearable Piezoelectric Nanogenerators. *Smart Mater. Struct.* **2018**, *27*, 095018.
(457) Zhou, Y.; He, J.; Wang, H.; Qi, K.; Nan, N.; You, X.; Shao, W.; Wang, L.; Ding, B.; Cui, S. Highly Sensitive, Self-Powered and Wearable Electronic Skin Based on Pressure-Sensitive Nanofiber Woven Fabric Sensor. *Sci. Rep.* **2017**, *7*, 12949.
(458) Lund, A.; Rundqvist, K.; Nilsson, E.; Yu, L.; Hagström, B.; Müller, C. Energy Harvesting Textiles for a Rainy Day: Woven Piezoelectrics Based on Melt-Spun PVDF Microfibres with a Conducting Core. *npj Flex. Electron.* **2018**, *2*, 9.
(459) Nilsson, E.; Lund, A.; Jonasson, C.; Johansson, C.; Hagstrom, B. Poling and Characterization of Piezoelectric Polymer Fibers for Use in Textile Sensors. *Sens. Actuators A: Phys.* **2013**, *201*, 477−486.
(460) Sim, H. J.; Choi, C.; Lee, C. J.; Kim, Y. T.; Spinks, G. M.; Lima, M. D.; Baughman, R. H.; Kim, S. J. Flexible, Stretchable and Weavable Piezoelectric Fiber. *Adv. Eng. Mater.* **2015**, *17*, 1270−1275.
(461) Song, S.; Yun, K. S. Design and Characterization of Scalable Woven Piezoelectric Energy Harvester for Wearable Applications. *Smart Mater. Struct.* **2015**, *24*, 045008.
(462) Ahn, Y.; Song, S.; Yun, K.-S. Woven Flexible Textile Structure for Wearable Power-Generating Tactile Sensor Array. *Smart Mater. Struct.* **2015**, *24*, 075002.
(463) Mokhtari, F.; Foroughi, J.; Zheng, T.; Cheng, Z. X.; Spinks, G. M. Triaxial Braided Piezo Fiber Energy Harvesters for Self-Powered Wearable Technologies. *J. Mater. Chem. A* **2019**, *7*, 8245−8257.
(464) Dagdeviren, C.; Joe, P.; Tuzman, O. L.; Park, K. I.; Lee, K. J.; Shi, Y.; Huang, Y. G.; Rogers, J. A. Recent Progress in Flexible and Stretchable Piezoelectric Devices for Mechanical Energy Harvesting, Sensing and Actuation. *Extreme Mech. Lett.* **2016**, *9*, 269−281.
(465) Dagdeviren, C.; Shi, Y.; Joe, P.; Ghaffari, R.; Balooch, G.; Usgaonkar, K.; Gur, O.; Tran, P. L.; Crosby, J. R.; Meyer, M.; et al. Conformal Piezoelectric Systems for Clinical and Experimental Characterization of Soft Tissue Biomechanics. *Nat. Mater.* **2015**, *14*, 728−736.
(466) Wu, N.; Cheng, X.; Zhong, Q.; Zhong, J.; Li, W.; Wang, B.; Hu, B.; Zhou, J. Cellular Polypropylene Piezoelectret for Human Body Energy Harvesting and Health Monitoring. *Adv. Funct. Mater.* **2015**, *25*, 4788−4794.
(467) Li, W.; Torres, D.; Díaz, R.; Wang, Z.; Wu, C.; Wang, C.; Lin Wang, Z.; Sepúlveda, N. Nanogenerator-Based Dual-Functional and Self-Powered Thin Patch Loudspeaker or Microphone for Flexible Electronics. *Nat. Commun.* **2017**, *8*, 15310.
(468) Liu, C.; Yu, A.; Peng, M.; Song, M.; Liu, W.; Zhang, Y.; Zhai, J. Improvement in the Piezoelectric Performance of a ZnO Nanogenerator by a Combination of Chemical Doping and Interfacial Modification. *J. Phys. Chem. C* **2016**, *120*, 6971−6977.
(469) Roundy, S.; Leland, E. S.; Baker, J.; Carleton, E.; Reilly, E.; Lai, E.; Otis, B.; Rabaey, J. M.; Wright, P. K.; Sundararajan, V. Improving Power Output for Vibration-Based Energy Scavengers. *IEEE Pervasive Comput* **2005**, *4*, 28−36.
(470) Du, S. J.; Jia, Y.; Chen, S. T.; Zhao, C.; Sun, B. Q.; Arroyo, E.; Seshia, A. A. A New Electrode Design Method in Piezoelectric Vibration Energy Harvesters to Maximize Output Power. *Sens. Actuators A: Phys.* **2017**, *263*, 693−701.
(471) Kim, M.; Dugundji, J.; Wardle, B. L. Effect of Electrode Configurations on Piezoelectric Vibration Energy Harvesting Performance. *Smart Mater. Struct.* **2015**, *24*, 045026.
(472) Cho, J.; Anderson, M.; Richards, R.; Bahr, D.; Richards, C. Optimization of Electromechanical Coupling for a Thin-Film PZT Membrane: II. Experiment. *J. Micromech. Microeng.* **2005**, *15*, 1804−1809.
(473) Zhao, J.; Zheng, X.; Zhou, L.; Zhang, Y.; Sun, J.; Dong, W.; Deng, S.; Peng, S. Investigation of a D_{15} Mode PZT-51 Piezoelectric Energy Harvester with a Series Connection Structure. *Smart Mater. Struct.* **2012**, *21*, 105006.
(474) Ren, B.; Or, S. W.; Zhang, Y.; Zhang, Q.; Li, X.; Jiao, J.; Wang, W.; Liu, D.; Zhao, X.; Luo, H. Piezoelectric Energy Harvesting Using Shear Mode 0.71Pb $(Mg_{1/3}\ Nb_{2/3})\ O_3$−0.29$PbTiO_3$ Single Crystal Cantilever. *Appl. Phys. Lett.* **2010**, *96*, 083502.
(475) Kulkarni, V.; Ben-Mrad, R.; Prasad, S. E.; Nemana, S. A Shear-Mode Energy Harvesting Device Based on Torsional Stresses. *IEEE/ASME Trans. Mechatronics* **2014**, *19*, 801−807.
(476) Uchino, K. In *Advanced Piezoelectric Materials*; Woodhead Publishing: Cambridge, UK, 2017; pp 385−451.
(477) Cui, H.; Hensleigh, R.; Yao, D.; Maurya, D.; Kumar, P.; Kang, M. G.; Priya, S.; Zheng, X. R. Three-Dimensional Printing of Piezoelectric Materials with Designed Anisotropy and Directional Response. *Nat. Mater.* **2019**, *18*, 234−241.
(478) Ghosh, S. K.; Mandal, D. High-Performance Bio-Piezoelectric Nanogenerator Made with Fish Scale. *Appl. Phys. Lett.* **2016**, *109*, 103701.
(479) Karan, S. K.; Maiti, S.; Kwon, O.; Paria, S.; Maitra, A.; Si, S. K.; Kim, Y.; Kim, J. K.; Khatua, B. B. Nature Driven Spider Silk as High Energy Conversion Efficient Bio-Piezoelectric Nanogenerator. *Nano Energy* **2018**, *49*, 655−666.
(480) Yang, Y.; Shen, Q. L.; Jin, J. M.; Wang, Y. P.; Qian, W. J.; Yuan, D. W. Rotational Piezoelectric Wind Energy Harvesting Using Impact-Induced Resonance. *Appl. Phys. Lett.* **2014**, *105*, 053901.
(481) Wang, D. A.; Liu, N. Z. A Shear Mode Piezoelectric Energy Harvester Based on a Pressurized Water Flow. *Sens. Actuators A: Phys.* **2011**, *167*, 449−458.

https://dx.doi.org/10.1021/acs.chemrev.9b00821
Chem. Rev. 2020, 120, 3668−3720

(482) Ilyas, M. A.; Swingler, J. Piezoelectric Energy Harvesting from Raindrop Impacts. *Energy* **2015**, *90*, 796−806.
(483) Chen, X. X.; Song, Y.; Su, Z. M.; Chen, H. T.; Cheng, X. L.; Zhang, J. X.; Han, M. D.; Zhang, H. X. Flexible Fiber-Based Hybrid Nanogenerator for Biomechanical Energy Harvesting and Physiological Monitoring. *Nano Energy* **2017**, *38*, 43−50.
(484) Jung, W. S.; Kang, M. G.; Moon, H. G.; Baek, S. H.; Yoon, S. J.; Wang, Z. L.; Kim, S. W.; Kang, C. Y. High Output Piezo/Triboelectric Hybrid Generator. *Sci. Rep.* **2015**, *5*, 9309.
(485) Li, X. H.; Lin, Z. H.; Cheng, G.; Wen, X. N.; Liu, Y.; Niu, S. M.; Wang, Z. L. 3D Fiber-Based Hybrid Nanogenerator for Energy Harvesting and as a Self-Powered Pressure Sensor. *ACS Nano* **2014**, *8*, 10674−10681.
(486) Han, M.; Zhang, X. S.; Meng, B.; Liu, W.; Tang, W.; Sun, X.; Wang, W.; Zhang, H. R-Shaped Hybrid Nanogenerator with Enhanced Piezoelectricity. *ACS Nano* **2013**, *7*, 8554−8560.
(487) Shi, B.; Zheng, Q.; Jiang, W.; Yan, L.; Wang, X.; Liu, H.; Yao, Y.; Li, Z.; Wang, Z. L. A Packaged Self-Powered System with Universal Connectors Based on Hybridized Nanogenerators. *Adv. Mater.* **2016**, *28*, 846−852.
(488) Huang, T.; Wang, C.; Yu, H.; Wang, H. Z.; Zhang, Q. H.; Zhu, M. F. Human Walking-Driven Wearable All-Fiber Triboelectric Nanogenerator Containing Electrospun Polyvinylidene Fluoride Piezoelectric Nanofibers. *Nano Energy* **2015**, *14*, 226−235.
(489) Yang, W.; Gong, W.; Hou, C.; Su, Y.; Guo, Y.; Zhang, W.; Li, Y.; Zhang, Q.; Wang, H. All-Fiber Tribo-Ferroelectric Synergistic Electronics with High Thermal-Moisture Stability and Comfortability. *Nat. Commun.* **2019**, *10*, 5541.
(490) Guo, Y. B.; Zhang, X. S.; Wang, Y.; Gong, W.; Zhang, Q. H.; Wang, H. Z.; Brugger, J. All-Fiber Hybrid Piezoelectric-Enhanced Triboelectric Nanogenerator for Wearable Gesture Monitoring. *Nano Energy* **2018**, *48*, 152−160.
(491) Chen, S.; Tao, X. M.; Zeng, W.; Yang, B.; Shang, S. M. Quantifying Energy Harvested from Contact-Mode Hybrid Nanogenerators with Cascaded Piezoelectric and Triboelectric Units. *Adv. Energy Mater.* **2017**, *7*, 1601569.
(492) Song, J.; Yang, B.; Zeng, W.; Peng, Z. H.; Lin, S. P.; Li, J.; Tao, X. M. Highly Flexible, Large-Area, and Facile Textile-Based Hybrid Nanogenerator with Cascaded Piezoelectric and Triboelectric Units for Mechanical Energy Harvesting. *Adv. Mater. Technol.* **2018**, *3*, 1800016.
(493) Zhu, M. L.; Shi, Q. F.; He, T. Y. Y.; Yi, Z. R.; Ma, Y. M.; Yang, B.; Chen, T.; Lee, C. Self-Powered and Self-Functional Cotton Sock Using Piezoelectric and Triboelectric Hybrid Mechanism for Healthcare and Sports Monitoring. *ACS Nano* **2019**, *13*, 1940−1952.
(494) Leonov, V.; Vullers, R. J. M. Wearable Thermoelectric Generators for Body-Powered Devices. *J. Electron. Mater.* **2009**, *38*, 1491−1498.
(495) Tarancón, A. Powering the IoT Revolution with Heat. *Nat. Electron.* **2019**, *2*, 270−271.
(496) Francioso, L.; De Pascali, C.; Farella, I.; Martucci, C.; Creti, P.; Siciliano, P.; Perrone, A. Flexible Thermoelectric Generator for Ambient Assisted Living Wearable Biometric Sensors. *J. Power Sources* **2011**, *196*, 3239−3243.
(497) Leonov, V.; Vullers, R. J. M. Wearable Electronics Self-Powered by Using Human Body Heat: The State of the Art and the Perspective. *J. Renewable Sustainable Energy* **2009**, *1*, 062701.
(498) Siddique, A. R. M.; Mahmud, S.; Van Heyst, B. A Review of the State of the Science on Wearable Thermoelectric Power Generators (TEGs) and Their Existing Challenges. *Renew. Sustain. Energy Rev.* **2017**, *73*, 730−744.
(499) Xue, H.; Yang, Q.; Wang, D. Y.; Luo, W. J.; Wang, W. Q.; Lin, M. S.; Liang, D. L.; Luo, Q. M. A Wearable Pyroelectric Nanogenerator and Self-Powered Breathing Sensor. *Nano Energy* **2017**, *38*, 147−154.
(500) Yang, Y.; Wang, S.; Zhang, Y.; Wang, Z. L. Pyroelectric Nanogenerators for Driving Wireless Sensors. *Nano Lett.* **2012**, *12*, 6408−6413.
(501) Cuadras, A.; Gasulla, M.; Ferrari, V. Thermal Energy Harvesting through Pyroelectricity. *Sens. Actuators A: Phys.* **2010**, *158*, 132−139.
(502) Thakre, A.; Kumar, A.; Song, H. C.; Jeong, D. Y.; Ryu, J. Pyroelectric Energy Conversion and Its Applications-Flexible Energy Harvesters and Sensors. *Sensors* **2019**, *19*, 2170.
(503) Ryu, H.; Kim, S. W. Emerging Pyroelectric Nanogenerators to Convert Thermal Energy into Electrical Energy. *Small* **2019**, 1903469.
(504) Sebald, G.; Guyomar, D.; Agbossou, A. On Thermoelectric and Pyroelectric Energy Harvesting. *Smart Mater. Struct.* **2009**, *18*, 125006.
(505) Zhou, M.; Al-Furjan, M. S. H.; Zou, J.; Liu, W. T. A Review on Heat and Mechanical Energy Harvesting from Human - Principles, Prototypes and Perspectives. *Renew. Sustain. Energy Rev.* **2018**, *82*, 3582−3609.
(506) Cataldi, P.; Cassinelli, M.; Heredia-Guerrero, J. A.; Guzman-Puyol, S.; Naderizadeh, S.; Athanassiou, A.; Caironi, M. Green Biocomposites for Thermoelectric Wearable Applications. *Adv. Funct. Mater.* **2020**, *30*, 1907301.
(507) Karalis, G.; Tzounis, L.; Lambrou, E.; Gergidis, L. N.; Paipetis, A. S. A Carbon Fiber Thermoelectric Generator Integrated as a Lamina within an 8-Ply Laminate Epoxy Composite: Efficient Thermal Energy Harvesting by Advanced Structural Materials. *Appl. Energy* **2019**, *253*, 113512.
(508) Nozariasbmarz, A.; Collins, H.; Dsouza, K.; Polash, M. H.; Hosseini, M.; Hyland, M.; Liu, J.; Malhotra, A.; Ortiz, F. M.; Mohaddes, F.; et al. Review of Wearable Thermoelectric Energy Harvesting: From Body Temperature to Electronic Systems. *Appl. Energy* **2020**, *258*, 114069.
(509) Pourkiaei, S. M.; Ahmadi, M. H.; Sadeghzadeh, M.; Moosavi, S.; Pourfayaz, F.; Chen, L. E.; Arab Pour Yazdi, M.; Kumar, R. Thermoelectric Cooler and Thermoelectric Generator Devices: A Review of Present and Potential Applications, Modeling and Materials. *Energy* **2019**, *186*, 115849.
(510) Varghese, T.; Dun, C. C.; Kempf, N.; Saeidi-Javash, M.; Karthik, C.; Richardson, J.; Hollar, C.; Estrada, D.; Zhang, Y. L. Flexible Thermoelectric Devices of Ultrahigh Power Factor by Scalable Printing and Interface Engineering. *Adv. Funct. Mater.* **2020**, *30*, 1905796.
(511) Vieira, E. M. F.; Pires, A. L.; Silva, J. P. B.; Magalhães, V. H.; Grilo, J.; Brito, F. P.; Silva, M. F.; Pereira, A. M.; Goncalves, L. M. High-Performance Mu-Thermoelectric Device Based on Bi_2Te_3/Sb_2Te_3 P-N Junctions. *ACS Appl. Mater. Interfaces* **2019**, *11*, 38946−38954.
(512) Vostrikov, S.; Somov, A.; Gotovtsev, P. Low Temperature Gradient Thermoelectric Generator: Modelling and Experimental Verification. *Appl. Energy* **2019**, *255*, 113786.
(513) Zheng, C. Z.; Xiang, L. Y.; Jin, W. L.; Shen, H. G.; Zhao, W. R.; Zhang, F. J.; Di, C. A.; Zhu, D. B. A Flexible Self-Powered Sensing Element with Integrated Organic Thermoelectric Generator. *Adv. Mater. Technol.* **2019**, *4*, 1900247.
(514) Hardy, J. D.; Dubois, E. F. Regulation of Heat Loss from the Human Body. *Proc. Natl. Acad. Sci. U. S. A.* **1937**, *23*, 624−631.
(515) Bhatnagar, V.; Owende, P. Energy Harvesting for Assistive and Mobile Applications. *Energy Sci. Eng.* **2015**, *3*, 153−173.
(516) *Thermoelectrics Handbook: Macro to Nano*; Rowe, D. M., Ed.; CRC Press: Boca Raton, FL, 2006.
(517) Kanatzidis, M. G. Nanostructured Thermoelectrics: The New Paradigm? *Chem. Mater.* **2010**, *22*, 648−659.
(518) Sootsman, J. R.; Chung, D. Y.; Kanatzidis, M. G. New and Old Concepts in Thermoelectric Materials. *Angew. Chem., Int. Ed.* **2009**, *48*, 8616−8639.
(519) Venkatasubramanian, R.; Siivola, E.; Colpitts, T.; O'Quinn, B. Thin-Film Thermoelectric Devices with High Room-Temperature Figures of Merit. *Nature* **2001**, *413*, 597−602.
(520) Kim, C. S.; Lee, G. S.; Choi, H.; Kim, Y. J.; Yang, H. M.; Lim, S. H.; Lee, S. G.; Cho, B. J. Structural Design of a Flexible Thermoelectric Power Generator for Wearable Applications. *Appl. Energy* **2018**, *214*, 131−138.

https://dx.doi.org/10.1021/acs.chemrev.9b00821
Chem. Rev. 2020, 120, 3668−3720

(521) Kim, C. S.; Yang, H. M.; Lee, J.; Lee, G. S.; Choi, H.; Kim, Y. J.; Lim, S. H.; Cho, S. H.; Cho, B. J. Self-Powered Wearable Electrocardiography Using a Wearable Thermoelectric Power Generator. *ACS Energy Lett* **2018**, *3*, 501−507.
(522) Wang, Y.; Yang, L.; Shi, X. L.; Shi, X.; Chen, L.; Dargusch, M. S.; Zou, J.; Chen, Z. G. Flexible Thermoelectric Materials and Generators: Challenges and Innovations. *Adv. Mater.* **2019**, *31*, 1807916.
(523) Ding, Y.; Qiu, Y.; Cai, K.; Yao, Q.; Chen, S.; Chen, L.; He, J. High Performance N-Type Ag_2Se Film on Nylon Membrane for Flexible Thermoelectric Power Generator. *Nat. Commun.* **2019**, *10*, 841.
(524) Zhang, L. S.; Lin, S. P.; Hua, T.; Huang, B. L.; Liu, S. R.; Tao, X. M. Fiber-Based Thermoelectric Generators: Materials, Device Structures, Fabrication, Characterization, and Applications. *Adv. Energy Mater.* **2018**, *8*, 1700524.
(525) Hyland, M.; Hunter, H.; Liu, J.; Veety, E.; Vashaee, D. Wearable Thermoelectric Generators for Human Body Heat Harvesting. *Appl. Energy* **2016**, *182*, 518−524.
(526) Liu, Z.; Lyu, J.; Fang, D.; Zhang, X. Nanofibrous Kevlar Aerogel Threads for Thermal Insulation in Harsh Environments. *ACS Nano* **2019**, *13*, 5703−5711.
(527) Lizák, P.; Mojumdar, S. C. Thermal Properties of Textile Fabrics. *J. Therm. Anal. Calorim.* **2013**, *112*, 1095−1100.
(528) Kim, M. K.; Kim, M. S.; Lee, S.; Kim, C.; Kim, Y. J. Wearable Thermoelectric Generator for Harvesting Human Body Heat Energy. *Smart Mater. Struct.* **2014**, *23*, 105002.
(529) Siddique, A. M.; Rabari, R.; Mahmud, S.; Van Heyst, B. Thermal Energy Harvesting from the Human Body Using Flexible Thermoelectric Generator (FTEG) Fabricated by a Dispenser Printing Technique. *Energy* **2016**, *115*, 1081−1091.
(530) Cao, Z.; Tudor, M. J.; Torah, R. N.; Beeby, S. P. Screen Printable Flexible BiTe-SbTe-Based Composite Thermoelectric Materials on Textiles for Wearable Applications. *IEEE Trans. Electron Devices* **2016**, *63*, 4024−4030.
(531) Kim, S. J.; We, J. H.; Cho, B. J. A Wearable Thermoelectric Generator Fabricated on a Glass Fabric. *Energy Environ. Sci.* **2014**, *7*, 1959−1965.
(532) Lu, Z. S.; Zhang, H. H.; Mao, C. P.; Li, C. M. Silk Fabric-Based Wearable Thermoelectric Generator for Energy Harvesting from the Human Body. *Appl. Energy* **2016**, *164*, 57−63.
(533) Allison, L. K.; Andrew, T. L. A Wearable All-Fabric Thermoelectric Generator. *Adv. Mater. Technol.* **2019**, *4*, 1800615.
(534) Hewitt, C. A.; Kaiser, A. B.; Roth, S.; Craps, M.; Czerw, R.; Carroll, D. L. Multilayered Carbon Nanotube/Polymer Composite Based Thermoelectric Fabrics. *Nano Lett.* **2012**, *12*, 1307−1310.
(535) Karttunen, A. J.; Sarnes, L.; Townsend, R.; Mikkonen, J.; Karppinen, M. Flexible Thermoelectric ZnO-Organic Superlattices on Cotton Textile Substrates by ALD/MLD. *Adv. Electron. Mater.* **2017**, *3*, 1600459.
(536) Finefrock, S. W.; Zhu, X.; Sun, Y.; Wu, Y. Flexible Prototype Thermoelectric Devices Based on Ag_2Te and PEDOT: PSS Coated Nylon Fibre. *Nanoscale* **2015**, *7*, 5598−5602.
(537) Li, P.; Guo, Y.; Mu, J. K.; Wang, H. Z.; Zhang, Q. H.; Li, Y. G. Single-Walled Carbon Nanotubes/Polyaniline-Coated Polyester Thermoelectric Textile with Good Interface Stability Prepared by Ultrasonic Induction. *RSC Adv.* **2016**, *6*, 90347−90353.
(538) Du, Y.; Xu, J. Y.; Wang, Y. Y.; Lin, T. Thermoelectric Properties of Graphite-PEDOT:PSS Coated Flexible Polyester Fabrics. *J. Mater. Sci.: Mater. Electron.* **2017**, *28*, 5796−5801.
(539) Kim, S. L.; Choi, K.; Tazebay, A.; Yu, C. Flexible Power Fabrics Made of Carbon Nanotubes for Harvesting Thermoelectricity. *ACS Nano* **2014**, *8*, 2377−2386.
(540) Du, Y.; Cai, K.; Chen, S.; Wang, H.; Shen, S. Z.; Donelson, R.; Lin, T. Thermoelectric Fabrics: Toward Power Generating Clothing. *Sci. Rep.* **2015**, *5*, 6411.
(541) Du, Y.; Cai, K. F.; Shen, S. Z.; Donelsonand, R.; Xu, J. Y.; Wang, H. X.; Lin, T. Multifold Enhancement of the Output Power of Flexible Thermoelectric Generators Made from Cotton Fabrics Coated with Conducting Polymer. *RSC Adv.* **2017**, *7*, 43737−43742.
(542) Kirihara, K.; Wei, Q.; Mukaida, M.; Ishida, T. Thermoelectric Power Generation Using Nonwoven Fabric Module Impregnated with Conducting Polymer PEDOT:PSS. *Synth. Met.* **2017**, *225*, 41−48.
(543) Wu, B.; Guo, Y.; Hou, C. Y.; Zhang, Q. H.; Li, Y. G.; Wang, H. Z. High-Performance Flexible Thermoelectric Devices Based on All-Inorganic Hybrid Films for Harvesting Low-Grade Heat. *Adv. Funct. Mater.* **2019**, *29*, 1900304.
(544) Zhou, C.; Dun, C.; Wang, Q.; Wang, K.; Shi, Z.; Carroll, D. L.; Liu, G.; Qiao, G. Nanowires as Building Blocks to Fabricate Flexible Thermoelectric Fabric: The Case of Copper Telluride Nanowires. *ACS Appl. Mater. Interfaces* **2015**, *7*, 21015−21020.
(545) Peng, J.; Witting, I.; Geisendorfer, N.; Wang, M.; Chang, M.; Jakus, A.; Kenel, C.; Yan, X.; Shah, R.; Snyder, G. J.; Grayson, M. 3D Extruded Composite Thermoelectric Threads for Flexible Energy Harvesting. *Nat. Commun.* **2019**, *10*, 5590.
(546) Qu, S. Y.; Chen, Y. L.; Shi, W.; Wang, M. D.; Yao, Q.; Chen, L. D. Cotton-Based Wearable Poly(3-Hexylthiophene) Electronic Device for Thermoelectric Application with Cross-Plane Temperature Gradient. *Thin Solid Films* **2018**, *667*, 59−63.
(547) Morata, A.; Pacios, M.; Gadea, G.; Flox, C.; Cadavid, D.; Cabot, A.; Tarancon, A. Large-Area and Adaptable Electrospun Silicon-Based Thermoelectric Nanomaterials with High Energy Conversion Efficiencies. *Nat. Commun.* **2018**, *9*, 4759.
(548) Yadav, A.; Pipe, K. P.; Shtein, M. Fiber-Based Flexible Thermoelectric Power Generator. *J. Power Sources* **2008**, *175*, 909−913.
(549) Liang, D.; Yang, H.; Finefrock, S. W.; Wu, Y. Flexible Nanocrystal-Coated Glass Fibers for High-Performance Thermoelectric Energy Harvesting. *Nano Lett.* **2012**, *12*, 2140−2145.
(550) Wu, Q.; Hu, J. Waterborne Polyurethane Based Thermoelectric Composites and Their Application Potential in Wearable Thermoelectric Textiles. *Compos. B. Eng.* **2016**, *107*, 59−66.
(551) Lee, J. A.; Aliev, A. E.; Bykova, J. S.; de Andrade, M. J.; Kim, D.; Sim, H. J.; Lepro, X.; Zakhidov, A. A.; Lee, J. B.; Spinks, G. M.; et al. Woven-Yarn Thermoelectric Textiles. *Adv. Mater.* **2016**, *28*, 5038−5044.
(552) Wu, Q.; Hu, J. A Novel Design for a Wearable Thermoelectric Generator Based on 3D Fabric Structure. *Smart Mater. Struct.* **2017**, *26*, 045037.
(553) Yamamoto, N.; Takai, H. Electrical Power Generation from a Knitted Wire Panel Using the Thermoelectric Effect. *Electr. Eng. Jpn.* **2002**, *140*, 16−21.
(554) Ito, M.; Koizumi, T.; Kojima, H.; Saito, T.; Nakamura, M. From Materials to Device Design of a Thermoelectric Fabric for Wearable Energy Harvesters. *J. Mater. Chem. A* **2017**, *5*, 12068−12072.
(555) Choi, J.; Jung, Y.; Yang, S. J.; Oh, J. Y.; Oh, J.; Jo, K.; Son, J. G.; Moon, S. E.; Park, C. R.; Kim, H. Flexible and Robust Thermoelectric Generators Based on All-Carbon Nanotube Yarn without Metal Electrodes. *ACS Nano* **2017**, *11*, 7608−7614.
(556) Zhang, T.; Li, K.; Zhang, J.; Chen, M.; Wang, Z.; Ma, S.; Zhang, N.; Wei, L. High-Performance, Flexible, and Ultralong Crystalline Thermoelectric Fibers. *Nano Energy* **2017**, *41*, 35−42.
(557) Ryan, J. D.; Lund, A.; Hofmann, A. I.; Kroon, R.; Sarabia-Riquelme, R.; Weisenberger, M. C.; Müller, C. All-Organic Textile Thermoelectrics with Carbon-Nanotube-Coated N-Type Yarns. *ACS Appl. Energy Mater.* **2018**, *1*, 2934−2941.
(558) Ryan, J. D.; Mengistie, D. A.; Gabrielsson, R.; Lund, A.; Müller, C. Machine-Washable PEDOT: PSS Dyed Silk Yarns for Electronic Textiles. *ACS Appl. Mater. Interfaces* **2017**, *9*, 9045−9050.
(559) Nan, K.; Kang, S. D.; Li, K.; Yu, K. J.; Zhu, F.; Wang, J.; Dunn, A. C.; Zhou, C.; Xie, Z.; Agne, M. T.; et al. Compliant and Stretchable Thermoelectric Coils for Energy Harvesting in Miniature Flexible Devices. *Sci. Adv.* **2018**, *4*, No. eaau5849.

https://dx.doi.org/10.1021/acs.chemrev.9b00821
Chem. Rev. 2020, 120, 3668−3720

(560) Sun, T.; Zhou, B.; Zheng, Q.; Wang, L.; Jiang, W.; Snyder, G. J. Stretchable Fabric Generates Electric Power from Woven Thermoelectric Fibers. *Nat. Commun.* **2020**, *11*, 572.
(561) Snyder, G. J.; Toberer, E. S. Complex Thermoelectric Materials. *Nat. Mater.* **2008**, *7*, 105−114.
(562) Bell, L. E. Cooling, Heating, Generating Power, and Recovering Waste Heat with Thermoelectric Systems. *Science* **2008**, *321*, 1457−1461.
(563) Yang, C.; Souchay, D.; Kneiß, M.; Bogner, M.; Wei, H. M.; Lorenz, M.; Oeckler, O.; Benstetter, G.; Fu, Y. Q.; Grundmann, M. Transparent Flexible Thermoelectric Material Based on Non-Toxic Earth-Abundant P-Type Copper Iodide Thin Film. *Nat. Commun.* **2017**, *8*, 16076.
(564) Bulman, G.; Barletta, P.; Lewis, J.; Baldasaro, N.; Manno, M.; Bar-Cohen, A.; Yang, B. Superlattice-Based Thin-Film Thermoelectric Modules with High Cooling Fluxes. *Nat. Commun.* **2016**, *7*, 10302.
(565) Rojas, J. P.; Singh, D.; Conchouso, D.; Arevalo, A.; Foulds, I. G.; Hussain, M. M. Stretchable Helical Architecture Inorganic-Organic Hetero Thermoelectric Generator. *Nano Energy* **2016**, *30*, 691−699.
(566) Wang, L.; Zhang, Z.; Geng, L.; Yuan, T.; Liu, Y.; Guo, J.; Fang, L.; Qiu, J.; Wang, S. Solution-Printable Fullerene/TiS_2 Organic/Inorganic Hybrids for High-Performance Flexible N-Type Thermoelectrics. *Energy Environ. Sci.* **2018**, *11*, 1307−1317.
(567) Kim, G. H.; Shao, L.; Zhang, K.; Pipe, K. P. Engineered Doping of Organic Semiconductors for Enhanced Thermoelectric Efficiency. *Nat. Mater.* **2013**, *12*, 719−723.
(568) Yang, P.; Liu, K.; Chen, Q.; Mo, X.; Zhou, Y.; Li, S.; Feng, G.; Zhou, J. Wearable Thermocells Based on Gel Electrolytes for the Utilization of Body Heat. *Angew. Chem., Int. Ed.* **2016**, *55*, 12050−12053.
(569) Duan, J.; Feng, G.; Yu, B.; Li, J.; Chen, M.; Yang, P.; Feng, J.; Liu, K.; Zhou, J. Aqueous Thermogalvanic Cells with a High Seebeck Coefficient for Low-Grade Heat Harvest. *Nat. Commun.* **2018**, *9*, 5146.
(570) Zhao, D.; Martinelli, A.; Willfahrt, A.; Fischer, T.; Bernin, D.; Khan, Z. U.; Shahi, M.; Brill, J.; Jonsson, M. P.; Fabiano, S.; Crispin, X. Polymer Gels with Tunable Ionic Seebeck Coefficient for Ultra-Sensitive Printed Thermopiles. *Nat. Commun.* **2019**, *10*, 1093.
(571) Peng, Y.; Chen, J.; Song, A. Y.; Catrysse, P. B.; Hsu, P. C.; Cai, L.; Liu, B.; Zhu, Y. Y.; Zhou, G.; Wu, D. S.; et al. Nanoporous Polyethylene Microfibres for Large-Scale Radiative Cooling Fabric. *Nat. Sustain.* **2018**, *1*, 105−112.
(572) Cai, L.; Song, A. Y.; Li, W.; Hsu, P. C.; Lin, D.; Catrysse, P. B.; Liu, Y.; Peng, Y.; Chen, J.; Wang, H.; et al. Spectrally Selective Nanocomposite Textile for Outdoor Personal Cooling. *Adv. Mater.* **2018**, *30*, 1802152.
(573) Cai, L.; Song, A. Y.; Wu, P.; Hsu, P. C.; Peng, Y.; Chen, J.; Liu, C.; Catrysse, P. B.; Liu, Y.; Yang, A.; et al. Warming up Human Body by Nanoporous Metallized Polyethylene Textile. *Nat. Commun.* **2017**, *8*, 496.
(574) Hsu, P. C.; Song, A. Y.; Catrysse, P. B.; Liu, C.; Peng, Y.; Xie, J.; Fan, S.; Cui, Y. Radiative Human Body Cooling by Nanoporous Polyethylene Textile. *Science* **2016**, *353*, 1019−1023.
(575) Jafar-Zanjani, S.; Salary, M. M.; Mosallaei, H. Metafabrics for Thermoregulation and Energy-Harvesting Applications. *ACS Photonics* **2017**, *4*, 915−927.
(576) Fan, P.; Zheng, Z. H.; Li, Y. Z.; Lin, Q. Y.; Luo, J. T.; Liang, G. X.; Cai, X. M.; Zhang, D. P.; Ye, F. Low-Cost Flexible Thin Film Thermoelectric Generator on Zinc Based Thermoelectric Materials. *Appl. Phys. Lett.* **2015**, *106*, 073901.
(577) Glatz, W.; Muntwyler, S.; Hierold, C. Optimization and Fabrication of Thick Flexible Polymer Based Micro Thermoelectric Generator. *Sens. Actuators A: Phys.* **2006**, *132*, 337−345.
(578) Liang, L. R.; Gao, C. Y.; Chen, G. M.; Guo, C. Y. Large-Area, Stretchable, Super Flexible and Mechanically Stable Thermoelectric Films of Polymer/Carbon Nanotube Composites. *J. Mater. Chem. C* **2016**, *4*, 526−532.
(579) Lv, S.; He, W.; Wang, L. P.; Li, G. Q.; Ji, J.; Chen, H. B.; Zhang, G. Design, Fabrication and Feasibility Analysis of a Thermo-Electric Wearable Helmet. *Appl. Therm. Eng.* **2016**, *109*, 138−146.
(580) Derler, S.; Schrade, U.; Gerhardt, L.-C. Tribology of Human Skin and Mechanical Skin Equivalents in Contact with Textiles. *Wear* **2007**, *263*, 1112−1116.
(581) Xiao, X.; Xia, H. Q.; Wu, R.; Bai, L.; Yan, L.; Magner, E.; Cosnier, S.; Lojou, E.; Zhu, Z.; Liu, A. Tackling the Challenges of Enzymatic (Bio)Fuel Cells. *Chem. Rev.* **2019**, *119*, 9509−9558.
(582) Jeerapan, I.; Sempionatto, J. R.; Wang, J. On-Body Bioelectronics: Wearable Biofuel Cells for Bioenergy Harvesting and Self-Powered Biosensing. *Adv. Funct. Mater.* **2019**, 1906243.
(583) Moehlenbrock, M. J.; Minteer, S. D. Extended Lifetime Biofuel Cells. *Chem. Soc. Rev.* **2008**, *37*, 1188−1196.
(584) Falk, M.; Shleev, S. Hybrid Dual-Functioning Electrodes for Combined Ambient Energy Harvesting and Charge Storage: Towards Self-Powered Systems. *Biosens. Bioelectron.* **2019**, *126*, 275−291.
(585) Katz, E.; MacVittie, K. Implanted Biofuel Cells Operating in Vivo - Methods, Applications and Perspectives - Feature Article. *Energy Environ. Sci.* **2013**, *6*, 2791−2803.
(586) Bandodkar, A. J. Wearable Biofuel Cells: Past, Present and Future. *J. Electrochem. Soc.* **2017**, *164*, H3007−H3014.
(587) Bullen, R. A.; Arnot, T. C.; Lakeman, J. B.; Walsh, F. C. Biofuel Cells and Their Development. *Biosens. Bioelectron.* **2006**, *21*, 2015−2045.
(588) Carrette, L.; Friedrich, K. A.; Stimming, U. Fuel Cells - Fundamentals and Applications. *Fuel Cells* **2001**, *1*, 5−39.
(589) Heller, A. Miniature Biofuel Cells. *Phys. Chem. Chem. Phys.* **2004**, *6*, 209−216.
(590) Cinquin, P.; Gondran, C.; Giroud, F.; Mazabrard, S.; Pellissier, A.; Boucher, F.; Alcaraz, J. P.; Gorgy, K.; Lenouvel, F.; Mathe, S.; et al. A Glucose Biofuel Cell Implanted in Rats. *PLoS One* **2010**, *5*, No. e10476.
(591) Cosnier, S.; Le Goff, A.; Holzinger, M. Towards Glucose Biofuel Cells Implanted in Human Body for Powering Artificial Organs: Review. *Electrochem. Commun.* **2014**, *38*, 19−23.
(592) Sakai, H.; Nakagawa, T.; Tokita, Y.; Hatazawa, T.; Ikeda, T.; Tsujimura, S.; Kano, K. A High-Power Glucose/Oxygen Biofuel Cell Operating under Quiescent Conditions. *Energy Environ. Sci.* **2009**, *2*, 133−138.
(593) Togo, M.; Takamura, A.; Asai, T.; Kaji, H.; Nishizawa, M. An Enzyme-Based Microfluidic Biofuel Cell Using Vitamin K_3-Mediated Glucose Oxidation. *Electrochim. Acta* **2007**, *52*, 4669−4674.
(594) Bandodkar, A. J.; Wang, J. Wearable Biofuel Cells: A Review. *Electroanalysis* **2016**, *28*, 1188−1200.
(595) Xie, X.; Hu, L.; Pasta, M.; Wells, G. F.; Kong, D.; Criddle, C. S.; Cui, Y. Three-Dimensional Carbon Nanotube-Textile Anode for High-Performance Microbial Fuel Cells. *Nano Lett.* **2011**, *11*, 291−296.
(596) Xie, X.; Ye, M.; Hu, L. B.; Liu, N.; McDonough, J. R.; Chen, W.; Alshareef, H. N.; Criddle, C. S.; Cui, Y. Carbon Nanotube-Coated Macroporous Sponge for Microbial Fuel Cell Electrodes. *Energy Environ. Sci.* **2012**, *5*, 5265−5270.
(597) Logan, B. E. Exoelectrogenic Bacteria That Power Microbial Fuel Cells. *Nat. Rev. Microbiol.* **2009**, *7*, 375−381.
(598) Minteer, S. D.; Liaw, B. Y.; Cooney, M. J. Enzyme-Based Biofuel Cells. *Curr. Opin. Biotechnol.* **2007**, *18*, 228−234.
(599) Rasmussen, M.; Abdellaoui, S.; Minteer, S. D. Enzymatic Biofuel Cells: 30 Years of Critical Advancements. *Biosens. Bioelectron.* **2016**, *76*, 91−102.
(600) Cracknell, J. A.; Vincent, K. A.; Armstrong, F. A. Enzymes as Working or Inspirational Electrocatalysts for Fuel Cells and Electrolysis. *Chem. Rev.* **2008**, *108*, 2439−2461.
(601) Wilson, R.; Turner, A. P. F. Glucose-Oxidase - an Ideal Enzyme. *Biosens. Bioelectron.* **1992**, *7*, 165−185.
(602) Huang, X.; Zhang, L.; Zhang, Z.; Guo, S.; Shang, H.; Li, Y.; Liu, J. Wearable Biofuel Cells Based on the Classification of Enzyme for High Power Outputs and Lifetimes. *Biosens. Bioelectron.* **2019**, *124*−*125*, 40−52.

https://dx.doi.org/10.1021/acs.chemrev.9b00821
Chem. Rev. 2020, 120, 3668−3720

(603) Reuillard, B.; Le Goff, A.; Agnes, C.; Holzinger, M.; Zebda, A.; Gondran, C.; Elouarzaki, K.; Cosnier, S. High Power Enzymatic Biofuel Cell Based on Naphthoquinone-Mediated Oxidation of Glucose by Glucose Oxidase in a Carbon Nanotube 3D Matrix. *Phys. Chem. Chem. Phys.* **2013**, *15*, 4892−4896.
(604) Zhu, Z.; Kin Tam, T.; Sun, F.; You, C.; Percival Zhang, Y. H. A High-Energy-Density Sugar Biobattery Based on a Synthetic Enzymatic Pathway. *Nat. Commun.* **2014**, *5*, 3026.
(605) Kang, Z.; Jiao, K.; Cheng, J.; Peng, R.; Jiao, S.; Hu, Z. A Novel Three-Dimensional Carbonized $PANI_{1600}$@ CNTS Network for Enhanced Enzymatic Biofuel Cell. *Biosens. Bioelectron.* **2018**, *101*, 60−65.
(606) Zebda, A.; Cosnier, S.; Alcaraz, J. P.; Holzinger, M.; Le Goff, A.; Gondran, C.; Boucher, F.; Giroud, F.; Gorgy, K.; Lamraoui, H.; Cinquin, P. Single Glucose Biofuel Cells Implanted in Rats Power Electronic Devices. *Sci. Rep.* **2013**, *3*, 1516.
(607) Jia, W.; Valdes-Ramirez, G.; Bandodkar, A. J.; Windmiller, J. R.; Wang, J. Epidermal Biofuel Cells: Energy Harvesting from Human Perspiration. *Angew. Chem., Int. Ed.* **2013**, *52*, 7233−7236.
(608) Bandodkar, A. J.; Gutruf, P.; Choi, J.; Lee, K.; Sekine, Y.; Reeder, J. T.; Jeang, W. J.; Aranyosi, A. J.; Lee, S. P.; Model, J. B.; et al. Battery-Free, Skin-Interfaced Microfluidic/Electronic Systems for Simultaneous Electrochemical, Colorimetric, and Volumetric Analysis of Sweat. *Sci. Adv.* **2019**, *5*, No. eaav3294.
(609) Calabrese Barton, S.; Gallaway, J.; Atanassov, P. Enzymatic Biofuel Cells for Implantable and Microscale Devices. *Chem. Rev.* **2004**, *104*, 4867−4886.
(610) Nasar, A.; Perveen, R. Applications of Enzymatic Biofuel Cells in Bioelectronic Devices - a Review. *Int. J. Hydrogen Energy* **2019**, *44*, 15287−15312.
(611) Cosnier, S.; Gross, A. J.; Le Goff, A.; Holzinger, M. Recent Advances on Enzymatic Glucose/Oxygen and Hydrogen/Oxygen Biofuel Cells: Achievements and Limitations. *J. Power Sources* **2016**, *325*, 252−263.
(612) Gamella, M.; Koushanpour, A.; Katz, E. Biofuel Cells - Activation of Micro- and Macro-Electronic Devices. *Bioelectrochemistry* **2018**, *119*, 33−42.
(613) Miyake, T.; Haneda, K.; Yoshino, S.; Nishizawa, M. Flexible, Layered Biofuel Cells. *Biosens. Bioelectron.* **2013**, *40*, 45−49.
(614) Ogawa, Y.; Takai, Y.; Kato, Y.; Kai, H.; Miyake, T.; Nishizawa, M. Stretchable Biofuel Cell with Enzyme-Modified Conductive Textiles. *Biosens. Bioelectron.* **2015**, *74*, 947−952.
(615) Jeerapan, I.; Sempionatto, J. R.; Pavinatto, A.; You, J. M.; Wang, J. Stretchable Biofuel Cells as Wearable Textile-Based Self-Powered Sensors. *J. Mater. Chem. A* **2016**, *4*, 18342−18353.
(616) Jia, W. Z.; Wang, X.; Imani, S.; Bandodkar, A. J.; Ramirez, J.; Mercier, P. P.; Wang, J. Wearable Textile Biofuel Cells for Powering Electronics. *J. Mater. Chem. A* **2014**, *2*, 18184−18189.
(617) Lv, J.; Jeerapan, I.; Tehrani, F.; Yin, L.; Silva-Lopez, C. A.; Jang, J. H.; Joshuia, D.; Shah, R.; Liang, Y. Y.; Xie, L. Y.; et al. Sweat-Based Wearable Energy Harvesting-Storage Hybrid Textile Devices. *Energy Environ. Sci.* **2018**, *11*, 3431−3442.
(618) Shitanda, I.; Takamatsu, K.; Niiyama, A.; Mikawa, T.; Hoshi, Y.; Itagaki, M.; Tsujimura, S. High-Power Lactate/O_2 Enzymatic Biofuel Cell Based on Carbon Cloth Electrodes Modified with MgO-Templated Carbon. *J. Power Sources* **2019**, *436*, 226844.
(619) Kwon, C. H.; Lee, S. H.; Choi, Y. B.; Lee, J. A.; Kim, S. H.; Kim, H. H.; Spinks, G. M.; Wallace, G. G.; Lima, M. D.; Kozlov, M. E.; et al. High-Power Biofuel Cell Textiles from Woven Biscrolled Carbon Nanotube Yarns. *Nat. Commun.* **2014**, *5*, 3928.
(620) Kwon, C. H.; Ko, Y.; Shin, D.; Kwon, M.; Park, J.; Bae, W. K.; Lee, S. W.; Cho, J. High-Power Hybrid Biofuel Cells Using Layer-by-Layer Assembled Glucose Oxidase-Coated Metallic Cotton Fibers. *Nat. Commun.* **2018**, *9*, 4479.
(621) Kwon, C. H.; Ko, Y.; Shin, D.; Lee, S. W.; Cho, J. Highly Conductive Electrocatalytic Gold Nanoparticle-Assembled Carbon Fiber Electrode for High-Performance Glucose-Based Biofuel Cells. *J. Mater. Chem. A* **2019**, *7*, 13495−13505.
(622) Yin, S. J.; Jin, Z. W.; Miyake, T. Wearable High-Powered Biofuel Cells Using Enzyme/Carbon Nanotube Composite Fibers on Textile Cloth. *Biosens. Bioelectron.* **2019**, *141*, 111471.
(623) Kwon, C. H.; Park, Y. B.; Lee, J. A.; Choi, Y. B.; Kim, H. H.; Lima, M. D.; Baughman, R. H.; Kim, S. J. Mediator-Free Carbon Nanotube Yarn Biofuel Cell. *RSC Adv.* **2016**, *6*, 48346−48350.
(624) Sim, H. J.; Lee, D. Y.; Kim, H.; Choi, Y. B.; Kim, H. H.; Baughman, R. H.; Kim, S. J. Stretchable Fiber Biofuel Cell by Rewrapping Multiwalled Carbon Nanotube Sheets. *Nano Lett.* **2018**, *18*, 5272−5278.
(625) Falk, M.; Blum, Z.; Shleev, S. Direct Electron Transfer Based Enzymatic Fuel Cells. *Electrochim. Acta* **2012**, *82*, 191−202.
(626) Ivnitski, D.; Branch, B.; Atanassov, P.; Apblett, C. Glucose Oxidase Anode for Biofuel Cell Based on Direct Electron Transfer. *Electrochem. Commun.* **2006**, *8*, 1204−1210.
(627) Zebda, A.; Gondran, C.; Le Goff, A.; Holzinger, M.; Cinquin, P.; Cosnier, S. Mediatorless High-Power Glucose Biofuel Cells Based on Compressed Carbon Nanotube-Enzyme Electrodes. *Nat. Commun.* **2011**, *2*, 370.
(628) Pang, S.; Gao, Y.; Choi, S. Flexible and Stretchable Microbial Fuel Cells with Modified Conductive and Hydrophilic Textile. *Biosens. Bioelectron.* **2018**, *100*, 504−511.
(629) Pang, S. M.; Gao, Y.; Choi, S. Flexible and Stretchable Biobatteries: Monolithic Integration of Membrane-Free Microbial Fuel Cells in a Single Textile Layer. *Adv. Energy Mater.* **2018**, *8*, 1702261.
(630) Chalasani, S.; Conrad, J. M. *A Survey of Energy Harvesting Sources for Embedded Systems*. Proceedings from the IEEE Southeastcon 2008, Huntsville, AL, April 3−6, 2008; pp 442− 447.
(631) Creutzig, F.; Agoston, P.; Goldschmidt, J. C.; Luderer, G.; Nemet, G.; Pietzcker, R. C. The Underestimated Potential of Solar Energy to Mitigate Climate Change. *Nat. Energy* **2017**, *2*, 17140.
(632) Gratzel, M. Solar Energy Conversion by Dye-Sensitized Photovoltaic Cells. *Inorg. Chem.* **2005**, *44*, 6841−6851.
(633) Lewis, N. S. Toward Cost-Effective Solar Energy Use. *Science* **2007**, *315*, 798−801.
(634) Alaaeddin, M.; Sapuan, S.; Zuhri, M.; Zainudin, E.; Al-Oqla, F. M. Photovoltaic Applications: Status and Manufacturing Prospects. *Renew. Sustain. Energy Rev.* **2019**, *102*, 318−332.
(635) Green, M. A. Third Generation Photovoltaics: Solar Cells for 2020 and Beyond. *Physica E* **2002**, *14*, 65−70.
(636) Green, M. A. *Third Generation Photovoltaics: Advanced Solar Energy Conversion*; Springer-Verlag: Berlin, 2006.
(637) Green, M. A.; Dunlop, E. D.; Levi, D. H.; Hohl-Ebinger, J.; Yoshita, M.; Ho-Baillie, A. W. Y. Solar Cell Efficiency Tables (Version 54). *Prog. Photovoltaics* **2019**, *27*, 565−575.
(638) Galagan, Y.; Rubingh, J.-E. J. M.; Andriessen, R.; Fan, C.-C.; Blom, P. W. M.; Veenstra, S. C.; Kroon, J. M. ITO-Free Flexible Organic Solar Cells with Printed Current Collecting Grids. *Sol. Energy Mater. Sol. Cells* **2011**, *95*, 1339−1343.
(639) Kymakis, E.; Savva, K.; Stylianakis, M. M.; Fotakis, C.; Stratakis, E. Flexible Organic Photovoltaic Cells with in Situ Nonthermal Photoreduction of Spin-Coated Graphene Oxide Electrodes. *Adv. Funct. Mater.* **2013**, *23*, 2742−2749.
(640) Zou, J.; Li, C. Z.; Chang, C. Y.; Yip, H. L.; Jen, A. K. Interfacial Engineering of Ultrathin Metal Film Transparent Electrode for Flexible Organic Photovoltaic Cells. *Adv. Mater.* **2014**, *26*, 3618−3623.
(641) Kuang, D.; Brillet, J.; Chen, P.; Takata, M.; Uchida, S.; Miura, H.; Sumioka, K.; Zakeeruddin, S. M.; Gratzel, M. Application of Highly Ordered TiO_2 Nanotube Arrays in Flexible Dye-Sensitized Solar Cells. *ACS Nano* **2008**, *2*, 1113−1116.
(642) Liao, J.-Y.; Lei, B.-X.; Chen, H.-Y.; Kuang, D.-B.; Su, C.-Y. Oriented Hierarchical Single Crystalline Anatase TiO_2 Nanowire Arrays on Ti-Foil Substrate for Efficient Flexible Dye-Sensitized Solar Cells. *Energy Environ. Sci.* **2012**, *5*, 5750−5757.
(643) Scalia, A.; Bella, F.; Lamberti, A.; Bianco, S.; Gerbaldi, C.; Tresso, E.; Pirri, C. F. A Flexible and Portable Powerpack by Solid-

https://dx.doi.org/10.1021/acs.chemrev.9b00821
Chem. Rev. 2020, 120, 3668−3720

State Supercapacitor and Dye-Sensitized Solar Cell Integration. *J. Power Sources* **2017**, *359*, 311−321.
(644) Shin, S. S.; Yang, W. S.; Noh, J. H.; Suk, J. H.; Jeon, N. J.; Park, J. H.; Kim, J. S.; Seong, W. M.; Seok, S. I. High-Performance Flexible Perovskite Solar Cells Exploiting Zn_2SnO_4 Prepared in Solution Below 100 °C. *Nat. Commun.* **2015**, *6*, 7410.
(645) Wang, X. Y.; Li, Z.; Xu, W. J.; Kulkarni, S. A.; Batabyal, S. K.; Zhang, S.; Cao, A. Y.; Wong, L. H. TiO_2 Nanotube Arrays Based Flexible Perovskite Solar Cells with Transparent Carbon Nanotube Electrode. *Nano Energy* **2015**, *11*, 728−735.
(646) Yang, D.; Yang, R.; Zhang, J.; Yang, Z.; Liu, S. F.; Li, C. High Efficiency Flexible Perovskite Solar Cells Using Superior Low Temperature TiO_2. *Energy Environ. Sci.* **2015**, *8*, 3208−3214.
(647) Yun, M. J.; Cha, S. I.; Seo, S. H.; Lee, D. Y. Highly Flexible Dye-Sensitized Solar Cells Produced by Sewing Textile Electrodes on Cloth. *Sci. Rep.* **2015**, *4*, 5322.
(648) Yun, M. J.; Cha, S. I.; Seo, S. H.; Kim, H. S.; Lee, D. Y. Insertion of Dye-Sensitized Solar Cells in Textiles Using a Conventional Weaving Process. *Sci. Rep.* **2015**, *5*, 11022.
(649) Zhen, H. Y.; Li, K.; Chen, C. J.; Yu, Y.; Zheng, Z. J.; Ling, Q. D. Water-Borne Foldable Polymer Solar Cells: One-Step Transferring Free-Standing Polymer Films onto Woven Fabric Electrodes. *J. Mater. Chem. A* **2017**, *5*, 782−788.
(650) Xu, X.; Fukuda, K.; Karki, A.; Park, S.; Kimura, H.; Jinno, H.; Watanabe, N.; Yamamoto, S.; Shimomura, S.; Kitazawa, D.; et al. Thermally Stable, Highly Efficient, Ultraflexible Organic Photovoltaics. *Proc. Natl. Acad. Sci. U. S. A.* **2018**, *115*, 4589−4594.
(651) Lee, S.; Lee, Y.; Park, J.; Choi, D. Stitchable Organic Photovoltaic Cells with Textile Electrodes. *Nano Energy* **2014**, *9*, 88−93.
(652) He, S. S.; Qiu, L. B.; Fang, X.; Guan, G. Z.; Chen, P. N.; Zhang, Z. T.; Peng, H. S. Radically Grown Obelisk-Like ZnO Arrays for Perovskite Solar Cell Fibers and Fabrics through a Mild Solution Process. *J. Mater. Chem. A* **2015**, *3*, 9406−9410.
(653) Arbab, A. A.; Sun, K. C.; Sahito, I. A.; Qadir, M. B.; Jeong, S. H. Multiwalled Carbon Nanotube Coated Polyester Fabric as Textile Based Flexible Counter Electrode for Dye Sensitized Solar Cell. *Phys. Chem. Chem. Phys.* **2015**, *17*, 12957−12969.
(654) Arumugam, S.; Li, Y.; Glanc-Gostkiewicz, M.; Torah, R. N.; Beeby, S. P. Solution Processed Organic Solar Cells on Textiles. *IEEE J. Photovolt.* **2018**, *8*, 1710−1715.
(655) Jung, J. W.; Bae, J. H.; Ko, J. H.; Lee, W. Fully Solution-Processed Indium Tin Oxide-Free Textile-Based Flexible Solar Cells Made of an Organic Inorganic Perovskite Absorber: Toward a Wearable Power Source. *J. Power Sources* **2018**, *402*, 327−332.
(656) Yun, M. J.; Sim, Y. H.; Cha, S. I.; Seo, S. H.; Lee, D. Y. Three-Dimensional Textile Platform for Electrochemical Devices and Its Application to Dye-Sensitized Solar Cells. *Sci. Rep.* **2019**, *9*, 2322.
(657) Yun, M. J.; Cha, S. I.; Kim, H. S.; Seo, S. H.; Lee, D. Y. Monolithic-Structured Single-Layered Textile-Based Dye-Sensitized Solar Cells. *Sci. Rep.* **2016**, *6*, 34249.
(658) Liu, J.; Li, Y.; Yong, S.; Arumugam, S.; Beeby, S. Flexible Printed Monolithic-Structured Solid-State Dye Sensitized Solar Cells on Woven Glass Fibre Textile for Wearable Energy Harvesting Applications. *Sci. Rep.* **2019**, *9*, 1362.
(659) Liu, J. Q.; Li, Y.; Li, M. L.; Arumugam, S.; Beeby, S. P. Processing of Printed Dye Sensitized Solar Cells on Woven Textiles. *IEEE J. Photovolt.* **2019**, *9*, 1020−1024.
(660) Pan, S.; Yang, Z.; Chen, P.; Deng, J.; Li, H.; Peng, H. Wearable Solar Cells by Stacking Textile Electrodes. *Angew. Chem., Int. Ed.* **2014**, *53*, 6110−6114.
(661) Lam, J. Y.; Chen, J. Y.; Tsai, P. C.; Hsieh, Y. T.; Chueh, C. C.; Tung, S. H.; Chen, W. C. A Stable, Efficient Textile-Based Flexible Perovskite Solar Cell with Improved Washable and Deployable Capabilities for Wearable Device Applications. *RSC Adv.* **2017**, *7*, 54361−54368.
(662) Zhang, Z. T.; Li, X. Y.; Guan, G. Z.; Pan, S. W.; Zhu, Z. J.; Ren, D. Y.; Peng, H. S. A Lightweight Polymer Solar Cell Textile That Functions When Illuminated from Either Side. *Angew. Chem., Int. Ed.* **2014**, *53*, 11571−11574.
(663) Wu, C. X.; Kim, T. W.; Guo, T. L.; Li, F. S. Wearable Ultra-Lightweight Solar Textiles Based on Transparent Electronic Fabrics. *Nano Energy* **2017**, *32*, 367−373.
(664) Jeong, E. G.; Jeon, Y.; Cho, S. H.; Choi, K. C. Textile-Based Washable Polymer Solar Cells for Optoelectronic Modules: Toward Self-Powered Smart Clothing. *Energy Environ. Sci.* **2019**, *12*, 1878−1889.
(665) Cho, S. H.; Lee, J.; Lee, M. J.; Kim, H. J.; Lee, S. M.; Choi, K. C. Plasmonically Engineered Textile Polymer Solar Cells for High-Performance, Wearable Photovoltaics. *ACS Appl. Mater. Interfaces* **2019**, *11*, 20864−20872.
(666) Yan, J.; Uddin, M. J.; Dickens, T. J.; Daramola, D. E.; Okoli, O. I. 3D Wire-Shaped Dye-Sensitized Solar Cells in Solid State Using Carbon Nanotube Yarns with Hybrid Photovoltaic Structure. *Adv. Mater. Interfaces* **2014**, *1*, 1400075.
(667) Zhang, L.; Shi, E.; Ji, C.; Li, Z.; Li, P.; Shang, Y.; Li, Y.; Wei, J.; Wang, K.; Zhu, H.; et al. Fiber and Fabric Solar Cells by Directly Weaving Carbon Nanotube Yarns with Cdse Nanowire-Based Electrodes. *Nanoscale* **2012**, *4*, 4954−4959.
(668) Zhang, Z. T.; Yang, Z. B.; Wu, Z. W.; Guan, G. Z.; Pan, S. W.; Zhang, Y.; Li, H. P.; Deng, J.; Sun, B. Q.; Peng, H. S. Weaving Efficient Polymer Solar Cell Wires into Flexible Power Textiles. *Adv. Energy Mater.* **2014**, *4*, 1301750.
(669) Zhang, Q. C.; Li, L. H.; Li, H.; Tang, L.; He, B.; Li, C. W.; Pan, Z. H.; Zhou, Z. Y.; Li, Q. L.; Sun, J.; et al. Ultra-Endurance Coaxial-Fiber Stretchable Sensing Systems Fully Powered by Sunlight. *Nano Energy* **2019**, *60*, 267−274.
(670) Zhang, Z.; Chen, X.; Chen, P.; Guan, G.; Qiu, L.; Lin, H.; Yang, Z.; Bai, W.; Luo, Y.; Peng, H. Integrated Polymer Solar Cell and Electrochemical Supercapacitor in a Flexible and Stable Fiber Format. *Adv. Mater.* **2014**, *26*, 466−470.
(671) Sugino, K.; Ikeda, Y.; Yonezawa, S.; Gennaka, S.; Kimura, M.; Fukawa, T.; Inagaki, S.; Konosu, Y.; Tanioka, A.; Matsumoto, H. Development of Fiber and Textile-Shaped Organic Solar Cells for Smart Textiles. *J. Fiber Sci. Technol.* **2017**, *73*, 336−342.
(672) Li, C.; Islam, M. M.; Moore, J.; Sleppy, J.; Morrison, C.; Konstantinov, K.; Dou, S. X.; Renduchintala, C.; Thomas, J. Wearable Energy-Smart Ribbons for Synchronous Energy Harvest and Storage. *Nat. Commun.* **2016**, *7*, 13319.
(673) Fu, X. M.; Sun, H.; Xie, S. L.; Zhang, J.; Pan, Z. Y.; Liao, M.; Xu, L. M.; Li, Z.; Wang, B. J.; Sun, X. M.; et al. A Fiber-Shaped Solar Cell Showing a Record Power Conversion Efficiency of 10%. *J. Mater. Chem. A* **2018**, *6*, 45−51.
(674) Wang, L.; Fu, X.; He, J.; Shi, X.; Chen, T.; Chen, P.; Wang, B.; Peng, H. Application Challenges in Fiber and Textile Electronics. *Adv. Mater.* **2020**, *32*, 1901971.
(675) Yang, Z.; Deng, J.; Sun, X.; Li, H.; Peng, H. Stretchable, Wearable Dye-Sensitized Solar Cells. *Adv. Mater.* **2014**, *26*, 2643−2647.
(676) Zhang, N.; Chen, J.; Huang, Y.; Guo, W.; Yang, J.; Du, J.; Fan, X.; Tao, C. A Wearable All-Solid Photovoltaic Textile. *Adv. Mater.* **2016**, *28*, 263−269.
(677) Gao, Z.; Liu, P.; Fu, X. M.; Xu, L. M.; Zuo, Y.; Zhang, B.; Sun, X. M.; Peng, H. S. Flexible Self-Powered Textile Formed by Bridging Photoactive and Electrochemically Active Fiber Electrodes. *J. Mater. Chem. A* **2019**, *7*, 14447−14454.
(678) Chai, Z.; Zhang, N.; Sun, P.; Huang, Y.; Zhao, C.; Fan, H. J.; Fan, X.; Mai, W. Tailorable and Wearable Textile Devices for Solar Energy Harvesting and Simultaneous Storage. *ACS Nano* **2016**, *10*, 9201−9207.
(679) Liu, P.; Gao, Z.; Xu, L. M.; Shi, X.; Fu, X. M.; Li, K.; Zhang, B.; Sun, X. M.; Peng, H. S. Polymer Solar Cell Textiles with Interlaced Cathode and Anode Fibers. *J. Mater. Chem. A* **2018**, *6*, 19947−19953.
(680) Yuan, J. Y.; Ford, M. J.; Xu, Y. L.; Zhang, Y. N.; Bazan, G. C.; Ma, W. L. Improved Tandem All-Polymer Solar Cells Performance by Using Spectrally Matched Subcells. *Adv. Energy Mater.* **2018**, *8*, 1703291.

https://dx.doi.org/10.1021/acs.chemrev.9b00821
Chem. Rev. 2020, 120, 3668−3720

(681) Li, Y.; Huang, H. H.; Wang, M. J.; Nie, W. Y.; Huang, W. X.; Fang, G. J.; Carroll, D. L. Spectral Response of Fiber-Based Organic Photovoltaics. *Sol. Energy Mater. Sol. Cells* **2012**, *98*, 273−276.
(682) Liu, J. W.; Namboothiry, M. A. G.; Carroll, D. L. Optical Geometries for Fiber-Based Organic Photovoltaics. *Appl. Phys. Lett.* **2007**, *90*, 133515.
(683) Zeng, W.; Wang, M. J.; Li, Y.; Wan, J. W.; Huang, H. H.; Tao, H.; Carroll, D. L.; Zhao, X. Z.; Zou, D. C.; Fang, G. J. Semi-Closed Tubular Light-Trapping Geometry Dye Sensitized Solar Cells with Stable Efficiency in Wide Light Intensity Range. *J. Power Sources* **2014**, *261*, 75−85.
(684) Park, T.; Na, J.; Kim, B.; Kim, Y.; Shin, H.; Kim, E. Photothermally Activated Pyroelectric Polymer Films for Harvesting of Solar Heat with a Hybrid Energy Cell Structure. *ACS Nano* **2015**, *9*, 11830−11839.
(685) Park, J.-S.; Chae, H.; Chung, H. K.; Lee, S. I. Thin Film Encapsulation for Flexible AM-OLED: A Review. *Semicond. Sci. Technol.* **2011**, *26*, 034001.
(686) Vishnuvarthanan, M.; Rajeswari, N. Effect of Mechanical, Barrier and Adhesion Properties on Oxygen Plasma Surface Modified PP. *Innovative Food Sci. Emerging Technol.* **2015**, *30*, 119−126.
(687) Tummala, R. R. Ceramic and Glass-Ceramic Packaging in the 1990s. *J. Am. Ceram. Soc.* **1991**, *74*, 895−908.
(688) Lopez, J.; Sun, Y.; Mackanic, D. G.; Lee, M.; Foudeh, A. M.; Song, M. S.; Cui, Y.; Bao, Z. A Dual-Crosslinking Design for Resilient Lithium-Ion Conductors. *Adv. Mater.* **2018**, *30*, 1804142.
(689) Lee, Y. I.; Jeon, N. J.; Kim, B. J.; Shim, H.; Yang, T. Y.; Seok, S. I.; Seo, J.; Im, S. G. A Low-Temperature Thin-Film Encapsulation for Enhanced Stability of a Highly Efficient Perovskite Solar Cell. *Adv. Energy Mater.* **2018**, *8*, 1701928.
(690) Seo, S.-W.; Chae, H.; Joon Seo, S.; Kyoon Chung, H.; Min Cho, S. Extremely Bendable Thin-Film Encapsulation of Organic Light-Emitting Diodes. *Appl. Phys. Lett.* **2013**, *102*, 161908.
(691) Zhou, Y. C.; Wang, H.; Wang, L.; Yu, K.; Lin, Z. D.; He, L.; Bai, Y. Y. Fabrication and Characterization of Aluminum Nitride Polymer Matrix Composites with High Thermal Conductivity and Low Dielectric Constant for Electronic Packaging. *Mater. Sci. Eng., B* **2012**, *177*, 892−896.
(692) Gong, J. W.; Liang, J.; Sumathy, K. Review on Dye-Sensitized Solar Cells (Dsscs): Fundamental Concepts and Novel Materials. *Renew. Sustain. Energy Rev.* **2012**, *16*, 5848−5860.
(693) Blakers, A. W.; Wang, A.; Milne, A. M.; Zhao, J. H.; Green, M. A. 22.8% Efficient Silicon Solar Cell. *Appl. Phys. Lett.* **1989**, *55*, 1363−1365.
(694) Parida, B.; Iniyan, S.; Goic, R. A Review of Solar Photovoltaic Technologies. *Renew. Sustain. Energy Rev.* **2011**, *15*, 1625−1636.
(695) Masuko, K.; Shigematsu, M.; Hashiguchi, T.; Fujishima, D.; Kai, M.; Yoshimura, N.; Yamaguchi, T.; Ichihashi, Y.; Mishima, T.; Matsubara, N.; et al. Achievement of More Than 25% Conversion Efficiency with Crystalline Silicon Heterojunction Solar Cell. *IEEE J. Photovolt.* **2014**, *4*, 1433−1435.
(696) Schmidt, S.; Horch, K.; Normann, R. Biocompatibility of Silicon-Based Electrode Arrays Implanted in Feline Cortical Tissue. *J. Biomed. Mater. Res.* **1993**, *27*, 1393−1399.
(697) Blakers, A. W.; Armour, T. Flexible Silicon Solar Cells. *Sol. Energy Mater. Sol. Cells* **2009**, *93*, 1440−1443.
(698) Fang, H.; Yu, K. J.; Gloschat, C.; Yang, Z.; Song, E.; Chiang, C.-H.; Zhao, J.; Won, S. M.; Xu, S.; Trumpis, M.; et al. Capacitively Coupled Arrays of Multiplexed Flexible Silicon Transistors for Long-Term Cardiac Electrophysiology. *Nat. Biomed. Eng.* **2017**, *1*, 0038.
(699) Wang, S.; Weil, B. D.; Li, Y. B.; Wang, K. X. Z.; Garnett, E.; Fan, S. H.; Cui, Y. Large-Area Free-Standing Ultrathin Single-Crystal Silicon as Processable Materials. *Nano Lett.* **2013**, *13*, 4393−4398.
(700) Chirilă, A.; Buecheler, S.; Pianezzi, F.; Bloesch, P.; Gretener, C.; Uhl, A. R.; Fella, C.; Kranz, L.; Perrenoud, J.; Seyrling, S.; et al. Highly Efficient Cu(In,Ga)Se_2 Solar Cells Grown on Flexible Polymer Films. *Nat. Mater.* **2011**, *10*, 857−861.
(701) Kessler, F.; Rudmann, D. Technological Aspects of Flexible Cigs Solar Cells and Modules. *Sol. Energy* **2004**, *77*, 685−695.
(702) Reinhard, P.; Chirila, A.; Blosch, P.; Pianezzi, F.; Nishiwaki, S.; Buecheler, S.; Tiwari, A. N. Review of Progress Toward 20% Efficiency Flexible CIGS Solar Cells and Manufacturing Issues of Solar Modules. *IEEE J. Photovolt.* **2013**, *3*, 572−580.
(703) Shi, J.; Liu, S.; Zhang, L.; Yang, B.; Shu, L.; Yang, Y.; Ren, M.; Wang, Y.; Chen, J.; Chen, W.; et al. Smart Textile-Integrated Microelectronic Systems for Wearable Applications. *Adv. Mater.* **2020**, *32*, 1901958.
(704) Kumari, P.; Mathew, L.; Syal, P. Increasing Trend of Wearables and Multimodal Interface for Human Activity Monitoring: A Review. *Biosens. Bioelectron.* **2017**, *90*, 298−307.
(705) Ryu, H.; Yoon, H. J.; Kim, S. W. Hybrid Energy Harvesters: Toward Sustainable Energy Harvesting. *Adv. Mater.* **2019**, *31*, 1802898.
(706) Bai, Y.; Jantunen, H.; Juuti, J. Energy Harvesting Research: The Road from Single Source to Multisource. *Adv. Mater.* **2018**, *30*, 1707271.
(707) Lee, J. H.; Lee, K. Y.; Gupta, M. K.; Kim, T. Y.; Lee, D. Y.; Oh, J.; Ryu, C.; Yoo, W. J.; Kang, C. Y.; Yoon, S. J.; et al. Highly Stretchable Piezoelectric-Pyroelectric Hybrid Nanogenerator. *Adv. Mater.* **2014**, *26*, 765−769.
(708) Wang, X.; Wang, Z. L.; Yang, Y. Hybridized Nanogenerator for Simultaneously Scavenging Mechanical and Thermal Energies by Electromagnetic-Triboelectric-Thermoelectric Effects. *Nano Energy* **2016**, *26*, 164−171.
(709) Yang, Y.; Zhang, H.; Lee, S.; Kim, D.; Hwang, W.; Wang, Z. L. Hybrid Energy Cell for Degradation of Methyl Orange by Self-Powered Electrocatalytic Oxidation. *Nano Lett.* **2013**, *13*, 803−808.
(710) You, M. H.; Wang, X. X.; Yan, X.; Zhang, J.; Song, W. Z.; Yu, M.; Fan, Z. Y.; Ramakrishna, S.; Long, Y. Z. A Self-Powered Flexible Hybrid Piezoelectric-Pyroelectric Nanogenerator Based on Non-Woven Nanofiber Membranes. *J. Mater. Chem. A* **2018**, *6*, 3500−3509.
(711) Lee, S.; Bae, S.-H.; Lin, L.; Ahn, S.; Park, C.; Kim, S.-W.; Cha, S. N.; Park, Y. J.; Wang, Z. L. Flexible Hybrid Cell for Simultaneously Harvesting Thermal and Mechanical Energies. *Nano Energy* **2013**, *2*, 817−825.
(712) Kim, M. K.; Kim, M. S.; Jo, S. E.; Kim, Y. J. Triboelectric-Thermoelectric Hybrid Nanogenerator for Harvesting Frictional Energy. *Smart Mater. Struct.* **2016**, *25*, 125007.
(713) Pan, C.; Li, Z.; Guo, W.; Zhu, J.; Wang, Z. L. Fiber-Based Hybrid Nanogenerators for/as Self-Powered Systems in Biological Liquid. *Angew. Chem., Int. Ed.* **2011**, *50*, 11192−11196.
(714) Pu, X.; Song, W. X.; Liu, M. M.; Sun, C. W.; Du, C. H.; Jiang, C. Y.; Huang, X.; Zou, D. C.; Hu, W. G.; Wang, Z. L. Wearable Power-Textiles by Integrating Fabric Triboelectric Nanogenerators and Fiber-Shaped Dye-Sensitized Solar Cells. *Adv. Energy Mater.* **2016**, *6*, 1601048.
(715) Wen, Z.; Yeh, M. H.; Guo, H.; Wang, J.; Zi, Y.; Xu, W.; Deng, J.; Zhu, L.; Wang, X.; Hu, C.; et al. Self-Powered Textile for Wearable Electronics by Hybridizing Fiber-Shaped Nanogenerators, Solar Cells, and Supercapacitors. *Sci. Adv.* **2016**, *2*, No. e1600097.
(716) Chen, J.; Huang, Y.; Zhang, N. N.; Zou, H. Y.; Liu, R. Y.; Tao, C. Y.; Fan, X.; Wang, Z. L. Micro-Cable Structured Textile for Simultaneously Harvesting Solar and Mechanical Energy. *Nat. Energy* **2016**, *1*, 16138.
(717) Hansen, B. J.; Liu, Y.; Yang, R.; Wang, Z. L. Hybrid Nanogenerator for Concurrently Harvesting Biomechanical and Biochemical Energy. *ACS Nano* **2010**, *4*, 3647−3652.
(718) Xu, C.; Wang, X.; Wang, Z. L. Nanowire Structured Hybrid Cell for Concurrently Scavenging Solar and Mechanical Energies. *J. Am. Chem. Soc.* **2009**, *131*, 5866−5872.
(719) Kim, K. H.; Kumar, B.; Lee, K. Y.; Park, H. K.; Lee, J. H.; Lee, H. H.; Jun, H.; Lee, D.; Kim, S. W. Piezoelectric Two-Dimensional Nanosheets/Anionic Layer Heterojunction for Efficient Direct Current Power Generation. *Sci. Rep.* **2013**, *3*, 2017.
(720) Liu, Y.; Das, A.; Xu, S.; Lin, Z. Y.; Xu, C.; Wang, Z. L.; Rohatgi, A.; Wong, C. P. Hybridizing ZnO Nanowires with

https://dx.doi.org/10.1021/acs.chemrev.9b00821
Chem. Rev. 2020, 120, 3668−3720

Micropyramid Silicon Wafers as Superhydrophobic High-Efficiency Solar Cells. *Adv. Energy Mater.* **2012**, *2*, 47−51.
(721) Pan, C.; Luo, Z.; Xu, C.; Luo, J.; Liang, R.; Zhu, G.; Wu, W.; Guo, W.; Yan, X.; Xu, J.; Wang, Z. L.; Zhu, J. Wafer-Scale High-Throughput Ordered Arrays of Si and Coaxial Si/Si_{1-x} Ge_x Wires: Fabrication, Characterization, and Photovoltaic Application. *ACS Nano* **2011**, *5*, 6629−6636.
(722) Shi, J.; Starr, M. B.; Wang, X. D. Band Structure Engineering at Heterojunction Interfaces via the Piezotronic Effect. *Adv. Mater.* **2012**, *24*, 4683−4691.
(723) Starr, M. B.; Shi, J.; Wang, X. D. Piezopotential-Driven Redox Reactions at the Surface of Piezoelectric Materials. *Angew. Chem., Int. Ed.* **2012**, *51*, 5962−5966.
(724) Yang, Y.; Zhang, H.; Liu, Y.; Lin, Z. H.; Lee, S.; Lin, Z.; Wong, C. P.; Wang, Z. L. Silicon-Based Hybrid Energy Cell for Self-Powered Electrodegradation and Personal Electronics. *ACS Nano* **2013**, *7*, 2808−2813.
(725) Yoon, G. C.; Shin, K. S.; Gupta, M. K.; Lee, K. Y.; Lee, J. H.; Wang, Z. L.; Kim, S. W. High-Performance Hybrid Cell Based on an Organic Photovoltaic Device and a Direct Current Piezoelectric Nanogenerator. *Nano Energy* **2015**, *12*, 547−555.
(726) Zhou, Y. S.; Liu, Y.; Zhu, G.; Lin, Z. H.; Pan, C.; Jing, Q.; Wang, Z. L. In Situ Quantitative Study of Nanoscale Triboelectrification and Patterning. *Nano Lett.* **2013**, *13*, 2771−2776.
(727) Zhou, Y. S.; Wang, S.; Yang, Y.; Zhu, G.; Niu, S.; Lin, Z. H.; Liu, Y.; Wang, Z. L. Manipulating Nanoscale Contact Electrification by an Applied Electric Field. *Nano Lett.* **2014**, *14*, 1567−1572.
(728) Pan, C.; Guo, W.; Dong, L.; Zhu, G.; Wang, Z. L. Optical Fiber-Based Core-Shell Coaxially Structured Hybrid Cells for Self-Powered Nanosystems. *Adv. Mater.* **2012**, *24*, 3356−3361.
(729) Lipomi, D. J.; Tee, B. C.; Vosgueritchian, M.; Bao, Z. Stretchable Organic Solar Cells. *Adv. Mater.* **2011**, *23*, 1771−1775.
(730) O'Connor, T. F.; Zaretski, A. V.; Savagatrup, S.; Printz, A. D.; Wilkes, C. D.; Diaz, M. I.; Sawyer, E. J.; Lipomi, D. J. Wearable Organic Solar Cells with High Cyclic Bending Stability: Materials Selection Criteria. *Sol. Energy Mater. Sol. Cells* **2016**, *144*, 438−444.
(731) Savagatrup, S.; Chan, E.; Renteria-Garcia, S. M.; Printz, A. D.; Zaretski, A. V.; O'Connor, T. F.; Rodriquez, D.; Valle, E.; Lipomi, D. J. Plasticization of PEDOT:PSS by Common Additives for Mechanically Robust Organic Solar Cells and Wearable Sensors. *Adv. Funct. Mater.* **2015**, *25*, 427−436.
(732) Bi, C.; Chen, B.; Wei, H.; DeLuca, S.; Huang, J. Efficient Flexible Solar Cell Based on Composition-Tailored Hybrid Perovskite. *Adv. Mater.* **2017**, *29*, 1605900.
(733) Park, M.; Kim, H. J.; Jeong, I.; Lee, J.; Lee, H.; Son, H. J.; Kim, D. E.; Ko, M. J. Mechanically Recoverable and Highly Efficient Perovskite Solar Cells: Investigation of Intrinsic Flexibility of Organic-Inorganic Perovskite. *Adv. Energy Mater.* **2015**, *5*, 1501406.
(734) Yang, Y.; Zhang, H. L.; Lin, Z. H.; Liu, Y.; Chen, J.; Lin, Z. Y.; Zhou, Y. S.; Wong, C. P.; Wang, Z. L. A Hybrid Energy Cell for Self-Powered Water Splitting. *Energy Environ. Sci.* **2013**, *6*, 2429−2434.
(735) Wang, S.; Wang, Z. L.; Yang, Y. A One-Structure-Based Hybridized Nanogenerator for Scavenging Mechanical and Thermal Energies by Triboelectric-Piezoelectric-Pyroelectric Effects. *Adv. Mater.* **2016**, *28*, 2881−2887.
(736) Chamanian, S.; Ciftci, B.; Ulusan, H.; Muhtaroglu, A.; Kulah, H. Power-Efficient Hybrid Energy Harvesting System for Harnessing Ambient Vibrations. *IEEE Trans. Circuits Syst. I, Reg. Papers* **2019**, *66*, 2784−2793.
(737) Lee, J. H.; Ryu, H.; Kim, T. Y.; Kwak, S. S.; Yoon, H. J.; Kim, T. H.; Seung, W.; Kim, S. W. Thermally Induced Strain-Coupled Highly Stretchable and Sensitive Pyroelectric Nanogenerators. *Adv. Energy Mater.* **2015**, *5*, 1500704.
(738) Broadhurst, M.; Davis, G.; McKinney, J.; Collins, R. Piezoelectricity and Pyroelectricity in Polyvinylidene Fluoride—a Model. *J. Appl. Phys.* **1978**, *49*, 4992−4997.
(739) Chen, Y.; Zhang, Y.; Yuan, F. F.; Ding, F.; Schmidt, O. G. A Flexible PMN-Pt Ribbon-Based Piezoelectric-Pyroelectric Hybrid Generator for Human-Activity Energy Harvesting and Monitoring. *Adv. Electron. Mater.* **2017**, *3*, 1600540.
(740) Li, J.; Zhao, J.; Rogers, J. A. Materials and Designs for Power Supply Systems in Skin-Interfaced Electronics. *Acc. Chem. Res.* **2019**, *52*, 53−62.
(741) Shu, R.; Zhou, Y.; Wang, Q.; Han, Z.; Zhu, Y.; Liu, Y.; Chen, Y.; Gu, M.; Xu, W.; Wang, Y.; et al. $Mg_{3+\delta}Sb_xBi_{2-x}$ Family: A Promising Substitute for the State-of-the-Art N-Type Thermoelectric Materials near Room Temperature. *Adv. Funct. Mater.* **2019**, *29*, 1807235.
(742) Dong, G.; Li, S.; Yao, M.; Zhou, Z.; Zhang, Y. Q.; Han, X.; Luo, Z.; Yao, J.; Peng, B.; Hu, Z.; et al. Super-Elastic Ferroelectric Single-Crystal Membrane with Continuous Electric Dipole Rotation. *Science* **2019**, *366*, 475−479.
(743) Alhawari, M.; Tekeste, T.; Mohammad, B.; Saleh, H.; Ismail, M. *Power Management Unit for Multi-Source Energy Harvesting in Wearable Electronics*, Proceedings from the 2016 IEEE 59th International Midwest Symposium on Circuits and Systems (MWSCAS), Abu Dhabi, UAE, October 16−19, 2016; pp 1−4.
(744) Zhou, Y.; Wang, C. H.; Lu, W.; Dai, L. Recent Advances in Fiber-Shaped Supercapacitors and Lithium-Ion Batteries. *Adv. Mater.* **2020**, *32*, 1902779.
(745) Zhai, S.; Karahan, H. E.; Wang, C.; Pei, Z.; Wei, L.; Chen, Y. 1D Supercapacitors for Emerging Electronics: Current Status and Future Directions. *Adv. Mater.* **2020**, *32*, 1902387.
(746) Chen, D.; Jiang, K.; Huang, T.; Shen, G. Recent Advances in Fiber Supercapacitors: Materials, Device Configurations, and Applications. *Adv. Mater.* **2020**, *32*, 1901806.
(747) Jost, K.; Dion, G.; Gogotsi, Y. Textile Energy Storage in Perspective. *J. Mater. Chem. A* **2014**, *2*, 10776−10787.
(748) Mo, F.; Liang, G.; Huang, Z.; Li, H.; Wang, D.; Zhi, C. An Overview of Fiber-Shaped Batteries with a Focus on Multifunctionality, Scalability, and Technical Difficulties. *Adv. Mater.* **2020**, *32*, 1902151.
(749) Jocic, D. Smart Textile Materials by Surface Modification with Biopolymeric Systems. *Res. J. Text. Apparel* **2008**, *12*, 58−65.
(750) Stoppa, M.; Chiolerio, A. Wearable Electronics and Smart Textiles: A Critical Review. *Sensors* **2014**, *14*, 11957−11992.
(751) Jost, K.; Perez, C. R.; McDonough, J. K.; Presser, V.; Heon, M.; Dion, G.; Gogotsi, Y. Carbon Coated Textiles for Flexible Energy Storage. *Energy Environ. Sci.* **2011**, *4*, 5060−5067.
(752) Horrocks, A. R.; Anand, S. C. *Handbook of Technical Textiles*; CRC Press: Boca Raton, 2000.
(753) Andrew, T. L.; Zhang, L.; Cheng, N.; Baima, M.; Kim, J. J.; Allison, L.; Hoxie, S. Melding Vapor-Phase Organic Chemistry and Textile Manufacturing to Produce Wearable Electronics. *Acc. Chem. Res.* **2018**, *51*, 850−859.
(754) Zhang, Y.; Ng, S.-W.; Lu, X.; Zheng, Z. Solution-Processed Transparent Electrodes for Emerging Thin-Film Solar Cells. *Chem. Rev.* **2020**, *120*, 2049.
(755) Liang, S.; Li, Y.; Zhou, T.; Yang, J.; Zhou, X.; Zhu, T.; Huang, J.; Zhu, J.; Zhu, D.; Liu, Y.; et al. Microfluidic Patterning of Metal Structures for Flexible Conductors by in Situ Polymer-Assisted Electroless Deposition. *Adv. Sci.* **2017**, *4*, 1600313.
(756) Jang, Y.; Kim, S. M.; Spinks, G. M.; Kim, S. J. Carbon Nanotube Yarn for Fiber-Shaped Electrical Sensors, Actuators, and Energy Storage for Smart Systems. *Adv. Mater.* **2020**, *32*, 1902670.
(757) Zhang, X.; Lu, W.; Zhou, G.; Li, Q. Understanding the Mechanical and Conductive Properties of Carbon Nanotube Fibers for Smart Electronics. *Adv. Mater.* **2020**, *32*, 1902028.
(758) Khair, N.; Islam, R.; Shahariar, H. Carbon-Based Electronic Textiles: Materials, Fabrication Processes and Applications. *J. Mater. Sci.* **2019**, *54*, 10079−10101.
(759) Lee, J.; Llerena Zambrano, B.; Woo, J.; Yoon, K.; Lee, T. Recent Advances in 1D Stretchable Electrodes and Devices for Textile and Wearable Electronics: Materials, Fabrications, and Applications. *Adv. Mater.* **2020**, *32*, 1902532.

https://dx.doi.org/10.1021/acs.chemrev.9b00821
Chem. Rev. 2020, 120, 3668−3720

(760) Dhanabalan, S. C.; Dhanabalan, B.; Chen, X.; Ponraj, J. S.; Zhang, H. Hybrid Carbon Nanostructured Fibers: Stepping Stone for Intelligent Textile-Based Electronics. *Nanoscale* **2019**, *11*, 3046−3101.
(761) Pierre, A. C.; Pajonk, G. M. Chemistry of Aerogels and Their Applications. *Chem. Rev.* **2002**, *102*, 4243−4265.
(762) Mecklenburg, M.; Schuchardt, A.; Mishra, Y. K.; Kaps, S.; Adelung, R.; Lotnyk, A.; Kienle, L.; Schulte, K. Aerographite: Ultra Lightweight, Flexible Nanowall, Carbon Microtube Material with Outstanding Mechanical Performance. *Adv. Mater.* **2012**, *24*, 3486−3490.
(763) Lefebvre, L. P.; Banhart, J.; Dunand, D. C. Porous Metals and Metallic Foams: Current Status and Recent Developments. *Adv. Eng. Mater.* **2008**, *10*, 775−787.
(764) Srivastava, V.; Srivastava, R. On the Polymeric Foams: Modeling and Properties. *J. Mater. Sci.* **2014**, *49*, 2681−2692.
(765) Hsu, Y. Y.; Gresser, J. D.; Trantolo, D. J.; Lyons, C. M.; Gangadharam, P. R.; Wise, D. L. Effect of Polymer Foam Morphology and Density on Kinetics of in Vitro Controlled Release of Isoniazid from Compressed Foam Matrices. *J. Biomed. Mater. Res.* **1997**, *35*, 107−116.
(766) He, W.; Zhang, G.; Zhang, X. X.; Ji, J.; Li, G. Q.; Zhao, X. D. Recent Development and Application of Thermoelectric Generator and Cooler. *Appl. Energy* **2015**, *143*, 1−25.
(767) Mokhothu, T. H.; John, M. J. Review on Hygroscopic Aging of Cellulose Fibres and Their Biocomposites. *Carbohydr. Polym.* **2015**, *131*, 337−354.
(768) Tritt, T. M. *Thermal Conductivity: Theory, Properties, and Applications*; Kluwer Academic/Plenum Publishers: New York, 2005.
(769) Park, S.; Vosguerichian, M.; Bao, Z. A Review of Fabrication and Applications of Carbon Nanotube Film-Based Flexible Electronics. *Nanoscale* **2013**, *5*, 1727−1752.
(770) Zhang, W.; Dehghani-Sanij, A. A.; Blackburn, R. S. Carbon Based Conductive Polymer Composites. *J. Mater. Sci.* **2007**, *42*, 3408−3418.
(771) Park, S.; Kim, J.; Park, C. H. Superhydrophobic Textiles: Review of Theoretical Definitions, Fabrication and Functional Evaluation. *J. Eng. Fibers Fabr.* **2015**, *10*, 1−18.
(772) Xue, X. Y.; Nie, Y. X.; He, B.; Xing, L. L.; Zhang, Y.; Wang, Z. L. Surface Free-Carrier Screening Effect on the Output of a ZnO Nanowire Nanogenerator and Its Potential as a Self-Powered Active Gas Sensor. *Nanotechnology* **2013**, *24*, 225501.
(773) Bryant, D.; Aristidou, N.; Pont, S.; Sanchez-Molina, I.; Chotchunangatchaval, T.; Wheeler, S.; Durrant, J. R.; Haque, S. A. Light and Oxygen Induced Degradation Limits the Operational Stability of Methylammonium Lead Triiodide Perovskite Solar Cells. *Energy Environ. Sci.* **2016**, *9*, 1655−1660.
(774) Meredith, M. T.; Minteer, S. D. Biofuel Cells: Enhanced Enzymatic Bioelectrocatalysis. *Annu. Rev. Anal. Chem.* **2012**, *5*, 157−179.
(775) Lu, H. L.; Shen, T. F. R.; Huang, S. T.; Tung, Y. L.; Yang, T. C. K. The Degradation of Dye Sensitized Solar Cell in the Presence of Water Isotopes. *Sol. Energy Mater. Sol. Cells* **2011**, *95*, 1624−1629.
(776) Nguyen, V.; Zhu, R.; Yang, R. S. Environmental Effects on Nanogenerators. *Nano Energy* **2015**, *14*, 49−61.
(777) Sauvage, F.; Decoppet, J. D.; Zhang, M.; Zakeeruddin, S. M.; Comte, P.; Nazeeruddin, M.; Wang, P.; Gratzel, M. Effect of Sensitizer Adsorption Temperature on the Performance of Dye-Sensitized Solar Cells. *J. Am. Chem. Soc.* **2011**, *133*, 9304−9310.
(778) Hu, Y.; Klein, B. D.; Su, Y.; Niu, S.; Liu, Y.; Wang, Z. L. Temperature Dependence of the Piezotronic Effect in ZnO Nanowires. *Nano Lett.* **2013**, *13*, 5026−5032.
(779) Gheibi, A.; Latifi, M.; Merati, A. A.; Bagherzadeh, R. Piezoelectric Electrospun Nanofibrous Materials for Self-Powering Wearable Electronic Textiles Applications. *J. Polym. Res.* **2014**, *21*, 469.
(780) Lee, D.; Sang, J. S.; Yoo, P. J.; Shin, T. J.; Oh, K. W.; Park, J. Machine-Washable Smart Textiles with Photothermal and Antibacterial Activities from Nanocomposite Fibers of Conjugated Polymer Nanoparticles and Polyacrylonitrile. *Polymers* **2019**, *11*, 16.
(781) Opwis, K.; Gutmann, J. S.; Lagunas Alonso, A. R.; Rodriguez Henche, M. J.; Ezquer Mayo, M.; Breuil, F.; Leonardi, E.; Sorbello, L. Preparation of a Textile-Based Dye-Sensitized Solar Cell. *Int. J. Photoenergy* **2016**, *2016*, 3796074.
(782) Wang, C.; Feng, R.; Yang, F. Enhancing the Hydrophilic and Antifouling Properties of Polypropylene Nonwoven Fabric Membranes by the Grafting of Poly(N-Vinyl-2-Pyrrolidone) via the ATRP Method. *J. Colloid Interface Sci.* **2011**, *357*, 273−279.
(783) Moon, H.; Seong, H.; Shin, W. C.; Park, W. T.; Kim, M.; Lee, S.; Bong, J. H.; Noh, Y. Y.; Cho, B. J.; Yoo, S.; et al. Synthesis of Ultrathin Polymer Insulating Layers by Initiated Chemical Vapour Deposition for Low-Power Soft Electronics. *Nat. Mater.* **2015**, *14*, 628−635.
(784) Xie, D. Y.; Qian, D.; Song, F.; Wang, X. L.; Wang, Y. Z. A Fully Biobased Encapsulant Constructed of Soy Protein and Cellulose Nanocrystals for Flexible Electromechanical Sensing. *ACS Sustainable Chem. Eng.* **2017**, *5*, 7063−7070.
(785) López-Escalante, M. C.; Fernández-Rodríguez, M.; Caballero, L. J.; Martín, F.; Gabás, M.; Ramos-Barrado, J. R. Novel Encapsulant Architecture on the Road to Photovoltaic Module Power Output Increase. *Appl. Energy* **2018**, *228*, 1901−1910.
(786) Scott, R.; Vidakovic, M.; Chikermane, S.; McKinley, B.; Sun, T.; Banerji, P.; Grattan, K. Encapsulation of Fiber Optic Sensors in 3D Printed Packages for Use in Civil Engineering Applications: A Preliminary Study. *Sensors* **2019**, *19*, 1689.
(787) Yan, W.; Dong, C.; Xiang, Y.; Jiang, S.; Leber, A.; Loke, G.; Xu, W.; Hou, C.; Zhou, S.; Chen, M.; et al. Thermally Drawn Advanced Functional Fibers: New Frontier of Flexible Electronics. *Mater. Today* **2020**, DOI: 10.1016/j.mattod.2019.11.006
(788) Abouraddy, A. F.; Bayindir, M.; Benoit, G.; Hart, S. D.; Kuriki, K.; Orf, N.; Shapira, O.; Sorin, F.; Temelkuran, B.; Fink, Y. Towards Multimaterial Multifunctional Fibres That See, Hear, Sense and Communicate. *Nat. Mater.* **2007**, *6*, 336−347.
(789) Yan, W.; Page, A.; Nguyen-Dang, T.; Qu, Y.; Sordo, F.; Wei, L.; Sorin, F. Advanced Multimaterial Electronic and Optoelectronic Fibers and Textiles. *Adv. Mater.* **2019**, *31*, 1802348.
(790) Adanur, S. *Handbook of Weaving*; Technomic Publishing Company: Lancaster, PA, 2001.
(791) Long, A. C. *Design and Manufacture of Textile Composites*; Woodhead Publishing Ltd., Cambridge, UK, 2005.
(792) Khan, G. A.; Terano, M.; Gafur, M.; Alam, M. S. Studies on the Mechanical Properties of Woven Jute Fabric Reinforced Poly (L-Lactic Acid) Composites. *J. King Saud Univ., Eng. Sci.* **2016**, *28*, 69−74.
(793) Hu, J. *Structure and Mechanics of Woven Fabrics*; Woodhead Publishing Ltd., Cambridge, UK, 2004.
(794) Dixit, A.; Mali, H. S. Modeling Techniques for Predicting the Mechanical Properties of Woven-Fabric Textile Composites: A Review. *Mech. Compos. Mater.* **2013**, *49*, 1−20.
(795) Skylar-Scott, M. A.; Mueller, J.; Visser, C. W.; Lewis, J. A. Voxelated Soft Matter via Multimaterial Multinozzle 3D Printing. *Nature* **2019**, *575*, 330−335.
(796) Qiu, J. H.; Yan, Y. G.; Luo, T. T.; Tang, K. C.; Yao, L.; Zhang, J.; Zhang, M.; Su, X. L.; Tan, G. J.; Xie, H. Y.; et al. 3D Printing of Highly Textured Bulk Thermoelectric Materials: Mechanically Robust Bisbte Alloys with Superior Performance. *Energy Environ. Sci.* **2019**, *12*, 3106−3117.
(797) López Marzo, A. M.; Mayorga-Martinez, C. C.; Pumera, M. 3D-Printed Graphene Direct Electron Transfer Enzyme Biosensors. *Biosens. Bioelectron.* **2020**, *151*, 111980.
(798) Ambrosi, A.; Moo, J. G. S.; Pumera, M. Helical 3D-Printed Metal Electrodes as Custom-Shaped 3D Platform for Electrochemical Devices. *Adv. Funct. Mater.* **2016**, *26*, 698−703.
(799) Chen, M.; Yang, J.; Wang, Z.; Xu, Z.; Lee, H.; Lee, H.; Zhou, Z.; Feng, S. P.; Lee, S.; Pyo, J.; et al. 3D Nanoprinting of Perovskites. *Adv. Mater.* **2019**, *31*, 1904073.
(800) Sun, J. M.; Pu, X.; Liu, M. M.; Yu, A. F.; Du, C. H.; Zhai, J. Y.; Hu, W. G.; Wang, Z. L. Self-Healable, Stretchable, Transparent

Triboelectric Nanogenerators as Soft Power Sources. *ACS Nano* **2018**, *12*, 6147−6155.

https://dx.doi.org/10.1021/acs.chemrev.9b00821
Chem. Rev. 2020, 120, 3668−3720